From Metabolite Sensing to Protein Regulation by *Synechococcus elongatus* PCC 7942 P_{II} Protein

Dissertation

der Mathematisch-Naturwissenschaftlichen Fakultät

der Eberhard Karls Universität Tübingen

zur Erlangung des Grades eines

Doktors der Naturwissenschaften

(Dr. rer. nat.)

vorgelegt von

Oleksandra Fokina

aus Kiew

Tübingen

2011

Tag der mündlichen Qualifikation:	29.11.11
Dekan:	Prof. Dr. Wolfgang Rosenstiel
1. Berichterstatter:	Prof. Dr. Karl Forchhammer
2. Berichterstatter:	Prof. Dr. Wolfgang Wohlleben
3. Berichterstatter:	Prof. Dr. Andreas Burkovski

Table of contents

Abstract

P_{II} signal transduction proteins have key functions in the coordination of central metabolism by integrating signals from the carbon, nitrogen and energy status of the cell. They bind the metabolites ATP, ADP and 2-oxoglutarate (2-OG) and control enzymes, transporters and transcription factors involved in nitrogen metabolism. Depending on its effector molecule binding status, P_{II} from *Synechococcus elongatus* binds a small protein termed PipX, which is a co-activator of the transcription factor NtcA, and regulates the key enzyme of the cyclic ornithine pathway, *N*-acetyl-L-glutamate kinase (NAGK). This study shows that P_{II} and NAGK from bacteria (*S. elongatus*) and plants (*Arabidopsis thaliana*) can functionally complement each other *in vitro*, demonstrating a strong conservation of this regulatory mechanism through 1.2 billion years of separate evolution. There are two contact interfaces in the P_{II}-NAGK complex from *S. elongatus.* One of the them includes a salt bridge of P_{II} E85 residue with R233 of NAGK. Consequently, E85-P_{II} mutants loose the ability to interact with NAGK. We found P_{II} variants (I86N and I86T) that were able to bind to a NAGK variant (R233A), which was previously shown to be unable to bind wild type P_{II} protein. Based on the crystal structure and biochemical analysis of the I86N P_{II} variant, we propose a two-step model for the mechanism of P_{II}-NAGK complex formation. In an initiating step, a contact between R233 of NAGK and E85 of P_{II} initiates the bending of the extended T-loop of P_{II}, followed by a second step, where a bended T-loop deeply inserts into the NAGK clefts to form the tight complex. 2-OG is a key molecule in the P_{II}-mediated signal transduction. Crystal structures of *S. elongatus* wild type P_{II} identified the site of 2-OG binding located in the vicinity of the ATP-binding site between the subunit clefts. The site is formed by the ATP-ligated Mg^{2+} ion and P_{II} residues of the T-loop itself, which adopts a unique bent conformation. The structures of P_{II} trimers with one or two bound 2-OG molecules explain the anticooperativity of the effector binding sites and demonstrate the inter-subunit communication inside the trimer. P_{II} binds ATP and 2-OG in a synergistic manner, with the ATP-binding sites also accepting ADP. Different ADP/ATP ratios strongly affected the properties of P_{II} signalling including 2-OG binding and interactions with its target proteins. ADP modulates P_{II} signalling to the receptor NAGK primarily at low 2-OG levels and antagonises the inhibitory effect of 2-OG for P_{II}-PipX interaction. Apparently P_{II} has a fine-tuned mechanism of sensing both changing energy charge and carbon/nitrogen balance at the same time.

Zusammenfassung

P_{II} Signalproteine spielen eine Schlüsselrole in der Regulation des zellulären Zentralmetabolismus in Bezug auf den Kohlenstoff-, Stickstoff- und Energiestatus der Zelle. Sie binden die Metabolite ATP, ADP und 2-OG (2-Oxoglutarat) und kontrollieren Enzyme, Transporter und Transkriptionsfaktoren, die am Stickstoffmetabolismus beteiligt sind. Abhängig von dem gebundenen Effektormolekül, interagiert P_{II} aus *Synechococcus elongatus* mit PipX, einen co-Aktivator des Transkriptionsfaktors NtcA, und reguliert das Schlüsselenzym des zyklischen Ornitinwegs, *N*-Acetyl-L-Glutamatkinase (NAGK). Im Komplex interagieren P_{II} und NAGK unter anderem über eine Salzbrücke zwischen E85 von P_{II} und R233 von NAGK. P_{II} Varianten, die eine Mutation an der Aminosäure 85 haben, verlieren die Fähigkeit mit NAGK zu interagieren. Wir haben zwei P_{II}-Varianten entdeckt, die die NAGK-Variante R233A binden können, obwohl dieses Enzym mit Wildtyp P_{II} nicht interagiert. Aufgrund der Kristallstruktur und biochemischen Analysen von I86N P_{II}, haben wir einen zweistufigen Mechanismus der P_{II}-NAGK-Komplexbildung vorgeschlagen. Außerdem haben wir gezeigt, dass P_{II} und NAGK aus Bakterien (*S. elongatus*) und Pflanzen (*Arabidopsis thaliana*) sich gegenseitig *in vitro* funktionell ersetzen können, was die starke Konservierung von P_{II}-Signaltransduktion demonstriert.

2-Oxoglutarat ist ein zentrales Molekül in der P_{II}-vermittelten Signaltransduktion. Kristallstrukturen von *S. elongatus* Wildtyp P_{II} haben die 2-OG-Bindungsstelle in der Nähe von der Nukleotidbindungsstelle identifiziert. Die 2-OG-Bindungsstelle wird vom ATP-gebundenen Mg^{2+}-Ion und vom P_{II}-T-loop gebildet. Dabei nimmt dieser Loop eine vorher nicht bekannte Konformation ein. P_{II}-Strukturen mit einem, zwei und drei gebundenen 2-OG Molekülen klären den Mechanismus der antikooperativen Ligandenbindung an P_{II} auf. ATP-Bindungstellen am P_{II}-Protein können auch von ADP besetzt werden. Verschiedene ATP/ADP-Verhältnisse beeinflussen die Signaltransduktioneigenschaften des P_{II}-Proteins. ADP verhindert 2-OG-Bindung an P_{II} und verringert den negativen Effekt von 2-OG auf die P_{II}-PipX-Interaktion. Die P_{II}-Regulation der NAG-Kinase wird durch ADP vor allem bei niedrigen 2-OG-Konzentrationen moduliert. Offensichtlich spricht P_{II} auf feinste Änderungen bezüglich des Energie- und Kohlenstoff/Stickstoff-Status der Zelle an und verändert entsprechend seine Eigenschaften als Signaltransduktionprotein.

A. Introduction

1. Cyanobacteria: Phylogeny and Ecological Impact

Cyanobacteria are a diverse and morphologically complex group of Gram-negative bacteria. They are the only bacteria that use water as an electron source for oxygenic photosynthesis. They are primary producers and therefore play a significant role in the planetary carbon cycle. Moreover, some cyanobacteria are capable of nitrogen fixation, which makes them also an important part of the nitrogen cycle.

Cyanobacteria occupy a distinct phylogenetic group with a unicellular photoautotroph as the last common ancestor (Sanchez-Baracaldo *et al.*, 2005). Traditional taxonomical classifications distinguished five groups depending on their morphology and developmental potential: from unicellular organisms as for example *Synechococcus* and *Gloeobacter* to complex multicellular cell-differentiating cyanobacteria (*Fischerella*) (Rippka *et al.*, 1979). Molecular sequence comparison showed phylogenetic affinities of taxa with similar filamentous and/or cell differentiation characteristics. On the other hand, more simple unicellular and filamentous cyanobacteria are more diverse (Giovannoni *et al.*, 1988; Turner *et al.*, 1999; Sanchez-Baracaldo *et al.*, 2005; Tomitani *et al.*, 2006). According to the endosymbiotic theory, oxygenic photosynthesis was introduced to eukaryotes by an ancient cyanobacterium 1.7 – 1.5 bio years ago (Cavalier-Smith, 1975).

Cyanobacteria populate almost all illuminated terrestrial, marine and fresh water habitats. They even occur in extreme environments, such as hot springs, salterns, desert crusts or different Antarctic biotopes. Furthermore, some cyanobacteria are capable to form stable symbiotic associations with eukaryotes, such as various protozoa, fungi or plants, for example mosses, an aquatic fern *Azolla* and angiosperms.

Historic relevance of cyanobacteria lies mainly in their invention of oxygenic photosynthesis and production of O_2 that allowed evolutionary changes towards aerobic metabolism on Earth.

2. Photosynthesis and Electron Transfer

Cyanobacteria are photoautothrophs, they regenerate ATP and reduction equivalents (NADPH) by converting solar energy into membrane potential through membrane-bound catalysts. The photosynthetic apparatus is localised on an intracellular membrane system termed thylakoid and consists of Photosystem II (PSII), the cytochrome b_6f complex, plastocyanin or cytochrome c_6, Photosystem I (PSI), ferrodoxin (Fd), ferrodoxin-$NADP^+$-Oxidoreductase and the ATP-Synthase (Krogmann, 1973; Bryant, 1994; Vermaas, 2001). PSII is a protein complex that contains a heterodimeric reaction centre (D1/D2) and a water-oxidising complex (oxygen evolving complex, OEC), together with numerous auxiliary proteins. The major light harvesting apparatus for PSII are the phycobilisomes. They are located on the stromal side of the thylacoid membrane and represent 50% of protein mass of a cyanobacterial cell. The phycobilisome consist of rods with light absorbing phycobiliproteins phycoerythrin, phycocyanine and core subunits with allophycocyanine. These pigmented proteins transfer energy to the primary electron donor in reaction centre of PSII P680, chlorophyll *a* (Chl *a*). Further electron transfer to plastoquinone is performed by a chain of electron carriers. Oxidised P680+ is re-reduced by the electron received from the oxidation of water to O_2 and $4H^+$, catalysed by the Mn-cluster of the OEC, with a TyrZ as an intermediate. Cytochrome b_6f complex receives electrons from PSII and transfers them to the luminal electron carrier proteins, for example plastocyanin. PSI captures light energy and transfers it to the Chl *a* in the reaction centre of PSI (P700). The electron is further transferred to ferredoxin and oxidised P700* is reduced by plastocyanin. Finally, the electron is used by the ferrodoxin-$NADP^+$-Oxidoreductase for reduction of $NADP^+$ to NADPH.
The electron transfer complexes pump protons across the membrane, creating a proton gradient that is used by ATP-Synthase to synthesise ATP from ADP and P_i.
ATP and reduced hydrogen in form of NADPH are used for example to fix CO_2 via the Calvin cycle and in nitrogen assimilation (see below).

3. Carbon Metabolism

Cyanobacteria use CO_2 fixation as the main carbon acquisition process, though some strains are capable of photomixotrophic or heterotrophic growth under certain

conditions. CO_2 enters into the cell by diffusion and is converted to HCO_3^- by two CO_2 uptake systems, NDH-1_4 (low affinity) and NDH-1_3 (high affinity). These systems involve thylakoid membrane-located NADPH-Dehydrogenase complexes (NDH-1) (Shibata *et al.*, 2001; Maeda *et al.*, 2002). There are also three HCO_3^- transporters located on the cytoplasmic membrane. One of them is a high affinity ABC-type transporter BCT1 that is encoded by the *cmpABCD* operon in *Synechococcus elongatus* PCC 7942 (Omata *et al.*, 1999; Maeda *et al.*, 2000). Another high affinity HCO_3^- transporter, SbtA, is sodium-dependent and was identified in *Synechocystis* sp. PCC 6803 (Shibata *et al.*, 2002a; Shibata *et al.*, 2002b). The third known HCO_3^- transporter, BicA, has a low affinity for its substrate and is induced by low CO_2 in *Synechococcus* PCC 7002 (Price *et al.*, 2004).

In the cell HCO_3^- diffuses into the carboxysomes (Reinhold *et al.*, 1991), subcellular polyhedral bodies consisting of RubisCO and carbonic anhydrase and enveloped by specific shell proteins. In the Carboxysome, HCO_3^- is converted to CO_2 by the carbonic anhydrase. This mechanism allows cyanobacteria to accumulate high concentrations of CO_2 in close proximity to Ribulose-1,5-bisphosphate carboxylase oxygenase (RubisCO) (Kaplan and Reinhold, 1999; Badger and Price, 2003). RubisCO catalyses the first reaction of the Calvin cycle – carboxylation of the ribulose-1,5-bisphosphate, thereby fixing inorganic carbon. The formed six-carbon intermediate is unstable and decays into two molecules of 3-phosphoglycerate. This product is used to regenerate the CO_2 acceptor ribulose-1,5-bisphosphate through the Calvin cycle, to synthesise glycogen, or it can be incorporated into the glycolysis and the oxidative branch of the tricarboxylic acid (TCA) cycle with the end product 2-oxoglutarate (2-OG). A characteristic feature of the cyanobacterial TCA cycle is the lack of 2-OG dehydrogenase (Stanier and Cohen-Bazire, 1977). The 2-OG serves only for anabolic purposes as a carbon skeleton in the assimilation of nitrogen and represents a direct link between carbon and nitrogen metabolism.

4. Nitrogen Assimilation

Cyanobacteria are capable to use the variety of inorganic and organic compounds as a source of nitrogen, for example ammonium, nitrate, nitrite, urea or a few amino acids. Some strains can grow diazotrophycally, fixing atmospheric nitrogen. Filamentous strains, such as *Anabaena* and *Nostoc*, differentiate specialised cells,

termed heterocysts, from vegetative cells under nitrogen starvation (Adams and Duggan, 1999). In heterocysts nitrogen is fixed by the enzyme nitrogenase in a microanoxic environment. To protect the nitrogenase from oxygen, these cells have several mechanisms, including a polysaccharide and glycolipid envelope, increased respiration and inactivated PSII to create a microoxic intracellular environment. Other diazotrophic cyanobacteria manage to protect the nitrogenase without cell differentiation (Berman-Frank *et al.*, 2001).

In non-diazotrophic strains, such as *Synechococcus elongatus* PCC 7942, nitrogen depletions causes specific stress responses including morphological and physiological changes that allow the cell to survive (Gorl *et al.*, 1998; Schwarz and Forchhammer, 2005). This process, termed chlorosis, is characterised by the deactivation of photosynthetic activities, degradation of pigments (phycobiliproteins, chlorophyll *a*) and general repression of many metabolic processes (Allen and Smith, 1969; Schwarz and Forchhammer, 2005).

Cyanobacteria take up the nitrogen-containing compounds and convert them intracellularly to ammonium, which is then assimilated (Fig. A1). For this reason ammonium is a preferred source of combined nitrogen and in its presence the assimilation of other nitrogen sources is repressed (Muro-Pastor and Florencio, 2003; Flores and Herrero, 2005). High-affinity transporters of the Amt family carry out ammonium uptake, if the concentration of the compound in environment is not high enough for a passive diffusion through the membrane (Montesinos *et al.*, 1998; Muro-Pastor *et al.*, 2005). In *S. elongatus* PCC 7942 the ammonium permease is encoded by the *amt1* gene that belongs to the NtcA regulon (Vazquez-Bermudez *et al.*, 2002).

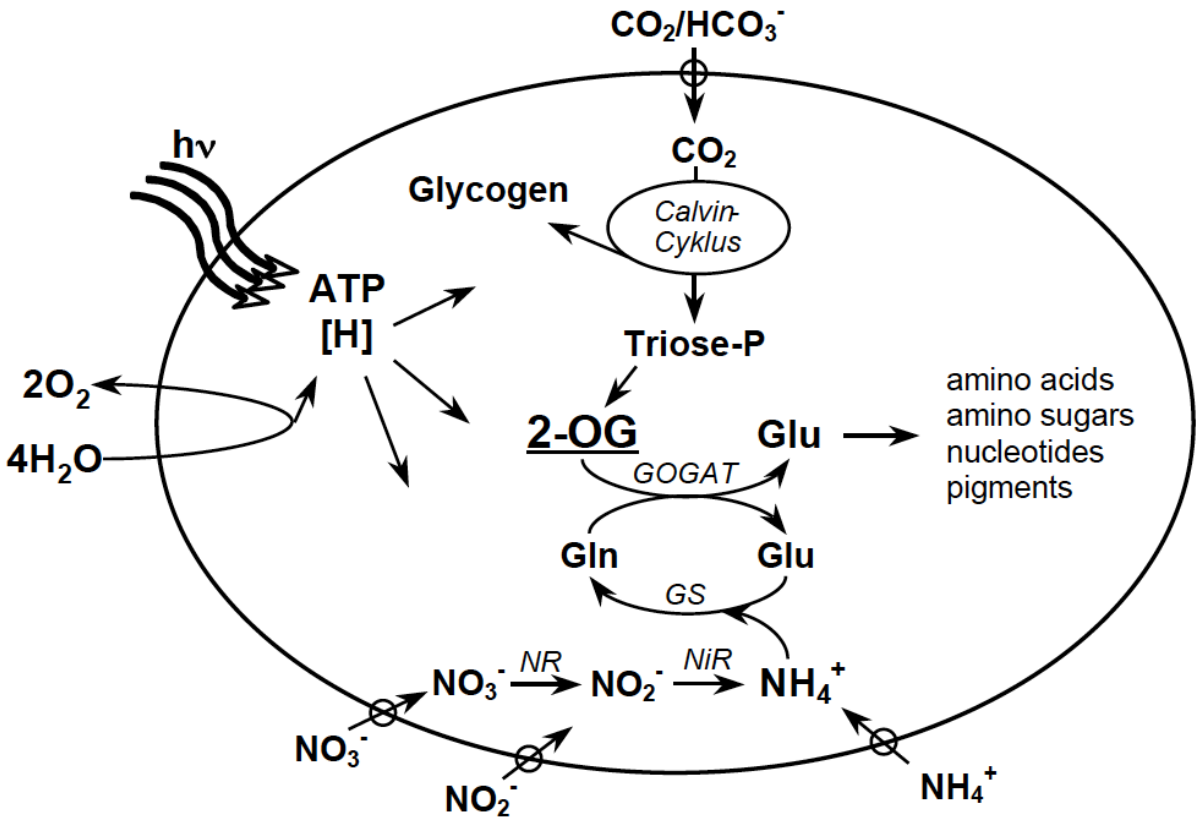

Figure A1. Schematic representation of carbon and nitrogen assimilation in non-diazotrophic cyanobacteria. GOGAT: glutamine-2-oxoglutarate-amido transferase; GS: glutamine synthetase; NR: nitrate reductase; NiR: nitrite reductase; 2-OG: 2-oxoglutarate. (Adapted from Luque and Forchhammer, 2008)

However, the most abundant source of nitrogen in many habitats is nitrate (Guerrero *et al.*, 1981). Both nitrate and nitrite require high-affinity uptake systems, since their concentrations in the environment are often low. Most fresh-water cyanobacteria, such as *S. elongatus*, *Synechocystis* and *Anabaena*, use an ABC-transporter, which allows nitrate and nitrite uptake in micromolar concentrations (Flores *et al.*, 2005). The transporter consists of four subunits: a periplasmatic substrate binding protein, NrtA, a transmembrane protein, NrtB, and two cytoplasmatic ATPases, NrtD and NrtC, with NrtC carrying an additional domain similar to NrtA (Maeda and Omata, 1997). In *Synechococcus elongatus,* the *nrtABCD* gene cluster forms a *nir*-operon together with the genes *narB* and *nirA*, which encode the nitrate and nitrite reductases (Omata *et al.*, 1993; Suzuki *et al.*, 1993). Most marine strains, for example the marine *Synechococcus* strains or *Trichodesmium* sp. WH 9601, possess a nitrate/nitrite permease that belongs to the major facilitator superfamily (MFS) and consists generally of a single polypeptide NrtP or NapA (Sakamoto *et al.*, 1999; Wang *et al.*, 2000; Flores *et al.*, 2005). Utilisation of nitrate includes two reduction

steps, first to nitrite by nitrate reductase (NR) and then to ammonium by nitrite reductase (NiR) (Fig. A1) (Flores *et al.*, 2005). Nitrate reductase is a monomer, containing one [4Fe-4S] cluster and a Mo-cofactor. For the reduction of one nitrate molecule NR requires two electrons, which are delivered from PSI-reduced ferredoxin (Manzano *et al.*, 1976). Nitrite reductase also is a monomeric enzyme with a [4Fe-4S] cluster and contains one siroheme as a prosthetic group. The reduction of nitrite to ammonium requires six electrons for three sequential reactions with NO and NH_2OH as intermediates.

Intracellular ammonium is assimilated in the two steps of the GS-GOGAT (glutamine synthetase – glutamine-2-oxoglutarate-amido transferase) cycle (Fig. A1) (Flores and Herrero, 1994). GS catalyzes the incorporation of ammonia into the carboxyl group of glutamate under consumption of ATP. The amido group of the formed glutamine is transferred by GOGAT to 2-oxoglutarate, creating two glutamate molecules. One of these molecules is amidated by GS and the other one is provided for the biosynthetic pathways.

Two types of GS have been identified in cyanobacteria. Glutamine synthetase type I (GSI), encoded by the gene *glnA*, is present in all analysed cyanobacteria except for *Pseudanabaena* sp. PCC 6903 (Muro-Pastor *et al.*, 2005). It consists of 12 identical subunits (approx. 50 kDa each) that form two hexagonal rings (Flores and Herrero, 1994; Merrick and Edwards, 1995). A second GS (GSIII), encoded by the *glnN* gene has first been discovered in *Synechocystis* PCC6803 (Reyes and Florencio, 1994). It is structurally different from GSI and consists of 8 identical subunits (approx. 75 kDa each). The enzyme is present exclusively in non-diazotrophic strains and is expressed only under nitrogen starvation (Reyes and Florencio, 1994; Garcia-Dominguez and Florencio, 1997). GSIII helps recovery of nitrogen-starved cells from chlorosis (Sauer *et al.*, 1999). *Pseudanabaena* sp. PCC 6903 contains only GS type III (GSIII).

The cyanobacterial GOGAT receives two electrons needed for 2-OG reduction from PSI-reduced ferredoxin (Marques *et al.*, 1992). The Fd-GOGAT is a monomer (170 kDa) with a [3Fe-4S] cluster and FMN as a prosthetic group, encoded by the *glsF* gene (Muro-Pastor *et al.*, 2005).

Another enzyme that can be considered a part of the nitrogen assimilatory system is isocitrate dehydrogenase (IDH). It produces 2-OG in the last step of the cyanobacterial TCA cycle solely for the purposes of nitrogen assimilation by the GS-

GOGAT cycle. The enzyme is a homodimer (55 kDa monomers), encoded by the *icd* gene (Muro-Pastor *et al.*, 2005). The 2-oxoglutarate serves as a link between carbon and nitrogen assimilation pathways.

5. Regulation of Nitrogen Metabolism

Cyanobacteria can assimilate a variety of nitrogen-containing compounds. As a result of highly developed acclimation mechanisms, nitrogen assimilation is tightly regulated by the carbon and nitrogen supply. For example, in the presence of ammonium, the preferred source of combined nitrogen, the assimilation of other nitrogen sources is repressed (Muro-Pastor and Florencio, 2003; Flores and Herrero, 2005). On the other hand, high intracellular levels of ammonium are toxic, so that enough 2-OG should be present to incorporate ammonium via the GS-GOGAT cycle (Flores and Herrero, 1994). Due to the lack of 2-oxoglutarate dehydrogenase, 2-OG is a final step of the oxidative branch of the TCA cycle and accumulates in the cell under nitrogen starvation, because it can't be processed (Stanier and Cohen-Bazire, 1977). This mechanism makes 2-OG not only a link between carbon and nitrogen metabolism, but also a perfect signalling molecule of the intracellular C/N balance.
This signal is sensed by the transcription factor NtcA (Luque *et al.*, 1994; Herrero *et al.*, 2004), which regulates expression of the genes involved in the nitrogen metabolism, and the signal transduction protein P_{II}, which controls a variety of intracellular processes via protein-protein interactions (Forchhammer, 2004).

5.1. P_{II}-mediated Signal Transduction

P_{II} signal transduction proteins are highly conserved and widely spread in bacteria, archaea and plants, where they coordinate metabolic processes depending on the carbon, nitrogen and energy status of the cell (Ninfa and Jiang, 2005; Leigh and Dodsworth, 2007; Forchhammer, 2008; Sant'Anna *et al.*, 2009). P_{II} proteins integrate metabolic signals by binding the effector molecules ATP, ADP and 2-OG and being subjected to reversible covalent modifications. The received information is transmitted to P_{II} target proteins, such as regulatory and metabolic enzymes, transcription factors and/or transport proteins (Forchhammer, 2004). The proteins of the P_{II} family can be classified into three subgroups depending on the encoding

gene, *glnB*, *glnK* and *nifI* (Arcondeguy *et al.*, 2001). The *glnB* and *glnK* homologues are quite common, though *nifI* encoded proteins are found only in archaea and some anaerobic bacteria.

The three-dimensional structure of the P_{II} proteins is highly conserved (Forchhammer, 2008). They are homotrimers of 12-13 kDa subunits with a central core of antiparallel β-sheets and laterally arranged α-helices (Fig. A2) (Xu *et al.*, 1998; Xu *et al.*, 2003; Sakai *et al.*, 2005). Three prominent loops (one T-loop per subunit) extend from the cylindrical body of the trimer outward into the solvent. These T-loops are highly flexible and adopt different conformations, taking part in binding of effector molecules and being the dominating structure in protein-protein interactions. Each subunit also contains two smaller loops: the B- and C-loop from the opposing subunits are facing each other in the intersubunit cleft and participate in the adenyl nucleotide binding.

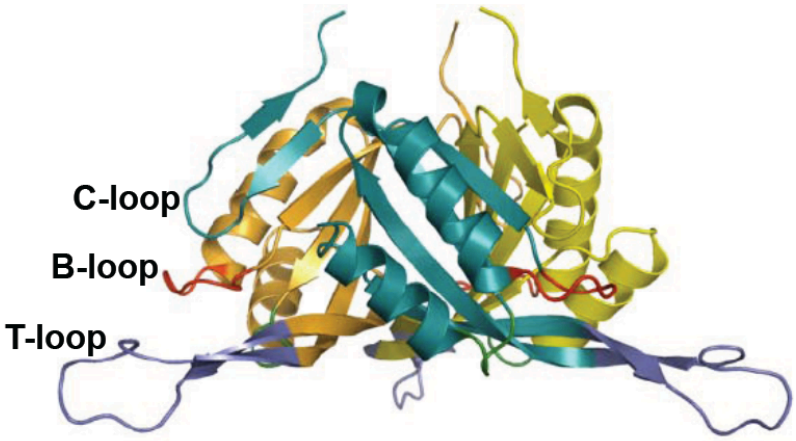

Figure A2. The P_{II} trimer from *Synechococcus elongatus as* a ribbon model with secondary structures and indicated T-, B- and C-loops (PDB ID 1QY7).

One P_{II} trimer has three nucleotide binding sites, which are highly similar in the P_{II} structures from all three domains of life, with ATP and ADP competing for the same site. Generally, in the presence of ATP, up to three 2-OG molecules can bind per trimer (Ninfa and Jiang, 2005). However, the P_{II} protein from *Arabidopsis thaliana* binds 2-OG also in the presence of ADP (Smith *et al.*, 2003). The data on location of the 2-OG-binding site has been controversial so far. According to the structural studies of a P_{II} paralogue from an archaeon *Methanococcus jannaschii*, GlnK1, a 2-OG-binding site was identified on the distal side of the T-loop (Yidiz *et al.*, 2007). On the other hand recent structure of a P_{II} homologue from *Azospirillum brasilience* showed that 2-OG was bound at the base of the T-loop near the ATP-binding site

(Truan *et al.*, 2010). The effector binding to the P_{II} protein is highly intriguing, because three ATP-sites as well as three 2-OG sites exhibit negative cooperativity (Forchhammer and Hedler, 1997; Jiang and Ninfa, 2007; Jiang and Ninfa, 2009a). To occupy the next site, a higher concentration of the ligand is required, which allows P_{II} proteins to sense metabolites in a wide range of concentrations. The second level of P_{II} signal integration is reversible covalent modification on the tips of the T-loops. This property is not conserved in all P_{II} proteins, also the type of modification differs in various bacteria. For example, P_{II} proteins in proteobacteria are subjected to uridylylation and in actinobacteria to adenylylation on tyrosyl-residue (Tyr51) (Son and Rhee, 1987; Jaggi *et al.*, 1996; Atkinson and Ninfa, 1999; Strosser *et al.*, 2004). Unicellular cyanobacteria exhibit phosphorylation/dephosphorylation of P_{II} on a seryl 49-residue (Forchhammer and de Marsac, 1994; Forchhammer and de Marsac, 1995). Depending on the bound effector molecules and the modification state, P_{II} proteins demonstrate fine-tuned and flexible control of their target proteins.

5.1.1. P_{II} signalling network in E. coli

GlnB from *E. coli* was discovered around 40 years ago and is one of the best characterised P_{II} proteins (Shapiro, 1969). It is regulated by the effector binding and the reversible uridylylation at Tyr51, catalysed by the signal transducing uridylyltransferase/uridylyl-removing enzyme (UTase/UR) at low glutamine levels, which correspond to nitrogen-poor conditions (Fig. A3) (Adler *et al.*, 1975; Jaggi *et al.*, 1996; Jiang *et al.*, 1998a). Glutamine inhibits the uridylyltransferase activity of the enzyme and activates its uridylyl-removing activity. GlnB controls the expression of genes involved in the nitrogen metabolism through the NRII (NrtB) histidine kinase of the NRI/NRII two-component regulatory system (Fig. A3) (Ninfa and Magasanik, 1986; Jiang *et al.*, 1998b). The unmodified P_{II} protein binds to NRII leading to its dephosphorylation, followed by the inactivation of the enhancer-binding transcription factor NRI (NtrC) (Jiang and Ninfa, 1999). On the other hand, under nitrogen deprivation, the uridylylated form of P_{II} can't form a complex with NRII, causing the phosphorylation of NRI and activation of nitrogen-regulated genes. The phosphorylation of NRI is also promoted by 2-oxoglutarate binding to P_{II} as a part of the nitrogen limitation response. The effector binds to the P_{II} protein in the presence of ATP and impairs the ability of P_{II} to cause dephosphorylation of the transcription factor.

Another known GlnB-receptor is glutamine synthetase adenylyltransferase (ATase) that catalyzes the reversible adenylylation of glutamine synthetase (GS), regulating its activity (Fig. A3) (Rhee *et al.*, 1985; Jiang *et al.*, 1998c). ATase forms a complex with non-modified GlnB as well as with the uridylylated form (Jaggi *et al.*, 1997). Non-modified GlnB stimulates the adenylyltransferase activity of ATase, whereas in the complex with modified GlnB, ATase deadenylates and activates GS. This way uridylylated P_{II} mediates GS activation under nitrogen-poor conditions. 2-OG, bound to the P_{II} protein, also promotes GS activation.

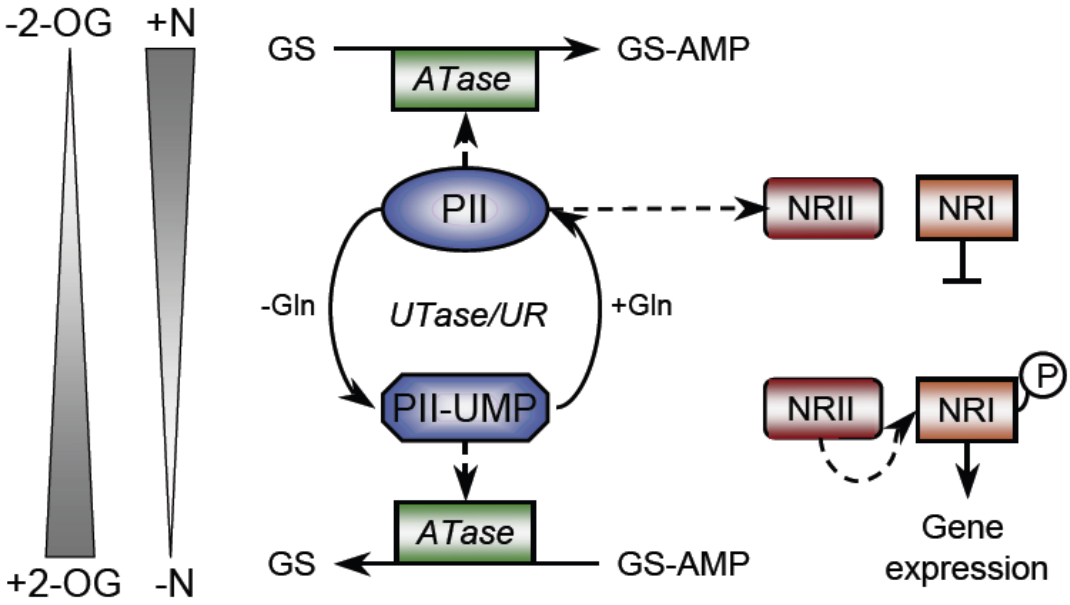

Figure A3. Schematic representation of the GlnB-mediated signal transduction in *E. coli*. Dashed lines represent direct protein-protein interactions. ATase: adenylyltransferase, GS: glutamine synthetase, NRI: NtrC transcription factor, NRII: NrtB histidine kinase, 2-OG: 2-oxoglutarate, UTase/UR: uridylyltransferase/uridylyl-removing enzyme.

E. coli possesses a second P_{II} paralogue, GlnK, that is produced under nitrogen-poor conditions (Atkinson *et al.*, 2002), unlike GlnB that is constitutively expressed (Liu and Magasanik, 1993). The P_{II} paralogues are structurally very similar (Xu *et al.*, 1998; Xu *et al.*, 2001) and GlnK is uridylylated by the UTase/UR enzyme as well. The function of GlnK is defined by the localisation of its gene in one operon with *amtB*, a gene encoding an ammonium transporter (Thomas *et al.*, 2000). In addition to the transcriptional linkage of these two genes, GlnK forms a complex with AmtB and inactivates it under nitrogen excess conditions (Coutts *et al.*, 2002; Javelle *et al.*, 2004). AmtB is a homotrimeric transmembrane protein with three hydrophobic pores for transportation of ammonia gas into the cell (Khademi *et al.*, 2004; Zheng *et al.*,

2004). In the GlnK-AmtB complex the non-uridylylated T-loops of the P_{II} protein adopt a stretched conformation and block the pores of the transporter (Conroy *et al.*, 2007; Gruswitz *et al.*, 2007). In this complex ADP was found bound to the nucleotide-binding site of GlnK. By contrast, 2-OG in the presence of Mg^{2+}-ATP has strong negative effect on AmtB-GlnK interaction (Durand and Merrick, 2006; Wolfe *et al.*, 2007).

P_{II} from *E.coli* can also act as a direct sensor of the adenylate energy charge *in vitro*. It was shown that ADP acted antagonistically to the signal of nitrogen deprivation, mediated by 2-OG. Through the GlnB protein, ADP promotes dephosphorylation of NRI in the NRI/NRII two-component system and adenylylation of glutamine synthetase by ATase (Jiang and Ninfa, 2007). In addition, uridylylation of GlnB by UTase is negatively influenced by ADP. Also ADP increases the stability of the GlnK-AmtB complex and antagonises the effect of 2-OG, demonstrating the P_{II} sensing of the adenylate energy charge (Radchenko *et al.*, 2010).

5.1.2. P_{II} protein in cyanobacteria

In cyanobacteria, P_{II} proteins have been mostly studied in unicellular strains *Synechococcus elongatus* and *Synechocystis* sp. PCC 6803, where they are phosphorylated and dephosphorylated on the Ser49 in response to the cellular 2-OG and ATP levels (Forchhammer and de Marsac, 1994; Forchhammer and de Marsac, 1995). However, some cyanobacteria, such as *Prochlorococcus* strains, do not exhibit P_{II} phosphorylation (Palinska *et al.*, 2002). P_{II} phosphorylation can be achieved *in vitro* in the presence of Mg^{2+}-ATP-2-OG (Forchhammer and de Marsac, 1995), though the P_{II} kinase hasn't been identified yet. In the absence of effectors P_{II} is dephosphorylated by the PP2C family phosphatase PphA, first found in *Synechocystis* sp. PCC 6803 (Ruppert *et al.*, 2002). The phosphatase activity is partially inhibited by ATP or ADP and strongly by Mg^{2+}-ATP-2-OG.

The regulatory role of P_{II} in cyanobacteria involves control of nitrate utilisation (Kloft and Forchhammer, 2005; Takatani *et al.*, 2006), gene expression, by sequestering the co-activator PipX of the general transcription factor NtcA (Espinosa *et al.*, 2006; Espinosa *et al.*, 2007; Llacer *et al.*, 2010), and arginine biosynthesis through N-acetyl-L-glutamate kinase (NAGK) (Fig. A4) (Burillo *et al.*, 2004; Heinrich *et al.*, 2004; Maheswaran *et al.*, 2004).

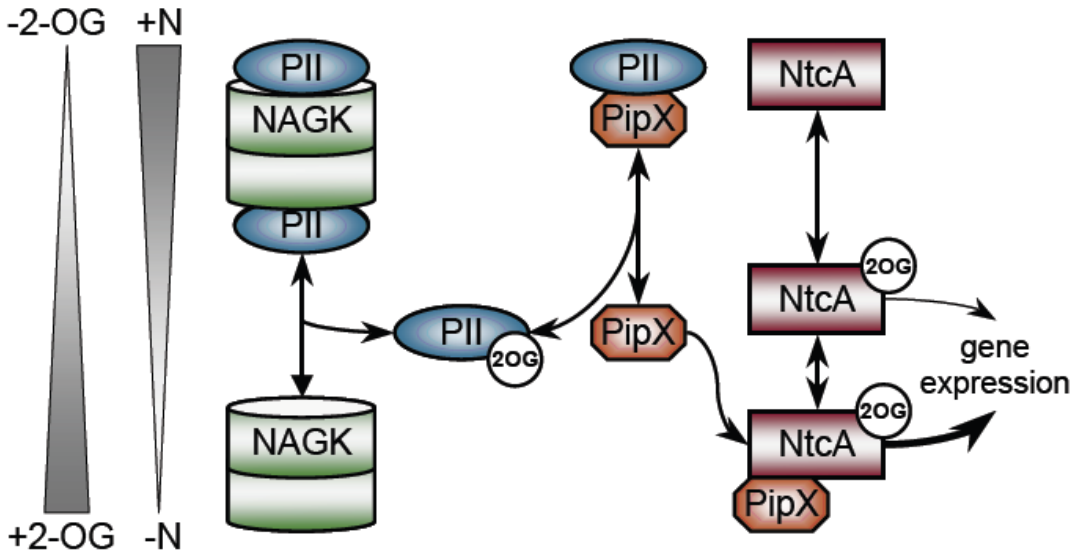

Figure A4. Schematic representation of the P_{II}-mediated signal transduction in *S. elongatus* PCC 7942. NAGK: N-acetyl-L-glutamate kinase, 2-OG: 2-oxoglutarate.

Nitrogen-regulated gene expression in cyanobacteria is provided by NtcA, which belongs to the cAMP receptor protein (CRP) family of transcription factors and was first discovered in *Synechococcus elongatus* PCC 7942 (Vega-Palas *et al.*, 1992).

NtcA binds to the promoters of genes subjected to metabolic control by ammonium, such as *glnA* (glutamine synthetase), *nir*-operon (nitrate reductase, nitrite reductase, nitrate/nitrite permease), its own gene (*ntcA*), and activates them (Wei *et al.*, 1993; Luque *et al.*, 1994). The NtcA regulon includes hundreds of other genes, including *glnB* (P_{II} protein), *idc* (isocitrate dehydrogenase), genes involved in uptake and transformation of nitrogen sources, regulatory genes that control heterocyst differentiation in filamentous cyanobacteria and many others (Muro-Pastor *et al.*, 1996; Garcia-Dominguez and Florencio, 1997; Lee *et al.*, 1999; Herrero *et al.*, 2004; Su *et al.*, 2005).

NtcA is a homodimer with approx. 50 kDa subunits that structurally resembles the bacterial transcription factor CRP and includes similar N- and C-terminal domains that have been identified as the regulatory and the DNA-binding domains in CRP protein (Weber and Steitz, 1987; Llacer *et al.*, 2010). The C-terminal domain of NtcA also includes an α-helix for interaction with a small protein termed PipX (Llacer *et al.*, 2010). The 2-oxoglutarate affects transcriptional activity of NtcA by enhancing its binding to DNA and it is also required for transcription initiation (Tanigawa *et al.*, 2002; Vazquez-Bermudez *et al.*, 2002). The binding site for 2-OG is similar to the cAMP-binding site of CRP and is located in the regulatory domain of NtcA. Two 2-OG

molecules can bind per NtcA dimer and promote the activated form of NtcA. In addition, NtcA is regulated by the P_{II} protein via the coactivator PipX (Espinosa *et al.*, 2006). PipX binds to NtcA under high 2-OG concentrations, stabilises its active form and possibly directly activates it (Espinosa *et al.*, 2007; Llacer *et al.*, 2010). Depending on the present 2-OG level, PipX changes its interaction partner from NtcA to P_{II}. In the P_{II}-PipX complex, the P_{II} T-loops exhibit a novel extended conformation, caging three PipX monomers bound to the P_{II} trimer and hiding the interacting groups for PipX-NtcA complex formation (Llacer *et al.*, 2010). Under low 2-OG concentrations P_{II} sequesters PipX thereby preventing the activation of NtcA mediated gene expression.

The control of arginine biosynthesis in cyanobacteria is achieved through arginine feedback inhibition of NAGK, which phosphorylates N-acetyl-*L*-glutamate (Caldovic and Tuchman, 2003; Llacer *et al.*, 2008). Nonphosphorylated P_{II} protein binds and activates the enzyme and relieves it from the feedback inhibition by arginine (Fig. A5) (Heinrich *et al.*, 2004; Maheswaran *et al.*, 2004).

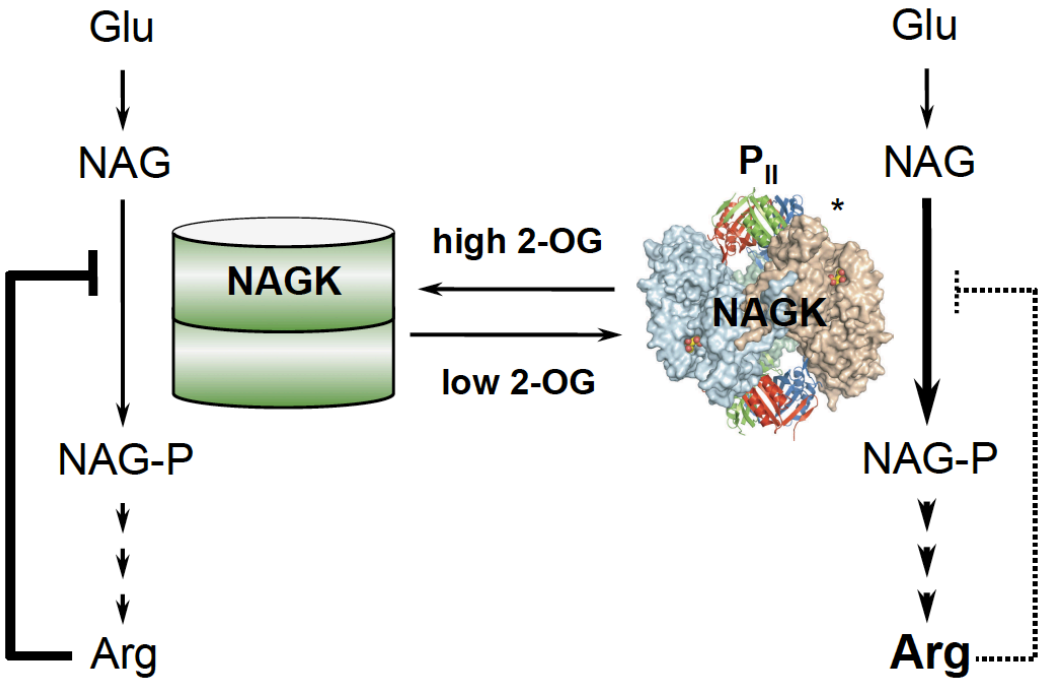

Figure A5. Schematic representation of the arginine biosynthesis control. P_{II} binds NAGK, induces its activity and protects it from the feed-back inhibition by arginine. Arg: arginine, Glu: glutamate, NAGK: N-acetyl-L-glutamate kinase. *Llacer *et al*. 2007.

The overall structure of the P_{II}-NAGK complex between cyanobacteria and plants is conserved, it consists of two P_{II} trimers at the poles, sandwiching a NAGK trimer of dimmers with the threefold axes of the proteins aligned (Llacer *et al.*, 2007; Mizuno *et al.*, 2007). One P_{II} subunit interacts with one NAGK subunit. The P_{II}-NAGK crystal structure from *S. elongatus* revealed two surfaces of P_{II} that are involved in the interaction with NAGK. The smaller one is on the P_{II} body, involving the residue E85 of the B-loop that forms a salt bridge with R233 of NAGK C-domain and residues F11, F13 at the β1-α1 junction as well as T83 engaged in hydrophobic interactions. The major surface for P_{II}-NAGK interaction is presented by the P_{II} T-loop, which adopts a unique bent conformation and is inserted into the interdomain cleft of NAGK. The T-loop residues R45 and E50 are engaged in an ion-pair network with the N-domain residues of NAGK and S49 is involved in a tight hydrogen bond. The binding of *S. elongatus* P_{II} causes a 4-fold increase of V_{max} and a significant decrease of the K_m of the enzyme (Maheswaran *et al.*, 2004). Free NAGK is also highly sensitive to arginine inhibition, but binding of the P_{II} protein changes the arginine inhibition and substrate binding sites, decreasing the affinity towards arginine and increasing it towards NAG (N-acetyl glutamate). P_{II}-NAGK complex formation is strongly regulated by the effector molecule binding to the P_{II} protein. In cyanobacteria PII-NAGK interaction is strongly inhibited by 2-OG in the presence of Mg^{2+}-ATP and negatively influenced by ADP (Maheswaran *et al.*, 2004).

Another P_{II} interaction partner in cyanobacteria is PamA, a putative membrane protein of unknown function (Osanai *et al.*, 2005). The *in vitro* interaction of the proteins responded to ATP and 2-OG and a *pamA* deficient mutant showed lower expression levels of several NtcA-regulated genes compared to the wild type. However, the mechanism of PamA influence on gene expression and the physiological connection to P_{II} are yet unknown.

P_{II} was also found to regulate an ABC-type NO^{2-}/NO^{3-} transporter. In the P_{II}-deficient mutants the activity of the transporter was not decreased in the presence of ammonium (Lee *et al.*, 1998). A subunit of the permease, NtrC, possesses a C-terminal domain that is not found in other ABC-type transporters and may be involved in the interaction with P_{II} (Kobayashi *et al.*, 1997), but no direct interaction between P_{II} and the permease has been found so far.

5.1.3. P_{II} protein in plants

The P_{II} protein found in plants is nuclear encoded, but is located in chloroplasts of *Arabidopsis thaliana* (Hsieh *et al.*, 1998; Smith *et al.*, 2002) and *Oryza sativa* (Sugiyama *et al.*, 2004). The protein is similar to the cyanobacterial P_{II} (Hsieh *et al.*, 1998; Smith *et al.*, 2003), but no covalent modification of the protein has been observed so far. The only found mutual interaction partner with cyanobacteria is NAGK (Chen *et al.*, 2006). The crystal structures of P_{II}-NAGK complexes from *S. elongatus* and *A. thaliana* showed major similarity to each other (Llacer *et al.*, 2007; Mizuno *et al.*, 2007). There are, however, some differences. An important one is the absence of the interactions between the P_{II} B-loop and NAGK C-domain in the *A. thaliana* P_{II}-NAGK complex. The impact of *A. thaliana* P_{II} binding on the enzymatic activity of plant NAGK is smaller in comparison to *S. elongatus* proteins. The activation of *A. thaliana* NAGK by P_{II} is characterised by only 30% increase of V_{max} and no change in K_m (Chen *et al.*, 2006). The enzyme is also 50-times less sensitive towards arginine inhibition than cyanobacterial NAGK. Concerning the regulation of P_{II}-NAGK complex formation by the metabolites: the study by Chen *et al.* (2006) suggested that in the plant P_{II}-NAGK system 2-OG, ATP and ADP have no significant effect on complex dissociation.

In plants the role of P_{II} has evolved over time to control the carbon metabolism pathway of fatty acid synthesis (Feria Bourrellier *et al.*, 2010). The *A. thaliana* P_{II} binds to the biotin carboxyl carrier protein (BCCP) subunits of the chloroplast acetyl-CoA carboxylase (ACCase). In the presence of Mg-ATP, P_{II} reduces the enzyme activity, but the presence of 2-OG leads to the complex dissociation *in vitro*, neutralising the P_{II}-mediated inhibition of the ACCase (Feria Bourrellier *et al.*, 2010). The discovery of this new signalling role of the P_{II} protein in *A. thaliana* is of great importance. It shows how a known and conserved P_{II}-mediated signalling pathway exists next to a completely novel one.

6. Research question

The P_{II}-mediated signal transduction is incredibly complex. One protein has evolved to sense signals of carbon, nitrogen and energy status of the cell and to regulate a large number of protein targets. These target proteins are very different and P_{II} has a unique interaction surface for each of them. In order to fulfil its role, the P_{II} protein

has to be extremely flexible. The cylindrical body of the trimer is strongly conserved even between different subfamilies, for example GlnK and GlnB proteins are structurally very similar. The major difference lies in the T-loop that can adopt various conformations, is subjected to covalent modifications and takes part in the interactions with proteins and smaller molecules (Forchhammer, 2008; Llacer *et al.*, 2010). However, molecular events leading to the observed conformational changes are unclear and were addressed in this study. This work includes the description of the mechanism behind P_{II}-NAGK complex formation and highlights unique features of novel P_{II} protein variants.

In cyanobacteria, P_{II} is reversibly phosphorylated by a specific kinase and can exist in three different forms - carrying three, two, one or zero phosphates. The identification of the P_{II} kinase remains an important subject of the research connected to P_{II}-mediated signal transduction in cyanobacteria. It is also possible that the plant P_{II}, which is highly similar to the cyanobacterial P_{II}, is also phosphorylated. The identification of the P_{II} kinase could help to determine, whether P_{II} in higher phototrophic eukaryots is subjected to covalent modification or has lost it in the evolutionary process. The fact that P_{II} in cyanobacteria and in plants regulates arginine biosynthesis through NAG kinase rises the question, whether the two proteins in these systems are mutually exchangeable. Several aspects of P_{II}-NAGK interaction in *S. elongatus* and in *A. thaliana* were compared in this work.

Reversible phosphorylation of P_{II}, mentioned above, is not important for all of the P_{II} interactions in *S. elongatu*s. PipX monomers bind to both phosphorylated and non-phosphorylated P_{II} subunits and the interaction is regulated by the metabolites. It seems that the role of the small effector molecules is more important than the covalent modification in some regulatory processes. According to the proposed model of the P_{II} phosphorylation cycle, the phosphorylated form of P_{II} is inhibitory for the nitrate/nitrite permease only in the absence of 2-OG-ATP (Forchhammer, 2008).

A characteristic feature of the P_{II} interaction with ATP and 2-OG is the negative cooperativity of the effector binding. If, for example, one ATP molecule binds to the trimer, higher concentration of effector is needed to occupy the second binding site, and even higher for the third site. It allows the protein to sense metabolites in a wide range of concentrations. The mechanism behind the negative cooperativity has remained unknown so far. This study demonstrated the binding site for 2-OG, partially formed by the T-loop in a novel conformation, and showed how the

anticooperativity is mediated via intersubunit communication. The structures of the P_{II} trimers with one, two and three bound 2-OG molecules revealed that intermolecular signalling is based on the highly conserved trimeric architecture of P_{II}.

For many years P_{II} proteins have been known mainly as sensors of nitrogen deprivation signal led by 2-OG. Lately, there have been evidences that they can also be direct sensor of the adenylate energy charge (EC) as well. In bacteria ADP acts as a signal of low energy charge and generally does not support 2-OG binding to P_{II} (Jiang and Ninfa, 2007; Radchenko *et al.*, 2010). In addition to other questions, this work addressed the ability of the cyanobacterial P_{II} to act as an EC sensor *in vitro* and demonstrated, how known P_{II} targets from *S. elongatus* responded to changing ADP/ATP ratios.

B. Publication 1

N-Acetyl-L-Glutamate Kinase (NAGK) from Oxygenic Phototrophs: P_{II} Signal Transduction across Domains of Life Reveals Novel Insights in NAGK Control

J. Mol. Biol. (2009) 389, 748–758

Contribution to publication:

I performed, analysed and interpreted the following experiments:

- SPR analysis of the 2-OG effect on the complex formation of *Se*NAGK or *Se*NAGKΔC and *Se*P_{II} or *At*P_{II}

doi:10.1016/j.jmb.2009.04.053 J. Mol. Biol. (2009) 389, 748–758

JMB

Available online at www.sciencedirect.com

ScienceDirect

ELSEVIER

N-Acetyl-L-Glutamate Kinase (NAGK) from Oxygenic Phototrophs: P_{II} Signal Transduction across Domains of Life Reveals Novel Insights in NAGK Control

Sabine Beez, Oleksandra Fokina, Christina Herrmann and Karl Forchhammer*

Institut für Mikrobiologie der Eberhard-Karls-Universität Tübingen, Auf der Morgenstelle 28, 72076 Tübingen, Germany

Received 29 October 2008; received in revised form 23 April 2009; accepted 27 April 2009
Available online 3 May 2009

N-Acetyl-L-glutamate kinase (NAGK) catalyzes the first committed step in arginine biosynthesis in organisms that perform the cyclic pathway of ornithine synthesis. In eukaryotic and bacterial oxygenic phototrophs, the activity of NAGK is controlled by the P_{II} signal transduction protein. Recent X-ray analysis of NAGK–P_{II} complexes from a higher plant (*Arabidopsis thaliana*) and a cyanobacterium (*Synechococcus elongatus*) revealed that despite several differences, the overall structure of the complex is highly similar. The present study analyzes the functional conservation of P_{II}-mediated NAGK regulation in plants and cyanobacteria to distinguish between universal properties and those that are specific for the different phylogenetic lineages. This study shows that plant and cyanobacterial P_{II} proteins can mutually regulate the NAGK enzymes across the domains of life, implying a high selective pressure to conserve P_{II}–NAGK interaction over more than 1.2 billion years of separate evolution. The non-conserved C-terminus of *S. elongatus* NAGK was identified as an element, which strongly enhances arginine inhibition and is responsible for most of the differences between *S. elongatus* and *A. thaliana* NAGK with respect to arginine sensitivity. Both P_{II} proteins relieve arginine inhibition of NAGK, and in both lineages, P_{II}-mediated relief from arginine inhibition is antagonized by 2-oxoglutarate. Together, these properties highlight the conserved role of P_{II} as a signal integrator of the C/N balance sensed as 2-oxoglutarate to regulate arginine synthesis in oxygenic phototrophs.

Keywords: arginine; 2-oxoglutarate; *Arabidopsis*; *Synechococcus*; enzyme activation

Edited by J. Karn

Introduction

P_{II} signal transduction proteins constitute an abundant protein family, present in bacteria, archaea and plants, where they control a wide range of processes related to nitrogen assimilation (for recent reviews, see Refs. 1–3). Generally, P_{II} proteins are signal integrators, which bind the key metabolites ATP, ADP and 2-oxoglutarate (2-OG) and which may be subjected to further signal-dependent covalent modification.[3,4] Depending on the signal input state (binding of metabolites and, where applicable, covalent modification), P_{II} proteins bind to various P_{II} receptors, including transcription factors, key regulatory enzymes, metabolic enzymes or transport proteins and thereby inhibit or activate the target's activity.

P_{II} proteins are homotrimers of 12- to 13-kDa subunits, and binding of the effector molecules takes place in the three clefts between the subunits. ATP is sandwiched between the B- and C-loops of two neighbouring subunits. Binding of 2-OG depends in many P_{II} proteins on the presence of ATP, apparently because ATP binding creates the conformation that is

*Corresponding author. E-mail address: karl.forchhammer@uni-tuebingen.de.

Abbreviations used: NAG, *N*-acetyl-L-glutamate; NAGK, *N*-acetyl-L-glutamate kinase; *Se*NAGK, NAGK from *Synechococcus elongatus*; *At*NAGK, NAGK from *Arabidopsis thaliana*; *At*P_{II} and *Se*P_{II}, P_{II} signal transduction protein from *A. thaliana* and *S. elongatus*, respectively; 2-OG, 2-oxoglutarate; SPR, surface plasmon resonance; FC, flow cell; RU, resonance unit.

able to bind 2-OG.[3,5] In the case of the cyanobacterial P_{II} protein studied here, the three 2-OG binding sites on the trimeric P_{II} protein have negative cooperativity, allowing P_{II} to sense this metabolite in a wide range of concentrations.[6,7] The remarkable functional versatility of P_{II} interactions can at least in part be attributed to a large, surface-exposed loop, termed the T-loop, which is flexible and is able to undergo extended conformational changes upon binding to receptors and/or binding of effector molecules.[3] In cases where P_{II} proteins are covalently modified, this modification takes place at the apex of the T-loop, such as tyrosyl-51 uridylylation in proteobacteria, tyrosyl-51 adenylylation in actinobacteria or seryl-49 phosphorlyation in unicellular cyanobacteria.[2,3]

In the cyanobacterium *Synechococcus elongatus*, P_{II} was shown to be involved in nitrate utilization by yet unknown mechanisms,[8,9] in activity regulation of the transcription factor NtcA through binding to an NtcA-activating factor, termed PipX,[10,11] and in control of arginine synthesis.[12–15] In the latter case, P_{II} binds in its non-phosphorylated state to *N*-acetyl-L-glutamate kinase (NAGK), the controlling enzyme of the arginine biosynthesis pathway (see below).[13,14,16] This P_{II} interaction seems to be a conserved feature of all oxygenic photosynthetic organisms[3,12,17] and has also been demonstrated in the chloroplasts of plants such as *Oryza sativa*[18] and *Arabidopsis thaliana*.[17]

Arginine biosynthesis in cyanobacteria and plants proceeds via a pathway that is controlled by arginine through feedback inhibition of NAGK, the enzyme that converts *N*-acetyl-L-glutamate (NAG) to *N*-acetyl glutamyl phosphate.[16,19] In cyanobacteria and plants, binding of the P_{II} signalling protein to NAGK results in a substantial relief of feedback control by arginine.[14,17] Recently, the crystal structures of NAGK–P_{II} complexes from the cyanobacterium *S. elongatus*[20] and from *A. thaliana*[21] could be resolved at 2.75 or 2.5 Å resolution, respectively, with both structures revealing a high degree of similarity.[16] In both cases, the complex consists of two P_{II} trimers sandwiching a hexameric (trimer of dimers) NAGK toroid, with the 3-fold axes of P_{II} and NAGK aligned. Each P_{II} subunit contacts one opposing NAGK subunit, whereby the contacts map in the inner circumference of the NAGK toroid and involve two regions of the P_{II} subunit. One region is on the P_{II} body and the other one is on the distal region of the T-loop, which adopts a similar compact conformation in both complexes. Of particular importance in complex formation are residues of the T-loop, including R45 and S49, which are signature residues for cyanobacterial P_{II} proteins and are also present in P_{II} proteins from eukaryotic phototrophs (with the exception of *Cyanidium caldarium*).[12,22]

Despite these similarities, several differences are apparent, with respect to the structure of the complex and at the level of enzyme regulation: An apparent difference in structure concerns the role of the B-loop of the P_{II} proteins in complex formation. Whereas in *S. elongatus*, residues from the B-loop of P_{II} (T83; E85) take part in interactions with the C-domain of NAGK,[20] no such interactions have originally been described for the *A. thaliana* complex,[21] although one corresponding salt bridge (E97-K240) in one subunit of the *A. thaliana* complex can be seen in the Protein Data Bank file 2rd5, as pointed out recently.[16] At the level of enzyme activity, *A. thaliana* NAGK (*At*NAGK) was shown to be only modestly activated by P_{II} complex formation (30% increase of V_{max} but no effect on K_m), whereas the *S. elongatus* enzyme was highly activated upon P_{II} binding, increasing V_{max} and lowering K_m.[14,17] The degree of arginine inhibition differs markedly between the two enzymes: *S. elongatus* NAGK (*Se*NAGK) was reported to be about 50-fold more sensitive towards arginine inhibition than the *A. thaliana* enzyme (IC_{50} of 15 μM Arg *versus* 730 μM Arg at saturating ATP levels). In both cases, complex formation with P_{II} relieves the inhibition by arginine by a factor of 4–7 as compared to free NAGK. ADP was shown to dissociate the *Se*NAGK–P_{II} complex,[14] but no such effect on *At*NAGK–P_{II} complex was reported.[17]

An intriguing difference between the plant and cyanobacterial NAGK–P_{II} system was reported with respect to the effect of 2-OG: In the case of *S. elongatus*, surface plasmon resonance (SPR) analysis showed that 2-OG in the presence of ATP inhibits complex formation. By contrast, enzymatic investigation of *At*NAGK revealed that 2-OG increased the catalytic efficiency of NAGK by 38%, mainly by increasing V_{max}. However, it should be noted that analysis of *Se*NAGK by activity measurements also failed to reveal the physically detectable inhibition of 2-OG on complex formation (compare Refs. 13 and 14), suggesting that the enzyme assay conditions may interfere with 2-OG action. In all previous studies, NAGK activity was monitored by a colorimetric assay, which requires a buffer containing 400 mM hydroxylamine, which might interfere with the effector molecules.

The present investigation was carried out to compare P_{II}-mediated NAGK regulation in plants and cyanobacteria, with a question in mind, that is, whether plant and cyanobacterial P_{II} and NAGK proteins are mutually exchangeable across the domains of life. Special attention was given to those aspects, where the NAGK–P_{II} system in cyanobacteria differs from that in plants, in particular, the contradictory results on the role of 2-OG on NAGK–P_{II} interaction and the sensitivity of the enzymes towards arginine inhibition.

Results and Discussion

Kinetic constants of *Se*NAGK and *At*NAGK determined by a coupled assay

Preparation of purified recombinant *Se*NAGK and *At*NAGK and P_{II} proteins is described in Materials and Methods. In previous studies, NAGK activity was tested by a colorimetric assay, which requires high concentrations of hydroxylamine.[14,17] Since

NAGK regulation may be affected by these artificial test conditions, an assay that measures the formation of ADP (product of the NAGK reaction) by coupling it to the oxidation of NADH was used[23] (for details, see Materials and Methods). The activity of NAGK in the coupled assay system resulted in a continuous and linear oxidation of NADH until consumption of NADH (not shown). The reaction velocity was directly proportional to the amount of NAGK added. Originally, the activities in various *Se*NAGK preparations were highly variable and unstable upon prolonged storage of the enzyme, in particular when assayed in the absence of P_{II}, whereas the *At*NAGK was much less sensitive (data not shown). Finally, stable enzyme activities could be achieved by preparing fresh solutions of reduced DTT that were added to the enzyme assays.

In a first set of experiments, the kinetic constants of plant and cyanobacterial NAGKs with and without P_{II} proteins from both sources were determined with NAG or ATP as variable substrates in the coupled assay (see Table 1). *Se*NAGK could be activated both by the cognate *S. elongatus* P_{II} protein (*Se*P_{II}) and, surprisingly, in a similar manner, by P_{II} from *A. thaliana* (*At*P_{II}). Compared to the previous colorimetric assays,[14] free *Se*NAGK had appreciably higher activity in the coupled assay, due to a lower K_m for NAG, whereas the difference between the assays faded away in the presence of *Se*P_{II} (see Table 1 for comparison, the previous results are shown in parentheses). Consequently, the apparent catalytic activation by P_{II} is less pronounced in the coupled assay (now 8-fold instead of the previously reported 40-fold increase in catalytic efficiency, k_{cat}/K_m). The higher activity of free *Se*NAGK under the new assay conditions could mostly be attributed to the presence of reduced DTT, which was not used previously (data not shown). In the coupled assay, free *At*NAGK displays considerably higher activities than the cyanobacterial enzyme, with a 10-fold higher k_{cat} and an almost 10-fold lower K_m, resulting in a 100-fold higher overall catalytic efficiency. These values for *At*NAGK activity were higher than those previously reported by the colorimetric assay,[17] due to an approximately 10-fold lower K_m for NAG, a 5-fold lower K_m for ATP and a 4-fold higher k_{cat} in the new assay. The reason for this difference remains elusive: *At*NAGK might be partially inhibited by hydroxylamine and/or by the products, which accumulate in the colorimetric assay (ADP and

Table 1. Kinetic parameters of NAGK enzymes from *S. elongatus* and *A. thaliana* and of a C-terminal truncated *Se*NAGK mutant in the absence or presence of *Se*P_{II} or *At*P_{II} signalling protein

					Arg	
	K_m (NAG) (mM)	K_m (ATP) (mM)	k_{cat} (s^{-1})	k_{cat}/K_m (s^{-1} M^{-1})	H	IC_{50} (mM)
*Se*NAGK	7.4±1.4	0.6±0.06	13.1±3.0	1.7×10^3	−4.1	0.02
(a)	(27.4)	(n.r.)	(11)	(0.4×10^3)	(−3.7)	(0.02)
*Se*NAGK+*Se*P_{II}	3.1±0.9	1.1±0.12	40.4±3.5	13×10^3	−1.5	0.19
(b)	(2.7)	(n.r.)	(43)	(16×10^3)	(−2.8)	(0.12)
*Se*NAGK+*At*P_{II}	3.2±1.0	0.9±0.07	41.4±3.8	13×10^3	−2.2	0.17
*At*NAGK	0.87±0.11	0.3±0.02	126.1±5.0	145×10^3	−6.5	1.0
(c)	(7.08)	(1.74)	(37.8)	(5.3×10^3)	(n.r.)	(0.73)
*At*NAGK/*At*P_{II}	0.85±0.14	0.4±0.04	187.5±9.2	220×10^3	−2.8	5.9
(d)	(7.55)	(2.03)	(46.2)	(6.1×10^3)	(n.r.)	(2.5)
*At*NAGK/*Se*P_{II}	0.65±0.12	0.6±0.10	135.3±6.6	208×10^3	−2.0	1.5
*At*NAGK+1 mM Arg	85±42	n.d.	115±13	1.3×10^3	n.a.	n.a.
*At*NAGK/*At*P_{II}/+1 mM Arg	17±6	n.d.	181±23	11×10^3	n.a.	n.a.
*At*NAGK/*Se*P_{II}/Arg+1 mM Arg	11±6	n.d.	82±43	8×10^3	n.a.	n.a.
*Se*NAGKΔC	3.6±0.6	3.0±0.4	18.9±0.8	6×10^3	−2.7	0.23
*Se*NAGKΔC/*Se*P_{II}	2.4±0.3	1.5±0.1	35.2±1.4	15×10^3	−1.3	1.4
*Se*NAGKΔC/*At*P_{II}	2.9±0.3	1.2±0.2	45.8±2.2	16×10^3	−1.9	1.8

For the determination of kinetic constants (apparent K_m and k_{cat}), the coupled assay was performed with varying NAG concentrations from 0.25 to 10 mM for *At*NAGK and from 1 to 50 mM NAG for *Se*NAG at a fixed concentration of 10 mM ATP or with varying ATP concentrations from 0.1 to 10 mM for both *At*NAGK and *Se*NAG at a fixed concentration of 50 mM NAG. Other assay conditions were as described in Materials and Methods. For the determination of arginine inhibition parameters, increasing concentrations of arginine were added at saturating NAG and ATP concentrations (50 and 10 mM, respectively). The values were analyzed by nonlinear regression analysis using sigmoidal dose–response (variable slope) fitting. Data sets from three independent experiments using two different enzyme preparations were employed for the calculation of kinetic parameters using the GraphPad Prism 4.03 software. k_{cat} and k_{cat}/K_m were calculated from the apparent V_{max} determined with NAG as a variable substrate at a fixed concentration of 10 mM ATP; the apparent k_{cat} with ATP as a variable substrate was almost equal. The k_{cat} values were calculated using the molecular mass of NAGK hexamers (see Materials and Methods).

n.a., not applicable; n.d., not determined; n.r., not reported.

H, Hill slope; IC_{50}, half-maximal inhibitory concentration; the 95% confidence intervals were within the limit of 25% difference from the given value.

(a) and (b) are the kinetic constants of free *Se*NAGK and of *Se*NAGK with *Se*P_{II}, respectively, determined by colorimetric assay with hexameric *Se*NAGK mass from Ref. 14.

(c) and (d) are the kinetic constants of free *At*NAGK and of *At*NAGK with *At*P_{II}, respectively, determined by colorimetric assay from Ref. 17. For comparison, the original k_{cat} values that were calculated with the monomeric NAGK mass were transformed by multiplication with 6 to yield the values for hexameric NAGK.

acetylglutamylhydroxamate). Apart from this general difference, the effect of AtP$_{II}$ on AtNAGK was similar to that reported previously[17] by only slightly stimulating catalytic activity through a moderate increase in k_{cat} whereas the SeP$_{II}$ protein was almost noneffective here.

Arginine inhibition of NAGK and its modulation by P$_{II}$ proteins

As a next step, arginine sensitivity of the two NAGK enzymes was determined in the coupled assay (Table 1 and Fig. 1). Generally, these results are in good agreement with the results reported by colorimetric assays.[14,17] When 50 mM NAG was used in the assays, much higher concentrations of arginine were needed for inhibiting AtNAGK (IC_{50}, 1 mM) than SeNAGK (IC_{50}, 20 μM). Adding cognate SeP$_{II}$ to SeNAGK relieved arginine inhibition by about 10-fold. Strikingly, the AtP$_{II}$ protein was as efficient in relieving SeNAGK from arginine inhibition as cognate SeP$_{II}$. More than just increasing the IC_{50} for arginine, the Hill slope became less negative, indicating that in complex with P$_{II}$, the cooperativity between the NAGK arginine inhibition sites diminishes. Addition of AtP$_{II}$ protein to AtNAGK raised the IC_{50} for arginine by approximately 6-fold. SeP$_{II}$ showed a weak effect on AtNAGK arginine inhibition, shifting the IC_{50} from 1 to 1.5 mM and flattening the Hill slope. To further substantiate the effect of SeP$_{II}$ on AtNAGK in the presence of arginine, the kinetic constants of AtNAGK for NAG were determined at a fixed concentration of 1 mM arginine, a concentration that is almost non-inhibitory for the AtNAGK–AtP$_{II}$ complex but inhibits the non-complexed AtNAGK by about 50%. As shown in Table 1 and Fig. 1b (inset), the stimulatory effect of SeP$_{II}$ on AtNAGK activity in the presence of arginine could be confirmed. Arginine impairs NAGK activity mainly through promoting a dramatic increase of K_m for NAG. The presence of both P$_{II}$ proteins attenuates the arginine-promoted K_m increase. This experiment now showed clearly that the SeP$_{II}$ protein is partially able to restore the catalytic efficiency of arginine-inhibited AtNAGK, confirming a productive interaction between SeP$_{II}$ and AtNAGK.

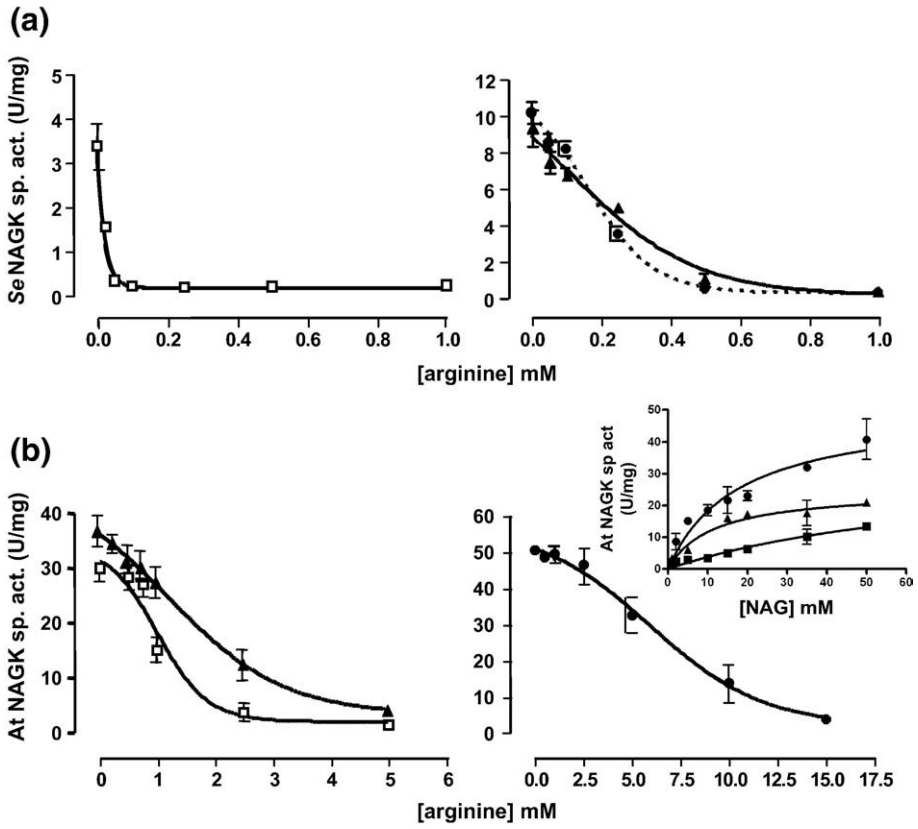

Fig. 1. Inhibition of NAGK activity by arginine in the absence and in the presence of P$_{II}$. Coupled NAGK assays were performed in the presence of 50 mM NAG and 10 mM ATP, together with increasing concentrations of arginine, as indicated. Assays were performed as indicated in Materials and Methods. (a) Left, SeNAGK in the absence of P$_{II}$ (open squares); right, SeNAGK in the presence of SeP$_{II}$ (filled triangles) or in the presence of AtP$_{II}$ (filled circles). (b) Left, AtNAGK in the absence of P$_{II}$ (open squares) or in the presence of SeP$_{II}$ (filled triangles); right, AtNAGK in the presence of AtP$_{II}$. The inset in (b) shows the catalytic activity of AtNAGK with or without P$_{II}$ proteins in the presence of 1 mM arginine, with NAG as a variable substrate at fixed 10 mM ATP. Squares, free AtNAGK; triangles, AtNAGK with SeP$_{II}$; circles, AtNAGK with AtP$_{II}$. The curves were fitted with GraphPad prism software. Standard deviations from triplicate experiments are indicated by error bars.

The role of 2-OG on NAGK activity

Conflicting results have been reported in previous analyses regarding the role of 2-OG for the regulation of NAGK by P_{II}. Enzyme assays carried out by the colorimetric assay failed to reveal any effect of 2-OG on P_{II} stimulation of NAGK activity.[13,17] Furthermore, gel-filtration analyses carried out in the presence of 0.1 mM 2-OG recovered *Se*P_{II} in the *Se*NAGK fraction[13] and pull-down experiments with *At*NAGK/P_{II}[17] recovered *At*P_{II} together with *At*NAGK even in the presence of 1 mM oxoglutarate and 5 mM ATP. By contrast to these data, SPR studies showed that 2-OG inhibits complex formation of *Se*NAGK with *Se*P_{II}.[14] To resolve this contradictory issue, a major goal of the use of the coupled assay was to find out whether there is any effect of 2-OG on the enzymatic activation of NAGK by P_{II}. The most apparent difference between free and P_{II}-complexed NAGK is observed in the presence of arginine. Therefore, an assay was devised, in which 2-OG was titrated to an NAGK-P_{II} mixture containing an amount of arginine that is almost non-inhibitory for the NAGK–P_{II} complex but already highly inhibitory for free NAGK. If 2-OG would impair P_{II}–NAGK interaction, NAGK would then become amenable to arginine inhibition. In the case of *Se*NAGK, such a discriminating concentration is 50 μM arginine (compare Fig. 1). Figure 2 shows the result of these analyses. Addition of 2-OG to the *Se*P_{II}–*Se*NAGK–arginine mixture indeed inhibited *Se*NAGK activity in a concentration-dependent manner. At high 2-OG levels, a basal NAGK activity was reached, which corresponded to the activity of free NAGK in the presence of 50 μM arginine (Fig. 2a). Control experiments were carried out to reveal whether 2-OG could directly affect the activity of NAGK. However, even 2 mM 2-OG did not affect the activity of free NAGK (data not shown, and compare Fig. 5, bars 1 and 2). Hyperbolic fitting of the inhibition curve showed a half-maximal inhibitory effect of 2-OG of about 35 μM. The same experiment was carried out with *At*P_{II} in combination with *Se*NAGK. As shown in Fig. 2a, almost the same curve was obtained as in the presence of *Se*P_{II}, further confirming the functional compatibility of *At*P_{II} with its cyanobacterial counterpart. Furthermore, these results confirm the inhibition of P_{II}–NAGK interaction by 2-OG, which was proposed on the basis of the SPR studies.[14]

With the same strategy as outlined above, the effect of 2-OG was investigated for the *At*NAGK–P_{II} complex. Here, a concentration of 5 mM arginine was chosen, since, at this concentration, free *At*NAGK was inhibited, whereas in the presence of *At*P_{II}, appreciable activity was maintained. As shown in Fig. 2b, an inhibition curve similar to that for SeNAGK was observed. At high 2-OG levels, the residual activity of 5 mM arginine-inhibited NAGK was obtained. About 36 μM 2-OG was required to obtain half-maximal inhibition. For studying the effect of 2-OG on *At*NAGK–*Se*P_{II} interaction, a discerning concentration of 1 mM arginine had to be chosen (compare Fig. 1b). Also, in this case, 2-OG lowered NAGK activity from the initial *Se*P_{II}-stimulated level down to the activity of free *At*NAGK in the presence of 1 mM arginine (Fig. 2b, inset). In this case, the half-maximal 2-OG effect was already achieved at a concentration of 8 μM, perhaps because the interaction between *Se*P_{II} and *At*NAGK is less tight.

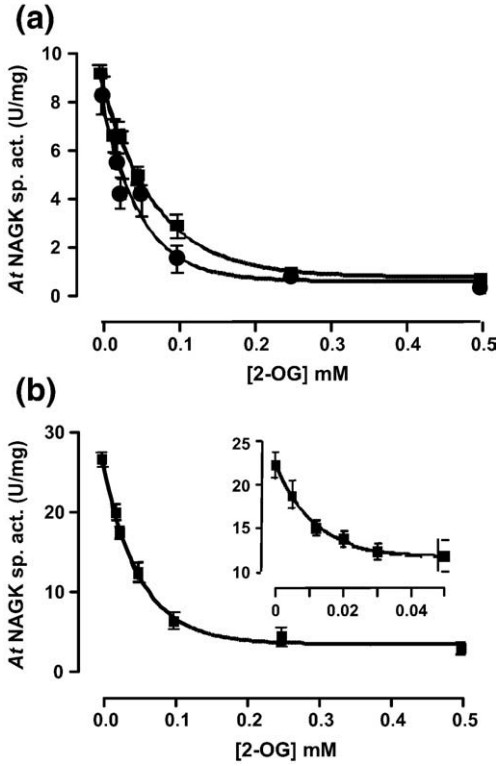

Fig. 2. 2-OG antagonizes the activation of NAGK by P_{II} in the presence of arginine. Standard coupled NAGK assays (see Materials and Methods) were performed in the presence of P_{II} proteins together with arginine as indicated below, and increasing 2-OG concentrations were added to the various reactions. The apparent reaction velocity of NAGK (in units per milligram) was plotted against the respective 2-OG concentration (the standard deviations from three individual measurements for each data point are indicated by error bars) and the data points were fitted to a hyperbolic curve. (a) *Se*NAGK with *Se*P_{II} (circles) or *At*P_{II} (squares) in the presence of 50 μM arginine. *Se*P_{II}, IC_{50} (oxoglutarate) of 35±1 μM; *At*P_{II}, IC_{50} (oxoglutarate) of 49±10 μM. (b) *At*NAGK with *At*P_{II} in the presence of 5 mM arginine. IC_{50} (oxoglutarate), 36±5 μM. Inset: *At*NAGK with *Se*P_{II} in the presence of 1 mM arginine. IC_{50} (oxoglutarate), 8±3 μM.

SPR studies of NAGK P_{II} binding

To further analyze the interactions between P_{II} and NAGK proteins across the domains of life, we measured complex formation by a direct physical method, SPR spectroscopy. First, the binding of P_{II} proteins to *Se*NAGK was analyzed. Confirming previous studies,[14] 2-OG in the presence of ATP

inhibited *Se*NAGK–*Se*P_{II} complex formation on the SPR sensor chip in a concentration-dependent manner (Fig. 3a). This inhibition correlates well with the 2-OG-promoted inhibition of NAGK activation by P_{II} as determined in the coupled assay (Fig. 2a). Using *At*P_{II} as an analyte, SPR analysis verified complex formation with *Se*NAGK (Fig. 3b). Furthermore, complex formation was impaired by 2-OG in a manner similar to that of the *Se*NAGK–*Se*P_{II} interaction. The major difference in the *At*P_{II} sensorgrams compared to those with *Se*P_{II} was the rapid dissociation of the complex following the injection phase, whereas the *Se*NAGK–*Se*P_{II} complex remained stable. This rapid dissociation indicates reduced stability of the *At*PII–*Se*NAGK complex, which may be the reason why prior yeast two-hybrid assays failed to reveal this interaction.[12]

Next, the interaction of *At*NAGK with *At*P_{II} was studied (Fig. 4). *At*NAGK–P_{II} interaction responded to nucleotides in a manner different from that of *Se*NAGK. Mg-ATP clearly favoured binding of *At*P_{II} to *At*NAGK (Fig. 4a) as revealed by the steeper association curve, compared to binding in the absence of nucleotides (dotted line). Whereas ADP is a potent inhibitor of *Se*NAGK–*Se*P_{II} interaction, *At*P_{II} binding to *At*NAGK was not affected by ADP, with or without ATP present. This property agrees with the reported *At*NAGK–P_{II} structure. Although the complex was crystallized in the presence of 10 mM ADP, ATP was found bound to P_{II}, which was interpreted as an indication that the complex of *At*P_{II} with *At*NAGK is highly selective for the ATP liganded form of P_{II}.[16,21] Analysis of the effect of 2-OG on *At*NAGK–*At*P_{II} interaction showed that up to 1 mM 2-OG complex formation was not affected (Fig. 4b). This result agrees with the previously reported stability of the complex towards 2-OG.[17] However, at 2-OG concentrations above 1 mM, gradual inhibition of complex formation could be observed. This result differs quantitatively from the effect of 2-OG in the coupled enzyme assay (Fig. 2b), where in the presence of 0.25 mM 2-OG, P_{II} was no longer able to protect NAGK from arginine inhibition. Binding of the cyanobacterial P_{II} protein to the plant NAGK could also be verified by SPR analysis (Fig. 4c and d), with ATP being absolutely required for complex formation (Fig. 4c). By contrast to *At*P_{II}, ADP efficiently impaired complex formation, indicating that this difference is due to P_{II} properties. The effect of 2-OG on *At*NAGK–*Se*PII interaction measured by SPR analysis correlated well with the 2-

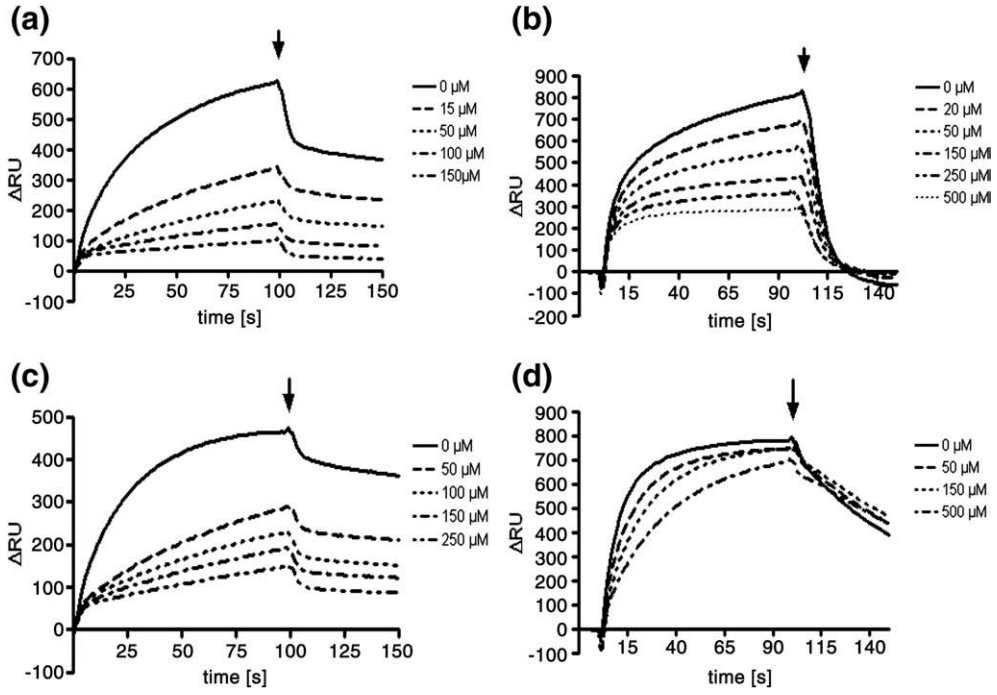

Fig. 3. SPR analysis of the 2-OG effect on complex formation between *Se*NAGK or *Se*NAGKΔC and *Se*P_{II} or *At*P_{II}. *Se*NAGK or *Se*NAGKΔC was bound to FC2 of a Ni^{2+}-loaded NTA sensor chip (see Materials and Methods) to give an increase in RU of approximately 3500 RU (corresponding to 3.5 ng protein bound per square millimeter of sensor surface). FC1 was used as background control. P_{II} proteins were injected as analyte with various concentrations of effector molecules, as indicated below, in a volume of 25 µl at a flow rate of 15 µl/min, and the response difference (ΔRU) between FC1 and FC2 during the injection phase is shown; the end of the injection phase is indicated by an arrow. (a) Binding of 200 nM *Se*P_{II} to *Se*NAGK in the presence of 1 mM ATP and 2-OG at concentrations of 0, 15, 50, 100 and 150 µM, as indicated. (b) Binding of *At*P_{II} (200 nM) to *Se*NAGK in the presence of 1 mM ATP and 2-OG at concentrations of 0, 20, 50, 150, 250 and 500 µM, as indicated. (c) Binding of *Se*P_{II} (200 nM) to *Se*NAGKΔC in the presence of 1 mM ATP and 2-OG at concentrations of 0, 50, 100, 150 and 250 µM, as indicated. (d) Binding of *At*P_{II} (200 nM) to *Se*NAGKΔC in the presence of 1 mM ATP and 2-OG at concentrations of 0, 50, 150, and 500 µM, as indicated.

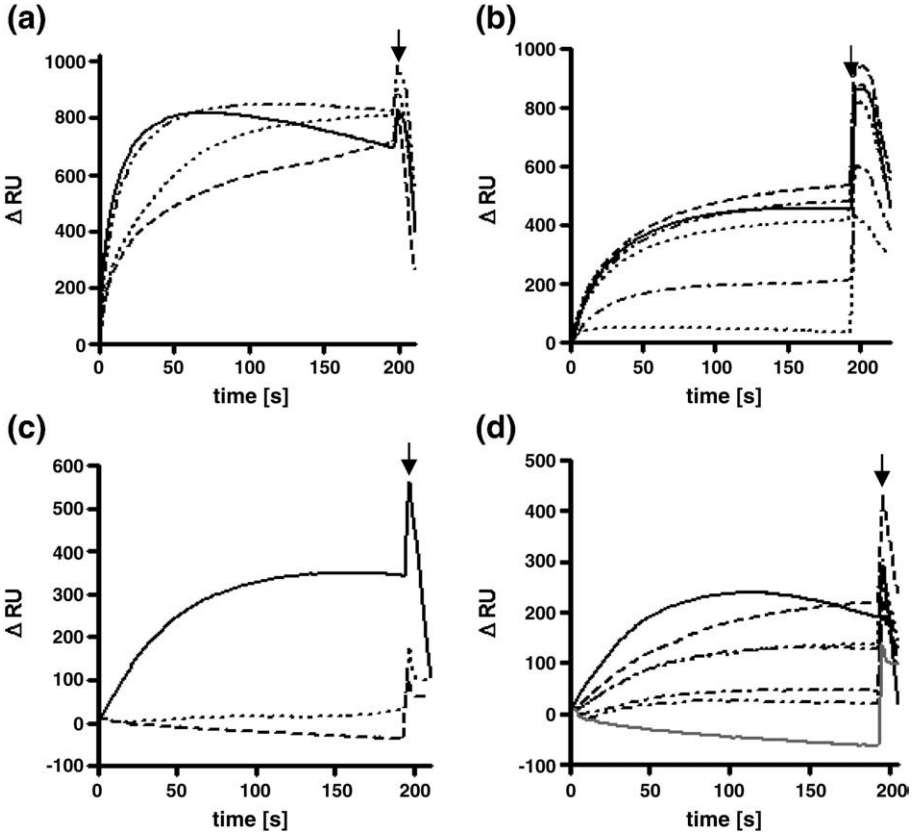

Fig. 4. SPR analysis of the influence of effector molecules on *At*NAGK–*At*P_{II} or *Se*P_{II} complex formation. Experimental conditions were as described in Fig. 3. (a) Binding of 150 nM *At*P_{II} to Ni-NTA-immobilized *At*NAGK in the absence of nucleotides (····), in the presence of 1 mM ATP (—) or 1 mM ADP (---), or 1 mM ATP together with 1 mM ADP (··–··). (b) Binding of 120 nM *At*P_{II} to Ni-NTA-immobilized *At*NAGK in the presence of 1 mM ATP and different 2-OG concentrations. 2-OG was used at concentrations of 100 μM (—), 250 μM (---), 500 μM (··–··), 1000 μM (····), 2500 μM (–·–) and 5000 μM (····). (c) Binding of 950 nM *Se*P_{II} to Ni-NTA-immobilized *At*NAGK in the absence of ATP (····) or in the presence of 1 mM ATP (—) or 1 mM ATP together with 1 mM ADP (---). (d) Influence of 2-OG on the binding of 950 nM *Se*P_{II} to *At*NAGK in the presence of 1 mM ATP. 2-OG was used at concentrations of 0 μM (—), 5 μM (---), 7,5 μM (····), 10 μM (–·–), 15 μM (–·–), 20 μM (··–··) and 500 μM (solid gray line).

OG response in the coupled enzyme assay (compare Figs. 4d and 2b).

Role of the P_{II} B-loop for binding *At*NAGK

In the *Se*NAGK–P_{II} complex, the B-loop plays an important role in NAGK interaction. B-loop residue E85 forms an important salt bridge with an arginine residue (R233) of NAGK. Consequently, mutation of E85 to alanine rendered the *Se*P_{II} E85A mutant inactive in NAGK binding.[20] Originally, the B-loop was not described as being involved in *At*NAGK interaction;[21] however, the existence of the corresponding salt bridge (E97-K240) in the *At*NAGK–*At*PII complex was seen in the structure of one subunit of the *A. thaliana* complex (see Protein Data Bank file 2rd5).[16] We tested, therefore, whether the *Se*P_{II}E85A mutant protein was able to bind to *At*NAGK. By SPR analysis, no binding of the *Se*P_{II} E85A mutant to the *At*NAGK surface could be detected even at elevated analyte concentration (Fig. 5a). To corroborate this finding, the interaction was also tested by enzymatic analysis. Stimulation of *At*NAGK by *Se*P_{II} in the presence of arginine is sufficiently large that it may be used as a test of interaction (see above). As shown in Fig. 5b, the E85A mutant, in contrast to wild-type *Se*PII, was not able to stimulate the arginine-inhibited *At*NAGK activity, confirming that the B-loop residue E85 is required for binding of *Se*P_{II} to *At*NAGK. This suggests that the corresponding E97-K240 salt bridge in the *A. thaliana* complex is indeed relevant for complex formation.

The C-terminus of *Se*NAGK enhances arginine sensitivity

One of the prominent differences between *Se*NAGK and *At*NAGK is the 50-fold higher sensitivity of the cyanobacterial enzyme towards arginine (see above). Primary-structure comparison pointed towards the C-terminal extension of 11 amino acids of the *Se*NAGK protein, which is not present in *At*NAGK. Since the C-terminus is close to the arginine binding site of *Se*NAGK, we speculated whether it could be involved in the different sensitivities towards arginine. Therefore, the 11 C-

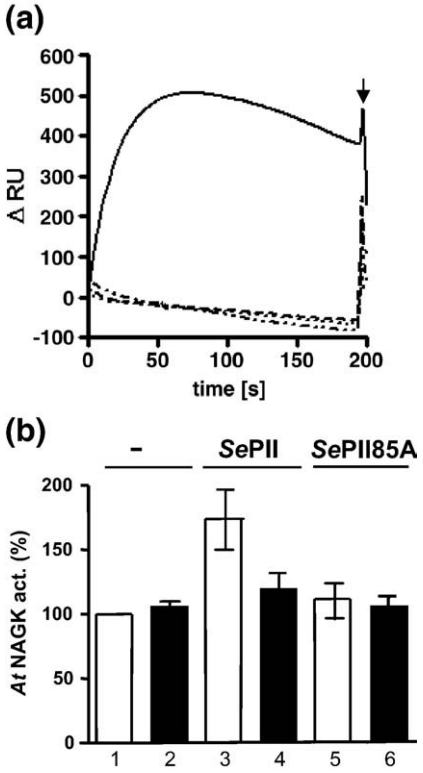

Fig. 5. *Se*P_{II}E85A mutant does not bind to *At*NAGK. (a) SPR analysis using Ni-NTA-immobilized *At*NAGK. *Se*P_{II}E85A was injected at concentrations of 950 and 2300 nM in the presence of 1 mM ATP as well as at a concentration of 2300 nM in the absence of ATP (····). No binding is detected. As a control, 950 nM wild-type *Se*P_{II} in the presence of 1 mM ATP showed efficient binding to *At*NAGK (—). (b) Activation of *At*NAGK by P_{II} proteins in the presence of 1 mM arginine, with or without 0.5 mM 2-OG. The activity of free *At*NAGK in the presence of 1 mM arginine was taken as 100%. The white bars show the activity in the absence of 2-OG, while the black bars show the activity in the presence of 2-OG. The addition of P_{II} proteins is indicated above the bars. Error bars indicate the standard deviation of triplicate experiments.

terminal amino acids were removed genetically and the resulting truncated *Se*NAGK (*Se*NAGKΔC) protein was characterized by the coupled assay. The enzymatic parameters are given in Table 1. In the absence of arginine, the free enzyme has a higher catalytic efficiency than the full-length protein, mostly due to lower K_m for NAG, whereas in the presence of P_{II}, the catalytic properties are almost the same as those of wild-type NAGK. Even more strikingly, the mutant has gained a considerably higher resistance towards arginine inhibition compared to the full-length enzyme (see Fig. 6 and Table 1): The IC_{50} of the free enzyme increased by more than 10-fold, and interestingly, the Hill slope was flattened, indicating decreased cooperativety between the arginine inhibition sites. The presence of *Se*P_{II} further alleviated arginine inhibition, such that even at 10 mM arginine, a residual activity of more than 25% of the uninhibited activity was retained and 1.4 mM arginine was required for half-maximal inhibition. *At*PII was at least as efficient as *Se*PII in activating the truncated *Se*NAGK in these assays. To further examine the interaction of the *Se*NAGKΔC mutant with the P_{II} proteins, we performed SPR analysis (shown in Fig. 3c and d). Compared to the binding of *Se*P_{II} to wild-type *Se*NAGK, complex association was accelerated as visualized by an earlier saturation of the binding curve. Furthermore, higher concentrations of 2-OG (in the presence of ATP) were necessary to inhibit complex formation, indicating a higher affinity of *Se*NAGKΔC towards *Se*P_{II} in the presence of the inhibitory molecule. Binding of *At*PII to *Se*NAGKΔC was even more strikingly improved: Whereas *At*PII rapidly dissociated from wild-type *Se*NAGK, dissociation from the *Se*NAGKΔC protein was diminished and 2-OG was much less effective in impairing complex formation (compare Fig. 3b and d). This indicates that *At*P_{II} accommodates much better to the C-terminal truncated mutant of *Se*NAGK than to the full-length protein. Thus, the truncated *Se*NAGKΔC enzyme adopts properties of the *At*NAGK enzyme, which also lacks the C-terminal peptide. Together, the C-terminus of *Se*NAGK appears to be important both for enhancing arginine sensitivity and for acting as a negative determinant in PII binding, in particular in the presence of 2-OG.

Conclusions

This study has demonstrated, for the first time, that bacterial and eukaryotic P_{II} signalling proteins could at least in part be functionally exchangeable *in vitro*. To our knowledge, it is the first example of a signal transduction system, which is functionally compatible between eukaryotes and bacteria. The

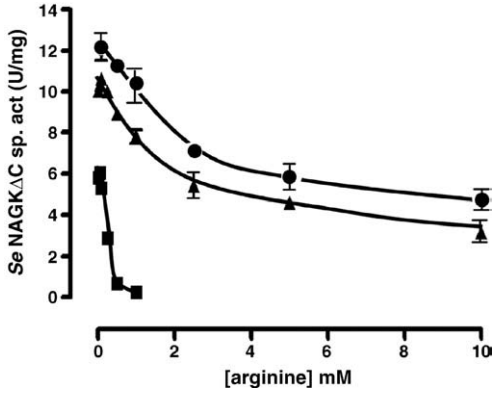

Fig. 6. Arginine inhibition of *Se*NAGKΔC. Coupled NAGK assays were performed with purified *Se*NAGKΔC protein in the presence of 50 mM NAG and 10 mM ATP, together with increasing concentrations of arginine, as indicated. Squares, free *Se*NAGKΔC; triangles, in the presence of *Se*P_{II}; circles, in the presence of *At*P_{II}. Assays were performed as indicated in Materials and Methods with an NAGK concentration of 3 μg/ml. Standard deviations from triplicate experiments are indicated by error bars.

AtP_{II} protein controls the cyanobacterial *Se*NAGK as efficient as its cognate P_{II} protein. *Vice versa*, *Se*P_{II} can at least partially complement *At*P_{II}. Therefore, *At*P_{II} must contain all requirements for efficient *Se*NAGK regulation, including the B-loop determinants. Conversely, the interaction of *At*NAGK with P_{II} requires properties that are not fully represented in *Se*P_{II}, since it can only partially replace *At*P_{II}. Indeed, the plant P_{II} protein has additional N- and C-terminal extensions, which are not present cyanobacterial P_{II} proteins.[24]

The *At*P_{II}–NAGK complex (as measured by SPR spectroscopy) is resistant towards concentrations of 2-OG, which are largely sufficient to antagonize the P_{II}-mediated NAGK activation in the presence of arginine. The presence of NAG and arginine in the enzymatic assay might facilitate complex dissociation at lower 2-OG concentrations. Another explanation could be that binding of low amounts of 2-OG to NAGK-bound *At*P_{II} might be sufficient to cause a conformational change of P_{II}, which impairs the relief from arginine inhibition, but which is not sufficient to promote full complex dissociation. For example, full contact of all three P_{II} subunits to NAGK on one side of the NAGK toroid may be required to achieve relief from arginine inhibition, whereas binding of only one subunit may still be detected as binding by SPR analysis. The cyanobacterial system is more simply in this regard, since loss of complex formation by 2-OG directly correlates with the loss of NAGK activation. Taken together, this study has revealed an important common property of P_{II}-dependent NAGK regulation in a cyanobacterium and a higher plant: In both systems, 2-OG renders the NAGK–P_{II} complex accessible to arginine inhibition, although the mechanism as to how this is achieved may differ in detail.

An apparent difference between *At*P_{II} and *Se*P_{II} is the response towards ADP in complex formation. Whereas ADP strongly inhibits complex formation of *Se*P_{II} with NAGK, binding of *At*P_{II} to *At*NAGK is not efficiently antagonized by this molecule. *At*P_{II} in complex with NAGK has apparently such a high affinity for ATP that ATP remains bound even at elevated ADP concentrations, as also suggested by the ATP molecule that was found in the complex crystallized in the presence of 10 mM ADP.[16,21] Plants and cyanobacteria may thus have evolved different strategies to sense and integrate the energy status for regulating P_{II}–NAGK interaction. In plants, NAGK–P_{II} complex formation would be favoured by ATP (when the energy status is high), whereas in cyanobacteria, a low-energy status would be measured as a high level of the antagonistic ADP molecule.[14]

Finally, we could resolve a structural basis for the different arginine sensitivities of *Se*NAGK and *At*NAGK. The non-conserved C-terminal peptide of *Se*NAGK appears to function as a negative determinant for NAGK activity and P_{II} interaction. It lowers the catalytic efficiency of non-complexed NAGK and enhances the inhibitory effect of arginine. Since this C-terminal peptide was not resolved in the *Se*NAGK structure,[20] it appears to be a flexible structure, and the way how it precisely affects NAGK activity and its interaction with P_{II} remains to be elucidated.

Despite some important differences in detail, this study reveals a striking functional conservation of NAGK–P_{II} interaction between different domains of life, allowing crosswise interaction between the partners. Considering the more than 1.2 billion years of separate evolution of cyanobacteria and plants,[25] this conservation can only be explained by a high selective pressure to maintain the P_{II}–NAGK interaction. Controlling arginine/ornithine biosynthesis in oxygenic phototrophs by the energy (sensed by ATP/ADP) and carbon/nitrogen (sensed through 2-OG) status must, therefore, be of deep fundamental importance and must be more important than actually presumed.[26]

Materials and Methods

Overexpression and purification of *Se*P_{II} and *Se*NAGK and *At*P_{II} and *At*NAGK

The recombinant proteins P_{II} and NAGK were overexpressed in *Escherichia coli* strain BL21(DE3)[27] from suitable vectors. Overexpression and purification of *Se*P_{II} with a C-terminal-fused Strep-tag II peptide (IBA, Göttingen) were performed as described previously.[13]

For overexpression of *At*P_{II}, an artificial gene with an optimized codon usage for *E. coli* expression was synthesized from Sloning Biotechnology GmbH (Puchheim, Germany). The DNA sequence was derived from the amino acid sequence of the mature, chloroplast-localized *At*P_{II} (starting with Gln63 of the non-processed *At*P_{II} sequence, accession number Q9ZST4) with its C-terminus fused to the Strep-tag II peptide. The synthetic gene was cloned into the NdeI and EcoRI sites of the pT7-7 expression vector[27] yielding pT7-*At*P_{II}. Overexpression of the recombinant *At*P_{II} protein was performed in *E. coli* BL21(DE3) containing pT7-*At*P_{II}, and the protein was affinity purified on Strep-Tactin columns as described previously for *Se*P_{II}.[13] The *Se*P_{II}E85A mutant protein was purified as described previously.[20]

His_6-tagged recombinant *Se*NAGK was overexpressed and purified as described previously.[14] For overexpression of *At*NAGK, an artificial gene with an optimized codon usage for *E. coli* expression was synthesized from Sloning Biotechnology GmbH. The DNA sequence was derived from the amino acid sequence of the mature, chloroplast-localized *At*NAGK (starting with Thr51 of the non-processed AtNAGK sequence, accession number Q9SCL7). The gene was cloned into the NdeI-XhoI sites of the His-tag fusion vector pET-15b (Novagene) to generate plasmid pET-*At*NAGK. Overexpression and purification of His_6-tagged *At*NAGK were performed according to the procedure described for His-*Se*NAGK.[14]

The C-terminal deletion mutant of *Se*NAGK was constructed by PCR amplification using the *Se*NAGK encoding pET-NAGK plasmid[14] as a template. The following primers were used: HIS-NAGK: forward (overlapping the 5′ NdeI restriction site), 5′-T*CATATG*TCTAGCGAGTTTATCGAAGCAG-3′ in combination with NAGK-C; reverse, 5′-GC*GGATCC***TTA**GCCAACAATCATCGTGCCAAT-3′, which contains a BamHI cloning site (in italics) and the

truncated C-terminus of *Se*NAGK with a TAA stop codon replacing the codon for the seryl residue located 11 amino acids apart from the native C-terminus (in boldface letters). The PCR product was cloned into NdeI/BamHI-restricted pET-15b, generating pET-NAGKΔC. Overexpression and purification of the C-terminal truncated *Se*NAGK were performed as described above for full-length NAGK.

Assay of NAGK activity by coupling NAG phosphorylation to NADH oxidation

Activity of purified His_6-NAGK was measured by coupling the ADP-generating phosphorylation of NAG from ATP via pyruvate kinase and lactate dehydrogenase to the oxidation of NADH. The reaction conditions were adapted from Ref. 23. The reaction buffer consisted of 50 mM imidazole, pH 7.5, 50 mM KCl, 20 mM $MgCl_2$, 0.4 mM NADH, 1 mM phosphoenolpyruvate, 10 mM ATP, 0.5 mM DTT, 11 U lactate dehydrogenase, 15 U pyruvate kinase and 50 mM NAG unless indicated otherwise. The reaction was started by the addition of 3 μg *Se*NAGK (16 μM NAGK hexamers) or 1.5 μg *At*NAGK (8 μM hexamers). Reactions in a volume of 1 ml were directly recorded over a period of 10 min in a SPECORD 200 photometer (Analytik Jena) at a wavelength of 340 nm. Phosphorylation of one molecule of NAG leads to the oxidation of one molecule of NADH, which leads to a linear decrease of absorbance at 340 nm over time.[23] The reaction velocity was calculated from the slope of the resulting time curve as change in absorbance at 340 nm per time. One unit of NAGK catalyses the conversion of 1 mmol of NAG min^{-1}, calculated with a molar absorption coefficient of NADH of ε_{340}=6178 L mol^{-1} cm^{-1}. When the reactions were carried out in the presence of P_{II}, P_{II} protein was added to the reaction mixture before the addition of NAGK (2.4 or 1.2 μg P_{II} to *Se*NAGK or *At*NAGK, respectively, corresponding to 64 or 32 μM). The enzymatic parameters K_m, k_{cat}, Hill slope and IC_{50} were calculated from the velocity slopes using the GaphPad Prism 4.03 software program (GraphPad Software, San Diego). The k_{cat} values were calculated from V_{max} values using the molecular mass of NAGK hexamers, that is, 207 kDa for *S. elongatus* His-tagged NAGK and 203 kDa for *A. thaliana* His-tagged NAGK.

SPR experiments

SPR experiments were performed using a BIAcore X biosensor system (Biacore AB, Uppsala, Sweden) as described previously.[14] Purified recombinant His-tagged NAGK proteins were bound to flow cell (FC) 2 of a Ni^{2+}-loaded NTA sensor chip, which was prepared according to BIAcore instructions, to give a binding signal of approximately 3500 resonance units (RU) (corresponding to a surface concentration change of 3.5 ng/mm^2) (for details of loading, see Ref. 14). Binding assays with His_6-*At*NAGK as ligand were carried out at a temperature of 18.5 °C. The flow buffer was composed of 20 mM Hepes, pH 7.5, 150 mM NaCl, 0.005% Nonidet P-40 and 2 mM $MgCl_2$. P_{II} protein solutions in flow buffer were used as analyte at the indicated protein concentrations. To test the effect of metabolites on P_{II} binding to NAGK, we pre-incubated P_{II} solutions for 5 min at 20 °C with the indicated effector molecules prior to injecting the solution to the sensor chip. Samples (25 μl) were injected to FC1 and FC2 of the sensor chip at a flow rate of 15 μl/min, and the response difference (FC1 − FC2) was recorded.

Acknowledgements

We thank Prof. A. Ninfa for the advice to assay NAGK activity by the coupled enzyme assay. K. Siedler is gratefully acknowledged for providing purified proteins. We further thank an anonymous reviewer for helpful suggestions. This work was supported by a grant from the Deutsche Forschungsgemeinschaft (Fo 195/4) and the Fachagentur für Nachwachsende Rohstoffe.

References

1. Ninfa, A. J. & Jiang, P. (2005). P_{II} signal transduction proteins: sensors of alpha-ketoglutarate that regulate nitrogen metabolism. *Curr. Opin. Microbiol.* **8**, 168–173.
2. Leigh, J. A. & Dodsworth, J. A. (2007). Nitrogen regulation in bacteria and archaea. *Annu. Rev. Microbiol.* **61**, 349–377.
3. Forchhammer, K. (2008). P_{II} signal transducers: novel functional and structural insights. *Trends Microbiol.* **16**, 65–72.
4. Jiang, P. & Ninfa, A. J. (2007). *Escherichia coli* P_{II} signal transduction protein controlling nitrogen assimilation acts as a sensor of adenylate energy charge in vitro. *Biochemistry*, **46**, 12979–12996.
5. Yildiz, Ö., Kalthoff, C., Raunser, S. & Kuhlbrandt, W. (2007). Structure of GlnK1 with bound effectors indicates regulatory mechanism for ammonia uptake. *EMBO J.* **26**, 589–599.
6. Forchhammer, K. & Hedler, A. (1997). Phosphoprotein P_{II} from cyanobacteria—analysis of functional conservation with the P_{II} signal-transduction protein from *Escherichia coli*. *Eur. J. Biochem.* **244**, 869–875.
7. Forchhammer, K. (2004). Global carbon/nitrogen control by P_{II} signal transduction in cyanobacteria: from signals to targets. *FEMS Microbiol. Rev.* **28**, 319–333.
8. Kloft, N. & Forchhammer, K. (2005). Signal transduction protein P_{II} phosphatase PphA is required for light-dependent control of nitrate utilization in *Synechocystis* sp. strain PCC 6803. *J. Bacteriol.* **187**, 6683–6690.
9. Takatani, N., Kobayashi, M., Maeda, S.-I. & Omata, T. (2006). Regulation of nitrate reductase by non-modifiable derivatives of P_{II} in the cells of *Synechococcus elongatus* strain PCC 7942. *Plant Cell Physiol.* **47**, 1182–1186.
10. Espinosa, J., Forchhammer, K., Burillo, S. & Contreras, A. (2006). Interaction network in cyanobacterial nitrogen regulation: PipX, a protein that interacts in a 2-OG dependent manner with PII and NtcA. *Mol. Microbiol.* **61**, 457–466.
11. Espinosa, J., Forchhammer, K. & Contreras, A. (2007). Role of the *Synechococcus* PCC 7942 nitrogen regulator protein PipX on NtcA controlled processes. *Microbiology*, **153**, 711–718.
12. Burillo, S., Luque, I., Fuentes, I. & Contreras, A. (2004). Interactions between the nitrogen signal transduction protein P_{II} and *N*-acetyl glutamate kinase in organisms that perform oxygenic photosynthesis. *J. Bacteriol.* **186**, 3346–3354.
13. Heinrich, A., Maheswaran, M., Ruppert, U. & Forchhammer, K. (2004). The *Synechococcus elongatus* P_{II} signal transduction protein controls arginine synthesis by complex formation with *N*-acetyl-L-glutamate kinase. *Mol. Microbiol.* **5**, 1303–1314.

14. Maheswaran, M., Urbanke, C. & Forchhammer, K. (2004). Complex formation and catalytic activation by the P_{II} signaling protein of *N*-acetyl-L-glutamate kinase from *Synechococcus elongatus* strain PCC 7942. *J. Biol. Chem.* **279**, 55202–55210.
15. Maheswaran, M., Ziegler, K., Lockau, W., Hagemann, M. & Forchhammer, K. (2006). P_{II}-regulated arginine synthesis controls the accumulation of cyanophycin in *Synechocystis* sp. strain PCC 6803. *J. Bacteriol.* **188**, 2730–2734.
16. Llacer, J. L., Fita, I. & Rubio, V. (2008). Arginine and nitrogen storage. *Curr. Opin. Struct. Biol.* **18**, 673–681.
17. Chen, Y. N., Ferrar, T., Lohmeir-Vogel, E., Morrice, N., Muzino, Y., Berenger, B. *et al.* (2006). The P_{II} signal transduction protein of *Arabidopsis thaliana* forms a metabolite regulated complex with plastid *N*-acetyl glutamate kinase. *J. Biol. Chem.* **281**, 5726–5733.
18. Sugiyama, K., Hayakawa, T., Kudo, T., Ito, T. & Yamaya, T. (2004). Interaction of *N*-acetylglutamate kinase with a P_{II}-like protein in rice. *Plant Cell Physiol.* **45**, 1768–1778.
19. Caldovic, L. & Tuchman, M. (2003). *N*-Acetylglutamate and its changing role through evolution. *Biochem. J.* **372**, 279–290.
20. Llacer, J. L., Contreras, A., Forchhammer, K., Marco-Marin, C., Gil-Ortiz, F., Maldonado, R. *et al.* (2007). The crystal structure of the complex of P_{II} and acetylglutamate kinase reveals how P_{II} controls the storage of nitrogen as arginine. *Proc. Natl. Acad. Sci. USA*, **104**, 17644–17649.
21. Mizuno, Y., Moorhead, G. B. G. & Ng, K. K. S. (2007). Structural basis for the regulation of *N*-acetylglutamate kinase by P_{II} in *Arabidopsis thaliana*. *J. Biol. Chem.* **282**, 35733–35740.
22. Palinska, K. A., Laloui, W., Bedu, S., Loiseaux-de Goer, S., Castets, A. M., Rippka, R. & Tandeau de Marsac, N. (2002). The signal transducer P_{II} and bicarbonate acquisition in *Prochlorococcus marinus* PCC 9511, a marine cyanobacterium naturally deficient in nitrate and nitrite assimilation. *Microbiology*, **148**, 2405–2412.
23. Jiang, P. & Ninfa, A. J. (1999). Regulation of autophosphorylation of *Escherichia coli* nitrogen regulator II by the P_{II} signal transduction protein. *J. Bacteriol.* **181**, 1906–1911.
24. Mizuno, Y., Berenger, B., Moorhead, B. G. B. & Ng, K. K. S. (2007). Crystal structure of *Arabidopsis* P_{II} reveals novel structural elements unique to plants. *Biochemistry*, **46**, 1477–1483.
25. Sheveleva, E. V. & Hallick, R. B. (2004). Recent horizontal intron transfer to a chloroplast genome. *Nucleic Acids Res.* **32**, 803–810.
26. Ferrario-Mery, S., Bouvet, M., Leleu, O., Savino, G., Hodges, M. & Meyer, C. (2005). Physiological characterization of *Arabidopsis* mutants affected in the expression of the putative regulatory protein P_{II}. *Planta*, **223**, 28–39.
27. Studier, F. W., Rosenberg, A. H., Dunn, J. J. & Dubendorff, J. W. (1990). Use of T7 RNA polymerase to direct expression of cloned genes. *Methods Enzymol.* **185**, 60–89.

C. Publication 2

A Novel Signal Transduction Protein P_{II} Variant from *Synechococcus elongatus* PCC 7942 Indicates a Two-Step Process for NAGK–P_{II} Complex Formation

J. Mol. Biol. (2010) 399, 410–421

Contribution to publication:

I performed, analysed and interpreted the following experiments:

- Overexpression and purification of the P_{II} and NAGK proteins
- SPR analysis
- Enzyme assays
- ITC analysis

I wrote the manuscript

doi:10.1016/j.jmb.2010.04.018 J. Mol. Biol. (2010) 399, 410–421

JMB

Available online at www.sciencedirect.com

ScienceDirect

ELSEVIER

A Novel Signal Transduction Protein P_{II} Variant from *Synechococcus elongatus* PCC 7942 Indicates a Two-Step Process for NAGK–P_{II} Complex Formation

Oleksandra Fokina[1], Vasuki-Ranjani Chellamuthu[2], Kornelius Zeth[2] and Karl Forchhammer[1]*

[1]*Interfakultäres Institut für Mikrobiologie und Infektionsmedizin der Eberhard-Karls-Universität Tübingen, Auf der Morgenstelle 28, 72076 Tübingen, Germany*

[2]*Max Planck Institute for Developmental Biology, Department of Protein Evolution, Spemannstrasse 35, 72076 Tübingen, Germany*

Received 15 December 2009; received in revised form 17 March 2010; accepted 13 April 2010
Available online
24 April 2010

P_{II} signal transduction proteins are highly conserved in bacteria, archaea and plants and have key functions in coordination of central metabolism by integrating signals from the carbon, nitrogen and energy status of the cell. In the cyanobacterium *Synechococcus elongatus* PCC 7942, P_{II} binds ATP and 2-oxoglutarate (2-OG) in a synergistic manner, with the ATP binding sites also accepting ADP. Depending on its effector molecule binding status, P_{II} (from this cyanobacterium and other oxygenic phototrophs) complexes and regulates the arginine-controlled enzyme of the cyclic ornithine pathway, *N*-acetyl-L-glutamate kinase (NAGK), to control arginine biosynthesis. To gain deeper insights into the process of P_{II} binding to NAGK, we searched for P_{II} variants with altered binding characteristics and found P_{II} variants I86N and I86T to be able to bind to an NAGK variant (R233A) that was previously shown to be unable to bind wild-type P_{II} protein. Analysis of interactions between these P_{II} variants and wild-type NAGK as well as with the NAGK R233A variant suggested that the P_{II} I86N variant was a superactive NAGK binder. To reveal the structural basis of this property, we solved the crystal structure of the P_{II} I86N variant at atomic resolution. The large T-loop, which prevails in most receptor interactions of P_{II} proteins, is present in a tightly bended conformation that mimics the T-loop of *S. elongatus* P_{II} after having latched onto NAGK. Moreover, both P_{II} I86 variants display a specific defect in 2-OG binding, implying a role of residue I86 in 2-OG binding. We propose a two-step model for the mechanism of P_{II}–NAGK complex formation: in an initiating step, a contact between R233 of NAGK and E85 of P_{II} initiates the bending of the extended T-loop of P_{II}, followed by a second step, where a bended T-loop deeply inserts into the NAGK clefts to form the tight complex.

Keywords: 2-oxoglutarate; nitrogen regulation; *Synechococcus*; metabolic signalling; arginine

Edited by I. B. Holland

Introduction

P_{II} proteins belong to a large protein family present in bacteria, plants and archaea, where they play pivotal roles as sensors and signal transducers in processes connected to nitrogen assimilation.[1–4] Generally, P_{II} proteins are signal integrators that bind the key metabolites ATP, ADP and 2-oxoglutarate (2-OG) and in many cases are subjected to reversible covalent modification in response to the carbon/nitrogen status of the cell.[3,5] Depending on the signal input state, P_{II} proteins bind and regulate the activity of key metabolic and regulatory enzymes, transcription factors or transport proteins.[1–3]

P_{II} proteins are homotrimers of 12- to 13-kDa subunits with a highly conserved three-dimensional structure. From the body of the trimer, which is almost hemispheric, three large T-loops, one per subunit, protrude into the solvent. The T-loops are

**Corresponding author.* E-mail address: karl.forchhammer@uni-tuebingen.de.

Abbreviations used: 2-OG, 2-oxoglutarate; NAGK, *N*-acetyl-L-glutamate kinase; SPR, surface plasmon resonance; ITC, isothermal titration calorimetry; FC, flow cell; RU, resonance units; NAG, *N*-acetyl-L-glutamate.

able to adopt multiple conformations and are the key to the versatile protein–protein interactions of P_{II} proteins.[3] Further to the T-loop, each subunit has two smaller loops: the B- and C-loop from opposing subunits face each other in the intersubunit clefts, where they are engaged in adenyl nucleotide binding.[6–8] The trimeric P_{II} protein thus contains three ATP/ADP binding sites, each one in the cleft between neighbouring subunits. In the presence of ATP, up to three 2-OG molecules can bind per trimer; however, the binding site for 2-OG is not clear hitherto.[1,6,9] For a P_{II} paralogue from *Methanococcus jannaschii*, GlnK1, one 2-OG molecule was shown to bind from outside to the distal side of the T-loop in the presence of Mg-ATP.[10] This finding is, however, in conflict with earlier data, which showed by deletion mutagenesis that this part of the T-loop is dispensable for 2-OG binding, at least for the P_{II} protein of *Escherichia coli*.[11] Recent studies suggest that, in *E. coli*, 2-OG controls the conformation of the T-loop after P_{II} binding to its receptor.[12] The binding of ATP and 2-OG are synergistic toward each other, meaning that the binding of ATP favours the binding of 2-OG and *vice versa*. However, the sites for ATP exhibit negative cooperativity toward the other ATP binding sites and the same holds true for the 2-OG binding sites. This feature of anti-cooperatively communicating metabolite binding sites allows P_{II} to sense these metabolites in a wide range of concentrations.[5,13]

In the cyanobacterium *Synechococcus elongatus* PCC 7942, P_{II} plays essential roles in control of nitrogen utilization.[8] Under nitrogen-poor conditions, P_{II} is phosphorylated at the T-loop residue S49 (P_{II}-P),[8] whereas under nitrogen-sufficient conditions, P_{II}-P is dephosphorylated.[14] Phosphorylation and dephosphorylation of P_{II} had been shown *in vitro* to depend on the 2-OG levels, with high 2-OG stimulating P_{II} phosphorylation and low 2-OG levels favouring the dephosphorylation of P_{II}-P. The known regulatory targets of P_{II} in *S. elongatus* involve regulation of gene expression controlled by transcription factor NtcA through binding to an NtcA-activating factor PipX[15] and control of arginine biosynthesis by activating *N*-acetyl-L-glutamate kinase (NAGK).[16–18] NAGK converts *N*-acetyl-L-glutamate (NAG) to *N*-acetyl-glutamyl phosphate, and its activity is regulated through feedback inhibition by arginine.[19] P_{II} exerts control over NAGK in the following manner: nonphosphorylated P_{II} protein, at low 2-OG concentrations, binds to NAGK. Complex formation not only increases enzymatic activity by affecting the K_m and V_{max} of the catalyzed reaction, but also relieves NAGK from arginine feedback inhibition by approximately 10-fold.[17] The P_{II}–NAGK complex consists of two P_{II} trimers sandwiching one NAGK hexamer (trimer of dimers) with their threefold axes aligned.[20] Two surfaces of each P_{II} subunit are involved in the contact with NAGK: at the body of the P_{II} protein, residues F11 and F13 at the β1–α1 junction of P_{II} make hydrophobic NAGK interactions; residue E85 of the B-loop of P_{II} forms a salt bridge with R233 of NAGK; and B-loop residue T83 is engaged in hydrophobic interactions. In the complexed state, the T-loop of P_{II} adopts a unique bended shape and inserts into the interdomain cavity of NAGK, making contact with the NAGK N domain, with R45 and E50 being engaged in an ion pair network and S49 in tight hydrogen-bond interactions with NAGK. This compact T-loop conformation requires that an intramolecular salt bridge between R47 and E85, which stabilizes an extended T-loop conformation of free P_{II} protein, is broken, so that the salt bridge between B-loop R45 and NAGK R233 can be formed. Almost the same structure as for the *S. elongatus* proteins was revealed for the P_{II}–NAGK complex from *Arabidopsis thaliana*,[21] and the mode of interaction has apparently been conserved throughout the evolution of eukaryotic phototrophs, highlighted by the fact that the cyanobacterial and plant proteins are able to functionally interact *in vitro* with each other.[22]

The current study was carried out to gain deeper insights into the molecular events leading to P_{II} interaction with NAGK. A random mutagenesis approach yielded novel P_{II} variants (I86N and I86T) that display unique features of NAGK and effector molecule binding. To explain these features, the structure of the I86N variant was solved, shedding new light on the process of how the P_{II} NAGK complex forms.

Results

Identification of a P_{II} variant with altered NAGK interaction

To investigate the process of interaction between *S. elongatus* P_{II} and its receptor NAGK, we created a randomly mutated *glnB* library (encoding P_{II}) cloned in a bacterial two-hybrid vector. In the course of this study, a P_{II} variant (carrying an E85-to-D substitution) was identified as being unable to interact with NAGK (not shown). Since the resulting variant has retained the negative charge required for a critical ion pair interaction with R233 in NAGK, the loss of interaction indicated a sophisticated role of the P_{II}-E85–NAGK-R233 interface for complex formation. To reveal this issue, a bacterial two-hybrid screening was performed using the *glnB* random mutant library against an *argB* bait that encodes an NAGK variant with an R233A substitution. This NAGK variant shows no interaction *in vitro* with P_{II} protein of wild-type sequence (wt P_{II}),[20] in yeast two-hybrid analysis interaction,[20] or in the actual bacterial two-hybrid assay (not shown). Screening this library for P_{II} variants capable of interacting with NAGK R233A yielded out of seven clones two types of complementing P_{II} variants, both containing substitutions at position 86 (I86T or I86N P_{II}). To analyze the interaction between NAGK R233A with the I86 P_{II} variants, the interaction of these proteins was measured by surface plasmon resonance (SPR) spectroscopy (Fig. 1a–c). Wild-type

P_{II} protein showed almost no interaction with immobilized NAGK R233A, either in the absence or in the presence of 100 μM ATP (Fig. 1a), confirming the previous results.[20] Strikingly, the two I86 P_{II} variants were able to form complexes with NAGK R233A, but only in the presence of nucleotides. ATP stimulated complex formation in a concentration-dependent manner (Fig. 1b and c). For the I86N variant, 1 μM ATP resulted in clearly detectable NAGK binding (Fig. 1b). Formation of the complex between the P_{II} variant I86T and NAGK R233A required higher ATP concentrations; the association occurred considerably slower than that of the I86N variant and the complex dissociated almost immediately at the end of analyte injection in the ATP-free running buffer (Fig. 1c). Furthermore, the influence of the two P_{II} variants on the enzymatic activity of the NAGK R233A variant was determined.[22] Arginine inhibition of NAGK activity was determined in the absence of P_{II} (IC_{50} for arginine, 14 μM) and with wt, I86N or I86T P_{II} proteins (Fig. 1d). The wt P_{II} protein and the I86T variant both slightly relieved R233A NAGK from arginine inhibition by increasing the IC_{50} for arginine to 40 or 32 μM, respectively. By contrast, the I86N P_{II} protein was much more efficient in relieving NAGK R233A from arginine inhibition by increasing the IC_{50} for arginine to 197 μM. This is in agreement with the result from the SPR analysis, which revealed efficient binding of I86N P_{II} to the R233A NAGK variant. Interestingly, wt P_{II} showed a weak effect on NAGK R233A in the enzyme assay but no interaction in bacterial two-hybrid screening or almost no binding by SPR analysis. This indicates that the arginine inhibition assay of NAGK is very sensitive and detects even very weak interactions, resulting in slightly enhanced NAGK activity. That the P_{II} I86T variant is not more efficient than wt P_{II} in protecting NAGK R233A from arginine inhibition may be attributed to the instability of the complex (as revealed by SPR analysis, see above) or could be a direct effect of this mutation, affecting the ability to relieve NAGK from arginine feedback inhibition (compare below).

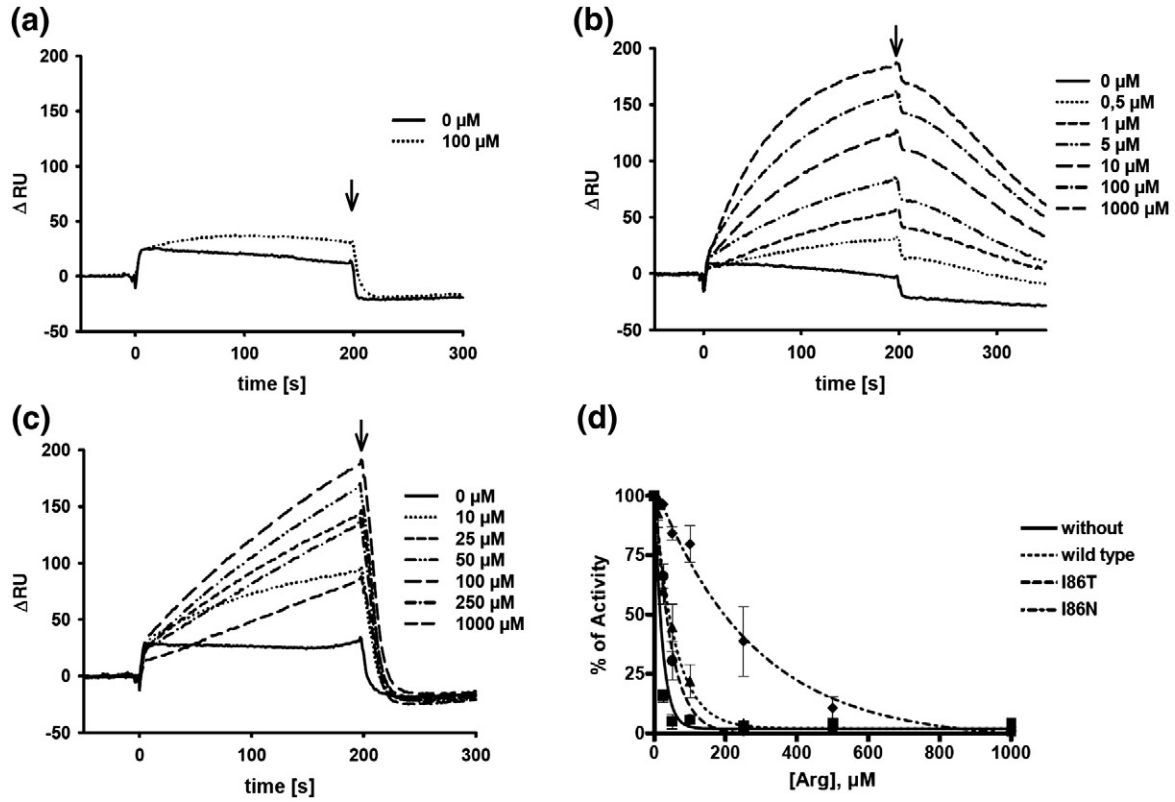

Fig. 1. Interaction of R233A NAGK with recombinant P_{II} proteins. (a)–(c), R233A NAGK was bound to FC2 of a Ni^{2+}-loaded NTA sensor chip (see Materials and Methods) and FC1 was used as background control. The response difference (ΔRU) between FC1 and FC2 is shown. An arrow indicates the end of the injection phase. (a) Binding of 100 nM wt P_{II} in the presence of 0 and 100 μM ATP, as indicated. (b) Influence of ATP on the complex formation of I86N P_{II} (100 nM) and R233A NAGK; ATP was used at a concentration of 0, 0, 5, 1, 5, 10, 100 and 1000 μM, as indicated. (c) Binding of I86T in the presence of ATP at a concentration of 0, 10, 25, 50, 100, 250 and 1000 μM, as indicated. (d) Inhibition of R233A NAGK activity by arginine in the absence and in the presence of P_{II}. Coupled NAGK assays were performed in the presence of 50 mM NAG and 10 mM ATP, together with increasing concentrations of arginine, as indicated, in the absence of P_{II} (squares) and in the presence of wt P_{II} (triangles), I86N (rhombus) or I86T (circles). The percentage of NAGK activity, using reaction velocity without analyte as 100%, was plotted against the respective analyte concentration (standard deviations from different measurements for each data point are indicated by error bars) and the data points were fitted to a hyperbolic curve.

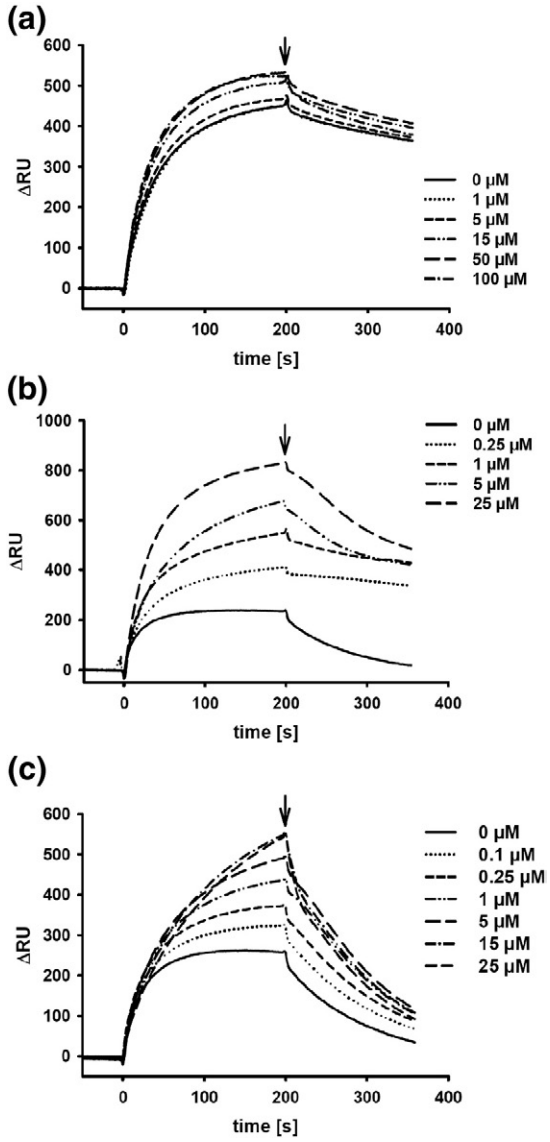

Fig. 2. SPR analysis of the effect of ATP on complex formation between wt NAGK and wt, I86N or I86T P_{II} proteins. SPR spectroscopy was performed as described in Materials and Methods. The response difference (ΔRU) between FC1 and FC2 is shown. An arrow indicates the end of the injection phase. (a) Binding of 100 nM wt P_{II} in the presence of 0, 1, 5, 15, 50 and 100 µM ATP, as indicated. (b) Influence of ATP on the complex formation of I86N P_{II} (100 nM) and wt NAGK; ATP was used at a concentration of 0, 0, 25, 1, 5 and 25 µM, as indicated. (c) Binding of I86T in the presence of ATP at a concentration of 0, 0,1, 0,25, 1, 5, 15 and 25 µM, as indicated.

Interaction of wt NAGK with P_{II} variants I86N and I86T

Next, the interaction of the P_{II} variants I86N and I86T with wild-type NAGK was analyzed to find out how the substitution of I86 in P_{II} affects its NAGK-binding properties. Complex formation was first assayed by SPR spectroscopy. Without effectors, both variants bound significantly weaker to NAGK compared to wt P_{II} and the complex appeared to be less stable, as revealed by the dissociation of the complex after the end of analyte injection (Fig. 2a–c, continuous lines; end of inject indicated by the arrow). However, binding to NAGK was significantly improved in the presence of adenyl nucleotides. The I86N variant responded to submicromolar concentrations of ATP. In the presence of 25 µM ATP, four times more binding was observed than without ATP, whereas wt P_{II} protein is only slightly affected by ATP (Fig. 2a).

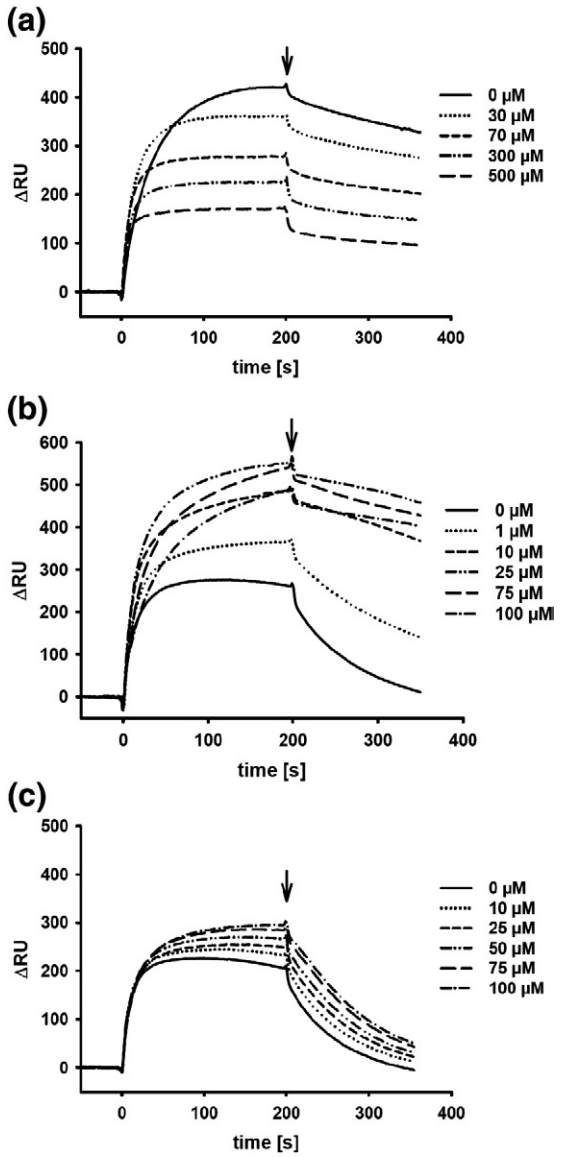

Fig. 3. SPR analysis of the effect of ADP on complex formation between wt NAGK and wt, I86N or I86T P_{II} proteins. SPR spectroscopy was performed as described in Materials and Methods. The response difference (ΔRU) between FC1 and FC2 is shown. An arrow indicates the end of the injection phase. (a) Binding of 100 nM wt P_{II} in the presence of 0, 30, 70, 300 and 500 µM ADP, as indicated. (b) Influence of ADP on the complex formation of I86N P_{II} and wt NAGK; ADP was used at a concentration of 0, 1, 10, 25, 75 and 100 µM, as indicated. (c) binding of I86T in the presence of ADP at a concentration of 0, 10, 25, 50, 75 and 100 µM, as indicated.

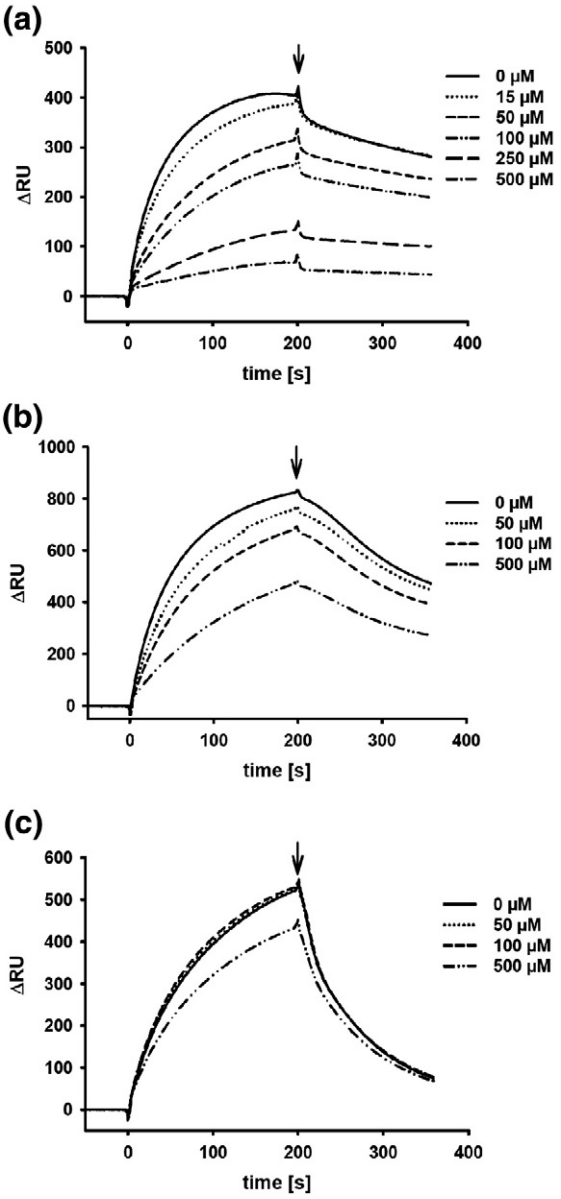

Fig. 4. SPR analysis of the effect of 2-OG on complex formation between wt NAGK and wt, I86N or I86T P_{II} proteins in the presence of 1 mM ATP. SPR spectroscopy was performed as described in Materials and Methods. The response difference (ΔRU) between FC1 and FC2 is shown. An arrow indicates the end of the injection phase. (a) Binding of 100 nM wt P_{II} in the presence of 1 mM ATP and 2-OG at a concentration of 0, 15, 50, 100, 250 and 500 μM, as indicated. (b) Influence of 2-OG on the complex formation of I86N P_{II} and wt NAGK in the presence of 1 mM ATP; 2-OG was used at a concentration of 0, 50, 100 and 500 μM, as indicated. (c) Influence of 2-OG on the complex formation of I86T P_{II} and wt NAGK in the presence of 1 mM ATP; 2-OG was added at a concentration of 0, 50, 100 and 500 μM, as indicated.

Compared to wt P_{II} protein in the presence of saturating ATP, the I86N variant bound even better to the NAGK surface and the complex was apparently stable (compare Fig. 2a and b), indicating that the I86N variant is a superactive NAGK binder. Concerning the P_{II} variant I86T, ATP also enhanced complex formation; however, the complex was unstable, as indicated by the rapid dissociation following the injection phase (Fig. 2c).

As demonstrated previously,[17] ADP negatively affects wt P_{II}–NAGK interaction (Fig. 3a). Apparently, ADP does not completely abolish P_{II}–NAGK interaction, but rather increases the dissociation constant, as deduced from the decreasing levels of P_{II} binding to the NAGK surface with increasing ADP concentrations. In striking contrast to wt P_{II}, ADP enhanced and stabilized the binding of both P_{II} I86 variants to NAGK (Fig. 3b and c). Addition of 1 μM ADP noticeably increased the binding of P_{II} variant I86N to NAGK, and a maximum was reached in the presence of 25 μM ADP, with higher ADP concentrations slightly reducing complex formation again. This P_{II} variant remained stably bound on the NAGK surface during the dissociation phase (Fig. 3b, right to the arrow) and in contrast to wt P_{II} could not be dissociated by injection of 1 mM of ADP (data not shown). In the case of the I86T variant, ADP only weakly stimulated NAGK interaction (Fig. 3c).

2-OG is known to be a major effector molecule involved in P_{II} signal transduction.[17] As shown in Fig. 4a, micromolar amounts of 2-OG in the presence of 1 mM ATP diminished wt P_{II}–NAGK interaction, and in the presence of 500 μM 2-OG, complex formation between wt P_{II} and NAGK was almost completely inhibited. Interestingly, addition of 2-OG to the I86N variant had only a small effect on complex formation, since significant binding was observed even in the presence of 500 μM 2-OG and 1 mM ATP (Fig. 4b). Even more strikingly, the I86T variant was almost completely insensitive toward 2-OG (Fig. 4c).

The interaction of I86 P_{II} variants with wt NAGK was further investigated by using the coupled NAGK enzyme assay (see above). As shown in Fig. 5a, the I86N P_{II} variant was as efficient as wt P_{II} in relieving NAGK from arginine inhibition (IC_{50} values of approximately 460 μM for wt P_{II} and 630 μM for P_{II} I86N). On the other hand, the I86T variant showed a much weaker effect on NAGK arginine inhibition (IC_{50}, 75 μM). In the absence of P_{II}, NAGK had an IC_{50} of 18 μM for arginine, as reported previously. These results correspond to SPR measurements shown above, where wt P_{II} and the I86N variant formed a stable complex with wt NAGK in the presence of ATP (ATP was also present in the coupled assay at 10 mM concentration). By contrast, the I86T variant dissociates rapidly from NAGK, leading to the conclusion that the stability of the P_{II}–NAGK complex could be important for relieving the enzyme from arginine inhibition.

The next step was to test the inhibitory effects of 2-OG on NAGK activation by P_{II} variants I86N and I86T via the coupled assay. Therefore, 2-OG was titrated to P_{II}–NAGK in a buffer containing 50 μM arginine. This amount of arginine is highly inhibitory for free NAGK, but only slightly inhibitory for the P_{II}–NAGK complex.[22] In the control experiment, NAGK activity in the presence of wt P_{II} was inhibited by the addition of 2-OG in a concentration-dependent

manner with an IC_{50} of 116 μM, as reported previously.[22] With both P_{II} variants, 2-OG was not effective in antagonizing the P_{II}-mediated protection of NAGK from arginine inhibition even at high concentrations (Fig. 5b). This result confirmed data from SPR experiments, which showed that P_{II} variants I86N or I86T are insensitive toward 2-OG.

Binding of effector molecules to P_{II} and its I86N and I86T variants

The experiments shown above indicated that the P_{II} variants I86N and I86T responded to the effector molecules ATP, ADP and 2-OG quite differently from wt P_{II}. Therefore, the effector-binding properties of these P_{II} variants were determined by isothermal titration calorimetry (ITC). Previously, the ligand-binding properties of *S. elongatus* P_{II} have not been determined by this method. Therefore, the ITC characteristics of wt P_{II} protein will be presented first in some detail. The measurements were performed with different ligand/protein concentrations to determine the conditions under which the best fitting to the binding model could be achieved. Subsequently, the experiments were repeated to confirm the result. As shown in Fig. 6a, wt P_{II} protein exhibits high affinity toward ATP. Optimal fitting of the raw data was obtained using a three sequential binding sites model (Fig. 6a, lower part). This analysis revealed a low dissociation constant for the first binding site ($K_d1 = 4$ μM) and increased K_d for binding sites 2 and 3 ($K_d2 = 12.5$ μM, $K_d3 = 47.4$ μM) as shown in Table 1, indicative of negative cooperativity between the binding sites, similar to values reported previously using equilibrium dialysis or ultrafiltration techniques.[13] Direct binding of ADP to *S. elongatus* P_{II} has so far never been reported. Here we show that ADP binds almost as efficiently as ATP (Fig. 6b), with similar anti-cooperativity among the three sites ($K_d1 = 10.6$ μM, $K_d2 = 19.3$ μM, $K_d3 = 133.4$ μM). Apparently, for each site, ATP binding is preferred over ADP. The binding isotherm for 2-OG was measured in the presence of 1 mM ATP (Fig. 6c). According to the model, assuming three sequential binding sites, the first two sites are occupied at low 2-OG concentrations ($K_d1 = 5.1$ μM, $K_d2 = 11.1$ μM), whereas occupation of the third site requires approximately 10-fold higher concentration of 2-OG ($K_d3 = 106.7$ μM). Interestingly, the dissociation constant of site 3 corresponds quite well to the IC_{50} of 2-OG for antagonizing the P_{II}-mediated protection of NAGK from arginine inhibition (116 μM, see above) or with the 2-OG concentration that is required to inhibit NAGK binding (as determined by SPR analysis; Fig. 4a). This suggests that for inhibiting the binding of P_{II} to NAGK, all three 2-OG sites have to be occupied.

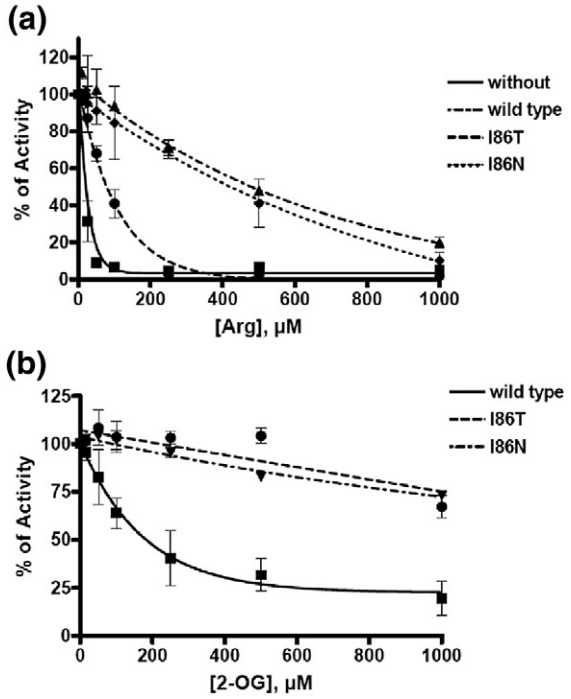

Fig. 5. Arginine inhibition of NAGK and influence of 2-OG in the presence of recombinant P_{II} proteins. Coupled NAGK assays were performed as described in Materials and Methods in the presence of 10 mM ATP. The percentage of NAGK activity, using reaction velocity without analyte as 100%, was plotted against the respective analyte concentration (standard deviations from different measurements for each data point are indicated by error bars) and the data points were fitted to a hyperbolic curve. (a) Inhibition of wt NAGK activity by increasing concentrations of arginine, as indicated, in the absence of P_{II} (squares) and in the presence of wt P_{II} (triangles), I86N (rhombus) or I86T (circles). (b) Effect of 2-OG on the activation of NAGK by P_{II} in the presence of arginine. Assays were performed in the presence 50 μM arginine and increasind 2-OG concentrations, as indicated, with wt P_{II} (squares), I86N (triangles) and I86T (circles).

The P_{II} variant I86N has completely lost the anti-cooperativity of the ATP binding sites: all three sites were occupied independently with a K_d of approximately 9.6 μM. The raw data could not be fitted properly using a three sequential binding sites model; therefore, a one-site binding model was used for these measurements. This model allowed us to determine three independent binding sites for a I86N trimer (Table 1). The I86T variant also showed lack of anti-cooperativity of the ATP binding sites. The affinity toward ADP in both variants was weaker than for wt P_{II}. For both P_{II} variants, addition of 2-OG in the presence of 1 mM ATP did not yield any calorimetric signals. This result agrees with data shown above, which demonstrate that these P_{II} variants are insensitive toward 2-OG (Fig. 4 and 5b), implying that I86 of the B-loop may take part in 2-OG binding.

Structure of the P_{II} I86N variant

The observation that P_{II} variant I86N, in particular, is able to bind to the NAGK variant R233A, whereas the wt P_{II} protein was unable to interact, clearly shows that the P_{II} E85–NAGK R233 interaction is not required for the I86N variant. This led us

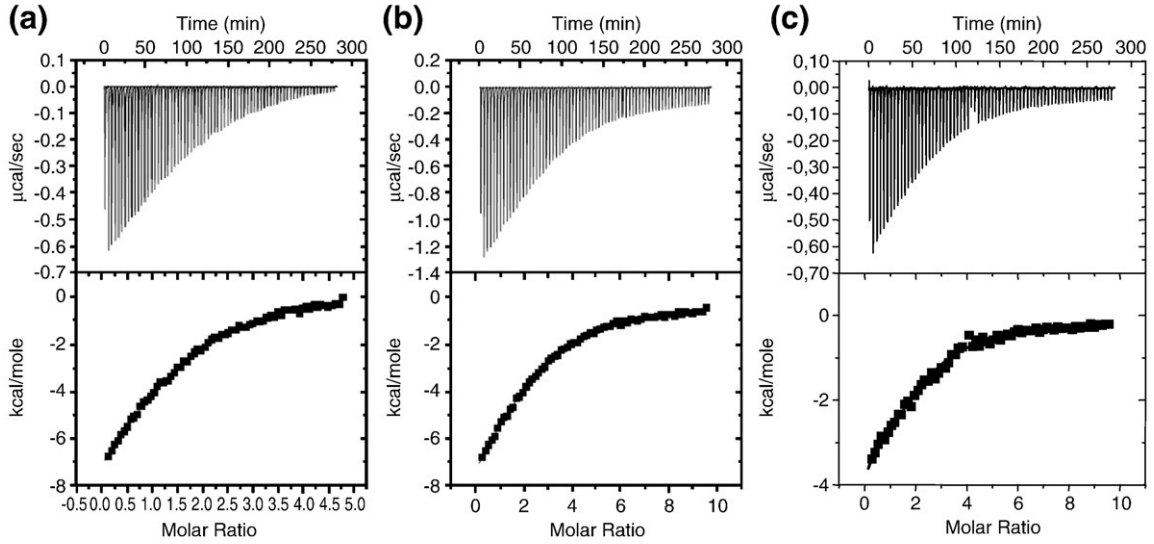

Fig. 6. ITC of ligand binding to wt P_{II} protein. The upper panels show the raw data in the form of the heat effect during the titration of 33 µM wt P_{II} solution (trimer concentration) with ligands. The lower panels show the binding isotherm and the best-fit curve according to the three sequential binding sites model. (a) ATP binding (titration from 2.1 to 146.8 µM). (b) ADP binding (4.2–293.7 µM). (c) 2-OG binding (4.2–293.7 µM) in the presence of 1 mM ATP.

to hypothesize that this variant may adopt a conformation that facilitates interaction with NAGK to make it independent of the NAGK R233 contact. To resolve this issue, the structure of the P_{II} I86N variant in the presence of ATP was solved by X-ray crystallography. Protein crystals diffracted to a resolution of 1.2 Å with one monomer of the protein in the asymmetric unit (see also Table 2). The structure was solved by molecular replacement using the structure of nonliganded *S. elongatus* P_{II} [Protein Data Bank (PDB) entry 1Q7Y] as the search model. As shown in Fig. 7, the backbone of the I86N variant is almost identical to that of the wt P_{II} structure[7] (r.m.s.d. of 1.9 Å for 100 aligned residues). In contrast to the nonliganded *S. elongatus* P_{II} protein (Fig. 7b), the T-loop adopts a compact conformation, which is very similar to that of the wt P_{II} protein in complex with NAGK[20] (Fig. 7a). The I86N substitution results in a newly formed hydrogen bond between the amido nitrogen of N86 and the backbone oxygen of T43, contracting the anterior part of the T-loop toward the body of P_{II} (Fig. 7c). This compact conformation is further stabilized by a salt bridge between E44 and K58. The same stabilizing salt bridge is observed in the compact T-loop of NAGK-bound P_{II} (Fig. 7a). Moreover, residues R45 and E50 at the tip of the T-loop are connected by another salt bridge in the I86N variant and E50 forms an additional H-bond with T43. The same interaction has been observed in NAGK-complexed P_{II}, where these surface-exposed residues organize an ion pair network with NAGK, which appears to be a major determinant for this interaction.[20] In the I86N variant, the hydroxyl group of S49 is surface-exposed to perfectly match the corresponding contact surface of NAGK. Overall, the structure of the I86N variant appears as a perfect mimic of wt P_{II} structure in complex with NAGK.

Mg-ATP is bound to the canonical ATP binding site of P_{II} proteins, which lies in the intersubunit clef between neighbouring subunits.[6,23] Accordingly, key contact residues for Mg-ATP binding are G27, T29, R101 and R103 from one subunit and G37, G87, G89 and K90 from the opposing subunit. The C-terminus of the I86N variant forms a short α-helix, which folds back toward the ATP binding pocket (Fig. 7a). This structure is reminiscent of the C-terminal end of *A. thaliana* P_{II}.[21] In the I86N P_{II} variant, this segment is well ordered until the C-terminal end of the native *S. elongatus* P_{II} sequence (amino acid 112). The additional 10 amino acids from the C-terminal fused Streptag II peptide are not ordered and therefore not visible, indicating that

Table 1. Dissociation constants of ATP, ADP and 2-OG binding to recombinant P_{II} proteins

	K_d1 (µM)	K_d2 (µM)	K_d3 (µM)	*N* (no. of sites in one-site model)
ATP				
wt	4.0±0.1	12.5±0.9	47.4±21.9	—
I86N		9.6±1.3		3.0±0.1
I86T		14.3±0.5		3.51±0.62
ADP				
wt	10.6±3.2	19.3±2.3	133.4±5.2	—
I86N	165.3±59.0	59.5±49.3	66.2±38.5	—
I86T	41.4±11.5	53.7±13.1	149.9±13.6	—
2-OG (+1 mM ATP)				
wt	5.1±4.0	11.1±1.8	106.7±14.8	—
I86N	n	n	n	—
I86T	n	n	n	—

n, not detectable.

Values for wt P_{II} correspond to the mean±SEM of three experiments for I86N and to the mean±SEM of two experiments for I86T.

The raw data for I86N- and I86T-ATP binding was fitted using a one-site binding model for a P_{II} trimer.

Table 2. Data collection and refinement statistics

	P_{II} I86N variant
Data collection	
Space group	$P2_13$
Cell dimensions	
a, *b*, *c* (Å)	80.68, 80.68, 80.68
α, β, γ (°)	90
Resolution (Å)	1.2 (1.27–1.2)
R_{sym} or R_{merge}	0.1 (0.64)
$I/\sigma I$	17 (2.3)
Completeness (%)	99.9 (99.7)
Redundancy	13.3 (10.3)
Refinement	
Resolution (Å)	36–1.2
No. of reflections	52,061
R_{work}/R_{free}	0.12/0.14
No. of atoms (all)	
Protein	919
Ligand/ion (ATP/Mg^{2+}/Cl)	31/1/1
Water	174
B-factors	
Protein	9.7
Ligand/ion (ATP/Mg^{2+}/Cl)	8.4/8.9/8.4
Water	31
r.m.s.d.	
Bond lengths (Å)	0.03
Bond angles (°)	2.7

Values in parentheses are for the highest-resolution shell.

this C-terminal extension is highly flexible and does not interfere with the P_{II} structure, in accord with the full functionality of the C-terminal Strep-tagged P_{II} protein compared to the untagged version with respect to effector molecule binding and NAGK interaction.[13,20]

Discussion

The structure of the novel P_{II} I86N variant together with its binding properties to NAGK offers a mechanistic explanation for the process of complex formation between P_{II} and NAGK and explains the role of the P_{II} 85E–NAGK 233R interface. In the complex of wt P_{II} and NAGK, there are two surfaces of interaction: a smaller exterior interface (303 A^2) is formed by the peripheral part of the NAGK C domain and the β1–α1 junction (F11–E15) and B-loop residues T83 and E85 of P_{II}, the latter forming a salt bridge with R233 of NAGK. The larger surface (393 A^2) involves the T-loop hairpin that is deeply buried within the NAGK interdomain cleft.[20] There is a drastic difference between this compact T-loop conformation and that of the nonliganded free P_{II}, where the T-loop exhibits an extended conformation. The extended T-loop of *S. elongatus* P_{II} may be a

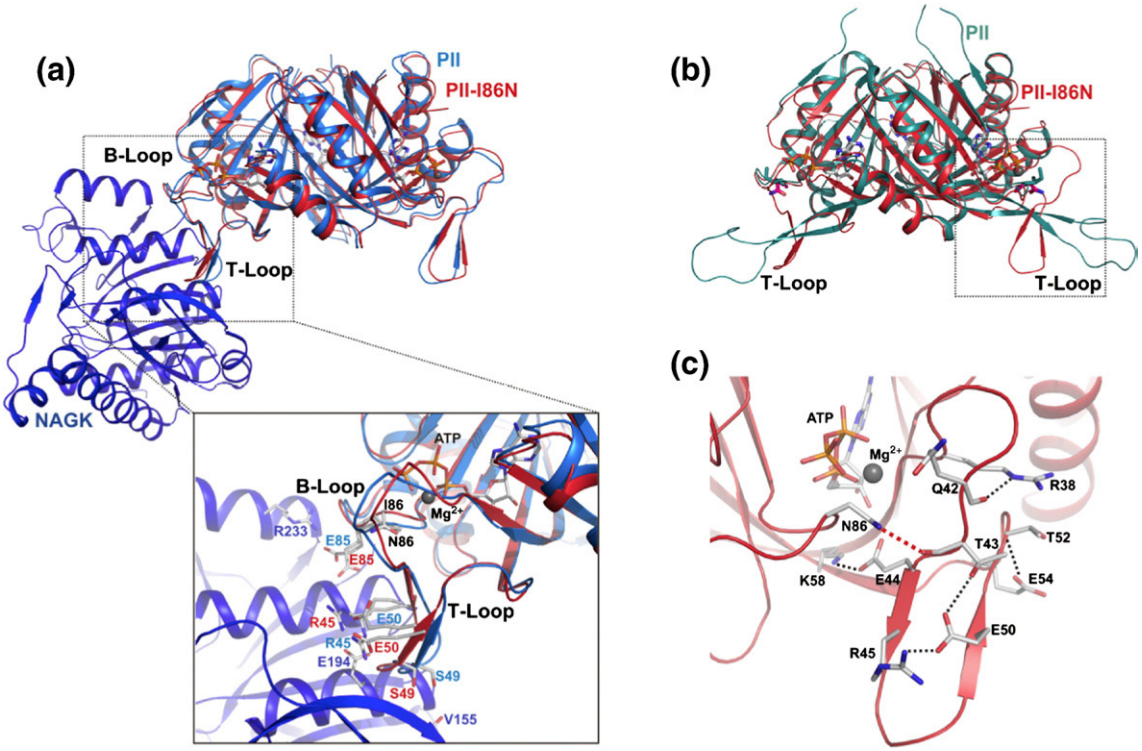

Fig. 7. The structure of the P_{II} I86N variant mimics the structure of *S. elongatus* P_{II} in complex with NAGK. Proteins are shown as strings and ribbons. ATP, residue side and main chains are shown as sticks and Mg^{2+} ions as spheres. (a) Superimposed structure of *S. elongatus* P_{II} in complex with NAGK coloured blue (PDB ID 2V5H) and the P_{II} variant I86N coloured red. The magnification below shows B- and T-loop residues important for NAGK interaction. Note the similar arrangement of residues R45, S49 and E50. (b) Superimposed structure of nonliganded *S. elongatus* P_{II} in green (PDB ID 1QY7) and the I86N variant (red). (c) T-loop of the I86N variant (red). Red broken lines show the hydrogen bond of the amido nitrogen of N86 with the backbone oxygen of T43; broken lines show the hydrogen bonds between E50 and T43 and, additionally, salt bridges R45–E50 and E44–K58, which stabilize the bent conformation.

specificity of cyanobacterial P_{II} proteins, since the R47–E85 pair, which apparently stabilizes this conformation, is only present in cyanobacterial P_{II} proteins. In agreement, from the numerous P_{II} structures that are available today, only the *S. elongatus* P_{II} structure exhibits this type of extended T-loop.[3,23] Obviously, in the process of NAGK–P_{II} complex formation, the R47–E85 bridge must be broken and the T-loop must undergo a large conformational rearrangement to adopt the compact bended structure. Based on the results of this study, we propose a two-step mechanism of P_{II} interaction with NAGK, giving the B-loop a key role in initiating this process. According to this model, in the first step, NAGK approaches P_{II} and the NAGK residue R233 triggers the break of the P_{II} R47–E85 bridge by presenting a more suitable partner for E85. In the second step, the extended T-loop collapses into the NAGK interdomain cleft, generating the large surface for P_{II} binding to NAGK and stabilizing the complex. As shown in this study, the salt bridge R233-NAGK–E85-P_{II} is not essential for binding *per se*, since the NAGK R233A variant is able to bind P_{II} variants I86N and I86T. According to the two-step model, wt P_{II} is not able to bind to NAGK R233A because the initiating step cannot take place. For the same reason, P_{II} variant E85A would be unable to bind wt NAGK. The P_{II} variant E85D may be impaired in performing the initiating step because the aspartate side chain could be too short to interact with R233 of NAGK. Binding of the P_{II} variant I86N to NAGK R233A is explained in light of the new structure. It binds to NAGK without the need of the initiating P_{II} E85–NAGK R233 interaction, because due to the I86N substitution, this P_{II} variant exhibits a conformation that *a priori* fits into NAGK. In this variant, the T-loop is fixed in a conformation that mimics that of the P_{II} T-loop in the NAGK complex. The interaction of the I86T variant with NAGK is weaker than that of the I86N variant. The location of the hydroxyl group of the T86 residue in this variant may be less favourable for hydrogen-bonding the backbone oxygen of T43 than the corresponding amide group of N86, resulting in a T-loop conformation that less perfectly fits into the NAGK binding pocket and may be less capable of relieving NAGK from arginine inhibition.

Whether a two-step binding process as proposed here for the NAGK–P_{II} interaction is a general mechanism occurring in P_{II} receptor interactions remains to be elucidated. Considering the wide variety of P_{II} interactions with different receptor proteins, there may be different processes of complex formation. However, in any case, the flexibility of the T-loop is predestined for highly sophisticated interactions involving multistage binding processes. A recent investigation of *E. coli* P_{II} interacting with its receptors NtrB and ATase implies that in *E. coli*, P_{II} binds its receptors in a first step independent of the effector molecule 2-OG. T-loop structural rearrangements, triggered by 2-OG binding, could occur in this case at a post-binding step, thereby modulating the regulation of receptors by 2-OG through P_{II}. Two distinct interaction surfaces were predicted for such a process, one that is insensitive toward 2-OG, and a second one that mediates the regulatory effects and responds to 2-OG.[12]

More than shedding light on the process of P_{II}–NAGK complex formation, the I86 variants reveal an unexpectedly important contribution of the I86 residue to effector molecule binding properties of P_{II}. First, the I86N variant has completely lost anti-cooperativity between the ATP binding sites, indicating a role for the B-loop in intersubunit signalling. Second, the failure to bind 2-OG is remarkable. Other P_{II} variants, which were reported previously to be unable to bind 2-OG, had in addition impaired ATP binding properties. This hampers the interpretation of the phenotype, since as a general rule for P_{II} proteins, 2-OG binding requires the previous binding of ATP.[1,13] Only upon ATP binding is the 2-OG binding site of P_{II} created; however, the position of the 2-OG binding site remains enigmatic so far. The I86 variants are the only P_{II} variants reported so far that have retained ATP binding, although modified, but are completely impaired in 2-OG binding. This suggests that this B-loop residue is probably directly involved in 2-OG binding, proposing a possible location of the 2-OG binding site near the B-loop and the binding site for ATP. This conclusion is supported by mutational studies of *E. coli* P_{II}, which revealed residue Q39 that lies at the base of the T-loop and opposing residue I86,[24] being involved in 2-OG binding.[11] A similar position for the 2-OG binding sites has already been proposed for the *Herbaspirillum seropedicae* GlnK protein (a member of the P_{II} family) based on sequence comparisons with other 2-OG binding proteins.[25] Alternatively (or in addition), the conformation of the T-loop adopted by the I86N variant could be incompatible with 2-OG binding. Since the same T-loop conformation is found in NAGK-bound P_{II}, which is able to respond to 2-OG, further conclusions could be made: 2-OG binding could unlock the bent T-loop conformation, ascribing the failure of the I86N variant to bind to 2-OG to the fact that the T-loop in this variant is fixed in the tightly bent conformation. Unlocking the bent T-loop would also provide a rationale for the antagonistic effect of 2-OG on P_{II}–NAGK binding. The location of the 2-OG binding site near the B-loop is in apparent contradiction with a recently reported structure of the P_{II} protein GlnK1 from the archaeon *M. jannaschii*. In the crystal structure soaked with 2-OG, the effector was found on the T-loop of GlnK1 with several hydrogen bonds between the keto-carboxyl group and main-chain NH of I52, V53 and D54.[10] Since a deletion of the corresponding residues in *E. coli* P_{II} did not affect 2-OG binding,[11] it is unlikely that this 2-OG-binding site of the archaeal P_{II} protein applies to bacterial P_{II} proteins. Furthermore, it is hardly conceivable how 2-OG could bind to such a site, once the complex with NAGK has formed, since in the complex the 2-OG site would be shielded by NAGK. However, a

binding site close to the B-loop would be accessible even in NAGK-complexed P_{II}. Resolution of the 2-OG binding site in bacterial P_{II} proteins is urgently needed to understand the regulatory function of this effector molecule in P_{II}-regulated processes.

Materials and Methods

Random mutagenesis of recombinant P_{II} protein and bacterial two-hybrid screen

Before mutagenesis, the *glnB* gene was cloned into the bacterial two-hybrid vector pBT (Stratagene) to generate pBT-*glnB* with the following oligonucleotides: glnB/pBTfor (5′-CGGAATTCCATGAAGAAGATTGAGGCGATTATT-3′), carrying an EcoRI restriction site, and glnB/pBTrev (5′-CGGGATCCCTGTTGTCGACGCTGACTTAGA-3′), carrying a BamHI restriction site. Random mutagenesis on pBT-*glnB* was performed with the GeneMorph II Random Mutagenesis Kit from Stratagene (La Jolla, CA) with the following oligonucleotides containing EcoRI and BamHI restriction sites: glnBRacefor (5′-CGGCCGCATCGAATTCCATGTAG-3′) and glnBRacerev (5′-TCGAGGATCCCTGTTGTCGACGTCGAC-3′), using 2.6 μg of pBT-*glnB* DNA as template. The randomly mutated PCR fragments were purified, restricted with EcoRI and BamHI and re-ligated into the pBT bait vector to produce the pBT-*glnB* random mutant library. For the *in vivo* assay of the P_{II}–NAGK interaction, the BacterioMatch II Two-Hybrid System Vector Kit from Stratagene was used. The *argB* gene from *S. elongatus*, coding for NAGK, was cloned into pTRG target vector (Stratagene) with the following primers: NAGK/pTRGfor (5′-CGGGATCCATGTCTAGCGAGTTTATCGAAGC-3′), carrying a BamHI restriction site, and NAGK/pTRGrev (5′-CCGCTCGAGTCACGGATCGCTCATTGCCAG-3′), carrying an XhoI restriction site, with *S. elongatus* chromosomal DNA as template. To screen for P_{II} variants that lost the ability to interact with NAGK, the pBT-*glnB* random mutant library was transformed into *E. coli* strain 200190 BacterioMatch II Screening Reporter Competent Cells (Stratagene) carrying pTRG-*argB*. The transformants were replica-plated on nonselective Cm/Tet Luria–Bertani (LB) plates and Cm/Tet/3-AT (3-amino-1,2,4-troazole) plates that only allow growth of cells, in which hybrid P_{II}–NAGK interaction occurs. Clones that failed to grow in the presence of the selective agent 3-AT were further investigated. To exclude *glnB* variants that produced instable or truncated versions of P_{II}, we grew the clones of interest in liquid LB-Cm/Tet and analyzed the integrity of P_{II} by immunoblot analysis using P_{II}-specific antibodies.[16] From clones that contained full-size P_{II} fusion protein, the mutant pBT-*glnB* plasmids were checked again by bacterial two-hybrid assay for loss of NAGK interaction; interaction-negative clones were isolated and the *glnB* gene was sequenced from both sides with primers glnB/pBTfor and glnB/pBTrev.

Overexpression and purification of recombinant P_{II} and NAGK

The mutant *glnB* genes were amplified from the respective mutant pBT-*glnB* plasmids by PCR using the following primers: glnBStrep-for (5′-GCAATTGGTCTCAAATGAAGAAGATTGAGGCGATTATTC-3′) and glnBStrep-rev (5′-GATCATGGTCTCAGCGCTGATTGCGTCGGCGTTTTTCTC-3′). The PCR products containing mutant *glnB* genes were cloned into the Strep-tag fusion vector pASK-IBA3 (IBA, Göttingen, Germany) as described previously.[16] Overexpression of mutant *glnB* in *E. coli* RB9060[26] and purification of recombinant P_{II} proteins with a C-terminal fused Strep-tag II peptide was performed according to Heinrich *et al*.[16]

The His_6-tagged recombinant wt NAGK from *S. elongatus* was overexpressed in *E. coli* strain BL21(DE3)[27] and purified as reported previously.[17]

The *argB* gene carrying a R233A mutation was cloned into expression vector pET15b with pUAGC569-*argB* plasmid as DNA template according to the protocol described previously.[17]

SPR detection

SPR experiments were performed with a BIAcore X biosensor system (Biacore AB, Uppsala, Sweden) as described previously at 25 °C in HBS-Mg buffer [10 mM Hepes, 150 mM NaCl, 1 mM $MgCl_2$, 0.005% Nonidet P-40 (pH 7.5)] at a flow rate of 15 μl/min.[17] The purified His_6-NAGK was immobilized on the Ni^+-loaded NTA sensor chip to flow cell 2 (FC2) in a volume of 50 μl at a concentration of 30 nM (hexamer) to receive a binding signal of approximately 3000 resonance units (RU), which corresponds to a surface concentration change of 3 ng/mm^2. To analyze the effect of ATP, ADP or the combined effect of 2-OG and ATP on binding of P_{II} variants to the His_6-NAGK surface compared to wt P_{II}, we incubated the analyte (100 nM), diluted in HBS-Mg buffer, with each of the effector molecules on ice for 5 min and injected (50 μl) it to both FC1 and FC2 on the sensor chip. The specific binding of P_{II} to NAGK was recorded as the response signal difference FC2 − FC1. P_{II} was removed from the His_6-NAGK surface by injecting 25 μl of 1 mM ADP. For novel reload of proteins on the NTA sensor chip, 25 μl of 0.4 M EDTA (ethylenediaminetetraacetic acid) (pH 7.5) was injected to remove His_6-NAGK and Ni^+. Subsequently, the chip could be loaded again with 5 mM $NiSO_4$ solution and His_6-NAGK as described above.

Isothermal titration calorimetry

ITC experiments were performed on a VP-ITC microcalorimeter (MicroCal, LCC) in 10 mM Hepes–NaOH, 50 mM KCl, 50 mM NaCl, and 1 mM $MgCl_2$ (pH 7.4) at 20 °C. For determination of ATP, ADP and 2-OG binding isotherms for wt P_{II} protein, 33 μM protein solution (trimer concentration) was titrated with 1 mM ATP, 2 mM ADP or 2 mM 2-OG (in the presence of 1 mM ATP), respectively. The ligand (3 μl) was injected 70 times into the 1.4285 ml cell with stirring at 350 rpm.

For determination of ATP, ADP and 2-OG binding isotherms for I86T and I86N P_{II} variants, 17 μM protein solution was titrated with 1 mM ATP, 1.5 mM ADP or 2 mM 2-OG (in the presence of 1 mM ATP), respectively. The ligand (5 μl) was injected 35 times. The binding isotherms were calculated from received data and fitted to a three-site binding model or one-site binding model with the MicroCal ORIGIN software (Northampton, MA) as indicated.

Coupled NAGK activity assay

The activity of NAGK was assayed by coupling NAG phosphorylation via pyruvate kinase and lactate

dehydrogenase to the oxidation of NADH. The assay was performed as described previously; the reaction buffer consisted of 50 mM imidazole (pH 7.5), 50 mM KCl, 20 mM $MgCl_2$, 0.4 mM NADH, 1 mM phosphoenolpyruvate, 10 mM ATP, 0.5 mM DTT, 11 U lactate dehydrogenase, 15 U pyruvate kinase and 50 mM NAGK.[22] The reaction was started by the addition of 3 μg NAGK. When needed, 1.2 μg P_{II} was added to the reaction mixture before beginning the assay. Phosphorylation of one molecule of NAG leads to oxidation of one molecule of NADH, followed by the linear decrease of absorbance at 340 nm.[28] The reaction was recorded in a volume of 1 ml over a period of 10 min with a SPECORD 200 photometer (Analytik Jena) at 340 nm. The reaction velocity was calculated from the slope of the resulting time curve as change in absorbance per time with 1 U of NAGK (ε_{340} = 6178 L mol^{-1} cm^{-1}) catalyzing the conversion of 1 mmol NAG per minute.

Crystallization of I86N P_{II} variant

Crystallization was performed with the sitting-drop technique by mixing 400 nl of the protein solution with equal amounts of the reservoir solution using the honeybee robot (Genomic Solutions Ltd). Drops were incubated at 20 °C and pictures were recorded by the RockImager system (Formulatrix, Waltham, MA). The protein buffer was composed of 10 mM Tris (pH 7.4), 0.5 mM EDTA, 100 mM NaCl, 1% glycerol, 2 mM ATP-Mg; crystals appeared after 7 days in a precipitant condition containing 0.1 M Mes (pH 6.5) and 25% PEG (polyethylene glycol) 1000. Crystals were mounted directly in cryoloops and flash-frozen in liquid nitrogen. Diffraction data were collected at the Swiss Light Source (SLS, Villigen, Switzerland). Diffraction images were recorded on a MarCCD camera 225 (Marreserarch, Norderstedt, Germany) and images were processed using the XDS/XSCALE software.[29] The structure was solved by molecular replacement using the program Molrep.[30] Rebuilding of the structure and structure refinement was performed using the programs Coot and Refmac.[31,32] The quality of the structure was analyzed by the Procheck program.[33] Figures were generated using PyMOL†.

PDB accession numbers

Coordinates and structure factors for the P_{II} I86N variant have been deposited in the PDB with accession number 2xbp.

Acknowledgements

We thank Dr. Gregor Meiss and Verena Schuenemann for their help in performing the ITC measurements. Ulrike Ruppert and Christina Herrmann are gratefully acknowledged for excellent technical assistance. We thank the Fonds der Chemischen Industrie for generous allocation of the BIAcore equipment and the Landesstiftung Baden-Württemberg program SI-BW for supporting the ITC equipment. This work was also supported by a grant from the DFG (Fo 194/4).

† http://www.pymol.org/

References

1. Ninfa, A. J. & Jiang, P. (2005). P_{II} signal transduction proteins: sensors of alpha-ketoglutarate that regulate nitrogen metabolism. *Curr. Opin. Microbiol.* **8**, 168–173.
2. Leigh, J. A. & Dodsworth, J. A. (2007). Nitrogen regulation in bacteria and archaea. *Annu. Rev. Microbiol.* **61**, 349–377.
3. Forchhammer, K. (2008). P(II) signal transducers: novel functional and structural insights. *Trends Microbiol.* **16**, 65–72.
4. Sant'Anna, F. H., Trentini, D. B., de Souto Weber, S., Cecagno, R., da Silva, S. C. & Schrank, I. S. (2009). The P_{II} superfamily revised: a novel group and evolutionary insights. *J. Mol. Evol.* **68**, 322–336.
5. Jiang, P. & Ninfa, A. J. (2007). *Escherichia coli* P_{II} signal transduction protein controlling nitrogen assimilation acts as a sensor of adenylate energy charge in vitro. *Biochemistry*, **46**, 12979–12996.
6. Xu, Y., Cheah, E., Carr, P. D., van Heeswijk, W. C., Westerhoff, H. V., Vasudevan, S. G. & Ollis, D. L. (1998). GlnK, a P_{II}-homologue: structure reveals ATP binding site and indicates how the T-loops may be involved in molecular recognition. *J. Mol. Biol.* **282**, 149–165.
7. Xu, Y., Carr, P. D., Clancy, P., Garcia-Dominguez, M., Forchhammer, K., Florencio, F. *et al.* (2003). The structures of the P_{II} proteins from the cyanobacteria *Synechococcus* sp. PCC 7942 and *Synechocystis* sp. PCC 6803. *Acta Crystallogr., Sect. D: Biol. Crystallogr.* **59**, 2183–2190.
8. Forchhammer, K. (2004). Global carbon/nitrogen control by P_{II} signal transduction in cyanobacteria: from signals to targets. *FEMS Microbiol. Rev.* **28**, 319–333.
9. Sakai, H., Wang, H., Takemoto-Hori, C., Kaminishi, T., Yamaguchi, H., Kamewari, Y. *et al.* (2005). Crystal structures of the signal transducing protein GlnK from *Thermus thermophilus* HB8. *J. Struct. Biol.* **149**, 99–110.
10. Yidiz, Ö., Kalthoff, C., Raunser, S. & Kühlbrandt, W. (2007). Structure of GlnK1 with bound effectors indicates regulatory mechanism for ammonia uptake. *EMBO J.* **26**, 589–599.
11. Jiang, P., Zucker, P., Atkinson, M. R., Kamberov, E. S., Tirasophon, W., Chandran, P. *et al.* (1997). Structure/function analysis of the P_{II} signal transduction protein of *Escherichia coli*: genetic separation of interactions with protein receptors. *J. Bacteriol.* **179**, 4343–4353.
12. Jiang, P. & Ninfa, A. J. (2009). alpha-Ketoglutarate controls the ability of the *Escherichia coli* P_{II} signal transduction protein to regulate the activities of NRII (NtrB) but does not control the binding of P_{II} to NRII. *Biochemistry*, **48**, 11514–11521.
13. Forchhammer, K. & Hedler, A. (1997). Phosphoprotein P_{II} from cyanobacteria—analysis of functional conservation with the P_{II} signal-transduction protein from *Escherichia coli*. *Eur. J. Biochem.* **244**, 869–875.
14. Kloft, N., Rasch, G. & Forchhammer, K. (2005). Protein phosphatase PphA from *Synechocystis* sp. PCC 6803: the physiological framework of P_{II}-P dephosphorylation. *Microbiology*, **151**, 1275–1283.
15. Espinosa, J., Forchhammer, K., Burillo, S. & Contreras, A. (2006). Interaction network in cyanobacterial nitrogen regulation: PipX, a protein that interacts in

a 2-oxoglutarate dependent manner with P_{II} and NtcA. *Mol. Microbiol.* **61**, 457–469.
16. Heinrich, A., Maheswaran, M., Ruppert, U. & Forchhammer, K. (2004). The *Synechococcus elongatus* P signal transduction protein controls arginine synthesis by complex formation with *N*-acetyl-L-glutamate kinase. *Mol. Microbiol.* **52**, 1303–1314.
17. Maheswaran, M., Urbanke, C. & Forchhammer, K. (2004). Complex formation and catalytic activation by the P_{II} signaling protein of *N*-acetyl-L-glutamate kinase from *Synechococcus elongatus* strain PCC 7942. *J. Biol. Chem.* **279**, 55202–55210.
18. Burillo, S., Luque, I., Fuentes, I. & Contreras, A. (2004). Interactions between the nitrogen signal transduction protein P_{II} and *N*-acetyl glutamate kinase in organisms that perform oxygenic photosynthesis. *J. Bacteriol.* **186**, 3346–3354.
19. Llacer, J. L., Fita, I. & Rubio, V. (2008). Arginine and nitrogen storage. *Curr. Opin. Struct. Biol.* **18**, 673–681.
20. Llacer, J. L., Contreras, A., Forchhammer, K., Marco-Marin, C., Gil-Ortiz, F., Maldonado, R. *et al.* (2007). The crystal structure of the complex of P_{II} and acetylglutamate kinase reveals how P_{II} controls the storage of nitrogen as arginine. *Proc. Natl. Acad. Sci. USA*, **104**, 17644–17649.
21. Mizuno, Y., Moorhead, G. B. & Ng, K. K. (2007). Structural basis for the regulation of *N*-acetylglutamate kinase by P_{II} in *Arabidopsis thaliana*. *J. Biol. Chem.* **282**, 35733–35740.
22. Beez, S., Fokina, O., Herrmann, C. & Forchhammer, K. (2009). *N*-Acetyl-L-glutamate kinase (NAGK) from oxygenic phototrophs: P(II) signal transduction across domains of life reveals novel insights in NAGK control. *J. Mol. Biol.* **389**, 748–758.
23. Nichols, C. E., Sainsbury, S., Berrow, N. S., Alderton, D., Saunders, N. J., Stammers, D. K. & Owens, R. J. (2006). Structure of the P_{II} signal transduction protein of *Neisseria meningitidis* at 1.85 Å resolution. *Acta Crystallogr., Sect. F: Struct. Biol. Cryst. Commun.* **62**, 494–497.
24. Carr, P. D., Cheah, E., Suffolk, P. M., Vasudevan, S. G., Dixon, N. E. & Ollis, D. L. (1996). X-ray structure of the signal transduction protein from *Escherichia coli* at 1.9 A. *Acta Crystallogr., Sect. D: Biol. Crystallogr.* **52**, 93–104.
25. Benelli, E. M., Buck, M., Polikarpov, I., de Souza, E. M., Cruz, L. M. & Pedrosa, F. O. (2002). *Herbaspirillum seropedicae* signal transduction protein P_{II} is structurally similar to the enteric GlnK. *Eur. J. Biochem.* **269**, 3296–3303.
26. Bueno, R., Pahel, G. & Magasanik, B. (1985). Role of *glnB* and *glnD* gene products in regulation of the glnALG operon of *Escherichia coli*. *J. Bacteriol.* **164**, 816–822.
27. Studier, F. W., Rosenberg, A. H., Dunn, J. J. & Dubendorff, J. W. (1990). Use of T7 RNA polymerase to direct expression of cloned genes. *Methods Enzymol.* **185**, 60–89.
28. Jiang, P. & Ninfa, A. J. (1999). Regulation of autophosphorylation of *Escherichia coli* nitrogen regulator II by the P_{II} signal transduction protein. *J. Bacteriol.* **181**, 1906–1911.
29. Kabsch, W. (2010). XDS. *Acta Crystallogr., Sect. D: Biol. Crystallogr.* **66**, 125–132.
30. Vagin, A. & Teplyakov, A. (1997). MOLREP: an automated program for molecular replacement. *J. Appl. Crystallogr.* **30**, 1022–1025.
31. Emsley, P. & Cowtan, K. (2004). Coot: model-building tools for molecular graphics. *Acta Crystallogr., Sect. D: Biol. Crystallogr.* **60**, 2126–2132.
32. Murshudov, G. N., Vagin, A. A. & Dodson, E. J. (1997). Refinement of macromolecular structures by the maximum-likelihood method. *Acta Crystallogr., Sect. D: Biol. Crystallogr.* **53**, 240–255.
33. Laskowski, R. A., Macarthur, M. W., Moss, D. S. & Thornton, J. M. (1993). Procheck—a program to check the stereochemical quality of protein structures. *J. Appl. Crystallogr.* **26**, 283–291.

D. Publication 3

Mechanism of 2-oxoglutarate signaling by the *Synechococcus elongatus* P_{II} signal transduction protein

Proc. Natl. Acad. Sci. U.S.A. (2010) 107, 19760-19765

Contribution to publication:

I performed, analysed and interpreted the following experiments:

- Cloning of the R9L and K58M P_{II} variants
- Overexpression and purification of the P_{II} and NAGK proteins
- SPR analysis
- Enzyme assays
- ITC analysis

I wrote the Materials and Methods section of the manuscript

Mechanism of 2-oxoglutarate signaling by the *Synechococcus elongatus* P_{II} signal transduction protein

Oleksandra Fokina[a], Vasuki-Ranjani Chellamuthu[b], Karl Forchhammer[a,1], and Kornelius Zeth[b,1]

[a]Interfakultäres Institut für Mikrobiologie und Infektionsmedizin der Eberhard-Karls-Universität Tübingen, Auf der Morgenstelle 28, 72076 Tübingen, Germany; and [b]Department of Protein Evolution, Max Planck Institute for Developmental Biology, Spemannstrasse 35, 72076 Tübingen, Germany

Edited by David L. Bain, University of Colorado Denver, Denver, CO, and accepted by the Editorial Board September 14, 2010 (received for review June 3, 2010)

P_{II} proteins control key processes of nitrogen metabolism in bacteria, archaea, and plants in response to the central metabolites ATP, ADP, and 2-oxoglutarate (2-OG), signaling cellular energy and carbon and nitrogen abundance. This metabolic information is integrated by P_{II} and transmitted to regulatory targets (key enzymes, transporters, and transcription factors), modulating their activity. In oxygenic phototrophs, the controlling enzyme of arginine synthesis, *N*-acetyl-glutamate kinase (NAGK), is a major P_{II} target, whose activity responds to 2-OG via P_{II}. Here we show structures of the *Synechococcus elongatus* P_{II} protein in complex with ATP, Mg^{2+}, and 2-OG, which clarify how 2-OG affects P_{II}–NAGK interaction. P_{II} trimers with all three sites fully occupied were obtained as well as structures with one or two 2-OG molecules per P_{II} trimer. These structures identify the site of 2-OG located in the vicinity between the subunit clefts and the base of the T loop. The 2-OG is bound to a Mg^{2+} ion, which is coordinated by three phosphates of ATP, and by ionic interactions with the highly conserved residues K58 and Q39 together with B- and T-loop backbone interactions. These interactions impose a unique T-loop conformation that affects the interactions with the P_{II} target. Structures of P_{II} trimers with one or two bound 2-OG molecules reveal the basis for anticooperative 2-OG binding and shed light on the intersubunit signaling mechanism by which P_{II} senses effectors in a wide range of concentrations.

metabolic signaling | nitrogen regulation | cyanobacteria | chloroplasts

The P_{II} proteins constitute one of the largest and most widely distributed family of signal transduction proteins present in archaea, bacteria, and plants. They control key processes of nitrogen metabolism in response to central metabolites ATP, ADP, and 2-oxoglutarate (2-OG), signaling cellular energy and carbon and nitrogen abundance (1–4). These effectors bind to P_{II} in an interdependent manner (see below), thereby transmitting metabolic information into structural states of this sensor protein (3, 5). Furthermore, P_{II} proteins may be posttranslationally modified (1, 6). Depending on the signal input states, P_{II} proteins bind and thereby regulate the activity of key metabolic and regulatory enzymes, transcription factors, or transport proteins (1–3). In cyanobacteria and plants, the controlling enzyme of arginine biosynthesis, *N*-acetyl-L-glutamate kinase (NAGK), is a major P_{II} target (7–9). Moreover, P_{II} affects gene expression in cyanobacteria through binding to the transcriptional coactivator of NtcA, PipX (10). In plants, acetyl-CoA carboxylase was recently shown to be regulated by P_{II}, providing an additional link between carbon and nitrogen regulation (11). Although these P_{II} targets share no common structural element, interaction with P_{II} is inhibited by 2-OG.

P_{II} proteins are homotrimers of 12- to 13-kDa subunits, built of a double ferredoxin-like fold-containing core (βαβ-βαβ), with a characteristic and highly conserved 3D structure, as revealed from numerous crystal structures (3, 12). The trimeric P_{II} architecture resembles a flattened barrel with long and flexible T loops extending outward, from the flat side (see Fig. 1 and Fig. S1). These T loops can adopt multiple conformations and mediate the versatile protein–protein interactions (3). Each subunit further comprises two small loops (B and C loop) in the intersubunit clefts, facing each other from opposing subunits and taking part in a unique mode of ATP-ADP binding (13–15). ADP and ATP compete here for the same site. In the presence of Mg-ATP, up to three 2-OG molecules can bind per trimer (1) with ADP antagonizing 2-OG binding (16). Notably, *Arabidopsis thaliana* P_{II} is an exception, because it binds 2-OG also in the presence of ADP (5, 17). Another feature characteristic for many P_{II} proteins is also intriguing: The three ATP-binding sites and the three 2-OG–binding sites each exhibit negative cooperativity. Anticooperativity implies strong conformational coupling between the subunits, and this feature probably allows P_{II} to sense a wide range of metabolite concentrations (5, 16, 18, 19). In contrast to the ATP-ADP–binding site, the 2-OG–binding site is controversial (3). From the crystal structure of a P_{II} paralogue from *Methanococcus jannaschii*, GlnK1, one 2-OG molecule was shown to bind from outside to the distal side of the T loop in the presence of Mg-ATP (20). By contrast, a recently published structure of a P_{II} homologue form *Azospirillum brasiliense* in complex with Mg-ATP and 2-OG revealed the 2-OG–binding site close to the base of the T loop and near the ATP-binding site (21). However, neither of these two structures was proved by biochemical studies nor could they explain the anticooperative binding of 2-OG.

The structures of complexes of P_{II} with its regulatory target NAGK from *Synechococcus elongatus* and *A. thaliana* are highly similar (22, 23), and the mode of interaction and regulation is apparently conserved in cyanobacteria and plants (24). The P_{II}–NAGK complex involves one hexameric (trimer of dimers) NAGK toroid sandwiched between two P_{II} trimers with the threefold axis aligned (23). Each P_{II} subunit engages two contact surfaces in NAGK binding: A smaller surface involves the B loop and a larger is formed by the T loop, which adopts a tightly bent conformation that fits into the interdomain crevice of NAGK. Binding of P_{II} enhances the catalytic activity of NAGK and alleviates feedback inhibition by arginine. To bind NAGK, free P_{II} has to contract its extended T loop. Recently, a two-step process of P_{II}–NAGK binding was proposed on the basis of the properties of a newly identified *S. elongatus* P_{II} variant (I86N), which mimics the P_{II} conformation in the NAGK-bound state (18): First, a salt bridge between P_{II}-E85 and NAGK-R233 forms,

Author contributions: K.F. and K.Z. designed research; O.F. and V.-R.C. performed research; O.F., K.F., and K.Z. analyzed data; and O.F., K.F., and K.Z. wrote the paper.

The authors declare no conflict of interest.

This article is a PNAS Direct Submission. D.L.B. is a guest editor invited by the Editorial Board.

Freely available online through the PNAS open access option.

Data deposition: The crystallography, atomic coordinates, and structure factors have been deposited in the Protein Data Bank, www.pdb.org (PDB ID codes 2XUL and 2XUN).

[1]To whom correspondence may be addressed. E-mail: karl.forchhammer@uni-tuebingen.de or kornelius.zeth@tuebingen.mpg.de.

This article contains supporting information online at www.pnas.org/lookup/suppl/doi:10.1073/pnas.1007653107/-/DCSupplemental.

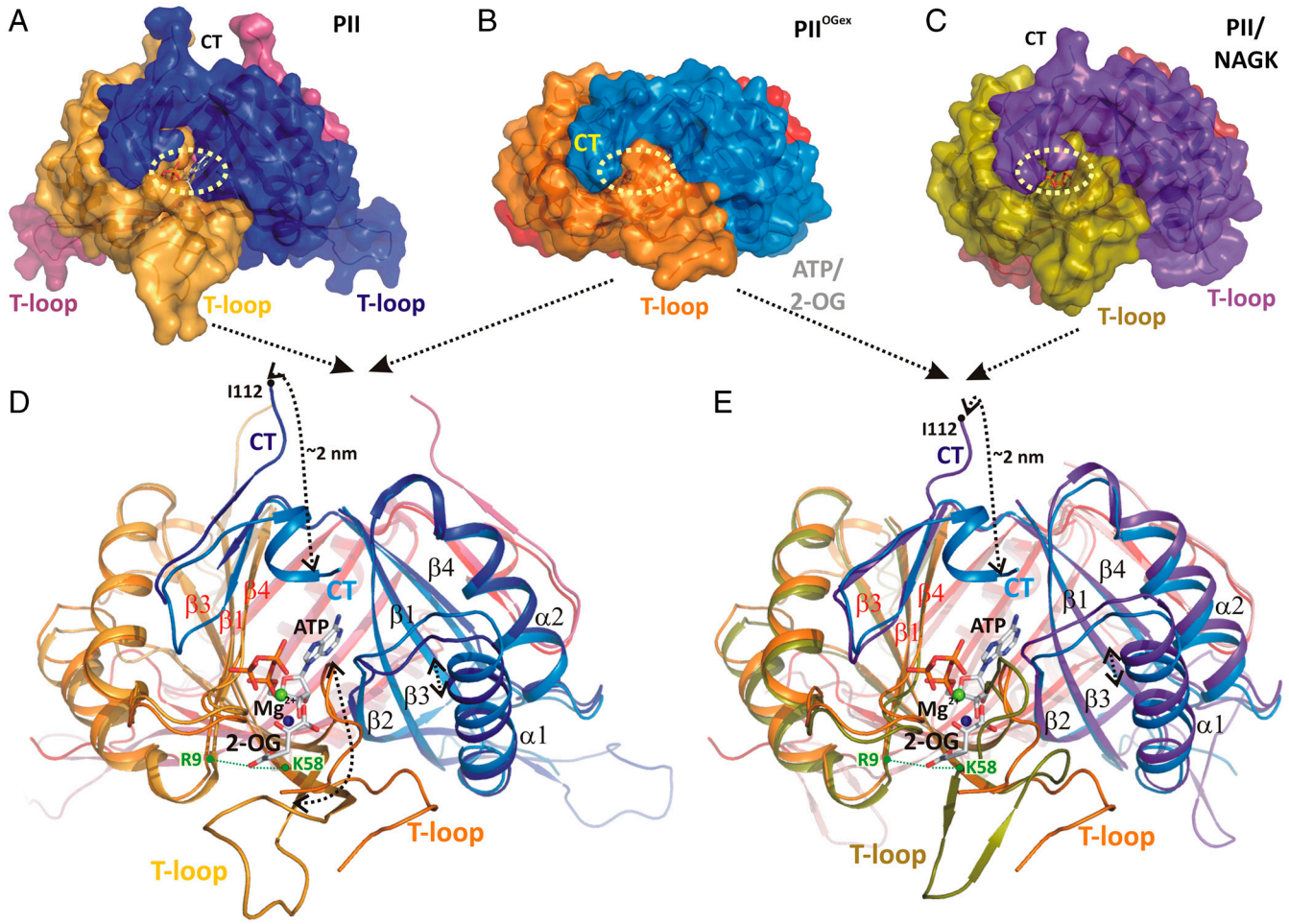

Fig. 1. Structural basis of P_{II} regulation by 2-oxoglutarate. (*A*–*C*) Side views of different *S. elongatus* P_{II} structures in surface representation. The location of the ATP-binding site is indicated by a yellow dashed circle; the red boxes highlight the structure part discussed detailed in *D*. (*A*) Ligand-free P_{II} modeled together with ATP (placed according to the superimposed P_{II}^{OGex} structure). The subunits are color coded in dark blue, light orange, and warm pink. The extended C termini and T loops of the proteins chains are marked CT and T-loop, respectively. (*B*) P_{II}/ATP/2-OG (P_{II}^{OGex}) complex structure; subunits color coded in orange, marine blue, and red. The structure adopts a compact conformation because of the back folding of the C terminus (CT) onto the core domain structure and the T loop observed in a partially disordered conformation. (*C*) Structure of P_{II} in the P_{II}–NAGK complex (PDB ID code: 2V5H) modeled together with ATP. Subunits are color coded in magenta, deep olive, and salmon. (*D*) Superposition of the ligand-free P_{II} and P_{II}^{OGex} structure as ribbon models in the color codes derived from *A* and *B*. Secondary structure elements are marked with β1–β5 and α1–α2 and ATP and 2-OG are shown in stick representation, whereas the Mg ion is marked in green. The sites of two mutations, R9L and K58M, introduced to prove the binding mode of 2-OG are marked with green dots. Remarkable conformational transitions are marked with dashed lines: movement of the C terminus, a shift of helix 1, and displacement of the T-loop base by 2-OG while the tip becomes disordered. (*E*) Superposition of P_{II}^{OGex} and P_{II}–NAGK structures as ribbon models in the color codes derived from *B* and *C*. Structural details are indicated as in *D*.

triggering the extended T loop to fold into the tightly bent conformation that fits into NAGK.

Detailed structural information together with the well-studied biochemical features and highly sensitive complex formation assays render the P_{II}–NAGK system ideal to study the transduction of metabolic signals into protein action. Until now, it was unclear how the 2-OG signal, perceived by P_{II}, results in inhibition of P_{II}–NAGK complex formation. To answer this question, we solved structures of P_{II} with ATP, Mg^{2+}, and 2-OG, revealing the mechanism by which the 2-OG signal is perceived by P_{II} and controls receptor interactions.

Results

Structure of P_{II} in Complex with ATP and 2-OG. Crystals of recombinant P_{II} protein from *S. elongatus* were obtained in the presence of excess 2-OG/Mg-ATP (P_{II}^{OGex}) and at substoichiometric amounts of 2-OG (P_{II}^{OG1-3}) (Table S1). All structures were solved by molecular replacement using the free *S. elongatus* P_{II} as a model [Protein Data Bank (PDB) ID code 1QY7]. The P_{II}^{OGex} crystal diffracting to 2.2 Å contains two identical trimers in the asymmetric unit (with an rmsd of 0.2 $Å^2$ for all C atoms superposed). Each trimer contains three Mg^{2+}, ATP, and 2-OG molecules. In Fig. 1, this structure is compared to the structures of ligand-free P_{II} (14) and P_{II} in complex with NAGK (23). In the ligand-free structure, the T loop, and the C terminus adopt highly extended conformations away from the ATP-binding site (see Fig. 1 *A* and *D*). Here, P_{II} offers an open binding cavity volume of approximately 1,000 $Å^3$ for the ligands. Upon ATP and 2-OG binding, a significant conformational change in the T loop and the C terminus occurs: The C-terminal β-sheet of the free form moves toward the ATP-binding site by up to 20 Å (for the terminal residue I112) to change into a small helix (see Fig. 1*D*). The T loop contracts and the tip (from residues 44–50) becomes disordered. Part of the flexible T loop moves toward the ATP-binding site to form a kink-like structure (residues 36–41), thereby forming the scaffold for proper ATP and 2-OG assembly. As a result, the ATP/2-OG–binding cavity is completely enclosed by this unique T-loop conformation and the movement of the C terminus (see Fig. 1*B*, yellow

circle). In the P_{II} structure complexed with NAGK, the T loop is clamped in a different conformation (see Fig. 1 *C* and *E*). Here, access to the ligand-binding cavity is slightly reduced compared to the ATP-free form because of a bend in the T-loop conformation, thereby reducing the cavity volume to about 600 $Å^3$.

The 2-OG–binding site of P_{II} is formed by an ATP-chelated Mg^{2+} ion and residues from one side of the intersubunit cleft (Fig. 2). The ATP molecule bound in the intersubunit cleft is ligated mainly by arginine residues (R38 from monomer A; R101 and R103 from monomer B) together with K90 from monomer A and a small number of hydrogen bonds. ATP fixed by these residues forms the scaffold for Mg^{2+}-mediated binding of 2-OG. The Mg^{2+} ion has an almost perfect hexagonal coordination sphere of oxygen atoms, three of which are contributed by oxo groups of the α-, β-, and γ-phosphate of ATP. Two additional ligating atoms are accounted for by the O2 and O5 of 2-OG. The last coordination position is contributed by the OE1 atom of residue Q39. Notably, the 2-OG–binding sphere mainly comprises residues from the T loop. Backbone atoms from residues Q39, K40, and G41 (all contacting O1 or O2 of 2-OG) together with the Q39 side-chain ligate the O5 atom and form one area of interactions. A second interaction region is composed of the backbone nitrogen of G87 (forming a second H bridge to O5) and a strong salt bridge of K58 toward the O3 and O4 atoms (distance of 2.7 Å). Furthermore, residue R9 approaches the O4 to 3.5 Å. All these residues with the exception of K40 are highly conserved in P_{II} proteins (4) (Fig. S1).

To validate that 2-OG in the crystal occupies the true binding site, P_{II} variants were constructed, in which residues K58 and R9, whose side chains according to the P_{II}^{OGex} structure specifically interact with 2-OG, were replaced by similar-sized uncharged residues (K58M and R9L). Binding of 2-OG in the presence of Mg-ATP was determined by isothermal calorimetry (ITC). Indeed, the P_{II} K58M variant was completely unable to bind 2-OG, although ATP could still be bound, showing that the loss of 2-OG binding is a specific effect of the K58 replacement. In further agreement with the structural prediction, the P_{II} R9L variant was strongly impaired in 2-OG binding (Table 1). Moreover, both P_{II} variants were impaired in NAGK binding, confirming that K58 is indeed pivotal for folding the T loop in the tightly bent structure. The R9 side chain is near the contact surface to NAGK and appears to stabilize the B-loop–T-loop interface (23) (Fig. S2).

Structural Basis of Sequential/Anticooperative 2-OG Binding. Crystallization of P_{II} protein in the presence of low 2-OG amounts yielded P_{II} structures with differing 2-OG content. The structure resolved at a resolution of 1.95 Å contains three P_{II} trimers in the asymmetric unit; one trimer contained three ATP, one Mg^{2+}, and one 2-OG (P_{II}^{OG1}), the second three ATP, two Mg^{2+}, and two 2-OG (P_{II}^{OG2}), and the third three each ATP, Mg^{2+}, and 2-OG (P_{II}^{OG3}) (Fig. 3 and Fig. S3). Additional details of structural parameters are given in *SI Text* (Tables S1 and S2). Binding of 2-OG does not significantly render the *B*-factor distribution of the three monomers significantly, unless the mobile elements (C terminus and T loop) contributing to binding are involved (Fig. S4). A superimposition of the three structurally similar trimers (Fig. 3 *A* and *B*) reveals the structure identity of the S1 site, which is occupied by 2-OG in all three P_{II}^{OG1-3} trimers, and the divergence in the S2 and S3 sites, respectively (Fig. 3*B*). The ligands are bound in S1 identical in topology to the mode described for the P_{II}^{OGex} structure (Figs. 2 and 3*B*). The P_{II}^{OG1} structure reveals that binding of the first 2-OG molecule to P_{II} (S1 site) generates unequal ligand-binding sites in the adjacent monomers, and, remarkably, sites not occupied by 2-OG also lack the Mg^{2+} ion. The conformational differences in the nonoccupied binding sites provide a structure-based explanation for the anticooperativity observed in biochemical experiments: After occupation of the first site, the K_d for the second site increases slightly, but after occupation of the second site, the K_d for the third site increases strongly (about 20-fold higher than the K_d for the first site; see Table 1). In P_{II}^{OG1}, the ATP molecule attached to the S2 site exhibits a significantly altered conformation of the phosphate moiety (Fig. 3 *B–D*); furthermore, the T-loop basis is displaced and the C terminus is ordered similar to the S1 site (Fig. 3 *C* and *D*). The S2 site in P_{II}^{OG1} resembles the S3 site of the P_{II}^{OG2} structure, which, according to the sequential 2-OG–binding mode, corresponds to the lowest affinity site (for detailed comparison of the binding sites, see Fig. S3). The S3 site of P_{II}^{OG2} exhibits further changes, visible most significantly in the T loop, the C terminus, and a small distortion in the β4-strand. Together these changes can lead to the strongly altered affinity of 2-OG toward the stereochemically differing S2 and S3 sites.

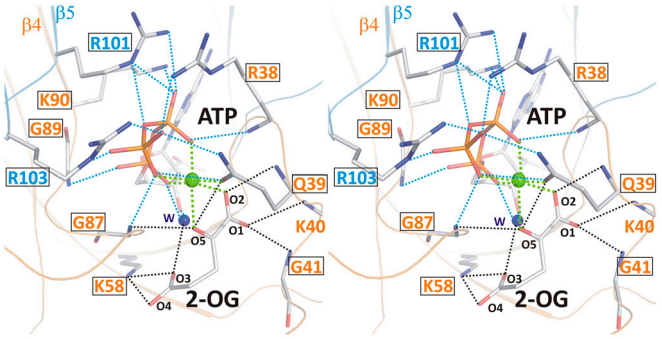

Fig. 2. Stereo image of the 2-OG–binding site. Residues involved in binding of 2-OG (atoms are marked with small numbers) and the hydrophilic portion of ATP are numbered according to the sequence. Cofactors as well as side- and main-chain atoms are marked in stick representation; Mg^{2+} is marked as a green sphere. Colors of residue numbers (orange and blue) correspond to those of the respective subunits. Residues conserved in standard alignments are boxed. Dashed blue lines represent bonds between residues and ATP and black lines indicate bonds for the ligation of 2-OG, whereas green lines mark the hexagonal coordination of the Mg^{2+} ion.

Table 1. Effector molecule binding to P_{II} variants R9L and K58M

	K_d1, μM	K_d2, μM	K_d3, μM
2-OG (+1 mM ATP)			
R9L	441 ± 40	123 ± 7	509 ± 116
K58M	ND	ND	ND
(WT)	(5.1 ± 4.0)	(11.1 ± 1.8)	(106.7 ± 14.8)
ATP			
R9L	NM	NM	NM
K58M	10 ± 5	262 ± 136	31 ± 15
(WT)	(4.0 ± 0.1)	(12.5 ± 0.9)	(47.4 ± 21.9)

Values correspond to the mean of two independent experiments ±SEM. The raw data were fitted by using a three-site binding model for a P_{II} trimer. For comparison, the original data for WT P_{II} protein are given in parentheses. ND, not detectable; NM, not measured.

Effect of 2-OG on the Dissociation of the P_{II}–NAGK Complex. The structure of the P_{II} Mg-ATP/2OG complex suggests that 2-OG prevents interaction of P_{II} with NAGK by hindrance of the T loop folding into the tightly bent conformation needed for NAGK binding: The NAGK-bound P_{II} structure involves a salt bridge between K58 and E44 (18, 23), but because K58 is an important ligand for 2-OG, formation of this salt bridge is prevented. Furthermore, binding of 2-OG introduces a significant bend in the backbone of residues 38–43 (Fig. 1*E*) and together with the side chain of residue 42 induces a new T-loop conformation, which is incompatible with NAGK binding. When the P_{II}–NAGK complex has already been formed, is 2-OG still able to bind to P_{II} and antagonize the P_{II}–NAGK complex? Because this issue has not yet been investigated, the dissociation of the P_{II}–NAGK complex by 2-OG was studied. First, complex dissociation was directly

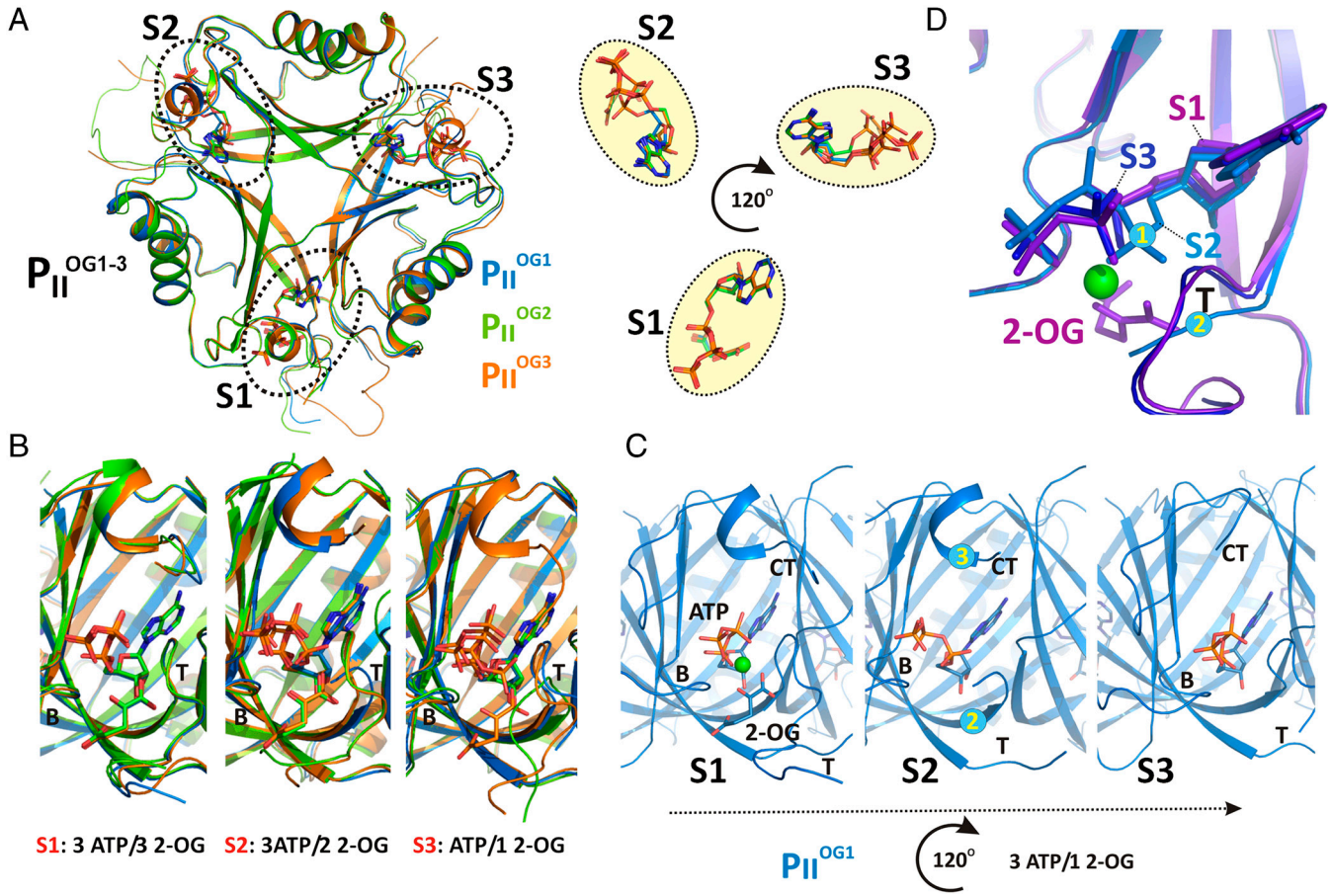

Fig. 3. Anticooperativity of 2-OG–binding sites. (*A*) Top view of the P_{II}^{OG} structure as a ribbon plot and superposition of the P_{II}^{OG1} (in blue), P_{II}^{OG2} (in green), and P_{II}^{OG3} (in orange) structures. The three ATP/2-OG–binding sites are marked by dashed circles and numbered (S1, S2, and S3). The picture on the right represents the cofactors bound in the individual sites (highlighted in yellow) with three ATP and 2-OG molecules in S1, three ATP and two 2-OG molecules in S2, and three ATP and one 2-OG molecules located in S3, respectively. The clockwise consecutive 120° binding into S1 → S2 → S3 sites is shown by an arrow. (*B*) Zoom in (side view) of the three binding sites after superposition of the molecules. The content of the individual binding sites is marked below the picture. T and B loops are marked with T and B, respectively, for clarity. (*C*) Binding sites S1, S2, and S3 of the P_{II}^{OG1} structure. In the S1 site, ATP, 2-OG, and Mg^{2+} (green sphere) are bound, whereas S2 and S3 contain only ATP and no Mg^{2+}. Significant changes in the C terminus and the T loop in site S2 are marked with numbered circles. (*D*) Superposition of effector molecules bound to sites S1, S2, and S3 in the P_{II}^{OG1} structure. The ATP molecule observed in the S2 site is significantly distorted relative to that in S1 and S3.

recorded by surface plasmon resonance (SPR) spectroscopy (Fig. 4*A*). The P_{II}–NAGK complex was formed on the sensor chip, and, subsequently, 2-OG was injected (Fig. 4*A*, arrow) to dissociate the complex. No dissociation was observed in the presence of Mg-ATP alone; with 0.5 mM 2-OG, the complex decayed slowly with a rate of 1.8×10^{-3} s^{-1}. With 1 mM 2-OG the decay rate increased to 9.0×10^{-3} s^{-1} and at 3 mM 2-OG to 28.6×10^{-3} s^{-1}. By comparison, association of the complex was inhibited by much lower 2-OG concentrations, with an IC_{50} of approximately 130 μM (18). In the second assay, the catalytic activity of NAGK/P_{II} in the presence of 50 μM arginine as an indicator of the degree of complex formation (24) was assayed (Fig. 4*B*). When 2-OG was added after formation of the P_{II}–NAGK complex, the inhibitory 2-OG concentration had an IC_{50} of 0.9 mM. By contrast, addition of 2-OG to P_{II} prior to the addition of NAGK inhibited the activity with an IC_{50} for 2-OG of approximately 120 μM (Fig. 4*B*, *Inset*) (18). Thus, 2-OG is able to dissociate the P_{II}–NAGK complex; however, one order of magnitude higher 2-OG concentrations are required to achieve dissociation compared to those required to inhibit association.

Discussion

The structures presented here explain the known features of P_{II}-mediated 2-OG signaling: A Mg^{2+} ion, chelated by the phosphates of ATP, ligates carboxylate oxygens of 2-OG, and, therefore, Mg-ATP binding is the prerequisite for 2-OG binding to P_{II}. Binding of 2-OG to *A. thaliana* P_{II} in the presence of Mg-

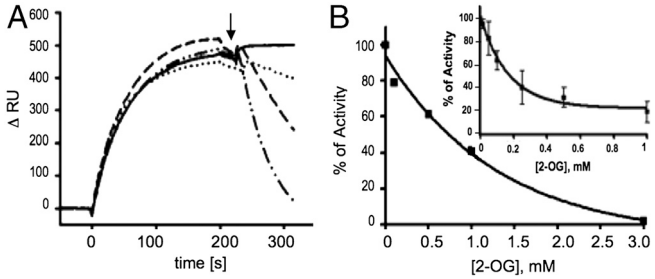

Fig. 4. The 2-OG effect on P_{II}–NAGK complex dissociation. (*A*) SPR analysis of 2-OG-induced dissociation of NAGK–P_{II} complex in the presence of 1 mM ATP. The response difference (ΔRU) between flow cells FC2 and FC1 (control) is shown. After binding of 100 nM P_{II} to NAGK in FC2, a mixture of 1 mM ATP, 1 mM $MgCl_2$, and 2-oxoglutarate [at a concentration of 0 (solid line), 0.5 (dotted line), 1 (dashed line), and 3 mM (dot-dashed line), as indicated] was injected at the point indicated by an arrow. (*B*) The effect of 2-OG on NAGK activity in the presence of 50 μM arginine. Increasing 2-OG concentrations were added to reaction mixtures after the formation of the P_{II}–NAGK complex, and NAGK activity was determined as detailed in *Materials and Methods*. (*Inset*) Effect of 2-OG on NAGK activity in the presence of P_{II}, when 2-OG was preincubated with P_{II}.

ADP could involve additional residues, possibly from its prolonged C-terminal segment, which contacts the effector molecule-binding site (22). The fact that all residues revealed here to be involved in 2-OG binding are highly conserved among P_{II} proteins (see also Fig. S1) strongly suggests that the reported mode of 2-OG binding could apply to all P_{II} proteins. The only contradiction is the previously reported structure of the P_{II} family member GlnK1 from *M. jannaschii*, where 2-OG bound from outside to the apex of a bent T loop (20). Because no biochemical evidence to support this binding mode was provided, it remains to be clarified whether this 2-OG binding mode is a peculiarity of the archaeal P_{II} protein or whether this mode of binding resulted from special crystallization conditions. In contrast, a recently described structure of the P_{II} homologue GlnZ from the proteobacterium *A. brasiliense* in complex with Mg-ATP and 2-OG revealed a mode of 2-OG binding, which is highly similar to the 2-OG binding described here, in particular the involvement of the Mg^{2+} ion and the highly conserved key residues Q39 and K58 (21). This one and our P_{II} structures perfectly agree with the properties of *S. elongatus* P_{II} variants bearing mutations in residues R9 and K58 described in this work and with the previously described I86N variant, displaying a closed 2-OG–binding site (18). Furthermore, they agree with previously reported properties of other P_{II} mutant variants. For instance, a Q39 mutation was shown to strongly impair 2-OG binding, whereas a deletion of the apical T-loop residues did not prevent 2-OG binding to *Escherichia coli* P_{II} (25). Furthermore, a K58 substitution abolished 2-OG signaling in *Rhodospirillum rubrum* P_{II} (26). Moreover, the actual structure reveals how precisely the carboxylate oxygens of 2-OG are probed by Mg^{2+} coordination and by interactions with protein backbone and side-chain atoms, explaining the high selectivity of P_{II} proteins for 2-OG (1, 16, 19). All together, these evidences strongly imply that the mode of 2-OG binding described here can be generalized for P_{II} proteins.

It has been shown that 2-OG controls P_{II} target interactions that involve the T loop, with X-ray structural information available for the *S. elongatus* and *A. thaliana* P_{II}–NAGK complex (22, 23), the *S. elongatus* P_{II}–PipX complex (27), and the *E. coli* GlnK–AmtB complex (28, 29). The mechanism of 2-OG-mediated P_{II}-target control was clarified here with the cognate P_{II}–NAGK complex. When P_{II} binds 2-OG, the base of the T loop (R38-G41) wraps around this metabolite, thereby adopting a unique retracted conformation. Furthermore, residues K58 and R9, which are involved in folding the T loop into the tightly bent conformation that fits into the NAGK crevice, perform ionic and H-bond interactions with the 2-OG γ-carboxylate oxygens, preventing formation of this fold. The IC_{50} for 2-OG to inhibit P_{II}–NAGK association (120–130 μM, depending on the method) matches the dissociation constant of the third, low-affinity 2-OG–binding site (approximately 110 μM). This correlation implies that all three sites in P_{II} have to be occupied by 2-OG in order to inhibit NAGK binding. Consequently, P_{II} partially loaded with 2-OG should be able to bind NAGK, whereby 2-OG should be displaced from P_{II}. The driving force squeezing out 2-OG could be provided by the encounter complex between P_{II} and NAGK, which, according to a recent analysis, could be formed by an ionic interaction of the B-loop residue E85 of P_{II} with R233 of NAGK (18).

The present study also revealed how 2-OG dissociates the P_{II}–NAGK complex. As shown in Fig. 1*C*, 2-OG can access its binding site from the P_{II} periphery, which is not shielded by NAGK in the complex. However, approximately 10-fold higher concentrations of 2-OG are required to dissociate the P_{II}–NAGK complex than to inhibit its association. The difference could be explained by the 2-OG–binding site being closed in the P_{II}–NAGK complex by the tightly bent T loop. The 2-OG should unlock this compact conformation to gain access to its binding site, and this process probably requires much higher concentrations than binding to the open sites, which are accessible when P_{II} is not attached to NAGK.

The structure of the second cyanobacterial P_{II} target complex, P_{II}–PipX, has been determined recently (27). It reveals three PipX molecules bound on the flat bottom surface of the P_{II} body (orientation of Fig. 1), trapped between vertically extended T loops whose tip residues grasp the PipX monomers. Notably, this extended T-loop conformation is incompatible with the T-loop fold imposed by Mg-ATP-2-OG binding (see structure overlay in Fig. S5). Binding of 2-OG to the P_{II}–PipX complex will retract the extended T loop, releasing the bound PipX molecules, which explains the biochemical data, showing that binding of PipX to P_{II} is antagonized by Mg-ATP/2-OG (10). A similar antagonistic mechanism of Mg-ATP/2-OG can be assumed for the complex of the P_{II} family member GlnK with the ammonium transport channel AmtB, as deduced from the complex structure of the *E. coli* proteins (28, 29). In complex with AmtB, the T loop is in a vertically extended structure, resembling the T loop of *S. elongatus* P_{II} in complex with PipX. In the AmtB complex, GlnK residue Q39 interacts with K58 and ADP is bound to the adenylate-binding pocket (28, 29). Given that the binding mode of Mg-ATP/2-OG to GlnK is identical as outlined above, the resulting T-loop conformation will be incompatible with formation of the GlnK–AmtB complex (21). Studies with other *E. coli* P_{II} receptors such as NtrB imply that 2-OG does not always inhibit complex formation, but it may affect receptor activity at a postbinding step (16). In this case, it is conceivable that receptor binding occurs apart from the T loop (like the B-loop interaction of P_{II} with NAGK) and the conformational changes of the T loop imposed by 2-OG binding to P_{II} are transduced into conformational changes in the receptor, thereby altering its activity.

P_{II} proteins are highly sophisticated devices for measuring the concentration of central metabolites ATP, ADP, and 2-OG in an interdependent manner. This study reveals the mechanisms underlying this process. Binding of one, two, or three 2-OG molecules generates, via intersubunit communication, distinct structural states of P_{II}. Intermolecular signaling is based on the highly conserved trimeric architecture of the P_{II} proteins. The β2-strands, which directly connect the three binding sites, could play an important role. Binding of 2-OG to one site affects the two neighboring sites asymmetrically, generating the anticooperativity that allows metabolite sensing in a wide concentration range. Moreover, the free site in clockwise orientation displays a characteristic T-loop structure. P_{II} receptors perceive the signal via intimate T-loop interactions, which affect binding or influence the receptor at a postbinding stage (16, 18). This mode of signal transduction by P_{II} is unique, and the complexity of interactions explains the remarkably high conservation of P_{II} proteins.

Materials and Methods

Full protocols are available in *SI Materials and Methods*.

Overexpression and Purification of Recombinant P_{II} and NAGK. The R9L and K58M variants were created with artificial *glnB* genes carrying the respective mutations and cloned into the Strep-tag fusion vector pASK-IBA3 (IBA) after restriction with BsaI as described previously (7). Overexpression of wild-type and mutant *S. elongatus glnB* in *E. coli* RB9060 (30) and purification of recombinant P_{II} proteins with a C-terminal-fused Strep-tag II peptide were performed according to Heinrich et al. (7). His_6-tagged recombinant NAGK from *S. elongatus* was overexpressed in *E. coli* strain BL21(DE3) (31) and purified as reported previously (8).

SPR Detection. SPR experiments were performed by using a BIAcore X biosensor system (GE Healthcare) at 25 °C in Hepes-buffered saline-Mg buffer as described previously (8). In order to analyze the effect of 2-OG on the dissociation of the P_{II}–NAGK complex, 100 nM P_{II} was first bound to immobilized His_6–NAGK in flow cell 2 (FC2) (ascending curves). Subsequently, 50 μL buffer containing 1 mM ATP and different concentrations of 2-OG was injected (start of injection indicated by the arrow). Binding and dissociation

of P_{II} to NAGK was recorded as the response signal difference (ΔRU) of FC2-FC1; FC1, reference cell without His_6–NAGK.

ITC. ITC experiments were performed on a VP-ITC microcalorimeter (MicroCal, LCC) in ITC buffer containing 10 mM Hepes-NaOH, pH 7.4, 50 mM KCl, 50 mM NaCl, and 1 mM $MgCl_2$ at 20 °C as described previously (18). For determination of ATP- and 2-OG–binding isotherms for P_{II} variants R9L and K58M, solutions with different protein concentration were titrated with 1 mM ATP or 4 mM 2-OG (in the presence of 1 mM ATP). The binding isotherms were calculated from received data and fitted to a three-site binding model using the MicroCal ORIGIN software (Northampton) as indicated.

Coupled NAGK Activity Assay. Activity of NAGK was assayed by a coupled assay (32) with modifications as described previously (24), in the buffer consisting of 50 mM imidazole, pH 7.5, 50 mM KCl, 20 mM $MgCl_2$, 0.4 mM NADH, 1 mM phosphoenolpyruvate, 10 mM ATP, 0.5 mM DTT, 11 U lactate dehydrogenase, 15 U pyruvate kinase, 50 μM arginine, 1.2 μg P_{II}, and 3 μg NAGK. The mixture was preincubated for 3 min to allow P_{II}–NAGK complex formation. Then the reaction was started by the addition of 50 mM NAG and 2-OG (to determine the effect of increasing 2-OG concentrations on disruption of P_{II}–NAGK complex in the presence of NAGK-inhibiting concentrations of arginine). Then, 20 s after addition of substrate, the change in absorbance at 340 nm was recorded for 10 min. Linear kinetics were observed over that period of time.

Crystallization of Recombinant *S. elongatus* P_{II} Protein. Crystallization was performed with the sitting-drop technique by mixing 400 nL of the protein solution with equal amounts of the reservoir solution by using the honeybee robot (Genomic Solutions Ltd). Drops were incubated at 20 °C, and pictures were recorded by the RockImager system (Formulatrix). The crystallization buffer was composed of 10 mM Tris (pH 7.4), 0.5 mM EDTA, 100 mM NaCl, 1% glycerol, and 2 mM ATP-Mg, and also 2 mM 2-OG was added; crystals appeared in a precipitant condition containing PEG 4000. Glycerol was used as the cryoprotectant, and the crystals were flash-frozen in liquid nitrogen. Diffraction data were collected at the Swiss Light Source. Diffraction images were recorded on a MarCCD camera 225 (Marresearch), and images were processed by using the XDS/XSCALE software (33). The structure was solved by molecular replacement using the program Molrep (34). Rebuilding of the structure and structure refinement was performed by using the programs Coot and Refmac (35, 36). The quality of the structure was analyzed by the Procheck program (37). Figures were generated by using PyMOL (www.pymol.org).

ACKNOWLEDGMENTS. We thank Gary Sawers for critically reading the manuscript. The help of Reinhard Albrecht in crystallization of P_{II} proteins and Christina Herrmann for technical assistance is gratefully acknowledged. This work was strongly supported by the Max Planck Society and the PXII Beamline personnel and grants from the Deutsche Forschungsgemeinschaft (Fo195).

1. Ninfa AJ, Jiang P (2005) P_{II} signal transduction proteins: Sensors of alpha-ketoglutarate that regulate nitrogen metabolism. *Curr Opin Microbiol* 8:168–173.
2. Leigh JA, Dodsworth JA (2007) Nitrogen regulation in bacteria and archaea. *Annu Rev Microbiol* 61:349–377.
3. Forchhammer K (2008) P(II) signal transducers: Novel functional and structural insights. *Trends Microbiol* 16:65–72.
4. Sant'Anna FH, et al. (2009) The P_{II} superfamily revised: A novel group and evolutionary insights. *J Mol Evol* 68:322–336.
5. Jiang P, Ninfa AJ (2007) *Escherichia coli* P_{II} signal transduction protein controlling nitrogen assimilation acts as a sensor of adenylate energy charge in vitro. *Biochemistry* 46:12979–12996.
6. Forchhammer K (2004) Global carbon/nitrogen control by P_{II} signal transduction in cyanobacteria: From signals to targets. *FEMS Microbiol Rev* 28:319–333.
7. Heinrich A, Maheswaran M, Ruppert U, Forchhammer K (2004) The *Synechococcus elongatus* P_{II} signal transduction protein controls arginine synthesis by complex formation with *N*-acetyl-L-glutamate kinase. *Mol Microbiol* 52:1303–1314.
8. Maheswaran M, Urbanke C, Forchhammer K (2004) Complex formation and catalytic activation by the P_{II} signaling protein of *N*-acetyl-L-glutamate kinase from *Synechococcus elongatus* strain PCC 7942. *J Biol Chem* 279:55202–55210.
9. Burillo S, Luque I, Fuentes I, Contreras A (2004) Interactions between the nitrogen signal transduction protein P_{II} and *N*-acetyl glutamate kinase in organisms that perform oxygenic photosynthesis. *J Bacteriol* 186:3346–3354.
10. Espinosa J, Forchhammer K, Burillo S, Contreras A (2006) Interaction network in cyanobacterial nitrogen regulation: PipX, a protein that interacts in a 2-oxoglutarate dependent manner with P_{II} and NtcA. *Mol Microbiol* 61:457–469.
11. Feria Bourrellier AB, et al. (2010) Chloroplast acetyl-CoA carboxylase activity is 2-oxoglutarate-regulated by interaction of P_{II} with the biotin carboxyl carrier subunit. *Proc Natl Acad Sci USA* 107:502–507.
12. Helfmann S, Lu W, Litz C, Andrade SL (2010) Cooperative binding of MgATP and MgADP in the trimeric P_{II} protein GlnK2 from *Archaeoglobus fulgidus*. *J Mol Biol* 402:165–177.
13. Xu Y, et al. (1998) GlnK, a P_{II}-homologue: Structure reveals ATP binding site and indicates how the T-loops may be involved in molecular recognition. *J Mol Biol* 282:149–165.
14. Xu Y, et al. (2003) The structures of the P_{II} proteins from the cyanobacteria *Synechococcus* sp. PCC 7942 and *Synechocystis* sp. PCC 6803. *Acta Crystallogr, Sect D: Biol Crystallogr* 59:2183–2190.
15. Sakai H, et al. (2005) Crystal structures of the signal transducing protein GlnK from *Thermus thermophilus* HB8. *J Struct Biol* 149:99–110.
16. Jiang P, Ninfa AJ (2009) Alpha-ketoglutarate controls the ability of the *Escherichia coli* P_{II} signal transduction protein to regulate the activities of NRII (NtrB) but does not control the binding of P_{II} to NRII. *Biochemistry* 48:11514–11521.
17. Smith CS, Weljie AM, Moorhead GB (2003) Molecular properties of the putative nitrogen sensor P_{II} from *Arabidopsis thaliana*. *Plant J* 33:353–360.
18. Fokina O, Chellamuthu VR, Zeth K, Forchhammer K (2010) A novel signal transduction protein P(II) variant from *Synechococcus elongatus* PCC 7942 indicates a two-step process for NAGK-P(II) complex formation. *J Mol Biol* 399:410–421.
19. Forchhammer K, Hedler A (1997) Phosphoprotein P_{II} from cyanobacteria—analysis of functional conservation with the P_{II} signal-transduction protein from *Escherichia coli*. *Eur J Biochem* 244:869–875.
20. Yidiz Ö, Kalthoff C, Raunser S, Kühlbrandt W (2007) Structure of GlnK1 with bound effectors indicates regulatory mechanism for ammonia uptake. *EMBO J* 26:589–599.
21. Truan D, et al. (2010) A new P_{II} protein structure identifies the 2-oxoglutarate binding site. *J Mol Biol* 400:531–539.
22. Mizuno Y, Moorhead GB, Ng KK (2007) Structural basis for the regulation of *N*-acetylglutamate kinase by P_{II} in *Arabidopsis thaliana*. *J Biol Chem* 282:35733–35740.
23. Llacer JL, et al. (2007) The crystal structure of the complex of P_{II} and acetylglutamate kinase reveals how P_{II} controls the storage of nitrogen as arginine. *Proc Natl Acad Sci USA* 104:17644–17649.
24. Beez S, Fokina O, Herrmann C, Forchhammer K (2009) *N*-acetyl-L-glutamate kinase (NAGK) from oxygenic phototrophs: P_{II} signal transduction across domains of life reveals novel insights in NAGK control. *J Mol Biol* 389:748–758.
25. Jiang P, et al. (1997) Structure/function analysis of the P_{II} signal transduction protein of *Escherichia coli*: Genetic separation of interactions with protein receptors. *J Bacteriol* 179:4342–4353.
26. Jonsson A, Nordlund S (2007) In vitro studies of the uridylylation of the three P_{II} protein paralogs from *Rhodospirillum rubrum*: The transferase activity of *R. rubrum* GlnD is regulated by alpha-ketoglutarate and divalent cations but not by glutamine. *J Bacteriol* 189:3471–3478.
27. Llacer JL, et al. (2010) Structural basis for the regulation of NtcA-dependent transcription by proteins PipX and PII. *Proc Natl Acad Sci USA* 107:15397–15402.
28. Conroy MJ, et al. (2007) The crystal structure of the *Escherichia coli* AmtB-GlnK complex reveals how GlnK regulates the ammonia channel. *Proc Natl Acad Sci USA* 104:1213–1218.
29. Gruswitz F, O'Connell J, 3rd, Stroud RM (2007) Inhibitory complex of the transmembrane ammonia channel, AmtB, and the cytosolic regulatory protein, GlnK, at 1.96 A. *Proc Natl Acad Sci USA* 104:42–47.
30. Bueno R, Pahel G, Magasanik B (1985) Role of glnB and glnD gene products in regulation of the glnALG operon of Escherichia coli. *J Bacteriol* 164:816–822.
31. Studier FW, Rosenberg AH, Dunn JJ, Dubendorff JW (1990) Use of T7 RNA polymerase to direct expression of cloned genes. *Methods Enzymol* 185:60–89.
32. Jiang P, Ninfa AJ (1999) Regulation of autophosphorylation of Escherichia coli nitrogen regulator II by the P_{II} signal transduction protein. *J Bacteriol* 181:1906–1911.
33. Kabsch W (2010) XDS. *Acta Crystallogr, Sect D: Biol Crystallogr* 66:125–132.
34. Vagin A, Teplyakov A (1997) MOLREP: An automated program for molecular replacement. *J Appl Crystallogr* 30:1022–1025.
35. Murshudov GN, Vagin AA, Dodson EJ (1997) Refinement of macromolecular structures by the maximum-likelihood method. *Acta Crystallogr, Sect D: Biol Crystallogr* 53:240–255.
36. Emsley P, Cowtan K (2004) Coot: Model-building tools for molecular graphics. *Acta Crystallogr, Sect D: Biol Crystallogr* 60:2126–2132.
37. Laskowski RA, Macarthur MW, Moss DS, Thornton JM (1993) Procheck—a program to check the stereochemical quality of protein structures. *J Appl Crystallogr* 26:283–291.

E. Publication 4

Signal transduction protein P_{II} from *Synechococcus elongatus* PCC 7942 senses low adenylate energy charge *in vitro*

Biochemical Journal, in press

Contribution to publication:

I performed, analysed and interpreted all experiments with the exception of:

- Cloning of the heterotrimeric Strep-tagged P_{II} protein
- Purification of AGPR and PipX proteins
- AGPR-coupled assay measurements of the ADP effect on the NAGK activity in the absence of P_{II} and on NAGK inhibition by arginine alone.

I wrote the manuscript

Signal transduction protein P_{II} from *Synechococcus elongatus* PCC 7942 senses low adenylate energy charge *in vitro*.

Short title: Adenylate energy charge sensing by cyanobacterial P_{II} protein

Oleksandra Fokina, Christina Herrmann and Karl Forchhammer[1]

Interfakultäres Institut für Mikrobiologie und Infektionsmedizin der Eberhard-Karls-Universität Tübingen, Auf der Morgenstelle 28, 72076 Tübingen, Germany

Synopsis

P_{II} proteins belong to a family of highly conserved signal transduction proteins widely spread in bacteria, archaea and plants. They respond to the central metabolites ATP, ADP and 2-oxoglutarate (2-OG) and control enzymes, transcription factors and transport proteins involved in nitrogen metabolism. Here we studied the effect of ADP on *in vitro* P_{II} signalling properties from the cyanobacterium *Synechococcus elongatus*, a model for oxygenic phototrophic organisms. Different ADP/ATP ratios strongly affected the properties of P_{II} signalling. Increasing ADP antagonized the binding of 2-oxoglutarate and directly affected the interactions of P_{II} with its target proteins. The resulting P_{II} signalling properties indicate that in mixtures of ADP and ATP, P_{II} trimers are occupied with mixtures of adenylate nucleotides. Binding and kinetic activation of *N*-acetyl-L-glutamate kinase (NAGK) (the controlling enzyme of arginine biosynthesis) by P_{II} was weakened by ADP, but relief from arginine inhibition remained unaffected. On the other hand, ADP enhanced the binding of P_{II} to PipX, a co-activator of transcription factor NtcA and furthermore, antagonised the inhibitory effect of 2-OG on P_{II}-PipX interaction. These results indicate that *S. elongatus* P_{II} directly senses the adenylate energy charge, resulting in target-dependent differential modification of the P_{II} signalling properties.

Key words: metabolic signalling, nitrogen regulation, 2-oxoglutarate, P_{II} protein, energy charge, cyanobacteria

Abbreviations used: EC, energy charge; 2-OG, 2-oxoglutarate; NAGK, *N*-acetyl-L-glutamate kinase; SPR, surface plasmon resonance; ITC, isothermal titration calorimetry; FC, flow cell; RU, resonance units; NAG, *N*-acetyl-L-glutamate

[1]To whom correspondence should be addressed (email karl.forchhammer@uni-tuebingen.de)

Introduction

ATP in the cell provides energy for metabolic reactions, serves as a substrate for nucleotide synthesis and regulates cell metabolism as a signal molecule. The adenylate energy charge (EC), [(adenosine triphosphate) + (adenosine diphosphate)]/[(adenosine triphosphate) + (adenosine diphosphate) + (adenosine monophosphate)] is a measure of the energy available for metabolism [1]. Since in bacteria the concentration of AMP is constantly low, the adenylate energy charge depends mainly on the ATP/ADP ratio [2]. However, sensors of the adenylate energy charge have been poorly characterized. Recently the P_{II} signal transduction proteins have been suggested to be involved in EC measurement. They respond to ATP, ADP and 2-oxoglutarate (2-OG) by binding these effectors in an interdependent manner [3-7], thereby transmitting metabolic information into structural states of the P_{II} sensor protein [8, 9]. P_{II} when fully occupied by either ATP or ADP corresponds to non-physiological extremes of EC. To understand how P_{II} responds to physiologically relevant changes in EC, experiments must be conducted with different ATP/ADP ratios that span physiological conditions.

P_{II} signal transduction proteins are widely distributed in bacteria, archaea and the chloroplasts of eukaryotes, where they regulate metabolic and regulatory enzymes, transcription factors and/or transport proteins [4, 10-12]. In addition to responding to the metabolites ATP, ADP and 2-oxoglutarate (2-OG), P_{II} proteins can furthermore be subjected to signal-dependent reversible covalent modification, which occurs on the large surface exposed T-loop [10, 13]. P_{II} proteins are compact homotrimers with each subunit exposing three surface-exposed loops, termed T-loop, B-loop and C-loop [4]. The large T-loop is highly flexible and adopts different conformations, taking part in binding of effector molecules and being the dominating structure in protein-protein interactions. The B- and C-loops from opposite subunits are facing each other in the intersubunit cleft and take part in adenylate nucleotide binding [14-16]. The P_{II} trimer contains three adenylate nucleotide-binding sites, one in each intersubunit cleft, with ATP and ADP competing for the same site. In the presence of Mg^{2+}-ATP, up to three 2-OG molecules can bind to the protein at the base of the T-loop in direct vicinity of the beta and gamma-phosphate of ATP, which ligate 2-OG through a bridging Mg^{2+} ion [8-10]. Through this type of interaction, binding of ATP and 2-OG at one effector molecule binding site is synergistic towards each other. However, the three effector molecule binding sites exhibit negative cooperativity towards each other [3, 6, 17, 18]. The anticooperativity is mediated via intersubunit signalling [19]. First structural insight in this process was obtained recently for sequential 2-OG binding [8]. Occupation of the first, high affinity site, creates structural differences in the two neighboring sites, with one site displaying a clear distortion in the conformation of the bound ATP molecule. The anticooperativity in the binding of the effector results in a subsensitive response of this stimulatory effect, which is ideal for accurate detection of a wide range of metabolite concentrations.

Adenyl nucleotide binding seems to be highly similar in all P_{II} proteins from the three domains of life. In bacterial P_{II} proteins, ADP generally does not support 2-OG binding [3, 7], whereas in a plant P_{II} protein (*Arabidopsis thaliana*) 2-OG binding was supported both by ATP and ADP [20]. Effects of different ADP/ATP ratios have so for only been studied *in vitro* with *E. coli* P_{II} protein [3, 18]. Increasing ADP levels act antagonistically to 2-OG in the UTase/UR-P_{II}-NRII-NRI signal transduction cascade *in vitro*. Furthermore, ADP acts through P_{II} as an activator of ATase catalyzed glutamine synthetase adenylylation in the ATase-GS monocycle. On the other hand, the uridylylation of P_{II} by UTase is negatively influenced by ADP [3]. ADP increases the stability of the complex of the P_{II}-family protein GlnK with the ammonium channel AmtB and antagonizes the effect of 2-OG, pointing at the P_{II} sensing of the adenylate energy charge [7]. In the photosynthetic bacterium *Rhodospirillum rubrum,* three P_{II} homologues are involved in the regulation of the transcription activator NifA and the DRAT/DRAG system for the posttranslational regulation of nitrogenase activity [21-23]. The DRAT/DRAG system responds to the energy state, pointing towards a connection of P_{II} with the energy status in the cell [22]. However, there is only slight

impact of low ATP levels alone on the P_{II} regulation of both processes, supposedly, the ratio of ADP/ATP is significant this response [5].
In cyanobacteria P_{II} is involved in nitrate utilization [24, 25], regulation of gene expression by sequestering the co-activator PipX of the general transcription factor NtcA [26-28], and in arginine biosynthesis by regulating the controlling enzyme, *N*-acetyl-L-glutamate kinase (NAGK) [29, 30]. Binding of P_{II} from the cyanobacterium *Synechococcus elongatus* enhances the activity of NAGK and relieves it from feedback inhibition by arginine [31]. In higher plants, P_{II} also regulates NAGK [32] and, moreover, *A. thaliana* P_{II} binds and inhibits a key enzyme of fatty acid metabolism, acetyl-CoA carboxylase [33], representing another link between P_{II} and carbon metabolism. The structure of the P_{II}-NAGK complex, NAGK regulation by P_{II} and its response towards 2-OG are highly conserved between higher plants and cyanobacteria [34-36]. In the presence of Mg^{2+}-ATP, 2-OG strongly inhibits P_{II}-NAGK complex formation. Whereas in cyanobacteria, Mg^{2+}-ATP alone has only a slight effect on complex formation [6, 31], it favours the binding of P_{II} to NAGK in *A. thaliana* [20]. ADP accelerates the dissociation of the cyanobacterial proteins but has no major effect on the *A. thaliana* proteins [36].
The *S. elongatus* P_{II} protein is subjected to phosphorylation and dephosphorylation in response to the cellular 2-OG and ATP levels [37]. *In vitro*, high concentrations of 2-OG in presence of ATP cause phosphorylation of seryl-residue 49, an exposed residue at the apex of the T-loop [38]. The P_{II} kinase has not been identified yet. The phosphatase of P_{II}-P, PphA from *Synechocystis* PCC 6803, readily dephosphorylates P_{II}-P in the absence of effector molecules. This reaction is partially inhibited by ATP or ADP, but strongly by Mg^{2+}-ATP-2-OG [39]. Combining different mixtures of ADP/ATP and 2-OG revealed that the P_{II} dephosphorylation reaction responded highly sensitive towards the 2-OG levels, however changing the ATP/ADP ratio had only little effect [40], since both adenylate nucleotides inhibit the dephosphorylation reaction. In contrast, preliminary data indicate that ATP and ADP antagonistically influence the binding of P_{II} with its targets NAGK or PipX. This could indicate that the interaction of P_{II} with its downstream signalling targets is indeed responsive to the ATP/ADP level, as was reported for the interaction of the P_{II} protein from *E. coli* with its targets NtrB and ATase [3].
In this study we investigate the ability of *S. elongatus* P_{II} to act as an EC sensor *in vitro*, and found that indeed it has such ability. Interestingly, the two targets, NAGK and PipX, respond differently to changing ADP/ATP ratios, with PipX being more sensitive towards low ADP levels. Furthermore, we observed that the effects of EC were mediated both indirectly, by changing the 2-OG binding properties of P_{II}, and directly, by the alteration of P_{II} output activities upon the binding of mixtures of nucleotides to P_{II}.

Experimental

Construction of heterotrimeric P_{II} protein

Heterotrimeric P_{II}-proteins, consisting of the Strep-tagged and non-tagged subunits were constructed as follows: two *glnB* genes from *Synechococcus elongatus*, one carrying Strep-tag fusion, another without Strep-tag, were cloned into pETDuet-1 vector (Merck KGaA, Darmstadt, Germany). First, native *glnB* was amplified using primers containing *AatII* and *AvrII* restriction sites: P_{II}nfwd2 (5′-ATGCGACGTCGATAACGAGGGCAAAA-3′) and P_{II}nrev2 (5′-ATGCCCTAGGGTAAACGGCAGACAAA-3′). The PCR product was restricted with *AatII* and *AvrII* and cloned into multiple cloning site 2 (MCS2) of pETDuet-1 vector. The resulting plasmid was restricted with *NcoI* and *HindIII* for the insertion of Strep-tag-fused *glnB* into multiple cloning site 1 (MCS1). The amplification of the second gene was done using following primers: P_{II}sfor (5′-ATGCCCATGGTTACCACTCCCTATCAGT-3′) and P_{II}srev (5′-ATGCAAGCTTCGCAGTAGCGGTAAAC-3′). The clones were checked by sequencing with the primers pET-Upstream (5′-ATGCGTCCGGCGTAGA-3′) for MCS1 and T7-Terminator (5′-GCTAGTTATTGCTCAGCGG-3′) for MCS2.

Overexpression and purification of recombinant P_{II}, NAGK, PipX and AGPR

The *glnB* gene *from Synechococcus elongatus*, cloned into the Strep-tag fusion vector pASK-IBA3 (IBA, Göttingen, Germany), was overexpressed in *E. coli* RB9060 [41] and purified using affinity chromatography as described previously [30]. The His_6-tagged recombinant NAGK from *S. elongatus,* His_6-tagged PipX and N-acetylglutamate-5-phosphate-reductase (AGPR) from *E. coli* were overexpressed in *E. coli* strain BL21(DE3) [42] and purified as reported previously [26, 30, 43]. Heterotrimeric P_{II} was overexpressed in *E. coli* strain BL21(DE3) and purified as described above with following modification: protein elution was made with a gradient of 30 µM, 200 µM and 1 mM desthiobiotin, and analysed by SDS-PAGE. P_{II} trimers with one/two Strep-tags were localized in 200 µM desthiobiotin fractions.

Surface Plasmon Resonance Detection (SPR)

SPR experiments were performed using a BIAcore X biosensor system (Biacore AB, Uppsala, Sweden) at 25°C in HBS-Mg buffer containing 10 mM HEPES, 150 mM NaCl, 1 mM $MgCl_2$ and 0.005% Nonidet P-40, pH 7.5 as described previously [31]. The purified His_6-NAGK was immobilized on the Ni^+-loaded NTA sensor chip to flow cell 2 (FC2) in a volume of 50 µl at a concentration of 30 nM (hexamer) to receive a binding signal of approximately 3000 resonance units (RU), which corresponds to a surface concentration change of 3 ng/mm^2. To determine the influence of different ATP/ADP ratios on the association and dissociation of the P_{II}-NAGK complex, a solution of 100 nM P_{II} was injected over the sensor-chip immobilized His_6-NAGK surface in the presence of 2 mM ATP with 0, 1, 2, 3, or 4 mM ADP as well as in the presence of 2 mM ADP alone. P_{II} was afterwards eluted by an injection of the same proportion of the metabolites. Furthermore, 100 nM P_{II} was bound over the immobilized NAGK with or without 1 mM ADP and eluted by an injection of 1 mM ADP. To load fresh proteins on the NTA sensor chip, bound proteins were first removed by injection of 25 µl of 0.4 M EDTA pH 7.5, subsequently, the chip could be loaded again with 5 mM Ni_2SO_4 solution and His_6-NAGK as described above.

P_{II}-PipX complex formation on the NTA chip was measured as described previously [26]. The His_6-PipX (500 nM) was preincubated with homotrimeric Strep-P_{II} (100 nM monomer) in the absence and in the presence of effectors and injected on the Ni^{2+}-loaded NTA chip. As a control, His_6-PipX was bound to the chip in the absence of P_{II}. The response difference between binding of His_6-PipX alone and in the presence of P_{II} at t = 197 s after start of the injection phase, was taken as a measure of protein binding.

To assay the binding of PipX to immobilized P_{II}, a CM5 sensor chip was treated with Amino Coupling Kit (Biacore AB, Uppsala, Sweden) to bind Strep-Tactin protein (50 µg/µl) in a volume 50 µl on the surface [28]. Thereafter, the purified heterotrimeric or homotrimeric-Strep-tagged P_{II} (40 ng/µl) was immobilized on the chip surface in flow cell 2 (FC2) in a volume of 20 µl. PipX (21 ng/µl) was injected in a volume of 20 µl in the presence of following effectors: 2 mM ADP, 2 mM ATP and 1 mM 2-OG. To remove P_{II} from the surface, the chip was washed with 5 mM desthiobiotin and regenerated by injecting HABA-buffer (IBA, Göttingen, Germany).

Isothermal Titration Calorimetry (ITC)

ITC experiments were performed on a VP-ITC microcalorimeter (MicroCal, LCC) in buffer containing 10 mM HEPES-NaOH, pH 7.4, 50 mM KCl, 50 mM NaCl and 1 mM $MgCl_2$ at 20°C.

Isotherms of 2-OG binding to P_{II} (33 µM trimer concentration) were determined in the presence of various ATP/ADP ratios: 1 mM/0.25 mM, 1 mM/0.5 mM, 1 mM/1 mM as well as only 1 mM ATP or 1 mM ADP. For one measurement 5 µl of 2 mM 2-OG was injected 35 times (4.2-293.7 µM) to the measuring cell containing P_{II} protein (cell volume 1.4285 ml) with stirring at 350 rpm. The binding isotherms were calculated from the recorded data and fitted to a one-site and a three-sites binding models using the MicroCal ORIGIN software (Northampton, USA) as indicated.

Direct coupled NAGK activity assay

The specific activity of NAGK from *S. elongatus* was assayed by coupling NAGK-dependent NAG phosphorylation to AGPR-catalyzed reduction of NAG-phosphate with NADPH as reductant and recording the change in absorbance at 340 nm [43]. The reaction buffer consisted of 50 mM potassium phosphate buffer (pH 7), 50 mM KCl, 20 mM $MgCl_2$, 0.2 mM NADPH and 0.5 mM DTT. Each reaction contained 10 µg AGPR, 50 mM NAG and 2.4 µg P_{II} with 6 µg NAGK or 1.2 µg P_{II} with 3 µg NAGK. The metabolites ATP, ADP, arginine and 2-OG varied depending on the experiment being performed. The reaction was started by the addition of NAGK. Phosphorylation of one molecule of NAG leads to oxidation of one molecule of NADPH, which is followed by the linear decrease of absorbance at 340 nm, recorded in a volume of 1 ml over a period of 10 min with a SPECORD 200 photometer (Analytik Jena). One unit of NAGK catalyzes the conversion of 1 mmol NAG per min. The reaction velocity was calculated with a molar absorption coefficient of NADH of ε_{340} = 6178 L mol^{-1} cm^{-1} from the slope of the change of absorbance per time.

P_{II}-PipX *in vitro* cross-linking

P_{II}-PipX interaction was analyzed using glutardialdehyde cross-linking. P_{II} (0.1 µg/µl) was preincubated with PipX (0.2 µg/µl) in the absence or in the presence of effectors ATP, ADP and 2-OG in 20 µl buffer containing 10 mM potassium phosphate buffer pH 7.4, 100 mM NaCl and 2 mM $MgCl_2$ at 4°C. After 5 min, 0.1% (w/w) glutardialdehyde was added and the samples were incubated for 5 min at 25°C. The cross-linking reaction was stopped by the addition of 100 mM Tris-HCl pH 7.4. The cross-link products were analyzed by 12.5% SDS-PAGE followed by immunoblot analysis with P_{II}-specific antibody as described previously [44].

Results

Different ATP/ADP ratios affect the activation of NAGK by P_{II} and its relief from arginine inhibition

The effect of different ADP/ATP ratios on the activation of NAGK by P_{II} and on the P_{II}-mediated relief from arginine inhibition could not be determined in the previously used assay, in which ATP consumption was coupled to NADH oxidation. However, by assaying the activity of NAGK in a reaction, where the phosphorylation of NAG is linked to the subsequent reduction of NAG-phosphate by AGPR with NADPH as a reductant [43], it is possible to determine the activity of NAGK under almost physiological conditions and at variable ATP/ADP levels. Increasing ATP concentrations from 0.5 mM to 4 mM enhanced the activity of NAGK both in the presence or absence of P_{II} (Fig. 1a and b), which was expected from the K_m of NAGK for ATP (without P_{II} K_m=0.6 mM, in the presence of P_{II} K_m=1.1 mM) [36]. Addition of ADP monotonically reduced the activity of P_{II}-complexed NAGK at any fixed ATP concentration. The higher the ADP concentration was, the more decreased the activity of NAGK. At a low constant ATP concentration, the relative decrease in NAGK activity by ADP addition was more pronounced than at high constant ATP concentration (6.4-fold decrease from 0 to 4 mM ADP at fixed 0.5 mM ATP compared to 2.6-fold decrease from 0 to 4 mM ADP at fixed 4 mM ATP). At the highest ADP/ATP ratio (4 mM ADP with 0.5. mM ATP), NAGK activity in presence of P_{II} was as low as NAGK activity in the absence of P_{II} (Fig. 1a and b). In the absence of P_{II}, NAGK responded only weakly to different ATP/ADP ratios (Fig. 1b), with a 1.8-fold reduction of activity comparing 0 and 4 mM ADP at any fixed ATP concentration. This indicates that the response of NAGK activity in presence of P_{II} towards different ADP/ATP ratios operates through the adenylate binding properties of P_{II}.

In the AGPR-coupled assay, NAGK was more sensitive to arginine inhibition than in the previously reported pyruvate kinase (PK)/ lactate dehydrogenase (LDH) coupled assay [31, 36], which keeps the ATP level constant at 10 mM. Using the AGPR-coupled assay, 10 µM arginine inhibited the free enzyme, but P_{II} relieved NAGK from arginine inhibition (Fig. 2a), as described previously for

the colorimetric assay and the PK/LDH coupled assay [31, 36]. The inhibitory effect of ADP on NAGK in the presence of P_{II} was tested at different arginine concentrations (20 µM, 40 µM and 60 µM), which are completely inhibitory for free NAGK but not or only moderately inhibitory to P_{II}-complexed NAGK. In these experiments ATP was fixed at 2 mM. Arginine inhibition was efficiently relieved by P_{II} in the presence of ATP alone; increasing concentrations of ADP increasingly diminished this effect, but didn't completely tune it down. If ADP would completely inhibit complex formation between P_{II} and NAGK, full inhibition of NAGK would be expected at high ADP concentrations in the presence of arginine. The lack of full inhibition implies that ADP did not fully prevent P_{II}-NAGK interaction in the presence of 2 mM ATP.

2-OG is a key effector molecule in P_{II} mediated signal transduction; micromolar amounts of 2-OG in the presence of ATP negatively affected P_{II}-NAGK complex formation [31]. Previous studies using the PK/LDH coupled assay could demonstrate the inhibitory effect of 2-OG on P_{II}-NAGK interaction by antagonizing the protective effect of P_{II} on NAGK activity in the presence of 50 µM arginine. In a similar experimental setting using the AGPR-coupled assay, NAGK activity decreased 10-fold when the 2-OG concentration was increased from 0 to 250 µM in the presence of P_{II}, 30 µM arginine and 2 mM ATP (Fig. 2b). The apparent half maximal inhibitory concentration (IC_{50}) of 2-OG was estimated to be 78 µM, a similar result as obtained in the previous study [6]. To reveal, how ADP affects the response towards 2-OG, the same experiment was performed in the presence of 2 mM ATP together with 2 mM ADP (Fig. 2b). The activity at zero 2-OG was 3-times lower than in the control in the absence of ADP, and it decreased 5-fold by titrating 2-OG up to 250 µM. The apparent IC_{50} for 2-OG in the presence of ADP was at about 145 µM, showing that 2-OG inhibited P_{II}-NAGK complex formation also in the presence of ADP, although moderately less efficiently.

Inhibitory effect of ADP on 2-OG binding of P_{II} in the presence of ATP

The 2-OG-binding site in P_{II} is created by a Mg^{2+} ion, which is coordinated by the gamma-phosphate of a bound ATP molecule and amino acid residues of one monomer of the P_{II} trimer itself. Binding of a single 2-OG molecule to P_{II} leads to a strong conformational change of the T-loop extending from the subunit, which ligates 2-OG, and moreover, to subtle changes in the other two binding sites as a result of negative cooperativity [8]. 2-OG binding in the presence of ATP was already measured by Isothermal Titration Calorimetry and the raw data could be fitted to a three sequential binding site model, that revealed the anticooperative occupation of the three binding sites [6]. Since ADP and ATP compete for the same binding site, an ADP molecule bound to one monomer of P_{II} might influence the affinity for 2-OG of the other two monomers because of the P_{II} intersubunit communication. Therefore, we next studied the effect of ADP on the binding of 2-OG to P_{II}. The raw data were tried to fit according to a three sequential binding model, but were also fitted using a one binding site model, because in a mixture of ATP and ADP, the number of available 2-OG-binding sites in P_{II} cannot be reliably predicted. Data fitting according to a model with three sequential binding sites could only be achieved for measurements done in excess of ATP over ADP (Table 1). At a molar ratio of 1:1 ADP/ATP, the binding isotherm was only consistent with the one-site model. Fitting to a one binding site model reveals a combined K_d of all binding sites and a mean stoichiometry of bound ligands. As shown in Fig. 3a, 2-OG exhibited high affinity towards P_{II} in the presence of 1 mM ATP. The combined K_d of 39 µM for all three binding sites was calculated from the binding isotherms of three independent experiments. On the other hand, in the presence of Mg^{2+}-ADP, titration with 2-OG didn't yield any calorimetric signals (Fig. 3b), obviously because ADP is not able to create the 2-OG-binding site. To reveal how ADP affects the binding of 2-OG to P_{II} in presence of ATP, 2-OG was titrated to various mixtures of ADP/ATP in presence of P_{II}. The addition of 0.25 mM ADP to 1 mM ATP (ADP/ATP ratio 1:4) had a negative effect on 2-OG binding (Fig 3c) with the apparent K_d increasing to 78 µM and the binding stoichiometry (N) decreasing from 1.73 to 1.35 (Table 1). Increasing concentrations of ADP led to further increase of the K_d for 2-OG binding and to a decrease in the binding stoichiometry (Fig 3d

and e, Table 1). In the presence of ATP alone, data fitting retrieved a mean stoichiometry of 1.73 2-OG molecules per P_{II} trimer. Since each P_{II} trimer has three binding sites for 2-OG, data fitting according to a one binding site model underestimates the actual number of binding sites, which could be due to the anticooperativity between the sites. The N value in the presence of 1 mM ATP and 1 mM ADP (1:1 ratio, N = 0.75) therefore indicates that one of the three binding sites can be efficiently occupied by 2-OG under theses conditions. Furthermore, ADP increases the K_d of the remaining 2-OG binding site to approximately 183 µM.

Different ATP/ADP ratios alter the association and dissociation of the P_{II}-NAGK complex

As shown previously, ADP negatively affects P_{II}-NAGK interaction by increasing the dissociation of the complex [6]. To reveal in more detail how ADP affects P_{II}-NAGK association, P_{II} was first loaded on the NAGK surface in the absence of effectors and was than eluted by injection of 1 mM ADP (Fig. 4a, left). Subsequently, the same amount of P_{II} was injected to the NAGK sensor surface in presence of 1 mM ADP, which resulted again in rapid complex formation. At the end of injection, after an initial drop of resonance units, dissociation ceased. A further injection of 1 mM ADP resulted again in rapid dissociation of bound P_{II} (Fig. 4a, right). Comparing the association curves shows that in presence of ADP, the curve reaches rapidly a plateau, which is approximately at one third of the maximal level obtained in absence of ADP. The steep initial increase of resonance units and rapid equilibration indicates that ADP enhances both the association and dissociation kinetics of P_{II}-NAGK complex formation. The fact that P_{II}-ADP didn't fully dissociate from NAGK after the end of the injection, but could again be rapidly dissociated after a further injection of ADP can be explained. At the end of the P_{II}-ADP injection, when the sensor ship is rinsed with ADP-free running buffer, ADP from P_{II} dissociates faster than P_{II}-ADP from NAGK, leaving ADP-free P_{II}, which can stay bound on NAGK.

The influence of various ADP/ATP ratios on P_{II}-NAGK interaction was investigated by injecting P_{II} on a sensor-chip with immobilized NAGK in the presence of different concentrations of ADP and ATP and subsequently injecting the same buffer in the absence of P_{II}, to determine the ATP/ADP-dependent dissociation of the complex (Fig. 4b). In the presence of ATP, rapid association of the P_{II}-NAGK was observed and injection of ATP to the complex didn't accelerate the dissociation. Addition of 1 mM ADP to 2 mM ATP had only a minor effect on complex formation (association was slightly faster and the maximal level slightly lower), but drastically accelerated complex dissociation (Fig. 4b). Higher concentrations of ADP (2 and 4 mM) at fixed 2 mM ATP lowered the steady state binding equilibrium during the first injection phase and increased the dissociation velocity to reach the velocity caused by ADP alone. Remarkably, in the excess of ADP over ATP, there was clearly more P_{II}-NAGK complex formation than with ADP alone, although complex dissociation was similarly fast in both cases.

Affinity of PipX to P_{II} in the presence of ADP

Three PipX monomers can bind to one P_{II} trimer in the absence of 2-OG [28]. However, at elevated 2-OG levels in the presence of ATP, P_{II}-PipX complex formation is impaired and free PipX can now bind to and activate the transcription factor NtcA [28]. These *in vitro* properties are correlated *in vivo* to nitrogen-limiting conditions. Here, we used SPR spectroscopy and glutardialdehyde cross-linking to determine the influence of ADP on 2-OG-modulated P_{II}-PipX complex formation.

In a first set of experiments, the His_6-PipX was preincubated with homotrimeric Strep-tagged P_{II} protein in the absence or in the presence of effectors and injected on the Ni^{2+}-loaded NTA chip. To ensure that all P_{II} trimers are fully occupied with PipX and enough free PipX is present, 5:1 PipX/P_{II} monomer ratio was used. In a control binding experiment His_6-PipX was loaded on the chip in the absence of P_{II}. PipX monomers alone showed relatively low binding to the chip due to the single short His_6-tag and therefore reached the equilibrium fast and dissociated after the end of the injection from the surface (Figure S1). Effectors had no influence on the interaction of His_6-PipX with Ni^{2+}-loaded NTA chip surface. Addition of P_{II} to PipX increased the binding signal in the sensorgram 2.5 times and decreased the dissociation rate, which can be explained by enhanced

binding of the P_{II}-PipX complexes, containing three His_6-tags that strongly bind to the surface, compared to monomeric PipX. P_{II} in the absence of PipX didn't bind to the chip surface. Thus, the increase of resonance units induced by the addition of P_{II} to PipX can be used to quantify P_{II}-PipX complex formation. Addition of 1 mM ADP to P_{II}-PipX had a strong positive effect on the binding signal, probably due to the stabilization of the P_{II}-PipX interaction, allowing more protein complexes to bind to the chip (Figure S1). The experiment was repeated in the presence of different ATD/ADP ratios and 2-OG. The increase of resonance units (ΔRU) from the start to the end of the injection indicates the amount of protein binding to the chip surface. The ΔRU values (at t = 197 s) for the binding of PipX without P_{II} was subtracted from the ΔRU values obtained in the presence of P_{II} and different effector molecules and the results are shown in the bar graph in Fig. 5a. In the absence of effectors the P_{II}-PipX complex binding reaches more than 800 RU. The amount of P_{II}-PipX complexes is enhanced by ADP and less efficiently by ATP; intermediate binding levels were obtained in a mixture of 1 mM ATP and ADP. Figure 5a shows that 2-OG in the presence of ATP is a strong inhibitor of P_{II}-PipX complex formation, the binding levels were almost the same as for free PipX. ADP acted antagonistically to 2-OG, even small amounts of ADP (0.05 mM) could significantly repress the 2-OG signal in the presence of 1 mM ATP *in vitro*. The amount of P_{II}-PipX complex in the presence of 1 mM ADP, ATP and 2-OG was even higher than in the absence of any effectors, showing that 1 mM ADP can almost completely erase the inhibitory effect of 2-OG.

This result was confirmed in a P_{II}-PipX binding assay, where proteins were preincubated under different conditions and cross-linked using glutardialdehyde. Subsequently, the products were visualized by SDS-PAGE and immunoblot analysis with P_{II}-specific antibody. As shown in Fig. 5b, in the absence of PipX, the cross-links of P_{II} trimers are prevalent and the dimeric form was only only slightly visible, the single P_{II} monomers were not present. Though in the presence of PipX alone no other bands were detected, with 1 mM ADP one additional band was observed, with higher molecular mass than the P_{II} trimer, consistent with a P_{II}-PipX cross-link product that could be formed, when ADP stabilized the complex. ATP had no such effect, but in the presence of both 1 mM ATP/ADP the characteristic band was also observed. In comparison to the SPR experiments, higher concentrations of ADP were needed to neutralize the negative effect of 2-OG.

The P_{II}-PipX interaction was also studied with C-terminal Strep-tagged P_{II} protein immobilized on a Strep-Tactin II-coated sensor chip surface, where PipX was injected as an analyte. Immobilized P_{II} protein was able to build a complex with PipX, but the interaction was insensitive to the effector molecules ATP and 2-OG (Fig. S2). We hypothesized, that by fixing the C-terminus of the P_{II} subunits on the chip surface, the conformational change of the C-terminus that occurs upon binding of ATP and 2-OG (a movement of the C-terminus towards the ATP-molecule) [8] is prevented and, therefore, the P_{II}-PipX complex was not affected by these effectors. To solve this question, a heterotrimeric Strep-tagged P_{II} protein was constructed by co-expressing Strep-tagged and untagged P_{II} subunits und purifying heterotrimers containing only one or two Strep-tagged subunits. If the above-mentioned assumption was true, the untagged subunits should be able to respond to the effectors. Heterotrimeric P_{II} was fixed on the Step-Tactin-coated chip and PipX could bind to this surface as efficient as to the homotrimeric Strep-tagged P_{II} protein (Fig. 5c). In contrast to the Strep-tagged P_{II} homotrimer, the interaction was indeed weakened by 1 mM 2-OG in the presence of 2 mM Mg^{2+}-ATP, although not completely, because of the remaining Strep-tagged P_{II} subunits. Injection of PipX in the presence of 2 mM ADP on the immobilized heterotrimeric P_{II} showed an enhanced velocity of complex association compared to binding in the absence of effector molecules. Furthermore, ADP was able to antagonize the negative effect of 2-OG on PipX-P_{II} binding: when ADP was added to a mixture of ATP and 2-OG, more PipX could bind to the P_{II} surface than in the absence of ADP.

Discussion

An important feature of cyanobacterial P_{II} signal transduction is the sensing of the balance of carbon and nitrogen status through binding of the central metabolite 2-OG. Results, presented here, indicate how P_{II} could also act as a sensor of adenylate energy charge in cyanobacteria. Binding of 2-OG to the ATP-ligated P_{II} protein is the fundament of P_{II}-mediated signal transduction. ADP was shown to occupy the ATP-site of P_{II} proteins [3, 14, 15]. Therefore, ADP binding prevents the coordination of the bridging Mg^{2+} ion by the γ-phosphate of ATP, which is essential for 2-OG binding [8]. In accord, no binding of 2-OG to ADP-occupied *S. elongatus* P_{II} protein occurs. When ATP and ADP are present simultaneously, as is the case in living cells, there will be competition for the three adenylate binding sites of the trimeric P_{II} protein. Moreover, it has to be considered, that the three binding sites are interacting in an anticooperative manner. In contrast to the *E.coli* system, where ADP binds better than ATP [3], the affinity of each of the three binding sites of the cyanobacterial P_{II} towards ADP (K_d of 10, 19 and 133 μM) is approximately 2-3 fold lower than towards ATP (K_d of 4, 12 and 47 μM) [6]. So, when P_{II} is exposed to a mixture of ATP and ADP, a mixed occupation of the adenylate binding sites is expected with a concomitant decreased capability to bind 2-OG. In agreement, the number of 2-OG binding sites per P_{II} trimer was reduced by the addition of ADP. As long as ATP stayed in excess over ADP, the 2-OG binding process could be fitted according to a three sequential binding model, but the average number of 2-OG-binding sites in the mixed population of P_{II} trimers decreased. This indicates that part of the P_{II} population didn't exhibit three 2-OG binding sites anymore. This part of the population has probably at least one ADP molecule bound. Furthermore, the affinity for 2-OG binding decreases. At a 1:1 molar ratio of ADP to ATP, the dominating P_{II} population should consist of P_{II} trimers with a mixed occupation of ATP and ADP. Considering the 2-3-higher affinity for ATP, the P_{II} species P_{II}-ATP_2ADP_1 should clearly prevail over the species P_{II}-ATP_1ADP_2. Under these conditions, on average, only one 2-OG molecule can apparently bind to P_{II}. The binding process can no more be fitted according to a three sequential binding site model. The affinity of the remaining 2-OG-binding site seems to be as low as that of the third, low-affinity 2-OG-binding site of ATP-ligated P_{II} (Tab. 1). This implies that binding of ADP to one site in P_{II} has a strong negative effect for the remaining 2-OG-binding sites, so that probably only one site can be efficiently occupied. The binding of 2-OG to the lowest affinity site appears to be crucial for inhibition of P_{II}-NAGK interaction, since the IC_{50} of 2-OG at a 1:1 ratio of ADP to ATP (145 μM) for inhibiting P_{II}-NAGK interaction is near the K_d measured for 2-OG binding at the same ADP/ATP concentrations (183 μM). This mechanism allows the P_{II}-NAGK complex to stay sensitive towards 2-OG under low energy conditions.

The ADP-ligated P_{II} protein appears to be able to bind to NAGK, but binding is clearly different for that of ATP-ligated P_{II}, as revealed by SPR spectroscopy. In particular, the dissociation rate of the P_{II}-NAGK complex was highly increased by ADP. The increased dissociation rate results in a lower steady state binding level of P_{II}-ADP to NAGK. P_{II}-species occupied with a mixture of ATP and ADP display intermediate binding properties: At 1:2 and 2:2 mM mixtures of ADP/ATP, the P_{II}-ATP_2ADP_1 species should prevail. These conditions already lead to enhanced complex dissociation. In mixtures of 3:2 or 4:2 mM ADP/ATP, more and more of the P_{II}-ATP_1ADP_2 species should appear, however, fully ADP-ligated P_{II} species are very unlikely. In accord, the binding curves under these two conditions were very similar towards each other and distinct from that of fully ADP-ligated P_{II} with NAGK.

We have previously suggested a two-step model for the binding of P_{II} to NAGK [6]. Following a transient encounter complex involving B-loop residues of P_{II}, the T-loop folds into a compact conformation, which tightly associates with NAGK. In ADP-ligated P_{II} protein, the T-loop may be impaired in folding into the perfect NAGK-binding conformation, explaining the fast dissociation of the complex. Measuring NAGK activity in mixtures of ATP, ADP and P_{II} suggests that P_{II} protein occupied with ATP/ADP mixtures is unable to enhance the catalytic activity of NAGK. On the other hand, NAGK, which forms a complex with ATP/ADP-occupied P_{II} is protected from arginine inhibition as efficient as by purely ATP-occupied P_{II}. These properties suggest that protection from arginine inhibition and activation of catalytic activity of NAGK by P_{II} operates by

different mechanisms: The loose binding of ATP/ADP-ligated P_{II} to NAGK is sufficient to relieve arginine inhibition, but is insufficient to rearrange the catalytic centre of NAGK, resulting in enhanced activity. This suggestion is in accord with two different contact surfaces of P_{II} with NAGK [35]. The rearrangement of the catalytic centre of NAGK by P_{II} has been shown to require a tight hydrogen-bonding and ion-pair network involving the distal part of the T-loop of P_{II} and the N-domain of NAGK, tightening the catalytic centre of NAGK [35]. The inability of ATP/ADP-ligated P_{II} to enhance NAGK activity is thus in accord with the lax binding of this P_{II} species, probably mediated by imperfect fit of the T-loop to the corresponding NAGK recognition site. By contrast, the relief from arginine inhibition appears to be mediated by the C-terminus of NAGK [36], interacting with the body of the P_{II} protein. In essence, NAGK complexed to partially ADP-ligated P_{II} is not catalytically induced but still relived from feedback inhibition by arginine. In such a state, P_{II}-complexed NAGK wouldn't support elevated arginine synthesis for efficient nitrogen storage but could quickly respond to increasing energy levels.

PipX is another known partner of P_{II} protein in *S. elongatus*. It switches between binding to P_{II} or NtcA, depending on the 2-OG concentration. Low adenylate energy charge (increased ADP/ATP ratio) enhances the association of the P_{II}-PipX complex *in vitro,* thereby antagonizing the signal of nitrogen limitation (elevated 2-OG levels). P_{II}-PipX complex formation is highly ADP-sensitive; ADP promotes complex formation and protects it from dissociation by 2-OG *in vitro*. Therefore, increasing ADP levels should decrease the activation of NtcA-dependent genes, which depends of PipX-NtcA interaction, due to efficient competition of P_{II} for PipX. Remarkably, the negative effect of 2-OG on P_{II}-PipX interaction was absent when Strep-tagged P_{II} was fixed with its C-terminus to the sensor surface but could partially be restored with heterotrimeric Strep-tagged P_{II}, which consists partially of untagged monomers with a free C-terminus. Although P_{II}-PipX binding itself doesn't involve conformational changes on the C-terminus of P_{II}, the movement of the C-terminus imposed by 2-OG binding is essential for the response to the effector molecules and incorporating metabolic signals [8, 9]. Together, this study shows how the *S. elongatus* P_{II} signal transduction protein is capable to respond in a fine-tuned manner to the change of the energy charge *in vitro*. Through P_{II}-dependent adenylate energy signalling, increasing ADP levels should diminish the NtcA-dependent activation of genes required for nitrogen assimilation under nitrogen-limiting conditions (high 2-OG levels). On the other hand, under nitrogen-excess conditions (low 2-OG levels), increased ADP levels, via P_{II} signalling, should diminish the activation of NAGK, thereby reducing the flux into the arginine biosynthesis pathway. In both cases, P_{II}-dependent signalling of increased ADP levels should dampen energetically expensive anabolic reactions. Comparing the response of PipX and NAGK to EC signalling by P_{II}, it appears that PipX is more sensitive towards low ADP levels.

The ability to bind 2-OG and adenyl nucleotides is conserved among P_{II} proteins in all three domains of life. Several studies indicated the involvement of P_{II} in sensing the energy status in various bacteria. It was suggested that P_{II} proteins in photosynthetic Proteobacterium *Rhodospirillum rubrum* responds to the cellular energy charge [22, 45]. Mutants of *Rhodospirillum rubrum* with impaired purine synthesis pathway were created and than provided with an exogenous adenine source to test the effect of different cellular ATP levels on P_{II} signal transduction. However, depleted ATP levels had little effect on P_{II}-mediated regulation of NifA and nitrogenase activity. It was suggested that the ADP/ATP ratio states the actual signal for P_{II} protein, but the direct effect of ADP/ATP ratios has not been shown yet [5]. Jiang and Ninfa showed for the first time with reconstituted signal transduction systems using the *E. coli* P_{II} protein and its receptors NtrB, ATase and UTase/UR, that ADP affected almost all signalling properties of *E. coli* P_{II} by antagonizing 2-OG mediated responses [3, 18]. The metabolite sensing involves intersubunit signalling in the P_{II} trimer itself with cooperation of the multiple effector binding sites [19]. Furthermore, ADP antagonized the inhibitory effect of 2-oxoglutarate on the binding of the P_{II} paralogue GlnK to the AmtB ammonium transport protein in E. coli [7]. The present study extends these insights: in the

case of the cyanobacterial system, ADP does not always antagonize the 2-OG signal but differentially affects the interaction of P_{II} with its targets. ADP modulates P_{II} signalling to the receptor NAGK primarily at low 2-OG levels without antagonizing the effect of 2-OG, whereas it antagonizes the inhibitory effect of 2-OG for P_{II}-PipX interaction. There is still discussion on how much unbound ATP is available in the cell at any given moment [46], but it appears that the ratio of ADP to ATP instead of the absolute concentration of ATP affects P_{II} signal transduction. Further studies using *in vivo* systems could shed light on the physiological impact of this remarkable and complex signalling system.

Acknowledgements

We thank Christopher Schuster and Sebastian Kindermann for their help in creating the heterotrimeric Strep-tagged P_{II} protein.

Funding

This work was supported by DFG grant Fo195/10.

Numbered references

1 Chapman, A. G., Fall, L. and Atkinson, D. E. (1971) Adenylate energy charge in *Escherichia coli* during growth and starvation. J. Bacteriol. **108**, 1072-1086

2 Franzen, J. S. and Binkley, S. B. (1961) Comparison of the acid-soluble nucleotides in *Escherichia coli* at different growth rates. J. Biol. Chem. **236**, 515-519

3 Jiang, P. and Ninfa, A. J. (2007) *Escherichia coli* P_{II} signal transduction protein controlling nitrogen assimilation acts as a sensor of adenylate energy charge *in vitro*. Biochemistry. **46**, 12979-12996

4 Forchhammer, K. (2008) P(II) signal transducers: novel functional and structural insights. Trends Microbiol. **16**, 65-72

5 Zhang, Y., Pohlmann, E. L. and Roberts, G. P. (2009) Effect of perturbation of ATP level on the activity and regulation of nitrogenase in *Rhodospirillum rubrum*. J. Bacteriol. **191**, 5526-5537

6 Fokina, O., Chellamuthu, V. R., Zeth, K. and Forchhammer, K. (2010) A Novel Signal Transduction Protein P(II) Variant from *Synechococcus elongatus* PCC 7942 Indicates a Two-Step Process for NAGK-P(II) Complex Formation. J. Mol. Biol. **399**, 410-421

7 Radchenko, M. V., Thornton, J. and Merrick, M. (2010) Control of AmtB-GlnK complex formation by intracellular levels of ATP, ADP, and 2-oxoglutarate. J. Biol. Chem. **285**, 31037-31045

8 Fokina, O., Chellamuthu, V. R., Forchhammer, K. and Zeth, K. (2010) Mechanism of 2-oxoglutarate signaling by the *Synechococcus elongatus* P_{II} signal transduction protein. Proc. Natl. Acad. Sci. U. S. A. **107**, 19760-19765

9 Truan, D., Huergo, L. F., Chubatsu, L. S., Merrick, M., Li, X. D. and Winkler, F. K. (2010) A new P(II) protein structure identifies the 2-oxoglutarate binding site. J. Mol. Biol. **400**, 531-539

10 Ninfa, A. J. and Jiang, P. (2005) P_{II} signal transduction proteins: sensors of alpha-ketoglutarate that regulate nitrogen metabolism. Curr. Opin. Microbiol. **8**, 168-173

11 Leigh, J. A. and Dodsworth, J. A. (2007) Nitrogen regulation in bacteria and archaea. Annu. Rev. Microbiol. **61**, 349-377

12 Sant'Anna, F. H., Trentini, D. B., de Souto Weber, S., Cecagno, R., da Silva, S. C. and Schrank, I. S. (2009) The P_{II} superfamily revised: a novel group and evolutionary insights. J. Mol. Evol. **68**, 322-336

13 Forchhammer, K. (2004) Global carbon/nitrogen control by P_{II} signal transduction in cyanobacteria: from signals to targets. FEMS Microbiol. Rev. **28**, 319-333

14 Xu, Y., Cheah, E., Carr, P. D., van Heeswijk, W. C., Westerhoff, H. V., Vasudevan, S. G. and Ollis, D. L. (1998) GlnK, a P_{II}-homologue: structure reveals ATP binding site and indicates how the T-loops may be involved in molecular recognition. J. Mol. Biol. **282**, 149-165

15 Xu, Y., Carr, P. D., Clancy, P., Garcia-Dominguez, M., Forchhammer, K., Florencio, F., Vasudevan, S. G., Tandeau de Marsac, N. and Ollis, D. L. (2003) The structures of the P_{II} proteins from the cyanobacteria *Synechococcus* sp. PCC 7942 and *Synechocystis* sp. PCC 6803. Acta. Crystallogr. D. Biol. Crystallogr. **59**, 2183-2190

16 Sakai, H., Wang, H., Takemoto-Hori, C., Kaminishi, T., Yamaguchi, H., Kamewari, Y., Terada, T., Kuramitsu, S., Shirouzu, M. and Yokoyama, S. (2005) Crystal structures of the signal transducing protein GlnK from *Thermus thermophilus* HB8. J. Struct. Biol. **149**, 99-110

17 Forchhammer, K. and Hedler, A. (1997) Phosphoprotein P_{II} from cyanobacteria--analysis of functional conservation with the P_{II} signal-transduction protein from *Escherichia coli*. Eur. J. Biochem. **244**, 869-875

18 Jiang, P. and Ninfa, A. J. (2009) Alpha-Ketoglutarate Controls the Ability of the *Escherichia coli* P_{II} Signal Transduction Protein To Regulate the Activities of NRII (NtrB) but Does Not Control the Binding of P_{II} to NRII. Biochemistry. **48**, 11514-11521

19 Jiang, P. and Ninfa, A. J. (2009) Sensation and Signaling of alpha-Ketoglutarate and Adenylylate Energy Charge by the *Escherichia coli* P_{II} Signal Transduction Protein Require Cooperation of the Three Ligand-Binding Sites within the P_{II} Trimer. Biochemistry. **48**, 11522-11531

20 Smith, C. S., Weljie, A. M. and Moorhead, G. B. (2003) Molecular properties of the putative nitrogen sensor P_{II} from *Arabidopsis thaliana*. Plant J. **33**, 353-360

21 Zhang, Y., Pohlmann, E. L., Halbleib, C. M., Ludden, P. W. and Roberts, G. P. (2001) Effect of P(II) and its homolog GlnK on reversible ADP-ribosylation of dinitrogenase reductase by heterologous expression of the *Rhodospirillum rubrum* dinitrogenase reductase ADP-ribosyl transferase-dinitrogenase reductase-activating glycohydrolase regulatory system in Klebsiella pneumoniae. J. Bacteriol. **183**, 1610-1620

22 Zhang, Y., Pohlmann, E. L., Ludden, P. W. and Roberts, G. P. (2001) Functional characterization of three GlnB homologs in the photosynthetic bacterium *Rhodospirillum rubrum*: roles in sensing ammonium and energy status. J. Bacteriol. **183**, 6159-6168
23 Zhang, Y. P., Pohlmann, E. L., Ludden, P. W. and Roberts, G. P. (2003) Regulation of nitrogen fixation by multiple P-II homologs in the photosynthetic bacterium *Rhodospirillum rubrum*. Symbiosis. **35**, 85-100
24 Kloft, N. and Forchhammer, K. (2005) Signal transduction protein P-II phosphatase PphA is required for light-dependent control of nitrate utilization in *Synechocystis* sp strain PCC 6803. Journal of Bacteriology. **187**, 6683-6690
25 Takatani, N., Kobayashi, M., Maeda, S. I. and Omata, T. (2006) Regulation of nitrate reductase by non-modifiable derivatives of P_{II} in the cells of *Synechococcus elongatus* strain PCC 7942. Plant and Cell Physiology. **47**, 1182-1186
26 Espinosa, J., Forchhammer, K., Burillo, S. and Contreras, A. (2006) Interaction network in cyanobacterial nitrogen regulation: PipX, a protein that interacts in a 2-oxoglutarate dependent manner with P_{II} and NtcA. Mol. Microbiol. **61**, 457-469
27 Espinosa, J., Forchhammer, K. and Contreras, A. (2007) Role of the *Synechococcus* PCC 7942 nitrogen regulator protein PipX in NtcA-controlled processes. Microbiology-Sgm. **153**, 711-718
28 Llacer, J. L., Espinosa, J., Castells, M. A., Contreras, A., Forchhammer, K. and Rubio, V. (2010) Structural basis for the regulation of NtcA-dependent transcription by proteins PipX and P_{II}. Proc. Natl. Acad. Sci. U. S. A. **107**, 15397-15402
29 Burillo, S., Luque, I., Fuentes, I. and Contreras, A. (2004) Interactions between the nitrogen signal transduction protein P_{II} and N-acetyl glutamate kinase in organisms that perform oxygenic photosynthesis. J. Bacteriol. **186**, 3346-3354
30 Heinrich, A., Maheswaran, M., Ruppert, U. and Forchhammer, K. (2004) The *Synechococcus elongatus* P signal transduction protein controls arginine synthesis by complex formation with N-acetyl-L-glutamate kinase. Mol. Microbiol. **52**, 1303-1314
31 Maheswaran, M., Urbanke, C. and Forchhammer, K. (2004) Complex formation and catalytic activation by the P_{II} signaling protein of N-acetyl-L-glutamate kinase from *Synechococcus elongatus* strain PCC 7942. J. Biol. Chem. **279**, 55202-55210
32 Chen, Y. M., Ferrar, T. S., Lohmeier-Vogel, E. M., Morrice, N., Mizuno, Y., Berenger, B., Ng, K. K. S., Muench, D. G. and Moorhead, G. B. G. (2006) The P_{II} signal transduction protein of *Arabidopsis thaliana* forms an arginine-regulated complex with plastid N-acetyl glutamate kinase.(vol 281, pg 5726, 2006). Journal of Biological Chemistry. **281**, 24084-24084
33 Bourrellier, A. B. F., Valot, B., Guillot, A., Ambard-Bretteville, F., Vidal, J. and Hodges, M. (2010) Chloroplast acetyl-CoA carboxylase activity is 2-oxoglutarate-regulated by interaction of P_{II} with the biotin carboxyl carrier subunit. Proc. Natl. Acad. Sci. U. S. A. **107**, 502-507
34 Mizuno, Y., Moorhead, G. B. and Ng, K. K. (2007) Structural basis for the regulation of N-acetylglutamate kinase by P_{II} in *Arabidopsis thaliana*. J. Biol. Chem. **282**, 35733-35740
35 Llacer, J. L., Contreras, A., Forchhammer, K., Marco-Marin, C., Gil-Ortiz, F., Maldonado, R., Fita, I. and Rubio, V. (2007) The crystal structure of the complex of P_{II} and acetylglutamate kinase reveals how P_{II} controls the storage of nitrogen as arginine. Proc. Natl. Acad. Sci. U. S. A. **104**, 17644-17649
36 Beez, S., Fokina, O., Herrmann, C. and Forchhammer, K. (2009) N-acetyl-L-glutamate kinase (NAGK) from oxygenic phototrophs: P(II) signal transduction across domains of life reveals novel insights in NAGK control. J. Mol. Biol. **389**, 748-758
37 Forchhammer, K. and Demarsac, N. T. (1995) Functional-Analysis of the Phosphoprotein P-Ii (Glnb Gene-Product) in the Cyanobacterium *Synechococcus* Sp Strain Pcc-7942. Journal of Bacteriology. **177**, 2033-2040
38 Forchhammer, K. and Demarsac, N. T. (1995) Phosphorylation of the P-Ii Protein (Glnb Gene-Product) in the Cyanobacterium *Synechococcus* Sp Strain Pcc-7942 - Analysis of *in vitro* Kinase-Activity. Journal of Bacteriology. **177**, 5812-5817
39 Ruppert, U., Irmler, A., Kloft, N. and Forchhammer, K. (2002) The novel protein phosphatase PphA from *Synechocystis* PCC 6803 controls dephosphorylation of the signalling protein P-II. Molecular Microbiology. **44**, 855-864
40 Forchhammer, K., Irmler, A., Kloft, N. and Ruppert, U. (2004) P-II signalling in unicellular cyanobacteria: analysis of redox-signals and energy charge. Physiologia Plantarum. **120**, 51-56
41 Bueno, R., Pahel, G. and Magasanik, B. (1985) Role of *glnB* and *glnD* gene products in regulation of the glnALG operon of *Escherichia coli*. J. Bacteriol. **164**, 816-822
42 Studier, F. W., Rosenberg, A. H., Dunn, J. J. and Dubendorff, J. W. (1990) Use of T7 RNA polymerase to direct expression of cloned genes. Methods Enzymol. **185**, 60-89
43 Takahara, K., Akashi, K. and Yokota, A. (2007) Continuous spectrophotometric assays for three regulatory enzymes of the arginine biosynthetic pathway. Analytical Biochemistry. **368**, 138-147
44 Forchhammer, K. and Demarsac, N. T. (1994) The P-Ii Protein in the Cyanobacterium *Synechococcus* Sp Strain Pcc-7942 Is Modified by Serine Phosphorylation and Signals the Cellular N-Status. Journal of Bacteriology. **176**, 84-91

45 Zhang, Y., Wolfe, D. M., Pohlmann, E. L., Conrad, M. C. and Roberts, G. P. (2006) Effect of AmtB homologues on the post-translational regulation of nitrogenase activity in response to ammonium and energy signals in *Rhodospirillum rubrum*. Microbiology. **152**, 2075-2089
46 Schneider, D. A. and Gourse, R. L. (2004) Relationship between growth rate and ATP concentration in *Escherichia coli* - A bioassay for available cellular ATP. Journal of Biological Chemistry. **279**, 8262-8268

Figure legends

Figure 1 Effect of ADP on NAGK activity in the AGPR-coupled assay
Assay was performed in the presence of ATP at a concentration of 4 mM (dashed line), 2 mM (solid line), 1 mM (dotted line) and 0.5 mM (dot-dashed line), as indicated. AGPR-coupled NAGK assays were performed as described in Experimental. The percents of NAGK activity were plotted against the respective analyte concentration (standard deviations from the different measurements for each data point are indicated by error bars) and the data points were fitted to a hyperbolic curve (**a**) Enzyme activity with P_{II} protein (**b**) Effect on NAGK without P_{II}.

Figure 2 Arginine inhibition and antagonistic effect of 2-OG on the NAGK activation by P_{II} in the presence of arginine
AGPR-coupled NAGK assays were performed as described in Experimental. The percents of the NAGK activity were plotted against the respective analyte concentration (standard deviations from the different measurements for each data point are indicated by error bars) and the data points were fitted to a hyperbolic curve (**a**) ADP enhances inhibition of the NAGK activity by arginine in the presence of 2 mM ATP. NAGK activity in the absence of P_{II} and ADP (solid line), in the presence of P_{II}: without ADP (dashed line), with 0.5 mM ADP (dotted line), with 1 mM ADP (thin solid line), with 2 mM ADP (dot-dashed line), with 4 mM ADP (dot-dot-dashed line). NAGK activity in the absence P_{II} and arginine (dot-dashed line) (**b**) 2-OG effect on NAGK induction by P_{II} in the presence of 2 mM ATP and 30 μM arginine without ADP (solid line) and with 2 mM ADP (dashed line).

Figure 3 ITC measurement of the 2-OG binding to P_{II} protein
The upper panels show the raw data in the form of the heat effect during the titration of 33 μM P_{II} solution (trimer concentration) with 2 mM 2-OG. The lower panels show the binding isotherm and the best-fit curve according to the one-site binding model (**a**) 2-OG binding (titration 4.2-293.7 μM) in the presence of 1 mM ATP (**b**) 2-OG binding in the presence of 1 mM ADP (**c**), (**d**) and (**e**) 2-OG binding in the presence of 1 mM ATP and 0.25 mM (C), 0.5 mM (D), 1 mM (E) ADP.

Figure 4 SPR analysis of the ADP/ATP ratio influence on the association and the dissociation of the P_{II}-NAGK complex
NAGK was bound to FC2 of a Ni^{2+} -loaded NTA sensor chip (see Experimental) and FC1 was used as a background control. The response difference (ΔRU) between FC1 and FC2 is shown (**a**) Effect of 1 mM ADP on the dissociation of wt P_{II}-NAGK complex following association without effectors (left) and in the presence of 1 mM ADP (right) (**b**) Association and dissociation of P_{II}-NAGK complex under influence of different ADP/ATP ratios: 2 mM ATP (solid line), 2 mM ATP + 1 mM ADP (dotted line), 2 mM ATP + 2 mM ADP (short dashed line), 2 mM ATP + 4 mM ADP (long dashed line) and 2 mM ADP (dot-dashed line).

Figure 5 Effect of ATP, ADP and 2-OG on P_{II}-PipX complex formation
(**a**) His_6-PipX (500 nM) was preincubated with homotrimeric Strep-P_{II} (100 nM) in the absence or in the presence of effectors, as indicated, and injected on the Ni^{2+}-loaded NTA chip for SPR detection. As a control, His_6-PipX was injected under the same conditions, but in the absence of P_{II}. The response signal at t = 197 s after start of the injection phase was taken as a measure of protein binding. The binding of His_6-PipX alone was subtracted from the results measured in the presence of P_{II}. Error bars indicate standard deviations from the three independent measurements. (**b**) P_{II}-PipX binding assay using the glutardialdehyde cross-linking *in vitro*. P_{II} was preincubated with PipX in the presence and in the absence of effectors, as indicated, and subsiqently cross-linked using glutardialdehyde. The cross-link products were analyzed by SDS-PAGE followed by immunoblot analysis with P_{II}-specific antibody. (**c**) Effect of ADP, ATP and 2-OG on PipX binding to immobilized heterotrimeric Strep-tagged P_{II} protein. P_{II} (3.2 μM) was bound to FC2 of a CM5

chip and FC1 was used as a background control. The response difference (ΔRU) between FC1 and FC2 is shown. PipX (2 μM) was injected in absence of effector molecules (solid line), in the presence of 2 mM ADP (long dashed line), 2 mM ATP + 1 mM 2-OG (middle dashed line), 2 mM ADP + 2 mM ATP + 1 mM 2-OG (short dashed line) and 4 mM ADP + 2 mM ATP + 1 mM 2-OG (dotted line)

Figure S1 SPR detection of P_{II}-PipX complexes using Ni^{2+}-loaded NTA chip
His_6-PipX (500 nM) was preincubated with homotrimeric Strep-P_{II} (100 nM) in the absence (dotted line) and in the presence of 1 mM ADP (dashed line) and injected on the Ni^{2+}-loaded NTA chip. Solid line corresponds to the control binding experiment of His_6-PipX in the absence of P_{II}. The sensorgram shows the increase of RU (resonance units) that represents the protein binding to the chip surface. The difference in the RU between binding experiments in the presence of P_{II} and the control (PipX alone) at t=197 s, indicated by an arrow, was used to quantify the amount of PipX-P_{II} complex formation.

Figure S2 SPR detection of P_{II}-PipX complexes using CM5 chip
Homotrimeric Step-P_{II} (3.2 μM) was immobilized to FC2 of the Strep-Tactin-coated CM5 chip and FC1 was used as a background control. His_6-PipX (2 μM) was injected in absence of effector molecules (solid line), in the presence of 1 mM ATP (dotted line) and of 1 mM ATP + 1 mM 2-OG (dashed line).

Tables and Figures

Table 1 2-OG binding to P_{II} in the presence of various ADP/ATP ratios

Values correspond to the mean of three experiments ± SEM. The raw data were fitted using one-site and three-sites binding models for a P_{II} trimer. For comparison, the 2-OG binding in the presence of 1 mM ATP data fitted according to the three sites binding model are given in parentheses. NF, non fittable.

	one-site binding model		three-sites binding model		
ADP:ATP	N, sites	K_d, µM	K_d1, µM	K_d2, µM	K_d3, µM
0:1	1.725 ± 0.01	38.9 ± 1.1	(5.1 ± 4.0)	(11.1 ± 1.8)	(106.7 ± 14.8)
0.25:1	1.35 ± 0.16	78.2 ± 18	12.2 ± 6.4	41.2 ± 28.8	263.5 ± 153.1
0.5:1	1.125 ± 0.15	95.0 ± 16.5	11.0 ± 6.0	19.8 ± 2.1	194.9 ± 45.0
1:1	0.75 ± 0.26	182.9 ± 4.3		NF	

Figure 1

A

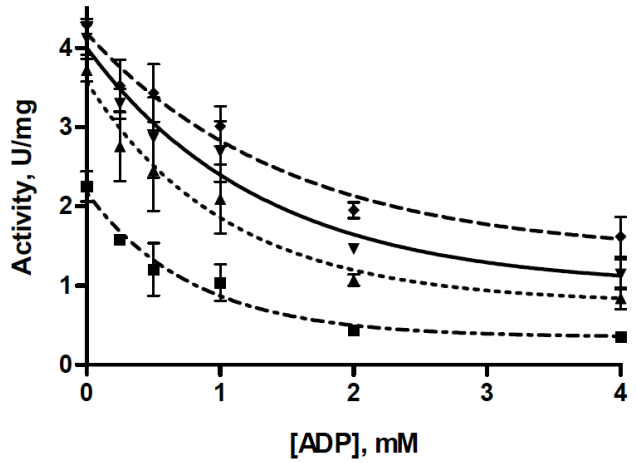

B

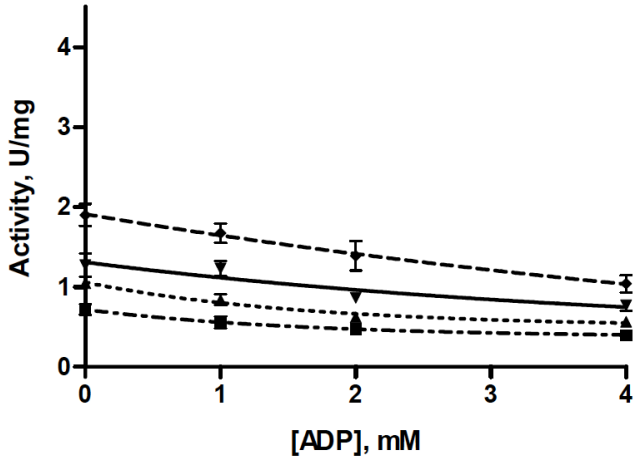

Figure 2

A

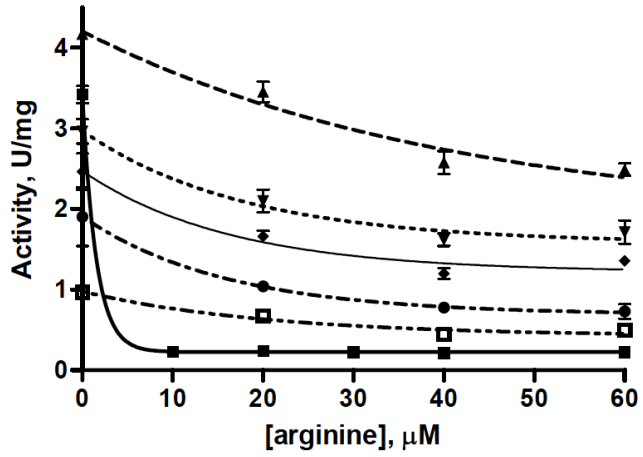
Activity, U/mg
0
1
2
3
4
0
10
20
30
40
50
60
[arginine], μM

B

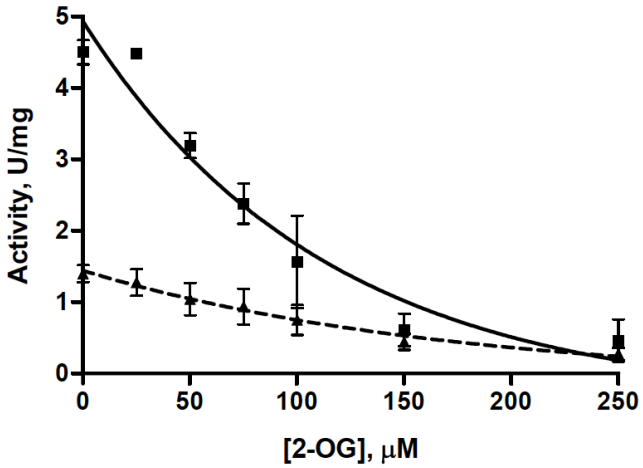
Activity, U/mg
0
1
2
3
4
5
0
50
100
150
200
250
[2-OG], μM

Figure 3

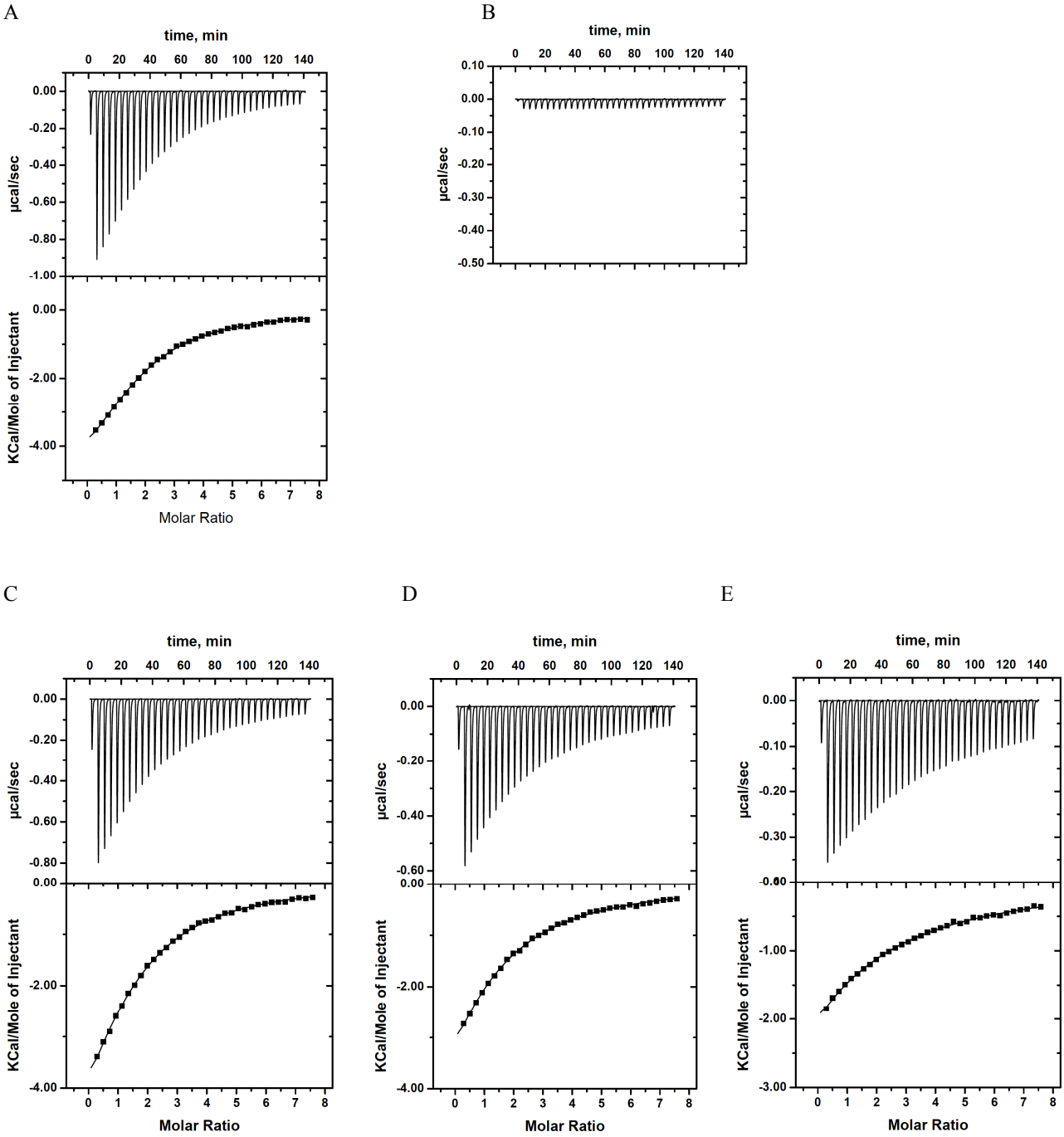
A
time, min
µcal/sec
KCal/Mole of Injectant
Molar Ratio
B
time, min
µcal/sec
C
time, min
µcal/sec
KCal/Mole of Injectant
Molar Ratio
D
time, min
µcal/sec
KCal/Mole of Injectant
Molar Ratio
E
time, min
µcal/sec
KCal/Mole of Injectant
Molar Ratio

Figure 4

A

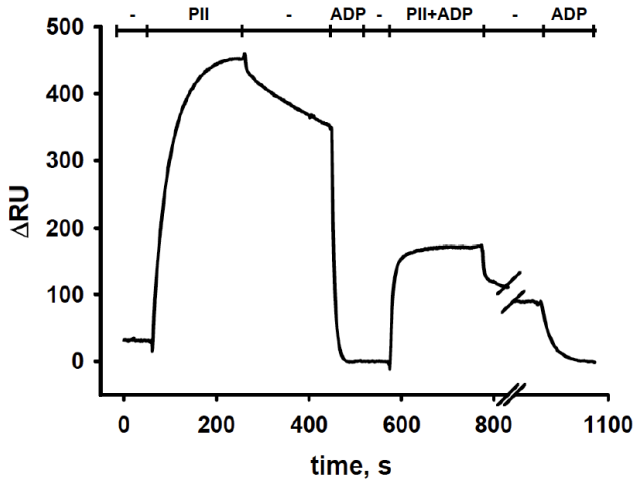
-
PII
-
ADP
-
PII+ADP
-
ADP
500
400
300
200
100
0
ΔRU
0
200
400
600
800
1100
time, s

B

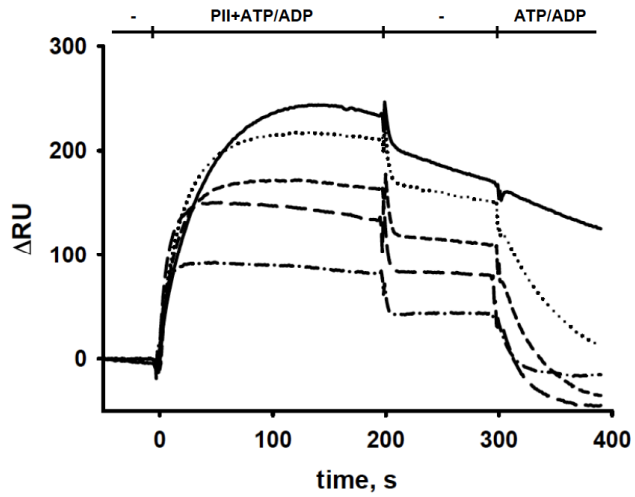
-
PII+ATP/ADP
-
ATP/ADP
300
200
100
0
ΔRU
0
100
200
300
400
time, s

Figure 5

A

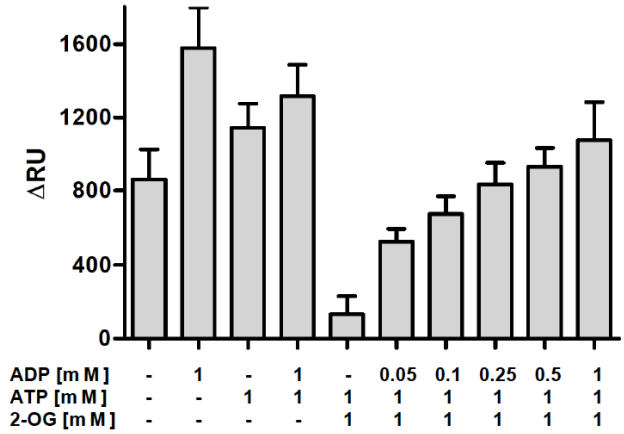
1600
1200
800
400
0
ΔRU
ADP [m M] - 1 - 1 - 0.05 0.1 0.25 0.5 1
ATP [m M] - - 1 1 1 1 1 1 1 1
2-OG [m M] - - - - 1 1 1 1 1 1

B

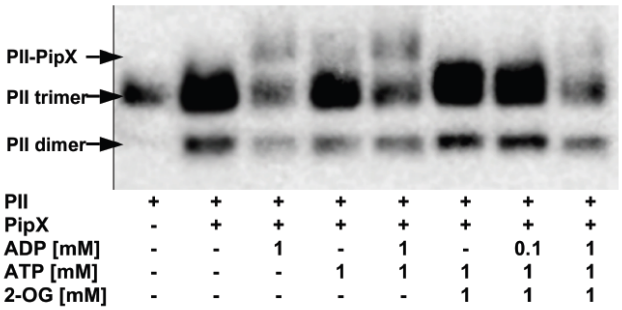
PII-PipX
PII trimer
PII dimer
PII + + + + + + + +
PipX - + + + + + + +
ADP [mM] - - 1 - 1 - 0.1 1
ATP [mM] - - - 1 1 1 1 1
2-OG [mM] - - - - - 1 1 1

C

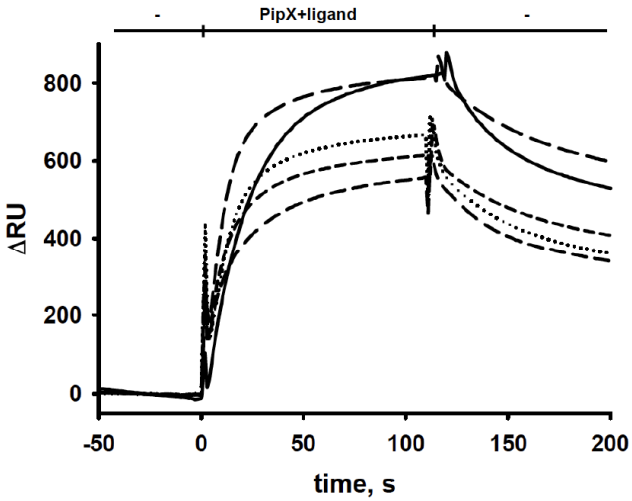
-
PipX+ligand
-
800
600
400
200
0
ΔRU
-50
0
50
100
150
200
time, s

F. Additional Research

Biochemical characterisation of P_{II} variants G84V, E85A, E85D and G89C

Sensing of a novel metabolite by genetically engineered P_{II} protein

Screening for a P_{II}-specific kinase using *Synechococcus elongatus* genomic library

1. Materials and Methods

1.1. Strains and growth conditions

Table F1. Bacterial strains

Strain	Relevant genotype	Reference
E. coli		
DH5α	F⁻ ϕ80d*lacZ*ΔM15Δ(*lacZ*YA-*argF*)U169 *end*A1 *rec*A1 *hsd*R17 *deoR thi-1 sup*E44 *gyr*A96 *rel*A1 λ-	(Hanahan, 1985)
FT8000	*rbs lacZ*::IS*1 gyr A hutC*$^{c}_{K}$ Δ*glnB1* ΩGm^{r} Δ*glnK1*	(Reyes-Ramirez *et al.*, 2001)
RB9060	Δ*glnB2306*	(Bueno *et al.*, 1985)
S. elongatus PCC 7942	wild type	(Kuhlemeier *et al.*, 1983)

Strains used in this study are listed in Table F1. *Escherichia coli* cells were grown in Luria-Bertani medium (Miller, 1972) at 37°C. Antibiotics ampicillin (Amp) and chloramphenicol (Cm) were added as necessary in concentrations of 50 and 34 µg ml^{-1} respectively. All cloning procedures were carried out in *Escherichia coli* DH5α using standard techniques (Sambrook *et al.*, 1989).

Synechococcus elongatus PCC 7942 cells were grown photoautotrophically at 25°C in liquid BG11 (BG11^{0}) medium (Rippka, 1988), with the addition of 5 mM $NaCO_3$. Either 17.6 mM $NaNO_3$ (BG11^{N}) or 5 mM NH_4^+ (BG11^{A}) were used as a nitrogen source. In low N medium 1 mM $NaNO_3$ was used. BG11^{A} medium was buffered with 20 mM HEPES/NaOH pH 7.5. The cell cultures were constantly shaken (150 rpm) at an illumination of 40 µmol photons s^{-1} m^{-2}. Growth of the cultures was monitored by measuring the optical density (OD_{750}).

1.2. Immunological detection of P_{II}-P

For the generation of a P_{II}-P-specific antiserum, a rabbit was immunised by intradermal injections of purified phosphopeptide CRYRG(pS)EYTV, generated from the P_{II} T-loop region, by the Pineda - Antikoerper-Service (Berlin, Germany). The activity and specificity of the received antiserum towards P_{II}-P was determined using immunoblot procedure. For the analysis, Ser49-phosphorylated P_{II} was purified from *S. elongatus* cells, grown in the low N BG11 medium to achieve maximal degree of *in*

vivo P_{II} phosphorylation, as described previously (Irmler and Forchhammer, 2001). To detect P_{II}-P in the cytoplasm extracts of *S. elongatus*, cells were grown in $BG11^{A}$ medium, harvested by centrifugation, washed in $BG11^{0}$ medium and resuspended in this medium to optical density (OD_{750}) of 0.7. Cytoplasm extracts were prepared according to the protocol of Forchhammer and de Marsac (1994). Purified P_{II}, cytoplasm extracts from $BG11^{A}$- or $BG11^{0}$-culture were loaded on the 15% SDS-PAGE. Afterwards, the proteins were blotted on the nitrocellulose membrane (Pall Corporation) and detected using the αP_{II}-P antiserum and peroxidase-coupled secondary antibody (Sigma) and chemoluminescent detection system (Roche).

Partial purification of the αP_{II}-P antiserum was achieved in several steps in solution and with immobilised proteins from *glnB* deficient *E. coli* RB9060 (Table F1) transformed with pASK-IBA3-*glnB* plasmid (Heinrich *et al.*, 2004). *E. coli* culture (200 ml) was grown at 37°C to an optical density (OD_{600}) of 0.8 and P_{II} expression was initiated by the addition of 0.2 µg ml^{-1} (w/v) anhydrotetracycline (AHT). After 40 min growth at 25°C, the cells (OD_{600}=1) were harvested by centrifugation and broken by sonification (Heinrich *et al.*, 2004). After removal of cell debris, one third of the supernatant was incubated with nitrocellulose membrane for 1 h at 25°C, one third - with 1% SDS for 10 minutes at 90°C and then put on the nitrocellulose membrane to bind proteins. Both membranes were separately washed in buffer (20 mM Tris/HCl pH 7.4, 0.9% NaCl) and saturated in 10% (w/v) milk solution. The last part of the supernatant was added directly to the αP_{II}-P antiserum (diluted 1:10 in 20 mM Tris/ HCl pH 7.4, 0.9% NaCl) for 4 hours at 25°C. Subsequently, the antiserum together with the *E. coli* proteins was incubated over night with a nitrocellulose membrane, carrying denaturated proteins from *E. coli*. Afterwards, the membrane was removed from the partially purified antiserum and the antibody was added to the membrane with non-denaturated proteins for 4 hours. The last step included another over night incubation with denaturated membrane bound proteins. The antibody after each purification step was analysed. Cytoplasm extracts of *E. coli* RB9060 (Table F1) without P_{II}, with overexpressed P_{II} and purified P_{II}-P from *S. elongatus* were loaded on the 15% SDS-PAGE and detected using the immunoblot analysis.

1.3. Cloning of the *S. elongatus glnB* gene in pACT3 vector

The *glnB* gene from *S. elongatus* was amplified by PCR with pASK-IBA3-glnB plasmid (Heinrich *et al.*, 2004) as a template with primer pair glnB-pACT3-for (5´-

CAGAGCTCATGAAGAAGATTGAGGCGATTA-3´) with *Sac*I site and glnB-pACT3-rev (5´-ATGGATCCTTAGATTGCGTCGGCGTTTTT-3´) with *Bam*HI site. The PCR product was cloned into the *Sac*I & *Bam*HI restricted and dephosphorylated pACT3 vector (Dykxhoorn *et al.*, 1996). The resulting plasmid was transformed into FT8000 *E. coli* (Table F1).

1.4. Library construction

Standard molecular cloning techniques (Sambrook *et al.*, 1989) were used to construct the genomic library of *S. elongatus*. Genomic DNA was purified from *S. elongatus* PCC 7942 cells grown in $BG11^N$ medium (Wilson, 1987). DNA was partially digested by *Sau*3AI for 30 min at 37°C. DNA fragments of approximately 3000-2000 bp, selected by excision from an agarose gel, were cloned into the *Bam*HI restricted and shrimp alkaline phosphatase (Roche) treated pEXT20 vector (Dykxhoorn *et al.*, 1996). For the screen, the library was transformed into FT8000 *E. coli* (Table F1) carrying pACT3-*glnB* plasmid.

1.5. Library screening

FT8000 cells containing pACT3-*glnB* plasmid and the library were plated on Cm/ Amp-LB medium without IPTG to get around 100 clones on one plate. From the master plate the cells were transferred on the replica Cm/Amp-plate with 1 mM IPTG and grown over night at 37°C. Afterwards, the cells from each plate were separately resuspended in M9 minimal medium (Sambrook *et al.*, 1989) containing 0.4% (w/v) glucose, 14 mM glutamine, 0.04% (w/v) thiamine and 0.1% (v/v) trace elements solution from BG11 medium (Rippka, 1988) and incubated shaking (150 rpm) for 2 hours with sufficient air supply at 25°C. After the incubation the cells were treated with SDS-sample buffer, denaturated at 90°C for 10 min and the modification status of the P_{II} protein was analysed by 15% SDS-PAGE followed by immunoblot analysis with P_{II}-P specific antibody. As a control, cytoplasm extracts from the wild type *S. elongatus* grown in low N BG11 medium were also loaded on the gel.

2. Results

2.1. Biochemical characterisation of P_{II} variants G84V, E85A, E85D and G89C

To identify *S. elongatus* P_{II} mutants that lost the ability to interact with NAG kinase, random mutagenesis of the P_{II}-encoding *glnB* gene was performed by error-prone PCR and the resulting random mutant library was cloned in the bacterial two-hybrid pBT vector (Ruppert and Forchhammer, unpublished). Subsequently, this library was used as a prey in an interaction screening against the NAGK encoding *argB* gene fused to the pTRG bait vector. Transformants were replica plated on selective and non-selective plates. Clones, which were unable to grow in selective conditions, indicative of a loss of interaction, were picked. These were subsequently tested for integrity of the P_{II} protein by immunoblot analysis, and those clones, which displayed full-length immunoreactive P_{II} fusion proteins and further confirmed to fail to grow on selective medium were further analysed by sequence analysis. In cases where several point mutations occurred, single mutants were generated and tested again as described above. Using this strategy following P_{II} mutations could be identified to result in loss of NAGK interaction: F11L, L13Q, I25V, R45C, G48D, S49G, S49D, S49P, S49W, I74N, G84V, E85D, G89C, G89S, F92S and R103H (Ruppert and Forchhammer, unpublished). Comparing these mutations with the structure of the P_{II}-NAGK complex (Llacer *et al.*, 2007) reveals a remarkable congruity: the β1-α1 junction of P_{II}, to which residues F11 and F13 belong, was shown to be involved in hydrophobic interactions with NAGK. Furthermore, the T-loop of P_{II} (in particular residues R45 – E50) inserts into the cleft between the N- and C-terminal NAGK domains, with R45 being engaged in an ion-pair network and S49 in tight hydrogen-bond interactions with NAGK. Another region of interaction concerns the B-loop of P_{II} with residues E85 forming a salt-bridge with R233 of NAGK and T83 being engaged in hydrophobic interactions. Considering the role of the E85 residue, the loss of interaction by the E85D mutation was unexpected, since the resulting mutant has retained the negative charge required for ion-pair interaction with NAGK.

2.1.1. Complex formation of wt NAGK with P_{II} variants: SPR analysis

Since the bacterial two-hybrid screens revealed an unexpected clustering of mutations in the B-loop region altering the P_{II}-NAGK interaction, the properties of B-loop P_{II} variants were further investigated. The wild type NAGK, P_{II} and the P_{II}

variants G84V, E85A, E85D and G89C were purified according to Fokina *et al.* 2010b. Using SPR analysis with wild type NAGK bound to the sensor chip performed as described previously (Fokina *et al.*, 2010b), the P_{II} variants were tested for interaction in the absence of effector molecules and in the presence of 1 mM ATP (Figure F1).

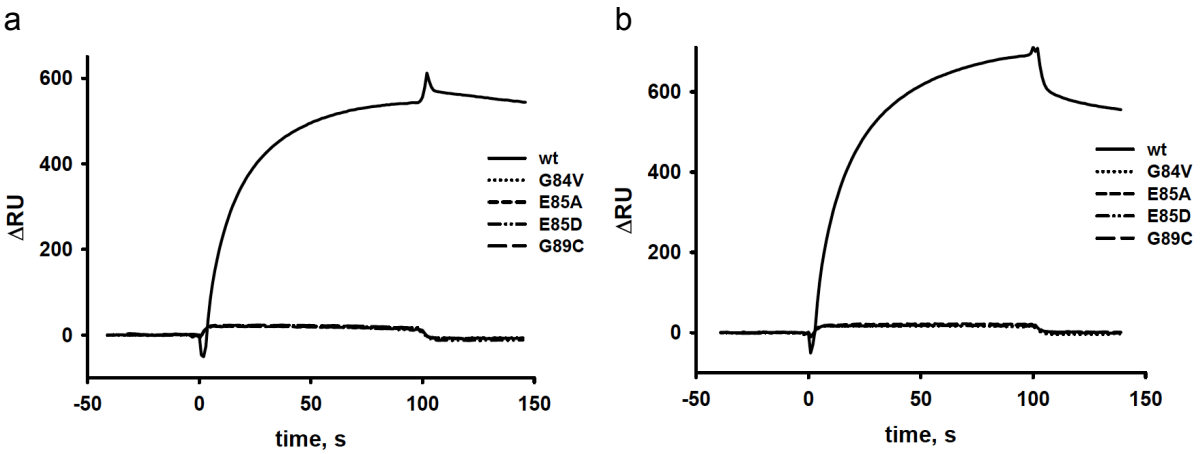

Figure F1. SPR analysis of NAGK interaction with recombinant P_{II} proteins. NAGK was bound to FC2 of a Ni^{2+}-loaded NTA sensor chip and FC1 was used as background control. The response difference (ΔRU) between FC1 and FC2 is shown. Wild type P_{II} and G84V, E85A, E85D and G89C variants, as indicated, were injected on the immobilised NAGK in the absence of effectors (a) and in the presence of 1 mM ATP (b).

Wild type P_{II} was injected on the immobilised NAGK in the control measurements with and without ATP and formed a stable complex with the enzyme. No binding to wt NAGK was revealed for variants G84V, E85A, E85D and G89C either without effector molecules or in the presence of 1 mM ATP, confirming the results obtained by bacterial two-hybrid study.

2.1.2. Isothermal Titration Calorimetry (ITC) studies of ATP, ADP and 2-OG binding to P_{II} proteins

P_{II} interactions are modulated by binding of the effector molecules ATP, ADP and 2-OG. Therefore we analysed the ATP-, ADP- and 2-OG-binding properties of wt P_{II} and B-loop mutant P_{II} variants using Isothermal Titration Calorimetry, performed according to Fokina *et al.* 2010b. Optimal fitting of the raw data was obtained using a three sequential binding sites model and the dissociation constants are shown in Table F2.

Table F2. Dissociation constants of ATP, ADP and 2-OG binding to recombinant P_{II} proteins

	K_d1 [µM]	K_d2 [µM]	K_d3 [µM]
ATP			
(wt)	(4.0±0.1)	(12.5±0.9)	(47.4±21.9)
G84V	95	146,2	3,4
E85A	16	38	49
E85D	26,7	10,1	3
G89C	n	n	n
ADP			
(wt)	(10.6±3.2)	(19.3±2.3)	133.4±5.3
G84V	138,5	107,9	278,5
E85A	2,8	3,1	17,4
E85D	92,6	263,1	1,5
G89C	n	n	n
2-OG (+1mM ATP)			
(wt)	5.1±4.0	11.1±1.8	106.7±14.8
G84V	581	243,3	93,4
E85A	408	203,7	621,1
E85D	32,9	21,5	111,2
G89C	n	n	n

n: not detectable

The P_{II} mutant G84V showed more than 10-fold weaker ATP-binding for the first two sites, but strong cooperativity for the third site. The affinity for ADP and 2-OG was strongly decreased compared to wt P_{II}. For G89C mutant addition of ATP, ADP or 2-OG (in the presence of 1 mM ATP) did not yield any calorimetric signals, suggesting that this mutant has lost the ability to interact with both ATP and ADP, and as a consequence, also with 2-OG. Both E85 P_{II} mutants, E85A and E85D, are not able to interact with NAGK, but showed highly different ligand-binding properties. The E85A mutant showed anti-cooperativity for all three ATP/ADP binding sites, though it bound ATP weaker and ADP stronger than wt P_{II} and the affinity towards 2-OG was very low. By contrast, the E86D P_{II} mutant has reverted ATP binding from anti-cooperative to cooperative. Affinity for ADP of sites one and two was much lower than in wt, but site three appeared to be occupied in a cooperative manner. The interaction with 2-OG was similar to the wild type.

2.2. Sensing of a novel metabolite by genetically engineered P_{II} protein

In the P_{II}-NAGK complex there are two contact surfaces: P_{II} B-loop with NAGK C-domain (E85-R233 salt bridge) and a larger one, P_{II} T-loop with NAGK N-domain. In the I86N P_{II} variant, the T-loop is locked in the tightly folded conformation with the E44 residue forming a salt-bridge to K58 (Fokina *et al.*, 2010b). This conformation is stabilised due to the hydrogen bond between N86 and the backbone carbonyl oxygen of T43. The inability of this variant to bind 2-OG can be explained by 2-OG not being able to open this conformation and accessing its ligands, and in consequence, this variant is a super-active NAGK binder (Fokina *et al.*, 2010b). In the crystallisation trials of this P_{II} variant, crystals revealed a Mg^{2+}-ATP complex with another physiologically relevant molecule, citrate.

To determine, whether in the I86N variant citrate functionally replaced 2-OG, the effect of citrate on binding of the P_{II} variant I86N to NAGK was assayed by SPR spectroscopy as described previously (Figure F2) (Fokina *et al.*, 2010b).

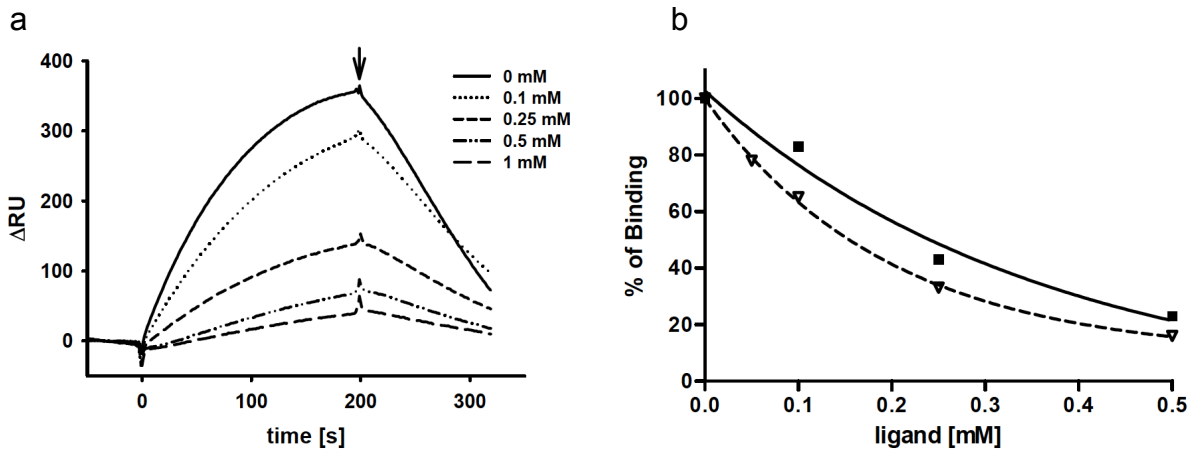

Figure F2. (a) SPR analysis of I86N P_{II} (100 nM) binding of to R233A NAGK in the presence of 1 mM ATP and citrate at concentrations of 0, 0.1, 0.25, 0.5 and 1 mM, as indicated. The response difference (ΔRU) between FC1 and FC2 is shown. An arrow indicates the end of the injection phase. (b) Association of I86N P_{II} and R233A NAGK in presence of citrate and 1mM ATP (—) compared to wt P_{II} and wt NAGK in presence of 2-OG and 1mM ATP (---).

Binding assays with the NAGK variant R233A showed a clear inhibitory effect of citrate (Figure F2a). The I86N binding levels in the presence of citrate were compared to the inhibition of wild type P_{II}-NAGK association by 2-OG (Figure F2b). The binding curves are highly similar, though 2-OG was a bit more efficient in preventing the wt P_{II}-NAGK interaction compared to citrate with R233A NAGK and I86N P_{II}.

2.3. Screening for a P_{II}-specific kinase using *Synechococcus elongatus* genomic library

P_{II}-mediated signal transduction in cyanobacteria is regulated directly and indirectly by the metabolites ATP, ADP and 2-OG. These effectors bind directly to P_{II} and change its conformation, so that the protein can regulate its targets NAGK and PipX. Another level of effector influence is reversible phosphorylation of P_{II} on the Ser49 in the presence of Mg^{2+}-ATP-2-OG. Though the P_{II}-specific kinase has not been identified yet, the *in vitro* phosphorylation could be achieved with whole cells extracts from *S. elongatus* (Forchhammer and de Marsac, 1995). In this study a genomic library of *S. elongatus* was created and transformed into the *E. coli* cells together with a plasmid carrying *S. elongatus glnB* gene. The purpose was to screen the clones for phosphorylated P_{II} with a specific antibody against phosphorylated P_{II}, which didn't react with non-phosphorylated P_{II}.

2.3.1. Production and characterisation of P_{II}-P specific antibody

For this study a specific antibody was needed, which would only detect phosphorylated P_{II} protein. A phosphopeptide CRYRG(pS)EYTV was generated from a part of the T-loop of P_{II} and used for immunisation of the rabbit. The sensitivity of antiserum after 175 days was tested against purified phosphorylated P_{II} ($P_{II}^{2,3}$) (Figure F3). The protein sample was loaded on the 15% SDS-PAGE and the proteins were blotted on the nitrocellulose membrane according to the standard protocol described in Section E. Different amounts of antiserum were applied in a total volume of 20 ml, resulting in dilutions 1:2000 (10 µl), 1:1000 (20 µl), 1:500 (40 µl) and 1:333 (60 µl).

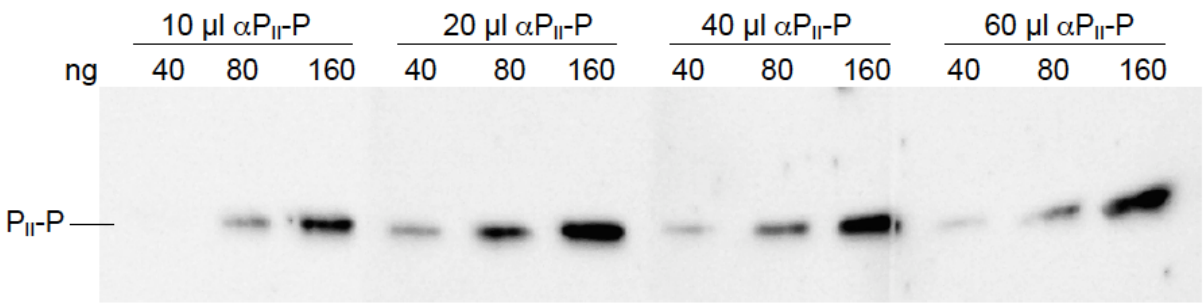

Figure F3. Sensitivity of αP_{II}-P antiserum towards purified αP_{II}-P protein. Different amounts of phosphorylated P_{II} protein, as indicated, were loaded on the 15% SDS-PAGE followed by immunoblot analysis. For the P_{II}-P detection, 10, 20, 40 and 60 µl of the αP_{II}-P antiserum were applied.

As shown in Fig. F3, 80 ng of the purified phosphorylated P_{II} could be detected by adding 10 µl of antiserum and 40 ng - by adding 20 µl. Further increase in concentration of αP_{II}-P had no effect on the signal intensity. Afterwards, 1:1000 (20 µl) dilution of antibody was used in the following experiments. The specificity of αP_{II}-P antibody was tested using purified non-phosphorylated P_{II} and cytoplasm extracts of wild type *S. elongatus*.

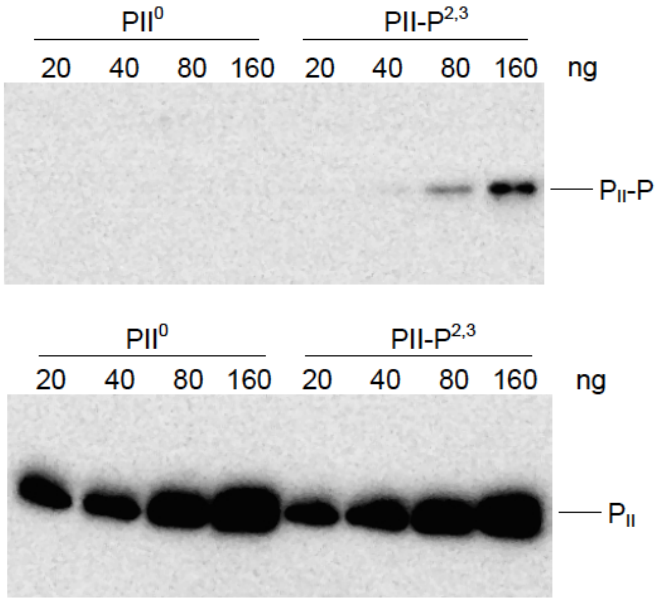

Figure F4. Analysis of αP_{II}-P antiserum specificity. Different amounts of purified non-phosphorylated (P_{II}^0) and phosphorylated ($P_{II}^{2,3}$) P_{II} protein were loaded on the 15% SDS-PAGE followed by immunoblot analysis, as indicated. The blots were incubated with αP_{II}-P antiserum (a) and αP_{II} antiserum (b).

The αP_{II}-P antibody didn't bind the non-phosphorylated P_{II} protein (P_{II}^0), but the P_{II}-P bands could be seen on the blot (Fig. F4a). As a control, the same amounts of protein were detected by the P_{II}-specific antibody (Forchhammer and de Marsac, 1994), which binds to the both modified and non-modified forms of P_{II} (Fig. F4b).

It was expected that a polyclonal antiserum could react unspecific with cell proteins in the *S. elongatus*. Cytoplasm extracts were obtained and cell proteins (35 µg and 75 µg total protein amount) were analysed by SDS-PAGE followed by immunoblot analysis with αP_{II}-P-specific antibody (Fig. F5).

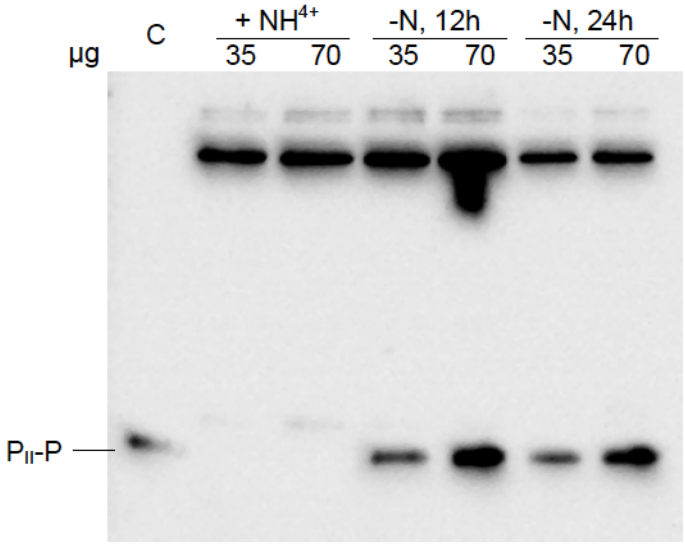

Figure F5. Detection of the phosphorylated P_{II} protein in cytoplasmic extracts using αP_{II}-P antiserum. *S. elongatus* cells were grown in the NH4+ BG11 medium and then shifted to nitrogen-free medium. Total cellular proteins (35 and 75 µg) were analysed via 15% SDS-PAGE followed by immunoblot analysis.

The cells were first grown in the ammonium-rich medium ($BG11^A$) to ensure sufficient nitrogen supply. Under these conditions P_{II} protein is non-phosphorylated (Forchhammer, 2004). As shown in Fig. F5, no P_{II}-P was detected by the αP_{II}-P antibody in the protein extract. Subsequently, the cells were shifted into nitrogen-free medium and analysed after 12 and 24 hours. Under nitrogen deprivation P_{II} protein binds ATP and 2-OG and is phosphorylated. The band, corresponding to the P_{II}-P, was detected in cytoplasm extracts after the shift (Fig. 5). The upper bands that were observed on the blot are unspecific and are present in all lanes with *S. elongatus* cytoplasm extracts.

The library screen to detect the P_{II} kinase was performed in the *E. coli*, so the antiserum was tested for unspecific reactions with *E. coli* cell proteins. Due to the many detected bands on the blot, the polyclonal antiserum was purified to remove the unspecific antibodies. Cytoplasm extracts of *glnB* deficient *E. coli* mutant without P_{II} and with overexpressed P_{II} from *S. elongatus* were analysed by SDS-PAGE followed by immunoblot analysis (Figure F6). Purified P_{II}-P was used as a control. After the western blot the membrane was cut in four and separate parts were incubated with αP_{II}-P antiserum after each purification step, as well as with non-purified antibody. The parts were put back together and developed using a chemoluminescent detection system. In the first step, antiserum was incubated for 4 hours with cell extract from *E. coli* and afterwards over night with a nitrocellulose

membrane, carrying denaturated proteins from *E. coli*. In the second step the partially purified antiserum was added to the membrane with bound native proteins from *E. coli* for 4 hours and the last step included another over night incubation with denaturated membrane bound proteins.

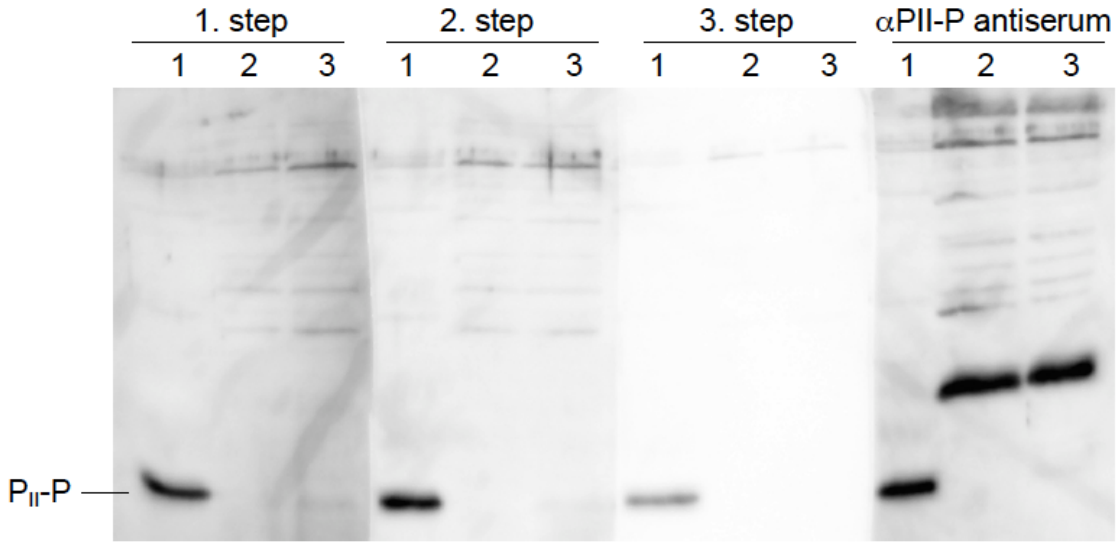

Figure F6. Purification of the αP_{II}-P antiserum. Protein samples were analysed by SDS-PAGE and immunoblot analysis. αP_{II}-P antiserum was purified in 3 steps as described in Material and Methods and the activity of the resulting solution was compared with the original antibody. 1 - purified P_{II}-P, 2 - *E. coli* cytoplasm extracts without P_{II}, 3 - *E. coli* extracts with overexpressed P_{II}.

The strong unspecific reaction of the antiserum towards *E. coli* cell proteins could be mostly removed in the first purification step without any detectable lost of the specific binding to P_{II}-P in the control lane (Fig. F6). After the second purification step no change was detected and the third step resulted into the weakening the specific detection of P_{II}-P. Therefore, large amount of antiserum was purified according to the protocol for the first purification step and applied in the library screen.

2.3.2. Cloning of the S. elongatus glnB gene and creation of the Synechococcus elongatus genomic library

To obtain both *glnB* and random gene from the *Synechococcus elongatus* PCC 7942 library overexpressed in the same *E. coli* FT8000 cell (Table F1), compatible expression vectors were chosen. The *glnB* gene was successfully cloned into pACT3 vector as described in Materials and Methods and clones were checked via PCR to confirm the presence of the gene (Fig. F7).

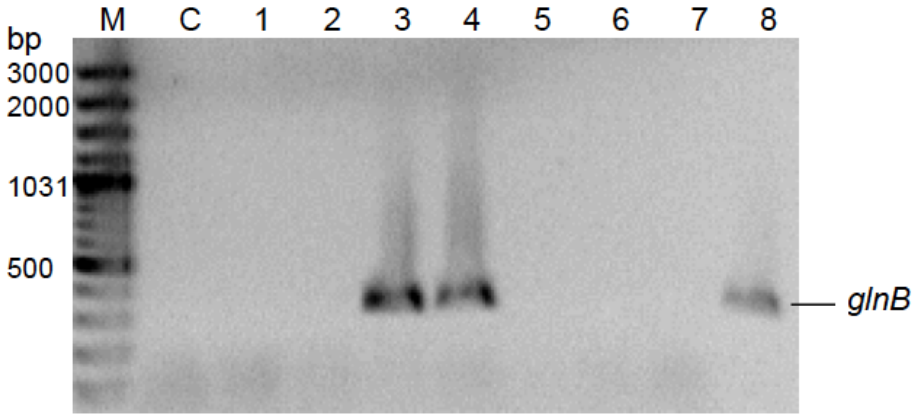

Figure F7. PCR analysis of the *glnB* gene presence in the plasmid after the cloning. M – DNA marker, C – control PCR with empty pACT3 vector, 1-8 clones 1-8.

Clones 3, 4 and 8 contained the *glnB* gene and clone 4 was checked by sequencing and used for transformation into *glnB*$^-$/*glnK*$^-$ FT8000 *E. coli*.

Genomic DNA of *S. elongatus* was partially digested with *Sau*3AI for 30 minutes. DNA fragments of approximately 3000-2000, 2000 and 1000 bp were isolated and analysed on the agarose gel together with *Bam*HI restricted pEXT20 vector (Figure F8).

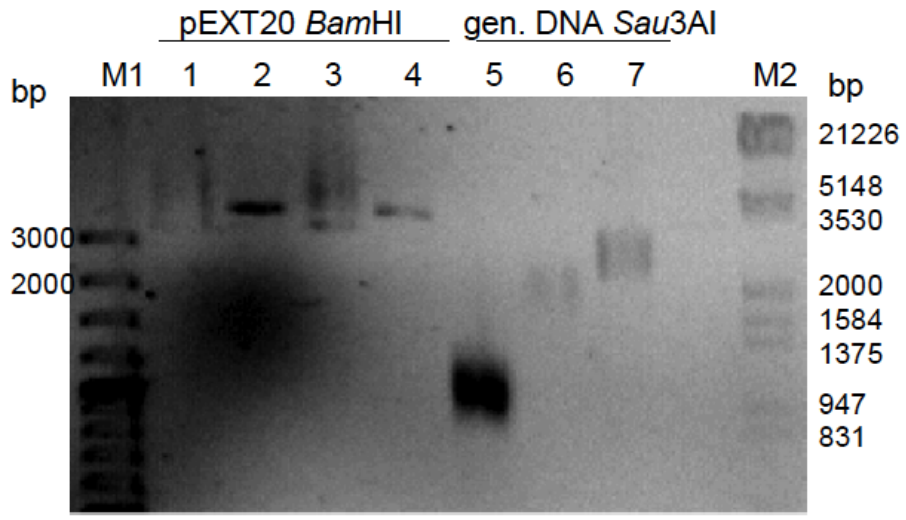

Figure F8. Analysis of the restriction digest of the pEXT20 vector and genomic DNA from *S. elongatus* before ligaton. M1 & M2 – DNA markers, 1-4 - *Bam*HI digested pEXT20 samples, 5-6 – *Sau*3AI digested genomic DNA.

The 3000-2000 bp *Sau*3AI fragments (lane 7) were cloned into pEXT20 vector (lane 2). The library was plated out and a total number of approximately 10000 clones was counted. The genome size of *S. elongatus* is around 2.7 Mb and the obtained

amount of clones was considered enough to perform a library screen. The library was transformed into *glnB*$^{-}$/*glnK*$^{-}$ FT8000 *E. coli* cells carrying a pACT3-*glnB* plasmid.

2.3.3. Screening for phosphorylated P_{II}

The library screen was performed to find phosphorylated P_{II} in the FT8000 *E. coli* cells, carrying plasmids with *glnB* and a random genome DNA fragment of *S. elongatus*. The cells were incubated in the minimal medium with Glc/Gln to create conditions for the P_{II}-phosphorylation. P_{II} and an unknown protein from the library were overexpressed after the addition of 1 mM IPTG. To optimise the method, two tests with FT8000 cells containing only pACT3-*glnB* were performed (Figure F9).

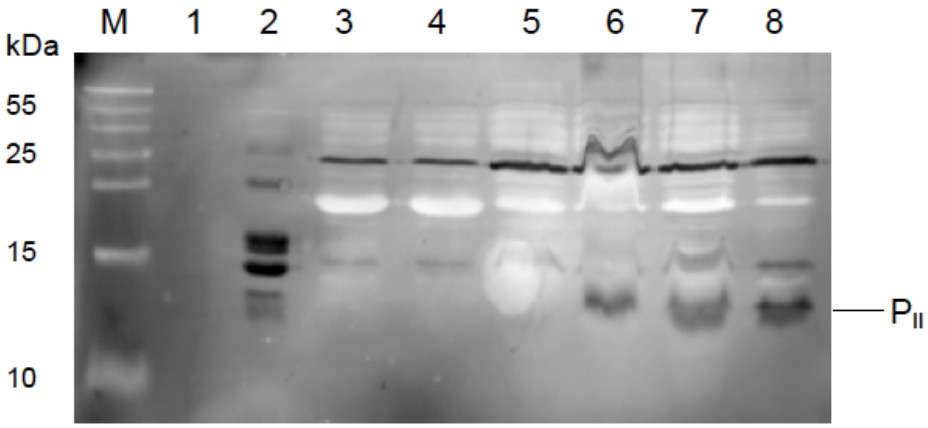

Figure F9. P_{II} overexpression in the FT8000 cells containing pACT3-*glnB* plasmid. Protein samples were analysed by SDS-PAGE and immunoblot analysis with αP_{II} antibody. M – protein marker, 1 – 10 ng purified P_{II}, 2 – protein extract of *S. elongatus*, 3 – test 1 protein extract from *E. coli* after over night incubation, 4 – test 1 proteins after addition of M9-Glc/Gln medium, 5 – test 1 proteins after incubation with 1 mM IPTG, 6 - test 2 protein extract from *E. coli* after over night incubation with IPTG, 7 – test 2 proteins after incubation with M9-Glc/Gln medium, 8 - protein extract from *E. coli* after standard overexpression of P_{II}.

In the first test the cells were grown on plates overnight, then resuspended in M9-Glc/Gln medium and afterwards incubated with 1 mM IPTG for two hours. The samples after each step were analysed using 15% SDS-PAGE and immunoblot analysis with P_{II} specific antibody. As shown in Figure F9 (lanes 3-5), no protein band corresponding to P_{II} protein was observed. The overexpression with IPTG didn't work due to presence of the glucose in the M9 medium. In the second test the cells were grown over night on the plates with 1 mM IPTG, then resuspended in the M9-Glc/Gln medium and incubated for two hours. P_{II} was present in the cells after the overnight incubation and after the addition of M9 medium (Fig. F9, lanes 6, 7). Cytoplasm extracts of FT8000 *E.coli* with P_{II}, overexpressed according to the standard protocol,

and of wild type *S. elongatus* PCC 7942 were used as positive control (Fig. F9, lanes 2, 8).

A total of approximately 6000 clones were analysed in the library screen. The library was transformed into the FT8000 cells with pACT3-*glnB*. The cells were plated on LB medium without IPTG to get around 100 clones on one plate. From the master plate the cells were put on the replica plate with IPTG and processed as in the test 2. After the incubation in the minimal medium with Glc/Gln, the modification status of the P_{II} protein was analysed by SDS-PAGE and immunoblot analysis with P_{II}-P specific antibody (Figure F10).

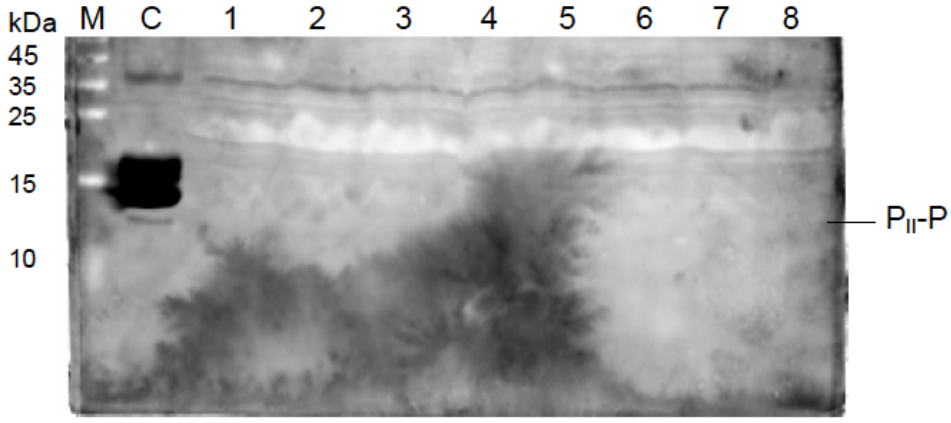

Figure F10. Screen for the phosphorylated P_{II} protein. Cytoplasm extracts from plates 1-8 were analysed by 15% SDS-PAGE and immunoblot analysis with αP_{II}-P antibody. M – protein marker, C - protein extract of *S. elongatus* with P_{II}-P, 1-8 – plates 1-8.

The cells from the first eight replica plates contained no phosphorylated P_{II}. However, it was detected in the control sample containing cell extract of *S. elongatus* grown under nitrogen starvation. To confirm that P_{II} was successfully overexpressed in the cells, the same samples were analysed with P_{II}-specific antibody (Figure F11).

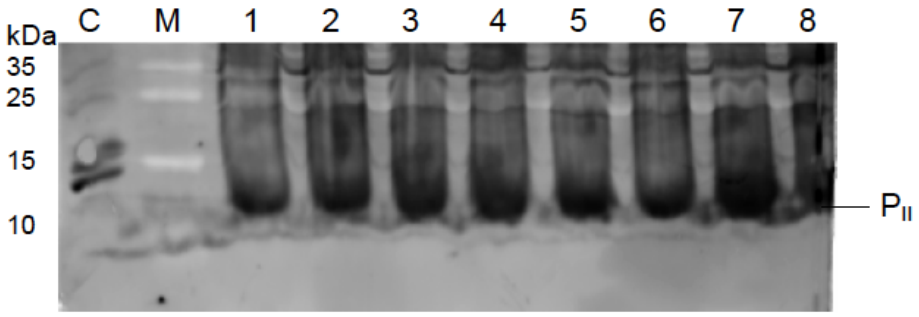

Figure F11. Detection of the overexpressed P_{II} in the cytoplasm extracts, used in the library screen. Samples from plates 1-8 were analysed by 15% SDS-PAGE and immunoblot analysis with αP_{II} antibody. M – protein marker, C - protein extract of *S. elongatus* with P_{II}-P, 1-8 – plates 1-8.

Large amounts of P_{II} proteins could be detected in all samples. Subsequently, the remaining 48 plates were analysed using the same method. No P_{II}-phosphorylation was observed.

There are several reasons for the absence of phosphorylated P_{II} in the analysed samples. Each sample contains P_{II} pool from approximately 100 cells, even though large amounts of P_{II} were present on the gel, the concentration of P_{II}-P could be insufficient for the detection. Since analysing each clone independently would require too much time, the method could be adapted. For example the cells could be transferred on the nitrocellulose membrane and P_{II}-P would be detected directly on the membrane. However, this method would require specific antibody without any unspecific reactions with other proteins. It is also possible that *E. coli* cells do not provide all the conditions needed for phosphorylation of the P_{II} protein or Ser-phosphotases in *E. coli* dephosphorylate P_{II}, the P_{II}-specific kinase could also be toxic for *E. coli*. Nevertheless, P_{II} kinase is an important part of the P_{II} signal transduction in cyanobacteria. The discovery of this enzyme is not only essential for all-round understanding of the P_{II} modification that is so far unique to cyanobacteria, but the protein would be a vital tool in the further laboratory studies concerning the P_{II} protein.

G. Discussion

This study has given intriguing new insights into the known aspects of the P_{II} interaction network with metabolites ATP, ADP and 2-OG and revealed P_{II} as a sensor of adenylate energy charge *in vitro*.

Variants of the *S. elongatus* P_{II} protein with point mutations in the B-loop region, obtained from random mutant library and bacterial-two-hybrid analysis, have pointed out the role of the B-loop in various P_{II}-involving interactions.

1. Role of the P_{II} B-loop in the effector binding

The B-loop variants of P_{II} were strongly impaired in the effector molecule binding compared to wild type P_{II}, as was detected by isothermal titration calorimetry (ITC) (Fokina *et al.*, 2010b). Optimal fitting of the raw data could be obtained by using a three sequential binding sites model for the three effector-binding sites of the P_{II} trimer. This analysis provided three different dissociation constants for the three sites of P_{II}, revealing sequential anticooperative occupation of the sites. The fact that binding of ATP and 2-OG to the *S. elongatus* P_{II} protein is anticooperative was previously determined by equilibrium dialysis, however the dissociation constants for the three effector binding site could not be obtained by this method (Forchhammer and Hedler, 1997). Here, for the first time, the binding characteristic of ADP to wild type P_{II} were determined. ADP binds to P_{II} almost as efficiently as ATP and also exhibits negative cooperativity.

Previous mutational analysis of *E. coli* P_{II} has already demonstrated the pivotal role of G89, both for effector molecule binding and receptor interactions, whereas mutation of the G84 residue had only a slight effect on effector molecule binding (Jiang *et al.*, 1997). The G84V variant of P_{II} from *Synechococcus* had a much lower affinity for effector molecules ATP, ADP and 2-OG than the wild type *S. elongatus* P_{II} and the corresponding *E. coli* G84A variant, indicating that the larger aliphatic side chain of valine (as compared to alanine) had a stronger effect on the B-loop structure and thereby impaired ATP and 2-OG binding more efficiently. The G89C variant has lost the ability to interact with both ATP and ADP, and probably as a consequence, also with 2-OG. The G89 residue is in close proximity to the α-phosphate of bound ATP in P_{II} from *S. elongatus* (Fokina *et al*., 2010a) and in GlnK from *E. coli* (Xu *et al.*,

1998), and apparently, introducing a side chain at this position impaired not only the binding of effector molecules, but distorted the conformation of the T-loop, which is responsible for most effector molecule interactions (Forchhammer, 2008), as revealed from the inability of the G89 P_{II} mutants in *E. coli* (Jiang *et al.*, 1997) and *S. elongatus* to interact with receptors.

In the absence of the effector molecules, the E85 residue of non-liganded P_{II} connects the B-loop with the T-loop by a salt bridge to R47 (Xu *et al.*, 2003; Llacer *et al.*, 2007). In the E85A mutant the negative cooperativity of ligand binding was still preserved, but weaker. The affinity for 2-OG was most strikingly impaired. This mutation also lowered the affinity for ATP, but at the same time enhanced affinity for ADP. Surprisingly, the E85D mutation reverted the binding properties for ATP from anti-cooperative to cooperative, whereas the binding of 2-OG (at saturating ATP levels) was not strongly affected. From structural analysis of P_{II} proteins one can assume that that the E85 residue is not directly involved in nucleotide binding, however, it seems to be involved in intermolecular signalling. The salt-bridge between E85 and R47 may be an important determinant for this purpose, but other interactions between structural elements of P_{II} seem to be involved as well, since the E85A mutant has not completely lost anticooperativity. The E85D mutation, by contrast, seems to lock the P_{II} protein in an unusual conformation: unable to interact with NAG kinase and cooperatively coupling the ATP binding sites.

The P_{II} variants I86N and I86T have completely lost the anticooperativity between the ATP-binding sites and were the only mutants that couldn't bind 2-OG and retained high affinity towards ATP (Fokina *et al.*, 2010b). The binding site for 2-OG is only formed upon ATP binding, so it was assumed that I86 was directly involved in 2-OG binding or was at least located near the 2-OG-binding site. This theory was supported by the mutational analysis in *E. coli* that determined Q39, which lies opposite to the I86 at the base of the T-loop, involved in 2-OG binding (Jiang *et al.*, 1997). The I86N variant has gained one remarkable feature compared to wild type P_{II}, it could bind citrate on the binding site, created by P_{II} and bound Mg^{2+}-ATP. Citrate has also functionally replaced 2-OG, by inhibiting the complex formation between I86N P_{II} and the R233A NAGK, but not wild type NAGK in the *in vitro* binding assay. The I86N variant in complex with citrate is a first example of a genetically engineered P_{II} protein sensing a novel metabolite.

2. Location of 2-OG binding site and mechanism of 2-OG signalling

Resolving the P_{II} crystal structure with bound Mg^{2+}-ATP and 2-OG was a decisive step towards understanding many remarkable features of P_{II}-mediated signal transduction. P_{II} with bound ATP-Mg^{2+}-2-OG adopts a compact structure due to the back-folding of the C-terminus and due to a novel T-loop conformation (Fokina *et al.*, 2010a). The ATP molecule is ligated by arginines R38, R101, R103 and K90 as well as hydrogen bridges. The 2-OG-binding site is created only after Mg^{2+}-ATP binding. It is located in the intersubunit cleft between P_{II} subunits and is formed by the ATP-chelated Mg^{2+} ion and backbone atoms from Q39, K40, G41, G87 and Q39, K58 salt bridges. The base of the T-loop (R38-G41) plays a major role in the interaction and wraps around 2-OG. The structure explains, why 2-OG has negative influence on the P_{II}-NAGK interaction. Conformational changes, caused by 2-OG binding, prevent the T-loop from folding into the conformation that fits into the NAGK.

2-OG is able to inhibit the P_{II}-NAGK complex formation and to cause its dissociation. However, 7.5-fold higher concentrations of 2-OG are required to dissociate the complex than to prevent its formation. The free P_{II} protein in solution can easily interact with 2-OG, if it has ATP-Mg^{2+} bound, however, in the complex with NAGK the tightly bent conformation of the T-loop prevents the 2-OG site from forming (Fig. G1).

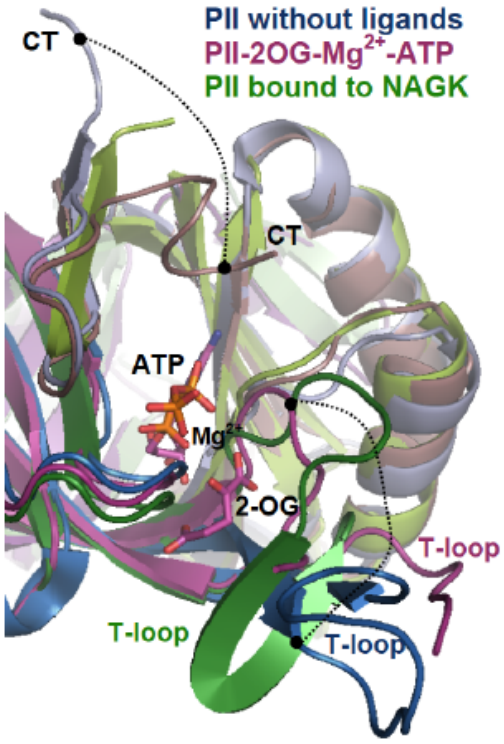

Figure G1. Conformational changes of the P_{II} protein from *S. elongatus*. Overlay of the P_{II} structures as ribbon models: without ligands coloured blue (PDB ID 1QY7), with 2-OG-Mg-ATP coloured pink (PDB ID 2XZW) and in the complex with NAGK coloured green (PDB ID 2V5H). The C-termini and T-loops are marked as CT and T-loop, respectively. ATP and 2-OG molecules are shown as sticks, Mg^{2+} ion as sphere. Large conformational transitions are marked with dashed lines.

Much higher concentrations of the ligand are needed to unlock the compact conformation and release the T-loop from NAGK to allow 2-OG binding. Interestingly, the IC_{50} for 2-OG to prevent P_{II}-NAGK association is approx. 125 µM and approaches the dissociation constant for the third 2-OG binding site (110 µM). Consequently, the occupation of the third site appears to be crucial for preventing the P_{II}-NAGK interaction. Therefore, partially 2-OG-occupied P_{II} should bind NAGK and thereby displace the 1-2 remaining 2-OG molecules. 2-OG is known to negatively affect the interaction between P_{II} and its second known target from *S. elongatus*, PipX. Considering the structure of the P_{II}-PipX complex with three extended T-loops around three PipX trimers bound to the bottom of the P_{II} body, solved recently (Llacer *et al.*, 2010), 2-OG could affect the complex in the similar way. The T-loop conformation in the complex is incompatible with the 2-OG-bound P_{II} T-loop, explaining the negative effect of 2-OG on the P_{II}-PipX interaction.

Sensing of 2-OG represents the main feature of the P_{II} proteins and all residues involved in the 2-OG binding are highly conserved (Fig. G2). Mutational studies showed that Q39 mutation strongly impaired 2-OG binding to P_{II} in *E. coli* (Jiang *et al.*, 1997) and K58 substitution destroyed the 2-OG signalling in *Rhodospirillum rubrum* (Jonsson and Nordlund, 2007).

Figure G2. Sequence conservation of the P_{II} proteins. Multiple sequence alignment was carried out using the P_{II} sequences from *S. elongatus*, *Nostoc sp*. strain 7120, *Prochlorococcus marinus* MIT 9301, *Thiobacillus denitrificans* ATCC25259, *E. coli* GlnB & GlnK, *Azospirillum brasiliense* GlnB & GlnK, *Bacillus subtilis* GlnK, *Lactococcus lactis subsp. cremoris* MG1363, *Streptomyces coelicolor* A3, *Methonococcus maripaludis* GlnB and *Methanocaldococcus jannaschii* DSM 2661 GlnB. Lower amino acid sequence belongs to the S. elongatus P_{II} protein with indication of the secondary structure elements and amino acids involved in ATP and 2-OG binding. Figure originates from Fokina *et al.*, 2010a.

The recently solved structure of the P_{II} homologue GlnZ from *Azospirillum brasiliense* with bound 2-OG-Mg^{2+}-ATP revealed the 2-OG binding site that is highly similar to the one presented in this study (Truan *et al.*, 2010). A remarkable feature of 2-OG interaction with P_{II} in *A. thaliana* is the ability of the effector molecule to bind in the presence of both Mg^{2+}-ATP and Mg^{2+}-ADP (Smith *et al.*, 2003). This process could involve additional residues of the P_{II} protein to compensate for the missing gamma-phosphate in the ADP, possibly from the back-folding C-terminus. The only study that revealed a different 2-OG binding site was performed with the P_{II} from *Methanococcus jannaschii* with the effector molecule binding to the outside apex of the T-loop (Yidiz *et al.*, 2007). Since this result was not confirmed by any biochemical research, it remains unclear, whether the mechanism of the 2-OG binding in archaea is different or the structure was a crystallisation artefact. The position of the 2-OG-binding site, identified in this study, perfectly agrees with mutational analysis done with P_{II} from *S. elongatus*. In particular, P_{II} variants R9L and K58M were impaired in the metabolite binding (Fokina *et al.*, 2010a). K58 and R9 were replaced with similar-sized amino acid, as a result the K58M P_{II} variant has lost the ability to bind 2-OG and R9L was strongly impaired in the 2-OG binding.

Crystal structures with one, two and three bound 2-OG molecules have revealed the mechanism behind negative cooperativity of the metabolite binding, characteristic for P_{II} proteins (Fokina *et al.*, 2010a). P_{II} proteins receive and process signals delivered by the metabolites ATP, ADP and 2-OG mainly via the T-loop interactions. Change of the T-loop conformation on one binding site upon 2-OG binding, unequally affects the two neighbouring sites, which can lead to the strongly altered affinity for the effector molecule. In the P_{II} trimer with one bound 2-OG molecule, the T-loop of the 2-OG-free site in clockwise orientation from the occupied site exhibits a conformation characteristic for the 2-OG-occupied site. As a result, this free site is more suitable for 2-OG binding than the other, which has the T-loop blocking the 2-OG pocket. The binding sites are directly connected by the β2-strands, which could be responsible for the delivering the signal inside the trimer. Such complex and unique mechanism of the intermolecular signalling is ensured by the highly conserved trimeric structure of the P_{II} proteins.

3. P_{II}-sensing of the adenylate energy charge

P_{II} proteins sense the signal of nitrogen deprivation, delivered by 2-oxoglutarate, but 2-OG binding is only possible to the Mg^{2+}-ATP-ligated P_{II} protein. The ATP binding site is strongly conserved (Fig. G2) and can be also occupied by ADP (Xu *et al.*, 1998; Xu *et al.*, 2003). There have been several studies, suggesting that P_{II} can act as a sensor of adenylate energy charge. The three P_{II} homologues from another photosynthetic bacterium, *Rhodospirillum rubrum*, regulate the transcriptional regulator NifA and DRAT/DRAG system, involved in regulation of the nitrogenase activity (Zhang *et al.*, 2001a; Zhang *et al.*, 2001b; Zhang *et al.*, 2003). The DRAT/ DRAG system responds to the cellular energy charge (Zhang *et al.*, 2001b), suggesting possible role of P_{II} in sensing the energy status of the cell. *In vitro* studies of the *E. coli* GlnB protein showed that ADP acted antagonistic to 2-OG in the P_{II} interactions with NtrB, ATase and UTase/UR (Jiang and Ninfa, 2007; Jiang and Ninfa, 2009b). Another member of the P_{II} family from *E. coli,* GlnK, is affected by ADP, which stabilises the complex with the ammonium transporter AmtB and negatively affects the 2-OG mediated response (Radchenko *et al.*, 2010).

The present study indicates that P_{II} from *S. elongatus* can act as an energy sensor *in vitro*. The decrease of the P_{II} affinity towards 2-OG is one of the effects of the ADP binding to P_{II} (Fokina *et al.*, 2011). The Mg^{2+} ion, needed for the formation of the 2-OG-binding site, is coordinated by the γ-phosphate of ATP, and this coordination is not possible with bound ADP. In living cells, ATP and ADP are present simultaneously and are competing for the same site on P_{II}, rendering the P_{II} sites either accessible or inaccessible for 2-OG (Fig. G3). The binding of the metabolites is anticooperative. ATP has a higher affinity towards each of the three binding site than ADP (Fokina *et al.*, 2010b). Therefore, at 1:1 molar ratio of ATP to ADP the amount of P_{II}-ATP_2ADP_1 trimers should prevail over the P_{II}-ATP_1ADP_2 population. Such a mixed population should exhibit lower affinity and reduced number of available sites for 2-OG, which was confirmed by the ITC experiments of 2-OG binding to P_{II} in the presence of ATP/ ADP (Fokina *et al.*, 2011). Also, at a 1:1 ATP/ADP ratio, 2-OG binding could no longer be fitted according to the three binding site model and approximately one 2-OG molecule could bind to P_{II}. The remaining 2-OG binding site showed low affinity towards 2-OG (K_d=183 μM), comparable to the third low-affinity site of the ATP-ligated P_{II} protein (K_d=106 μM). It means that ADP, bound to one site, has negative

impact on the 2-OG interaction with the ATP-occupied site in the P_{II} trimer of the mixed ADP/ATP-population.

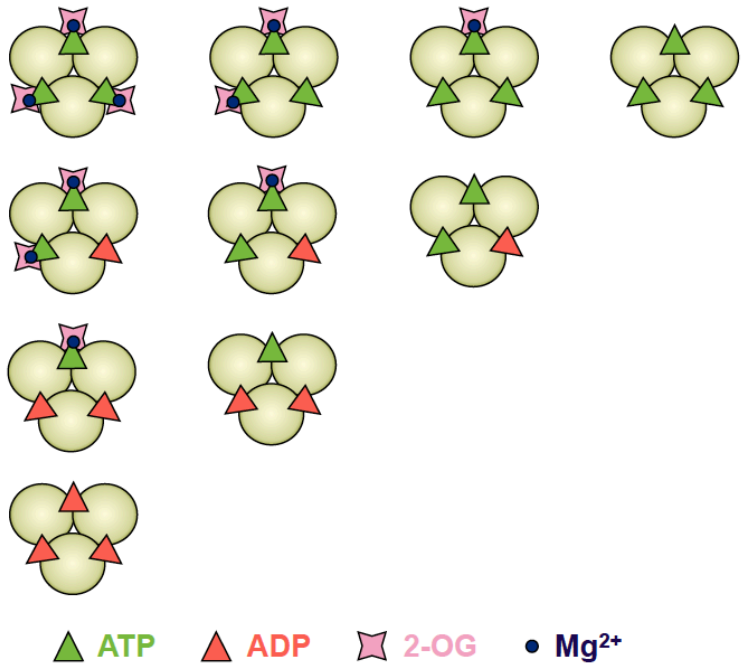

Figure G3. Possible signalling states of the *S. elongatus* P_{II} protein, in which all three nucleotide binding sites are occupied. Three linked circles represent the P_{II} trimer. P_{II}, fully occupied by the ATP/ADP molecules, can exist in 10 different forms depending on its 2-OG-binding status.

ADP affects the interaction of P_{II} with the NAG kinase in *S. elongatus,* by increasing the dissociation rate of the P_{II}-NAGK complex. Complex formation was observed even at high ADP concentrations. However, due to the higher dissociation rate, the steady-state binding levels of ADP-ligated P_{II} to NAGK in the SPR experiments were lowered, compared to the free or ATP-bound P_{II} (Fokina *et al.*, 2011). P_{II} species, occupied by a mixture of ATP and ADP, showed lower steady-state binding levels and enhanced dissociation of the P_{II}-NAGK complex. Even when ADP was in excess over ATP, the binding curves were still different from the ones with fully ADP-ligated P_{II}. This result showed that even if ADP is in excess over ATP, fully ADP-ligated P_{II} species are unlikely and the existence of the P_{II}-ATP_1ADP_2 species is more probable. In addition to affecting complex formation, ADP also influences the catalytic activity of NAGK in the complex with P_{II} (Fokina *et al.*, 2011). The effect could be mediated by the T-loop, which can't fold into the perfect NAGK-conformation after the initiating step of the P_{II}-NAGK interaction, described above. From the enzyme assay, performed with different ATP/ADP ratios, it could be concluded that P_{II} species with bound ATP/ADP mixtures were not able to enhance the NAGK activity, but still

efficiently protected the enzyme from arginine inhibition. Clearly, NAGK induction and protection from arginine inhibition are mediated by P_{II} via two different mechanisms and it is also known, that P_{II} and NAGK have two interaction surfaces (Llacer *et al.*, 2007). The C-terminus of NAGK is interacting with the body of the P_{II} protein, which is not strongly affected by binding of ADP, and appears to be involved in the relief of the enzyme from arginine inhibition (Beez *et al.*, 2009). On the other hand, induction of the NAG-kinase activity by P_{II} requires rearrangements in the catalytic centre of the enzyme, including hydrogen-bonding and ion-pairs involving the T-loop and the N-domain of NAGK (Llacer *et al.*, 2007). The T-loop conformation of the ADP-ligated P_{II} protein probably is insufficient or too flexible to have such an effect on the NAGK catalytic centre. P_{II}-NAGK interaction is inhibited by 2-OG in the presence of Mg^{2+}-ATP (Maheswaran *et al.*, 2004), and in the presence of 1:1 ATP/ADP the complex stays sensitive towards 2-OG. We already concluded that binding of 2-OG to the third site on the P_{II} trimer is crucial for preventing the P_{II}-NAGK interaction (Fig. G4). This is also true for the P_{II} species with mixed occupation of ATP and ADP. In the presence of 1:1 ATP/ADP, the IC_{50} for 2-OG in the NAGK enzyme assay with P_{II} was 145 µM, close to the K_d (183 µM) for the 2-OG binding to the remaining site in the ATP/ADP-occupied P_{II} species. This way NAGK can stay sensitive towards nitrogen deprivation under low energy conditions. Furthermore, under nitrogen-excess conditions, ADP should diminish the NAGK activation by P_{II}, thereby dampening the energetically expensive anabolic reactions.

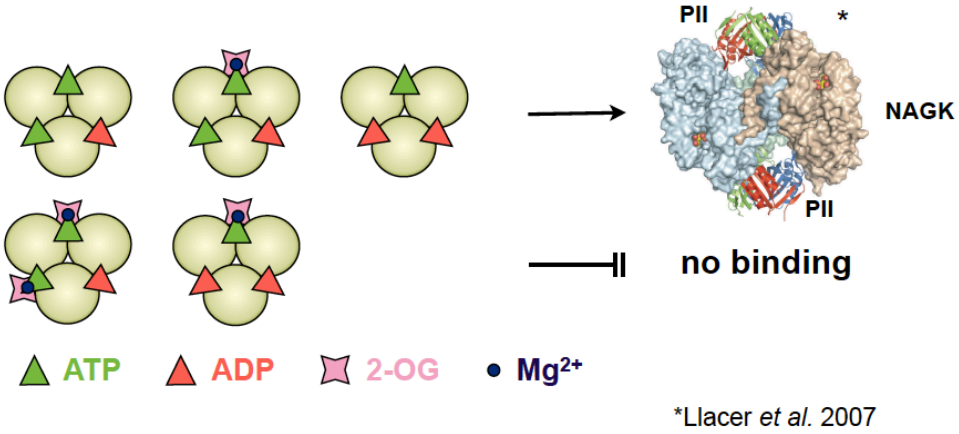

Figure G4. Model describing the role of the effector molecules ATP, ADP and 2-OG in the P_{II}-NAGK complex formation. Three linked circles represent the P_{II} trimer. In the presence of 1:1 ATP/ADP 2-OG can bind to both P_{II}-ATP_2ADP_1 and P_{II}-ATP_1ADP_2 trimers. The occupation of the last available 2-OG-binding site is crucial for inhibiting the P_{II}-NAGK interaction.

4. Two-step mechanism of the P_{II}-NAGK complex formation

Characterisation of the P_{II} variants I86N and I86T also led to a discovery of the two-step mechanism of the P_{II}-NAGK complex formation (Fokina *et al.*, 2010b). The interaction studies of I86N P_{II} with NAGK, including the binding and enzyme assays, and the I86N PII crystal structure clarified the role of the P_{II}85E-NAGK233R interface in the PII-NAGK binding. There are two interaction surfaces in the P_{II}-NAGK complex (Llacer *et al.*, 2007). The larger surface involves the T-loop in a compact bent form that is inserted into the interdomain cleft of NAGK. A smaller interface is formed by the C-terminal domain of NAGK and the P_{II} residues F11, F13 at the β1-α1 junction, T83, involved in hydrophobic interactions, and E85 that forms a salt bridge with R233 of NAGK. The major difference between the structure of the free non-ligated P_{II} protein and the NAGK-bound P_{II} protein from *Synechococcus elongatus* lies in the conformation of the T-loop (Xu *et al.*, 2003; Llacer *et al.*, 2007). In free P_{II}, the T-loop exhibits an extended conformation that is apparently stabilised by a salt bridge between the R47 and E85 residues (Fig. G5). This conformation is only observed in the cyanobacterial P_{II} proteins, because the R47-E85 pair is not present in other P_{II} proteins and the characteristic T-loop form was not found in other resolved P_{II} structures available today (Nichols *et al.*, 2006; Forchhammer, 2008).

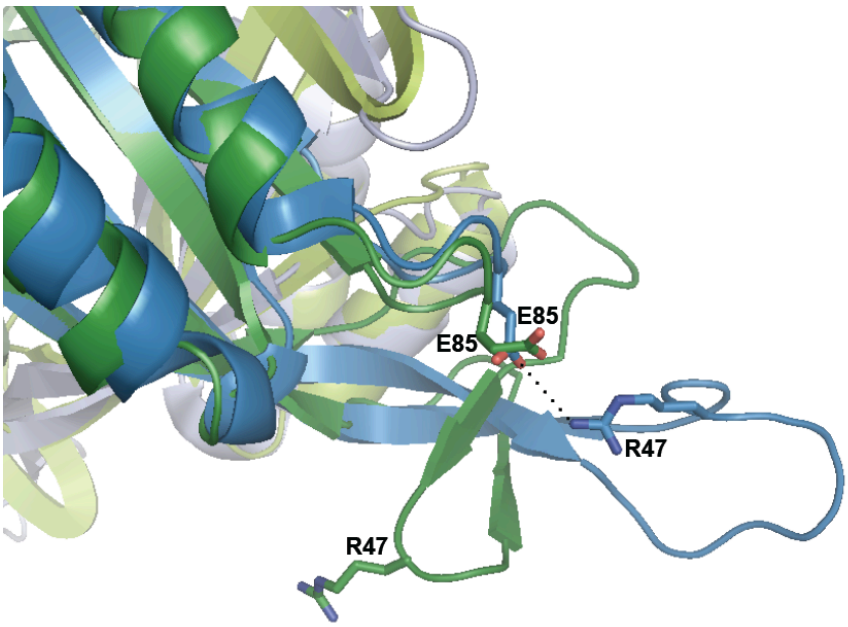

Figure G5. Conformation of the P_{II} T-loop before and after the P_{II}-NAGK complex formation. Overlay of the P_{II} structures as ribbon models: without ligands coloured blue (PDB ID 1QY7), and in the complex with NAGK coloured green (PDB ID 2V5H). Broken line shows the E85-R47 salt bridge.

The R47-E85 bridge is broken in the NAGK-bound P_{II} protein and E85 is interacting with R233 of NAGK. This interaction is crucial for the P_{II}-NAGK complex formation, because the P_{II} variant E85A can't bind wild type NAGK, and R233A NAGK can't bind wild type P_{II}. However, the existence of the E85-R233 bridge itself is not needed for maintaining the complex, because R233A NAGK was able to bind the two P_{II} variants, I86N and I86T. Crystal structure of the I86N P_{II} variant showed that this protein, in the free unbound form, mimicked the conformation of the wild type NAGK-bound P_{II} and fitted into NAGK even without the E85-R233 bridge (Fokina *et al.*, 2010b). Based on these results, a two-step model of the wild-type P_{II}-NAGK complex formation was proposed. In the first step NAGK residue R233 triggers the break of the P_{II} R47-E85 bridge by presenting a more suitable partner for E85. In step two the T-loop, which is no longer stabilised by the R47-E85 bridge, collapses into the compact conformation and creates a larger surfaces for P_{II} binding to NAGK stabilising the complex. The interaction of the I86T variant with the enzyme is weaker and less stable than that of the I86N P_{II}. The T-loop conformation is less suitable for complex with NAGK, probably due to the hydroxyl group of the side chain that is less favourable for hydrogen bonding. The lack of E85D binding to NAGK can be explained by the size of the aspartate side chain that may be too short for the interaction with R233 residue or, as mentioned above, the E85D variant could be locked in the conformation unsuitable for P_{II}-NAGK complex formation. The variants G84V and G89C have lost the ability to bind NAGK due to the general deformation of the B-loop.

5. Conservation of the P_{II}-NAGK interaction in cyanobacteria and plants

Though the P_{II}-NAGK interaction is conserved in cyanobacteria and plants, there are some differences between the two systems, as for example the absence of interactions between the P_{II} B-loop and the NAGK C-domain in the *A. thaliana* P_{II}-NAGK complex (Mizuno *et al.*, 2007). Since the B-loop E85 residue plays an essential role in the two-step complex formation in *S. elongatus*, plant system has some differences in the mechanism of the P_{II}-NAGK interaction. However, as presented in this study, the bacterial and the eukaryotic PII and NAGK proteins were at least partially exchangeable *in vitro* (Beez *et al.*, 2009). P_{II} from *A. thaliana* can fully control NAGK from *S. elongatus*. It means that *At*P_{II} has kept all the essential components for the *Se*NAGK regulation. On the other hand, P_{II} from *S. elongatus*

can only partially complement *At*P_{II}. The plant P_{II} protein has additional N- and C-terminal extensions that are not present in *Se*P_{II} (Mizuno *et al.*, 2007). The *A. thaliana* P_{II}-NAGK complex formation is less sensitive towards 2-OG than the cyanobacterial one, as shown in the binding assays. However, 2-OG concentrations, which are not high enough to prevent complex formation, antagonise the P_{II} mediated induction of *At*NAGK in the enzyme assay. It is possible that low amounts of 2-OG bind to the P_{II} protein and cause conformational changes that prevent the NAGK activation, but the complex remains intact. Despite this difference, in both plant and bacterial systems 2-OG binds to the NAGK-bound P_{II} protein and makes the enzyme exposed to arginine inhibition. As reported previously, plant NAGK is also 50-times less sensitive towards arginine inhibition than the cyanobacterial kinase (Chen *et al.*, 2006). This study has found an explanation for this observation in the structural characteristics of NAGK from *S. elongatus*. *Se*NAGK carries a 11 amino acids long C-terminal peptide, which is not present in the plant enzyme. It has negative influence on the activity of NAGK, makes it more sensitive towards arginine and is affecting the interaction with the P_{II} protein (Beez *et al.*, 2009). Strikingly, *At*P_{II} formed a more stable complex with *Se*NAGK that lacked the C-terminal peptide, than with the wild type cyanobacterial enzyme and the complex was also less sensitive towards 2-OG. The peptide was not resolved in the structure of *Se*NAGK and could be a flexible structure (Llacer *et al.*, 2007). The P_{II}-NAGK interaction is surprisingly well conserved and even partially functionally exchangeable *in vitro*. Only high selective pressure and the importance of the P_{II}-mediated control over the arginine biosynthesis could maintain the interaction over 1.2 billion years of evolution.

6. Antagonistic effect of ADP and 2-OG on the P_{II}-PipX interaction

In *S. elongatus*, P_{II} also controls transcription factor NtcA by binding its activator protein, PipX. Depending on the 2-OG concentration, PipX switches its interaction partner from P_{II} to NtcA (Espinosa *et al.*, 2006). In this work we demonstrated, how low energy charge (increased ADP/ATP ratio) acted antagonistically to the 2-OG mediated effect, by enhancing and stabilising the P_{II}-PipX interaction *in vitro* (Fokina *et al.*, 2011). Compared to the P_{II}-NAGK interaction, PipX binding is much more sensitive towards ADP. Interestingly, the effect of the metabolites on the P_{II}-PipX interaction was diminished, if the C-terminus of the P_{II} protein has been immobilised, as shown in the SPR assay with Strep-tag P_{II}. Therefore, the movement of the C-

terminus, observed for example upon binding 2-OG-Mg^{2+}-ATP (Fig. G1), is essential for incorporation of metabolic signals. Though the study was performed *in vitro*, it is known that nitrogen deprivation correlates with increased intracellular 2-OG levels. Increasing ADP levels should decrease the activity of NtcA, by keeping the P_{II}-PipX complex stable, and thereby prevent the expression of genes required for nitrogen assimilation even at elevated 2-OG levels.

This work extends our knowledge of the P_{II}-mediated signal transduction in cyanobacteria. Metabolite binding is crucial for the P_{II} protein sensing of both nitrogen deprivation and low energy charge. Understanding the basic mechanisms behind the response to effector molecules can help us not only to understand, but also to manipulate the P_{II}-controlled signal transduction or even introduce new metabolites into the system, as in the case of the *in vitro* citrate sensing by the I86N P_{II} variant. Though the study, presented above, has been performed *in vitro*, it gives clear and logical models of the P_{II}-NAGK complex formation and the regulation of the NAGK and PipX proteins by P_{II}, depending on the ADP/ATP balance and the 2-OG levels in *S. elongatus*. Also, complex intersubunit signalling in the P_{II} trimer itself allows communication of the multiple effector binding sites and presents a fine-tuned response to a wide range of metabolite concentrations. The reversible modification by the P_{II}-specific kinase makes this system even more complex. However, all attempts to identify this enzyme have been unsuccessful so far. Finding the kinase and using an *in vivo* system to study the physiological combination of changing energy charge and carbon/nitrogen balance could shed light on the remarkable and yet unknown aspects of the P_{II} controlled signalling system.

I. References

Adams, D. G. and P. S. Duggan. 1999. Heterocyst and akinete differentiation in cyanobacteria. *New Phytologist* **144**: 3-33.

Adler, S. P., D. Purich and E. R. Stadtman. 1975. Cascade control of *Escherichia coli* glutamine synthetase. Properties of the P_{II} regulatory protein and the uridylyltransferase-uridylyl-removing enzyme. *J Biol Chem* **250**: 6264-72.

Allen, M. M. and A. J. Smith. 1969. Nitrogen chlorosis in blue-green algae. *Arch Mikrobiol* **69**: 114-20.

Arcondeguy, T., R. Jack and M. Merrick. 2001. P(II) signal transduction proteins, pivotal players in microbial nitrogen control. *Microbiol Mol Biol Rev* **65**: 80-105.

Atkinson, M. R., T. A. Blauwkamp, V. Bondarenko, V. Studitsky and A. J. Ninfa. 2002. Activation of the *glnA*, *glnK*, and *nac* promoters as *Escherichia coli* undergoes the transition from nitrogen excess growth to nitrogen starvation. *J Bacteriol* **184**: 5358-63.

Atkinson, M. R. and A. J. Ninfa. 1999. Characterization of the GlnK protein of *Escherichia coli*. *Mol Microbiol* **32**: 301-13.

Badger, M. R. and G. D. Price. 2003. CO_2 concentrating mechanisms in cyanobacteria: molecular components, their diversity and evolution. *J Exp Bot* **54**: 609-22.

Beez, S., O. Fokina, C. Herrmann and K. Forchhammer. 2009. N-acetyl-L-glutamate kinase (NAGK) from oxygenic phototrophs: P(II) signal transduction across domains of life reveals novel insights in NAGK control. *J Mol Biol* **389**: 748-58.

Berman-Frank, I., P. Lundgren, Y. B. Chen, H. Kupper, Z. Kolber, B. Bergman and P. Falkowski. 2001. Segregation of nitrogen fixation and oxygenic photosynthesis in the marine cyanobacterium *Trichodesmium*. *Science* **294**: 1534-1537.

Bryant, D. 1994. *The Molecular Biology of Cyanobacteria*. Kluwer Acadamic Publishers.

Bueno, R., G. Pahel and B. Magasanik. 1985. Role of *glnB* and *glnD* gene products in regulation of the *glnALG* operon of *Escherichia coli*. *J Bacteriol* **164**: 816-22.

Burillo, S., I. Luque, I. Fuentes and A. Contreras. 2004. Interactions between the nitrogen signal transduction protein P_{II} and N-acetyl glutamate kinase in organisms that perform oxygenic photosynthesis. *J Bacteriol* **186**: 3346-54.

Caldovic, L. and M. Tuchman. 2003. N-acetylglutamate and its changing role through evolution. *Biochem J* **372**: 279-90.

Cavalier-Smith, T. 1975. The origin of nuclei and of eukaryotic cells. *Nature* **265**: 463-468.

Chen, Y. M., T. S. Ferrar, E. M. Lohmeier-Vogel, N. Morrice, Y. Mizuno, B. Berenger, K. K. Ng, D. G. Muench and G. B. Moorhead. 2006. The P_{II} signal transduction protein of *Arabidopsis thaliana* forms an arginine-regulated complex with plastid N-acetyl glutamate kinase. *J Biol Chem* **281**: 5726-33.

Conroy, M. J., A. Durand, D. Lupo, X. D. Li, P. A. Bullough, F. K. Winkler and M. Merrick. 2007. The crystal structure of the *Escherichia coli* AmtB-GlnK complex reveals how GlnK regulates the ammonia channel. *Proc Natl Acad Sci U S A* **104**: 1213-8.

Coutts, G., G. Thomas, D. Blakey and M. Merrick. 2002. Membrane sequestration of the signal transduction protein GlnK by the ammonium transporter AmtB. *EMBO J* **21**: 536-45.

Durand, A. and M. Merrick. 2006. In vitro analysis of the *Escherichia coli* AmtB-GlnK complex reveals a stoichiometric interaction and sensitivity to ATP and 2-oxoglutarate. *J Biol Chem* **281**: 29558-67.

Dykxhoorn, D. M., R. St Pierre and T. Linn. 1996. A set of compatible *tac* promoter expression vectors. *Gene* **177**: 133-6.

Espinosa, J., K. Forchhammer, S. Burillo and A. Contreras. 2006. Interaction network in cyanobacterial nitrogen regulation: PipX, a protein that interacts in a 2-oxoglutarate dependent manner with P_{II} and NtcA. *Mol Microbiol* **61**: 457-69.

Espinosa, J., K. Forchhammer and A. Contreras. 2007. Role of the *Synechococcus* PCC 7942 nitrogen regulator protein PipX in NtcA-controlled processes. *Microbiology-Sgm* **153**: 711-718.

Feria Bourrellier, A. B., B. Valot, A. Guillot, F. Ambard-Bretteville, J. Vidal and M. Hodges. 2010. Chloroplast acetyl-CoA carboxylase activity is 2-oxoglutarate-regulated by interaction of P_{II} with the biotin carboxyl carrier subunit. *Proc Natl Acad Sci U S A* **107**: 502-7.

Flores, E., J. E. Frias, L. M. Rubio and A. Herrero. 2005. Photosynthetic nitrate assimilation in cyanobacteria. *Photosynthesis Research* **83**: 117-133.

Flores, E. and A. Herrero. 1994. Assimilatory nitrogen metabolism and its regilation. In The Molecular Biology of Cyanobacteria. (D. Bryant) Dordrecht, NL, Kluwer Academic Publishers**:** p. 488-517.

Flores, E. and A. Herrero. 2005. Nitrogen assimilation and nitrogen control in cyanobacteria. *Biochemical Society Transactions* **33**: 164-167.

Fokina, O., V. R. Chellamuthu, K. Forchhammer and K. Zeth. 2010a. Mechanism of 2-oxoglutarate signaling by the *Synechococcus elongatus* P_{II} signal transduction protein. *Proc Natl Acad Sci U S A* **107**: 19760-5.

Fokina, O., V. R. Chellamuthu, K. Zeth and K. Forchhammer. 2010b. A Novel Signal Transduction Protein P(II) Variant from *Synechococcus elongatus* PCC 7942 Indicates a Two-Step Process for NAGK-P(II) Complex Formation. *J Mol Biol* **399**: 410-421.

Fokina, O., C. Herrmann and K. Forchhammer. 2011. Signal transduction protein P_{II} from *Synechococcus elongatus* PCC 7942 senses low adenylate energy charge in vitro. *Biochem J* in press.

Forchhammer, K. 2004. Global carbon/nitrogen control by P_{II} signal transduction in cyanobacteria: from signals to targets. *FEMS Microbiol Rev* **28**: 319-33.

Forchhammer, K. 2008. P(II) signal transducers: novel functional and structural insights. *Trends Microbiol* **16**: 65-72.

Forchhammer, K. and N. T. de Marsac. 1994. The P_{II} Protein in the Cyanobacterium *Synechococcus Sp* Strain Pcc-7942 Is Modified by Serine Phosphorylation and Signals the Cellular N-Status. *Journal of Bacteriology* **176**: 84-91.

Forchhammer, K. and N. T. de Marsac. 1995. Phosphorylation of the $P\text{-}_{II}$ Protein (Glnb Gene-Product) in the Cyanobacterium *Synechococcus* Sp Strain Pcc-7942 - Analysis of in-Vitro Kinase-Activity. *Journal of Bacteriology* **177**: 5812-5817.

Forchhammer, K. and A. Hedler. 1997. Phosphoprotein P_{II} from cyanobacteria--analysis of functional conservation with the P_{II} signal-transduction protein from Escherichia coli. *Eur J Biochem* **244**: 869-75.

Garcia-Dominguez, M. and F. J. Florencio. 1997. Nitrogen availability and electron transport control the expression of *glnB* gene (encoding P_{II} protein) in the cyanobacterium *Synechocystis sp.* PCC 6803. *Plant Mol Biol* **35**: 723-34.

Giovannoni, S. J., S. Turner, G. J. Olsen, S. Barns, D. J. Lane and N. R. Pace. 1988. Evolutionary relationships among cyanobacteria and green chloroplasts. *J Bacteriol* **170**: 3584-92.

Gorl, M., J. Sauer, T. Baier and K. Forchhammer. 1998. Nitrogen-starvation-induced chlorosis in *Synechococcus* PCC 7942: adaptation to long-term survival. *Microbiology-Uk* **144**: 2449-2458.

Gruswitz, F., J. O'Connell, 3rd and R. M. Stroud. 2007. Inhibitory complex of the transmembrane ammonia channel, AmtB, and the cytosolic regulatory protein, GlnK, at 1.96 A. *Proc Natl Acad Sci U S A* **104**: 42-7.

Guerrero, M. G., J. M. Vega and M. Losada. 1981. The assimilatory nitrate-reducing system and its regulation. *Annu Rev Plant Physiol* **32**: 169-204.

Hanahan, D. 1985. *Techniques for transformation of Escherichia coli.* In *DNA cloning.* (D. E. Glover). Oxford: IRL Press.

Heinrich, A., M. Maheswaran, U. Ruppert and K. Forchhammer. 2004. The *Synechococcus elongatus* PII signal transduction protein controls arginine synthesis by complex formation with N-acetyl-L-glutamate kinase. *Mol Microbiol* **52**: 1303-14.

Herrero, A., A. M. Muro-Pastor, A. Valladares and E. Flores. 2004. Cellular differentiation and the NtcA transcription factor in filamentous cyanobacteria. *FEMS Microbiol Rev* **28**: 469-87.

Hsieh, M. H., H. M. Lam, F. J. van de Loo and G. Coruzzi. 1998. A P_{II}-like protein in Arabidopsis: putative role in nitrogen sensing. *Proc Natl Acad Sci U S A* **95**: 13965-70.

Irmler, A. and K. Forchhammer. 2001. A PP2C-type phosphatase dephosphorylates the P_{II} signaling protein in the cyanobacterium *Synechocystis* PCC 6803. *Proc Natl Acad Sci U S A* **98**: 12978-83.

Jaggi, R., W. C. van Heeswijk, H. V. Westerhoff, D. L. Ollis and S. G. Vasudevan. 1997. The two opposing activities of adenylyl transferase reside in distinct homologous domains, with intramolecular signal transduction. *EMBO J* **16**: 5562-71.

Jaggi, R., W. Ybarlucea, E. Cheah, P. D. Carr, K. J. Edwards, D. L. Ollis and S. G. Vasudevan. 1996. The role of the T-loop of the signal transducing protein P_{II} from Escherichia coli. *FEBS Lett* **391**: 223-8.

Javelle, A., E. Severi, J. Thornton and M. Merrick. 2004. Ammonium sensing in *Escherichia coli*. Role of the ammonium transporter AmtB and AmtB-GlnK complex formation. *J Biol Chem* **279**: 8530-8.

Jiang, P. and A. J. Ninfa. 1999. Regulation of autophosphorylation of *Escherichia coli* nitrogen regulator II by the P_{II} signal transduction protein. *J Bacteriol* **181**: 1906-11.

Jiang, P. and A. J. Ninfa. 2007. *Escherichia coli* P_{II} signal transduction protein controlling nitrogen assimilation acts as a sensor of adenylate energy charge in vitro. *Biochemistry* **46**: 12979-96.

Jiang, P. and A. J. Ninfa. 2009a. Alpha-Ketoglutarate Controls the Ability of the *Escherichia coli* P_{II} Signal Transduction Protein To Regulate the Activities of NRII (NtrB) but Does Not Control the Binding of P_{II} to NRII. *Biochemistry* **48**: 11514-11521.

Jiang, P. and A. J. Ninfa. 2009b. Sensation and Signaling of alpha-Ketoglutarate and Adenylylate Energy Charge by the *Escherichia coli* P_{II} Signal Transduction Protein Require Cooperation of the Three Ligand-Binding Sites within the P_{II} Trimer. *Biochemistry* **48**: 11522-11531.

Jiang, P., J. A. Peliska and A. J. Ninfa. 1998a. Enzymological characterization of the signal-transducing uridylyltransferase/uridylyl-removing enzyme (EC 2.7.7.59) of *Escherichia coli* and its interaction with the P_{II} protein. *Biochemistry* **37**: 12782-94.

Jiang, P., J. A. Peliska and A. J. Ninfa. 1998b. Reconstitution of the signal-transduction bicyclic cascade responsible for the regulation of Ntr gene transcription in *Escherichia coli. Biochemistry* **37**: 12795-801.

Jiang, P., J. A. Peliska and A. J. Ninfa. 1998c. The regulation of *Escherichia coli* glutamine synthetase revisited: role of 2-ketoglutarate in the regulation of glutamine synthetase adenylylation state. *Biochemistry* **37**: 12802-10.

Jiang, P., P. Zucker, M. R. Atkinson, E. S. Kamberov, W. Tirasophon, P. Chandran, B. R. Schefke and A. J. Ninfa. 1997. Structure/function analysis of the P_{II} signal transduction protein of *Escherichia coli*: genetic separation of interactions with protein receptors. *J Bacteriology* **179**: 4343-4353.

Jonsson, A. and S. Nordlund. 2007. In vitro studies of the uridylylation of the three P_{II} protein paralogs from *Rhodospirillum rubrum*: the transferase activity of *R. rubrum* GlnD is regulated by alpha-ketoglutarate and divalent cations but not by glutamine. *J Bacteriol* **189**: 3471-8.

Kaplan, A. and L. Reinhold. 1999. CO2 concentrating mechanisms in photosynthetic microorganisms. *Annual Review of Plant Physiology and Plant Molecular Biology* **50**: 539-+.

Khademi, S., J. O'Connell, 3rd, J. Remis, Y. Robles-Colmenares, L. J. Miercke and R. M. Stroud. 2004. Mechanism of ammonia transport by Amt/MEP/Rh: structure of AmtB at 1.35 A. *Science* **305**: 1587-94.

Kloft, N. and K. Forchhammer. 2005. Signal transduction protein P-II phosphatase PphA is required for light-dependent control of nitrate utilization in *Synechocystis sp* strain PCC 6803. *Journal of Bacteriology* **187**: 6683-6690.

Kobayashi, M., R. Rodriguez, C. Lara and T. Omata. 1997. Involvement of the C-terminal domain of an ATP-binding subunit in the regulation of the ABC-type nitrate/nitrite transporter of the Cyanobacterium *Synechococcus sp.* strain PCC 7942. *J Biol Chem* **272**: 27197-201.

Krogmann, D. W. 1973. *The Biology of Blue-green Algae.* (N. Carr and B. Whitton) Oxford. Blackwell Scientific.

Kuhlemeier, C. J., A. A. Thomas, A. van der Ende, R. W. van Leen, W. E. Borrias, C. A. van den Hondel and G. A. van Arkel. 1983. A host-vector system for gene cloning in the cyanobacterium *Anacystis nidulans* R2. *Plasmid* **10**: 156-63.

Lee, H. M., E. Flores, A. Herrero, J. Houmard and N. Tandeau de Marsac. 1998. A role for the signal transduction protein P_{II} in the control of nitrate/nitrite uptake in a cyanobacterium. *FEBS Lett* **427**: 291-5.

Lee, H. M., M. F. Vazquez-Bermudez and N. T. de Marsac. 1999. The global nitrogen regulator NtcA regulates transcription of the signal transducer P_{II} (GlnB) and influences its phosphorylation level in response to nitrogen and carbon supplies in the Cyanobacterium *Synechococcus* sp. strain PCC 7942. *J Bacteriol* **181**: 2697-702.

Leigh, J. A. and J. A. Dodsworth. 2007. Nitrogen regulation in bacteria and archaea. *Annu Rev Microbiol* **61**: 349-77.

Liu, J. and B. Magasanik. 1993. The glnB region of the *Escherichia coli* chromosome. *J Bacteriol* **175**: 7441-9.

Llacer, J. L., A. Contreras, K. Forchhammer, C. Marco-Marin, F. Gil-Ortiz, R. Maldonado, I. Fita and V. Rubio. 2007. The crystal structure of the complex

of P_{II} and acetylglutamate kinase reveals how P_{II} controls the storage of nitrogen as arginine. *Proc Natl Acad Sci U S A* **104**: 17644-9.

Llacer, J. L., J. Espinosa, M. A. Castells, A. Contreras, K. Forchhammer and V. Rubio. 2010. Structural basis for the regulation of NtcA-dependent transcription by proteins PipX and P_{II}. *Proceedings of the National Academy of Sciences of the United States of America* **107**: 15397-15402.

Llacer, J. L., I. Fita and V. Rubio. 2008. Arginine and nitrogen storage. *Curr Opin Struct Biol* **18**: 673-81.

Luque, I., E. Flores and A. Herrero. 1994. Molecular mechanism for the operation of nitrogen control in cyanobacteria. *EMBO J* **13**: 2862-9.

Luque, I. and K. Forchhammer. 2008. Nitrogen assimilation and C/N balance sensing. in *The Cyanobacteria*. (Herrero, A. and E. Flores) Norfolk, UK: Caister Academic Press.

Maeda, S., M. R. Badger and G. D. Price. 2002. Novel gene products associated with NdhD3/D4-containing NDH-1 complexes are involved in photosynthetic CO_2 hydration in the cyanobacterium, *Synechococcus* sp PCC7942. *Molecular Microbiology* **43**: 425-435.

Maeda, S., G. D. Price, M. R. Badger, C. Enomoto and T. Omata. 2000. Bicarbonate binding activity of the CmpA protein of the cyanobacterium *Synechococcus* sp strain PCC 7942 involved in active transport of bicarbonate. *Journal of Biological Chemistry* **275**: 20551-20555.

Maeda, S. I. and T. Omata. 1997. Substrate-binding lipoprotein of the cyanobacterium *Synechococcus* sp strain PCC 7942 involved in the transport of nitrate and nitrite. *Journal of Biological Chemistry* **272**: 3036-3041.

Maheswaran, M., C. Urbanke and K. Forchhammer. 2004. Complex formation and catalytic activation by the P_{II} signaling protein of N-acetyl-L-glutamate kinase from *Synechococcus elongatus* strain PCC 7942. *J Biol Chem* **279**: 55202-10.

Manzano, C., P. Candau, C. Gomez-Moreno, A. M. Relimpio and M. Losada. 1976. Ferredoxin-dependent photosynthetic reduction of nitrate and nitrite by particles of Anacystis nidulans. *Mol Cell Biochem* **10**: 161-9.

Marques, S., F. J. Florencio and P. Candau. 1992. Purification and characterization of the ferredoxin-glutamate synthase from the unicellular cyanobacterium *Synechococcus* sp. PCC 6301. *Eur J Biochem* **206**: 69-77.

Merrick, M. J. and R. A. Edwards. 1995. Nitrogen Control in Bacteria. *Microbiological Reviews* **59**: 604-&.

Miller, J. H. 1972. *Experiments in Molecular Genetics*. Cold Spring Harbor Laboratory Press.

Mizuno, Y., G. B. Moorhead and K. K. Ng. 2007. Structural basis for the regulation of N-acetylglutamate kinase by P_{II} in *Arabidopsis thaliana*. *J Biol Chem* **282**: 35733-40.

Montesinos, M. L., A. M. Muro-Pastor, A. Herrero and E. Flores. 1998. Ammonium/Methylammonium permeases of a cyanobacterium - Identification and analysis of three nitrogen-regulated amt genes in *Synechocystis* sp. PCC 6803. *Journal of Biological Chemistry* **273**: 31463-31470.

Muro-Pastor, M. I. and F. J. Florencio. 2003. Regulation of ammonium assimilation in cyanobacteria. *Plant Physiology and Biochemistry* **41**: 595-603.

Muro-Pastor, M. I., J. C. Reyes and F. J. Florencio. 1996. The NADP+-isocitrate dehydrogenase gene (icd) is nitrogen regulated in cyanobacteria. *J Bacteriol* **178**: 4070-6.

Muro-Pastor, M. I., J. C. Reyes and F. J. Florencio. 2005. Ammonium assimilation in cyanobacteria. *Photosynthesis Research* **83**: 135-150.

Nichols, C. E., S. Sainsbury, N. S. Berrow, D. Alderton, N. J. Saunders, D. K. Stammers and R. J. Owens. 2006. Structure of the P_{II} signal transduction protein of *Neisseria meningitidis* at 1.85 A resolution. *Acta Crystallogr Sect F Struct Biol Cryst Commun* **62**: 494-7.

Ninfa, A. J. and P. Jiang. 2005. P_{II} signal transduction proteins: sensors of alpha-ketoglutarate that regulate nitrogen metabolism. *Curr Opin Microbiol* **8**: 168-73.

Ninfa, A. J. and B. Magasanik. 1986. Covalent modification of the glnG product, NRI, by the glnL product, NRII, regulates the transcription of the *glnALG* operon in Escherichia coli. *Proc Natl Acad Sci U S A* **83**: 5909-13.

Omata, T., X. Andriesse and A. Hirano. 1993. Identification and Characterization of a Gene-Cluster Involved in Nitrate Transport in the Cyanobacterium *Synechococcus* Sp-Pcc7942. *Molecular & General Genetics* **236**: 193-202.

Omata, T., G. D. Price, M. R. Badger, M. Okamura, S. Gohta and T. Ogawa. 1999. Identification of an ATP-binding cassette transporter involved in bicarbonate uptake in the cyanobacterium *Synechococcus* sp strain PCC 7942. *Proceedings of the National Academy of Sciences of the United States of America* **96**: 13571-13576.

Osanai, T., S. Sato, S. Tabata and K. Tanaka. 2005. Identification of PamA as a P_{II}-binding membrane protein important in nitrogen-related and sugar-catabolic gene expression in *Synechocystis* sp. PCC 6803. *J Biol Chem* **280**: 34684-90.

Palinska, K. A., W. Laloui, S. Bedu, S. Loiseaux-de Goer, A. M. Castets, R. Rippka and N. Tandeau de Marsac. 2002. The signal transducer P(II) and bicarbonate acquisition in *Prochlorococcus marinus* PCC 9511, a marine cyanobacterium naturally deficient in nitrate and nitrite assimilation. *Microbiology* **148**: 2405-12.

Price, G. D., F. J. Woodger, M. R. Badger, S. M. Howitt and L. Tucker. 2004. Identification of a SulP-type bicarbonate transporter in marine cyanobacteria. *Proc Natl Acad Sci U S A* **101**: 18228-33.

Radchenko, M. V., J. Thornton and M. Merrick. 2010. Control of AmtB-GlnK complex formation by intracellular levels of ATP, ADP, and 2-oxoglutarate. *J Biol Chem* **285**: 31037-45.

Reinhold, L., R. Kosloff and A. Kaplan. 1991. A Model for Inorganic Carbon Fluxes and Photosynthesis in Cyanobacterial Carboxysomes. *Canadian Journal of Botany-Revue Canadienne De Botanique* **69**: 984-988.

Reyes, J. C. and F. J. Florencio. 1994. A New-Type of Glutamine-Synthetase in Cyanobacteria - the Protein Encoded by the Glnn Gene Supports Nitrogen Assimilation in *Synechocystis* Sp Strain Pcc-6803. *Journal of Bacteriology* **176**: 1260-1267.

Reyes-Ramirez, F., R. Little and R. Dixon. 2001. Role of Escherichia coli nitrogen regulatory genes in the nitrogen response of the *Azotobacter vinelandii* NifL-NifA complex. *J Bacteriol* **183**: 3076-82.

Rhee, S. G., P. B. Chock and E. R. Stadtman. 1985. Glutamine synthetase from *Escherichia coli*. *Methods Enzymol* **113**: 213-41.

Rippka, R. 1988. Isolation and purification of cyanobacteria. *Methods Enzymol* **167**: 3-27.

Rippka, R., J. Deruelles, J. B. Waterbury, M. Herdman and R. Y. Stanier. 1979. Generic Assignments, Strain Histories and Properties of Pure Cultures of Cyanobacteria. *J Gen Microbiol* **111**: 1-61.

Ruppert, U., A. Irmler, N. Kloft and K. Forchhammer. 2002. The novel protein phosphatase PphA from *Synechocystis* PCC 6803 controls dephosphorylation of the signalling protein P-II. *Molecular Microbiology* **44**: 855-864.

Sakai, H., H. Wang, C. Takemoto-Hori, T. Kaminishi, H. Yamaguchi, Y. Kamewari, T. Terada, S. Kuramitsu, M. Shirouzu and S. Yokoyama. 2005. Crystal structures of the signal transducing protein GlnK from *Thermus thermophilus* HB8. *J Struct Biol* **149**: 99-110.

Sakamoto, T., K. Inoue-Sakamoto and D. A. Bryant. 1999. A novel nitrate/nitrite permease in the marine cyanobacterium *Synechococcus* sp strain PCC 7002. *Journal of Bacteriology* **181**: 7363-7372.

Sambrook, J., E. F. Fritsch and T. Maniatis. 1989. *Molecular Cloning: a laboratory manual*. Cold Spring Harbor Laboratory Press.

Sanchez-Baracaldo, P., P. K. Hayes and C. E. Blank. 2005. Morphological and habitat evolution in the Cyanobacteria using a compartmentalization approach. *Geobiology* **3**: 145-165.

Sant'Anna, F. H., D. B. Trentini, S. de Souto Weber, R. Cecagno, S. C. da Silva and I. S. Schrank. 2009. The P_{II} superfamily revised: a novel group and evolutionary insights. *J Mol Evol* **68**: 322-36.

Sauer, J., M. Gorl and K. Forchhammer. 1999. Nitrogen starvation in synechococcus PCC 7942: involvement of glutamine synthetase and NtcA in phycobiliprotein degradation and survival. *Arch Microbiol* **172**: 247-55.

Schwarz, R. and K. Forchhammer. 2005. Acclimation of unicellular cyanobacteria to macronutrient deficiency: emergence of a complex network of cellular responses. *Microbiology-Sgm* **151**: 2503-2514.

Shapiro, B. M. 1969. The glutamine synthetase deadenylylating enzyme system from *Escherichia coli.* Resolution into two components, specific nucleotide stimulation, and cofactor requirements. *Biochemistry* **8**: 659-70.

Shibata, M., H. Katoh, M. Sonoda, H. Ohkawa, M. Shimoyama, H. Fukuzawa, A. Kaplan and T. Ogawa. 2002a. Genes essential to sodium-dependent bicarbonate transport in cyanobacteria - Function and phylogenetic analysis. *Journal of Biological Chemistry* **277**: 18658-18664.

Shibata, M., H. Ohkawa, T. Kaneko, H. Fukuzawa, S. Tabata, A. Kaplan and T. Ogawa. 2001. Distinct constitutive and low-CO2-induced CO2 uptake systems in cyanobacteria: Genes involved and their phylogenetic relationship with homologous genes in other organisms. *Proceedings of the National Academy of Sciences of the United States of America* **98**: 11789-11794.

Shibata, M., H. Ohkawa, H. Katoh, M. Shimoyama and T. Ogawa. 2002b. Two CO2 uptake systems in cyanobacteria: four systems for inorganic carbon acquisition in *Synechocystis* sp strain PCC6803. *Functional Plant Biology* **29**: 123-129.

Smith, C. S., A. M. Weljie and G. B. Moorhead. 2003. Molecular properties of the putative nitrogen sensor P_{II} from *Arabidopsis thaliana. Plant J* **33**: 353-60.

Smith, C. S., S. T. Zaplachinski, D. G. Muench and G. B. Moorhead. 2002. Expression and purification of the chloroplast putative nitrogen sensor, P_{II}, of *Arabidopsis thaliana*. *Protein Expr Purif* **25**: 342-7.

Son, H. S. and S. G. Rhee. 1987. Cascade control of Escherichia coli glutamine synthetase. Purification and properties of P_{II} protein and nucleotide sequence of its structural gene. *J Biol Chem* **262**: 8690-5.

Stanier, R. Y. and G. Cohen-Bazire. 1977. Phototrophic prokaryotes: the cyanobacteria. *Annu Rev Microbiol* **31**: 225-74.

Strosser, J., A. Ludke, S. Schaffer, R. Kramer and A. Burkovski. 2004. Regulation of GlnK activity: modification, membrane sequestration and proteolysis as regulatory principles in the network of nitrogen control in *Corynebacterium glutamicum*. *Mol Microbiol* **54**: 132-47.

Su, Z., V. Olman, F. Mao and Y. Xu. 2005. Comparative genomics analysis of NtcA regulons in cyanobacteria: regulation of nitrogen assimilation and its coupling to photosynthesis. *Nucleic Acids Res* **33**: 5156-71.

Sugiyama, K., T. Hayakawa, T. Kudo, T. Ito and T. Yamaya. 2004. Interaction of N-acetylglutamate kinase with a P_{II}-like protein in rice. *Plant Cell Physiol* **45**: 1768-78.

Suzuki, I., T. Sugiyama and T. Omata. 1993. Primary Structure and Transcriptional Regulation of the Gene for Nitrite Reductase from the Cyanobacterium *Synechococcus* PCC 7942. *Plant Cell Physiol* **34**: 1311-1320.

Takatani, N., M. Kobayashi, S. I. Maeda and T. Omata. 2006. Regulation of nitrate reductase by non-modifiable derivatives of P_{II} in the cells of *Synechococcus elongatus* strain PCC 7942. *Plant and Cell Physiology* **47**: 1182-1186.

Tanigawa, R., M. Shirokane, S. Maeda Si, T. Omata, K. Tanaka and H. Takahashi. 2002. Transcriptional activation of NtcA-dependent promoters of *Synechococcus* sp. PCC 7942 by 2-oxoglutarate *in vitro*. *Proc Natl Acad Sci U S A* **99**: 4251-5.

Thomas, G., G. Coutts and M. Merrick. 2000. The glnKamtB operon. A conserved gene pair in prokaryotes. *Trends Genet* **16**: 11-4.

Tomitani, A., A. H. Knoll, C. M. Cavanaugh and T. Ohno. 2006. The evolutionary diversification of cyanobacteria: molecular-phylogenetic and paleontological perspectives. *Proc Natl Acad Sci U S A* **103**: 5442-7.

Truan, D., L. F. Huergo, L. S. Chubatsu, M. Merrick, X. D. Li and F. K. Winkler. 2010. A new P(II) protein structure identifies the 2-oxoglutarate binding site. *J Mol Biol* **400**: 531-9.

Turner, S., K. M. Pryer, V. P. Miao and J. D. Palmer. 1999. Investigating deep phylogenetic relationships among cyanobacteria and plastids by small subunit rRNA sequence analysis. *J Eukaryot Microbiol* **46**: 327-38.

Vazquez-Bermudez, M. F., J. Paz-Yepes, A. Herrero and E. Flores. 2002. The NtcA-activated *amt1* gene encodes a permease required for uptake of low concentrations of ammonium in the cyanobacterium *Synechococcus* sp PCC 7942. *Microbiology-Sgm* **148**: 861-869.

Vega-Palas, M. A., E. Flores and A. Herrero. 1992. NtcA, a global nitrogen regulator from the cyanobacterium *Synechococcus* that belongs to the Crp family of bacterial regulators. *Mol Microbiol* **6**: 1853-9.

Vermaas, W. 2001. Encyclopedia of Life Sciences. Photosynthesis and respiration in cyanobacteria.

Wang, Q. F., H. Li and A. F. Post. 2000. Nitrate assimilation genes of the marine diazotrophic, filamentous cyanobacterium *Trichodesmium* sp strain WH9601. *Journal of Bacteriology* **182**: 1764-1767.

Weber, I. T. and T. A. Steitz. 1987. Structure of a complex of catabolite gene activator protein and cyclic AMP refined at 2.5 A resolution. *J Mol Biol* **198**: 311-26.

Wei, T. F., T. S. Ramasubramanian, F. Pu and J. W. Golden. 1993. *Anabaena* sp. strain PCC 7120 *bifA* gene encoding a sequence-specific DNA-binding protein cloned by in vivo transcriptional interference selection. *J Bacteriol* **175**: 4025-35.

Wilson, K. 1987. *Current protocols in molecular biology.* Wiley, New York.

Wolfe, D. M., Y. Zhang and G. P. Roberts. 2007. Specificity and regulation of interaction between the P_{II} and AmtB1 proteins in *Rhodospirillum rubrum*. *J Bacteriol* **189**: 6861-9.

Xu, Y., P. D. Carr, P. Clancy, M. Garcia-Dominguez, K. Forchhammer, F. Florencio, S. G. Vasudevan, N. Tandeau de Marsac and D. L. Ollis. 2003. The structures of the P_{II} proteins from the cyanobacteria *Synechococcus* sp. PCC 7942 and *Synechocystis* sp. PCC 6803. *Acta Crystallogr D Biol Crystallogr* **59**: 2183-90.

Xu, Y., P. D. Carr, T. Huber, S. G. Vasudevan and D. L. Ollis. 2001. The structure of the P_{II}-ATP complex. *Eur J Biochem* **268**: 2028-37.

Xu, Y., E. Cheah, P. D. Carr, W. C. van Heeswijk, H. V. Westerhoff, S. G. Vasudevan and D. L. Ollis. 1998. GlnK, a P_{II}-homologue: structure reveals ATP binding site and indicates how the T-loops may be involved in molecular recognition. *J Mol Biol* **282**: 149-65.

Yidiz, Ö., C. Kalthoff, S. Raunser and W. Kühlbrandt. 2007. Structure of GlnK1 with bound effectors indicates regulatory mechanism for ammonia uptake. *EMBO* **26**: 589-599.

Zhang, Y., E. L. Pohlmann, C. M. Halbleib, P. W. Ludden and G. P. Roberts. 2001a. Effect of P(II) and its homolog GlnK on reversible ADP-ribosylation of dinitrogenase reductase by heterologous expression of the Rhodospirillum rubrum dinitrogenase reductase ADP-ribosyl transferase-dinitrogenase reductase-activating glycohydrolase regulatory system in *Klebsiella pneumoniae*. *J Bacteriol* **183**: 1610-20.

Zhang, Y., E. L. Pohlmann, P. W. Ludden and G. P. Roberts. 2001b. Functional characterization of three GlnB homologs in the photosynthetic bacterium *Rhodospirillum rubrum*: roles in sensing ammonium and energy status. *J Bacteriol* **183**: 6159-68.

Zhang, Y. P., E. L. Pohlmann, P. W. Ludden and G. P. Roberts. 2003. Regulation of nitrogen fixation by multiple P-II homologs in the photosynthetic bacterium *Rhodospirillum rubrum*. *Symbiosis* **35**: 85-100.

Zheng, L., D. Kostrewa, S. Berneche, F. K. Winkler and X. D. Li. 2004. The mechanism of ammonia transport based on the crystal structure of AmtB of *Escherichia coli*. *Proc Natl Acad Sci U S A* **101**: 17090-5.

J. Abbreviations

ABC	ATP-binding cassette
ADP	adenosine diphosphate
AHT	anhydrotetracycline
Amp	ampicillin
ATase	adenylyltransferase
***At*NAGK**	NAGK from *Arabidopsis thaliana*
***At*P_{II}**	P_{II} from *Arabidopsis thaliana*
ATP	adenosine triphosphate
bp	base pair
C	carbon
°C	degree Celsius
Chl *a*	chlorophyll *a*
Cm	chloramphenicol
CRP	cAMP receptor protein
DNA	deoxyribonucleic acid
EDTA	ethylenediaminetetraacetic acid
FC1	flow cell 1
FC2	flow cell 2
Fd	ferredoxin
Fig.	figure
Glc	glucose
Gln	glutamine
GOGAT	glutamine-2-oxoglutarate-amido transferase
GS	glutamine synthetase
GSI	glutamine synthetase type I
GSIII	glutamine synthetase type III
HEPES	4-(2-hydroxyethyl)-1-piperazineethanesulfonic acid

IDH	isocitrate dehydrogenase
IPTG	isopropyl β-D-1-thiogalactopyranoside
kDa	kilo-Dalton
LB	Luria-Bertani
MFS	major facilitator superfamily
N	nitrogen
NADPH	nicotinamide adenine dinucleotide phosphate
NAG	*N*-acetyl-L-glutamate
NAGK	*N*-acetyl-L-glutamate kinase
NiR	nitrite reductase
NR	nitrate reductase
NTA	nitrilotriacetic acid
OD	optical density
PCR	polymerase chain reaction
P_i	Inorganic phosphate
PSI	photosystem I
PSII	photosystem II
RU	resonance units
RubisCO	ribulose-1,5-bisphosphate carboxylase oxygenase
SDS-PAGE	sodium dodecyl sulfate polyacrylamide gel electrophoresis
***Se*NAGK**	NAGK from *Synechococcus elongatus*
***Se*P_{II}**	P_{II} from *Synechococcus elongatus*
SPR	surface plasmon resonance
Tab.	table
TCA	tricarboxylic acid
UTase/UR	uridylyltransferase/uridylyl-removing enzyme
wt	wild type
2-OG	2-oxoglutarate

Acknowledgement

My sincere thanks to everyone who helped and supported me during the last years.

Especially I would like to thank:

Prof. Dr. K. Forchhammer for giving me the opportunity to work on such an interesting topic. His supervision, guidance, scientific ideas and experiences allowed me to fulfil this work.

Prof. Dr. W. Wohlleben for the assessment of this work.

Nikole and Grit for helping me out in the beginning of my research, when I had no idea what I was doing.

Susanne, Max, Peter and Josef not only for their help, advices and interesting discussions, but moreover for wonderful working atmosphere and all the fun we had together.
Everyone else at the institute for the friendly and comfortable working environment. Iris for always finding the time to give me a helpful advice and for the great time spent together. Michaela for all her help in the official institute matters. Herr Hantke for useful discussions. Christina for her technical assistance that supported my work.

My friends for always being there for me, when I needed them.

Special thanks to my parents for their interest in my research and scientific carrier. Their faith in me and support are always giving me the strength to continue.